

AN ABSTRACT OF THE DISSERTATION OF

Britton C. Goodale for the degree of Doctor of Philosophy in Toxicology presented on August 12, 2013.

Title: Developmental Toxicity of Polycyclic Aromatic Hydrocarbons: Defining Mechanisms with Systems-based Transcriptional Profiling

Abstract approved: _____
Robert L. Tanguay

Polycyclic aromatic hydrocarbons (PAHs) are ubiquitous in the environment as components of fossil fuels and by-products of combustion. Defining toxicity mechanisms for this large family of multi-ring structures and substituted derivatives is a substantial challenge. Several PAHs, such as benzo(a)pyrene (BaP), are mutagenic, toxic to wildlife, and classified as probable carcinogens to humans. PAHs are present in the environment both in the gaseous phase as well as associated with particulates, and exposures occur via complex mixtures; combustion emissions contain PAHs along with many other contaminants. Cardiac dysfunction and adverse birth outcomes associated with exposure to airborne PAHs suggest that this family of compounds may have non-mutagenic biological activities that affect human health. Some PAHs exert toxic effects via binding the aryl hydrocarbon receptor (AHR), a ligand-activated transcription factor that mediates transcription of many downstream target genes, including cytochrome P450 metabolizing enzymes. Unlike planar halogenated hydrocarbons, such as 2,3,7,8-tetrachlorodibenzo-p-dioxin (TCDD), PAHs are readily metabolized by CYP1A, CYP1B1 and other enzymes, which create reactive intermediates and/or facilitate excretion. Mechanisms of PAH toxicity therefore include canonical AHR signaling, induction of oxidative stress, and other lesser-understood activities that do not require the AHR. We employed zebrafish as a model to rapidly assess developmental toxicity, global transcriptional responses and AHR activation in embryos exposed to parent and oxygenated PAHs (OPAHs). Using comparative analysis of mRNA expression profiles from microarrays with embryos exposed to benz(a)anthracene (BAA), dibenzothiophene (DBT) and pyrene (PYR), we identified expression biomarkers and

disrupted biological processes that precede developmental abnormalities. These transcriptional responses were associated with PAH body burdens in the embryos detected by GC-MS. We found that uptake data were essential for discerning molecular pathways from dose-related differences, and identified two primary toxicity profiles. While BAA disrupted transcripts involved in vasculogenesis, DBT and PYR misregulated ion homeostasis and muscle-related genes. NfKB signaling was predicted to be involved in both responses, but canonical AHR signaling was only activated by BAA. In order to study the role of the AHR in mediating toxicity of PAHs, we developed an AHR2 mutant zebrafish line, which has a mutation in the transactivation domain of AHR2. We used AHR agonists TCDD and leflunomide as toxicological probes to characterize AHR activity in the mutant line, and determined that the mutants were functionally null. Finally, we used AHR2 deficient zebrafish embryos to investigate mechanisms by which two four-ring OPAHs induced developmental effects. 1,9 benz-10-anthrone (BEZO) and benz(a)anthracene-7,12-dione (7,12-B[a]AQ) both caused malformations in developing embryos, but they differentially induced CYP1A expression. Despite this difference, the toxicity produced from both compounds was AHR2-dependent. We used mRNA-seq to compare the transcriptional profiles of BEZO and 7,12-B[a]AQ, and identified transcriptional networks that will be investigated further to determine how ligands differentially modulate AHR activity. We also discovered novel transcripts that are potentially important mediators of AHR toxic effects. Comparison across all five parent and OPAHs highlighted clusters of genes that, surprisingly, were similarly expressed in response to the OPAHs, DBT and PYR. These commonly-regulated transcripts may be important to consider when investigating toxicity of PAH mixtures. Together, these studies show that PAHs act via different transcriptional mechanisms, but can be categorized based on transcriptional profiles and differential AHR activation. The clusters of transcripts identified may be involved in common pathways; further investigation of transcription factors and coactivators that interact with mixexpressed genes is a promising area of research for elucidating diverse functions of the AHR.

©Copyright by Britton C. Goodale

August 12, 2013

All Rights Reserved

Developmental Toxicity of Polycyclic Aromatic Hydrocarbons: Defining Mechanisms with
Systems-based Transcriptional Profiling

by

Britton C. Goodale

A DISSERTATION

submitted to

Oregon State University

in partial fulfillment of
the requirements for the
degree of
Doctor of Philosophy

Presented August 12, 2013

Commencement June 2014

Doctor of Philosophy dissertation of Britton C. Goodale presented on August 12, 2013.

APPROVED:

Major Professor, representing Toxicology

Head of the Department of Environmental and Molecular Toxicology

Dean of the Graduate School

I understand that my dissertation will become part of the permanent collection of Oregon State University libraries. My signature below authorizes release of my dissertation to any reader upon request.

Britton C. Goodale, Author

ACKNOWLEDGEMENTS

The completion of this dissertation has by no means been a solitary effort, and I am grateful to the many people who made it possible. I would like to express my sincere gratitude to my graduate mentor, Robert Tanguay, for giving me the opportunity to join the lab and pursue what were, five years ago, fairly specific interests in toxicology. Thank you for sharing your endless excitement about new ideas, and for broadening my perspective and enthusiasm for this field of research more than I could have imagined. None of the work presented here would have been possible without the support I had during my time at OSU, and I am appreciative of the excellent resources that the Tanguay lab has provided. I would like to thank the many members of the Tanguay lab who have helped me over the years: Jane La Du, for her humor and for always being there to help in a pinch; Kate Saili, Tamara Tal, Lisa Truong, Galen Miller and Sumitra Sengupta for providing training in the lab, and for their mentorship and friendship; Andrea Knecht, Mike Simonich, and Annika Swanson for their help and patience with the OPAH studies; Leah Wehmas, Derik Haggard, Siba Das and Cory Gerlach for editing, experiment assistance, and helping me through this final year with excellent company in the lab; Sean Bugel for sharing the office with the window and the challenge assay, providing thoughtful answers to my many questions, and for the excellent discussions; Jill Franzosa for encouragement and advice, both in the lab and on the climbing wall; and Margaret Corvi for helping me keep perspective, making the OPAH body burden studies possible, and being an inspiration to work with. All of the studies in this dissertation were truly made possible by the SARL staff, and I am thankful to Carrie Barton and Cari Buchner for their dedication to the zebrafish colony, particularly the AHR2 mutants (they will some day express their gratitude, too, I'm sure). Thank you to Greg Gonnerman, Chapell Miller for screening help, and to all of the other staff who have kept SARL running.

I would like to thank others at OSU for their support; I am grateful to my committee members Daniel Sudakin, Michael Freitag, Kim Anderson, Barbara Taylor and Jeffrey Greenwood for their wisdom and guidance of this project. The Anderson lab welcomed me to OSU, and I can't imagine my time here without them. Thank you to the many folks who helped me with chemistry questions, compound requests, advised me on environmental

relevance for my studies, and gave me good excuses to go to campus. I thank the EMT department for making my graduate work possible, especially department head Craig Marcus for helping me accomplish many goals, and all of the EMT office staff for making things run smoothly.

I am especially grateful to my friends who, from near and far, supported me through every step of graduate school. Thank you for being my family when I arrived, exploring the west coast with me, and making Oregon home. Since graduate work feels, much of the time, like a process of many failures, successes in other arenas were an essential part of life the past five years. Thank you to everyone who buoyed my sanity with triumphant climbs, bikes, and foraging adventures. I am so thankful to Erik Endrulat, for his support through this endeavor, and for gently reminding me to think about balance. I was unable to conduct a controlled study on the topic, but nevertheless attribute my perplexing decrease in flu susceptibility the past two years to the good food and abundance of laughter I've enjoyed with him. Most of all, I am forever grateful to my family, for their love and support through this entire journey, especially when I chose to move across the country. To my sister, Jane: thank you for your incredible insight, and for your gift of finding the humor in whatever situation I presented you with. Thank you to my Dad, Steve, for teaching me to be a problem solver, and continually giving me new things to think about. To my Mom, Anne: thank you for your words of advice, even when I didn't want to hear it, cheering for me always, and the steadfast assurance that I wasn't doing this on my own.

CONTRIBUTION OF AUTHORS

Many people at Oregon State University and Pacific Northwest National Lab contributed to the studies presented in this thesis. In Chapter 2, Susan Tilton statistically analyzed the microarray data, conducted transcription factor enrichment/pathway analysis, provided guidance and training for other bioinformatics techniques employed, and contributed intellectually to the manuscript. Margaret Corvi contributed experiment planning guidance and assisted with all aspects of sample preparation for the PAH body burden studies. Glenn Wilson conducted GC-MS analysis of PAH body burden samples. Derek Janszen statistically analyzed the PAH developmental toxicity data. Kim Anderson and Katrina Waters both contributed training and intellectual guidance for the manuscript.

In Chapter 3, Jane La Du conducted outcrossing and screening for *ahr2*^{hu3335} carriers, and assisted with characterization and AHR knockdown studies. William Bisson conducted the in silico AHR docking studies. Derek Janszen carried out statistical analysis of developmental toxicity data. Katrina Waters provided statistical expertise and contributed intellectually to the studies.

In Chapter 4, Susan Tilton provided bioinformatic support and conducted transcription factor network prediction and enrichment analysis for biological functions associated with RNA-seq transcripts. Christopher Sullivan processed RNA-seq data, and provided bioinformatic core support for mapping, assembly, and statistical analysis of RNA-seq data.

TABLE OF CONTENTS

	<u>Page</u>
Chapter 1 - Introduction	2
Human exposure to PAHs.....	3
Emerging concerns: cardiac function and effects during development.....	5
Mechanisms of PAH toxicity: activation of the aryl hydrocarbon receptor.....	6
Effects of PAH exposure on fish development	8
Discovering endogenous functions of the AHR	10
The zebrafish model	11
Substituted PAHs: adding complexity to toxicity evaluation.....	12
Categorizing compounds, predicting PAH toxicity	13
Summary and study objectives	14
References.....	16
Chapter 2 - Structurally distinct polycyclic aromatic hydrocarbons induce differential transcriptional responses in developing zebrafish	25
Abstract.....	26
Introduction	27
Methods	29
Results and discussion.....	34
Acknowledgements.....	49
References.....	50
Chapter 3 - AHR2 mutant reveals functional diversity of aryl hydrocarbon receptors in zebrafish	72
Abstract.....	73
Introduction	74

Results	76
Discussion	80
Materials and Methods	85
Acknowledgments	89
References.....	89
Chapter 4 - Ahr-dependent developmental toxicity and differential transcriptional profiles induced by 4-ring oxygenated PAHs	104
Abstract.....	105
Introduction	106
Materials and Methods	107
Results	112
Discussion	122
Acknowledgements.....	127
References.....	128
Chapter 5 - Discussion	168
References.....	171
Chapter 6 - Future Directions	172
Bibliography.....	174
Appendices	187

LIST OF FIGURES

<u>Figure</u>	<u>Page</u>
Figure 1-1 Schematic diagram of the aryl hydrocarbon receptor pathway	22
Figure 1-2 Zebrafish early development.....	23
Figure 1-3 Polycyclic aromatic hydrocarbon structures.....	24
Figure 2-1 PAHs induce abnormalities in developing zebrafish.....	55
Figure 2-2 Body burdens of PAH detected in embryos.....	56
Figure 2-3 Differentially expressed transcripts in PAH-exposed embryos.....	57
Figure 2-4 Direct comparison of PYR and DBT expression values	58
Figure 2-5 Comparison of AHR, RELA and JUN regulatory networks.....	59
Figure 3-1 Schematic diagram of predicted AHR2 protein in <i>ahr2</i> ^{hu3335} zebrafish	94
Figure 3-2 Fin and skeletal abnormalities in <i>ahr2</i> ^{hu3335} zebrafish	95
Figure 3-3 <i>ahr2</i> ^{hu3335} embryos are resistant to TCDD developmental abnormalities	96
Figure 3-4 <i>ahr2</i> ^{hu3335} embryos are resistant to TCDD-induced CYP induction	97
Figure 3-5 Molecular docking of TCDD and Leflunomide in zebrafish AHR isoforms.....	98
Figure 3-6 CYP1A protein expression patterns	99
Figure 4-1 Structures of BEZO, 7,12-B[a]AQ and BAA	132
Figure 4-2 Developmental toxicity of 7,12-B[a]AQ and BEZO at 120 hpf.....	133
Figure 4-3 Cyp1 expression and morphology in OPAH-exposed embryos at 48 hpf.....	135
Figure 4-4 Heatmap of transcripts significantly induced by BAA exposure at 48 hpf.....	138
Figure 4-5 Comparison of transcripts induced by BEZO and 7,12-B[a]AQ exposure	139
Figure 4-6 qRT-PCR analysis of OPAH targets in control and AHR2 morphants.....	142
Figure 4-7 Biological processes affected by BEZO and 7,12-B[a]AQ exposure.....	144
Figure 4-S1 Comparative expression across 5 PAH structures.....	149

LIST OF TABLES

<u>Table</u>	<u>Page</u>
Table 2-2 Comparison of malformations induced by PAH treatments	61
Table 2-3 Biological functions affected by PAH exposure at 24 hpf.....	62
Table 2-4 Biological functions affected by PAH exposure at 48 hpf.....	64
Table 2-4 (Continued).....	65
Table 2-4 (Continued).....	66
Table 2-S1 Primer sequences used for qRT-PCR.....	67
Table 2-S2 Percent recovery by GC-MS for PAH body burden studies.....	68
Table 2-S4 Gene expression values detected by microarray and qRT-PCR	69
Table 2-S5 Predicted transcription factors for PAH responses.....	70
Table 3-1 Primer sequences for PCR experiments	100
Table 3-2 Concentration responses for developmental effects.....	101
Table 3-3 Predicted binding energy values for zebrafish AHR2, AHR1B and AHR1A	102
Table 3-4 Summary of zebrafish AHR ligand binding, activity and expression.....	103
Table 4-1 Cross-platform comparison of expression data for genes differentially induced by PAHs	147
Table 4-2 Biological processes misregulated by OPAHs	148
Table 4-S1 Primers used for qRT-PCR analysis	150
Table 4-S2 Sequencing mapping	151
Table 4-S3 7,12-B[a]AQ significantly misexpressed transcripts	152
Table 4-S4 BEZO significantly misexpressed transcripts	160

DEDICATION

This dissertation is dedicated to my grandparents, Edith and John Artz, Walter Goodale, and Garrett and Pearl Morrell, whose love and support of all educational and creative endeavors have been incredible gifts to me.

Developmental toxicity of polycyclic aromatic hydrocarbons: defining mechanisms with systems-based transcriptional profiling

Chapter 1 - Introduction

Combustion of fuels for transportation, heating and industrial activities produces volatile and fine particulate matter emissions that decrease air quality and contribute to environmental contamination, particularly in urban areas. Polycyclic aromatic hydrocarbons (PAHs), a group of chemicals comprised of multiple fused benzene rings, are formed from these combustion (pyrogenic) processes and are components of fossil fuels (petrogenic sources). Environmental samples contain a diversity of parent PAHs, which differ in the number and arrangement of rings, as well as substituted (alkyl-, nitro-, amino-, and oxy-) structures (Ciganek et al. 2004). PAHs are contaminants of extant concern because of their carcinogenic properties and ubiquity both in high-population areas and hazardous waste sites (Schoeny 1993; Collins et al. 1998). Recently, PAH exposure has been associated with non-cancer health effects such as immune system deficiency, cardiovascular disease, low birth weight, neural tube defects and learning deficits in children (Burstyn et al. 2005; Choi et al. 2006; Hertz-Picciotto et al. 2008; Perera et al. 2009; Lee et al. 2011; Ren et al. 2011). Both pyrogenic and petrogenic PAHs are ubiquitous in the natural world, but anthropogenic activities such as automobile combustion, fossil fuel burning, oil refining and coal tar seal coating have contributed to increasing concentrations in local environments (Mahler et al. 2005; Polidori et al. 2010; Van Metre and Mahler 2010). Humans and wildlife are inveterately exposed to this family of compounds; however, certain environmental conditions, occupational settings, residential combustion practices and dietary habits are associated with increased disease risk that compelled the inclusion of 16 PAHs in the EPA list of priority pollutants (EPA 2012).

PAH-containing mixtures such as soot, coal tar mixtures and tobacco smoke have long been known carcinogens in humans (Bostrom et al. 2002). Animal studies have provided data on the ability of individual PAH structures to induce tumors, as well as shed light on the mechanisms by which PAHs induce toxicity. Carcinogenic mechanisms of Benzo(a)pyrene (BaP), a commonly detected PAH classified as a probable human carcinogen, have been well-studied in a variety of animal and cell models. In order to estimate cancer risk for environmental mixtures, which contain multiple PAH structures, the US EPA employed a Toxic Equivalency Factor (TEF) approach with available data to rank seven PAHs for

potency as carcinogens in comparison to BaP (Schoeny 1993). Since then, potency equivalency factors and risk assessments have been published for a wider range of PAHs, and the EPA has provided a draft document on the development of a relative potency factor (RPF) approach for PAH mixtures (Collins et al. 1998; Bostrom et al. 2002; EPA 2010). Assessment of health risk from PAH exposure is driven primarily by carcinogenicity data for parent PAHs, as data is limited and uncertainty surrounds the toxicity endpoints of non-carcinogenic PAHs (Jennings 2012)

Determining the contribution of individual PAHs to the increased risk of morbidity such as heart attack, asthma and low birth weight remains a daunting challenge, as the mechanisms by which PAHs may cause these effects are not defined. Though PAHs are not new to the human exposure paradigm, the recent epidemiological associations of PAH exposure with multiple diseases, as well as increased ability to detect a broad spectrum of substituted PAHs in environmental samples, is cause to consider them emerging contaminants of concern to human health. The goal of this work is to investigate biological activity and group PAHs based on proposed molecular mechanisms, providing an important step towards understanding the mechanisms by which this diverse family of chemicals affects the health of humans and wildlife.

Human exposure to PAHs

Exposure to PAHs in the general population occurs primarily via inhalation of aerosols or fine particulate matter from smoke (combustion emissions as well as cigarette), and through ingestion of smoked or grilled meats, fish and charred foods. Dermal exposures can also occur from exposure to petroleum products, and accidental ingestion of PAHs through house dust is a concern for small children (Ramesh et al. 2004). Cigarette smoke is a primary source of PAHs for individuals who smoke or are exposed regularly to second-hand smoke. Several studies have shown that for non-smoking individuals, the largest contributor to PAH exposures is the diet (Menzie et al. 1992). This is true particularly for the higher molecular weight (and more carcinogenic) PAHs, which are less volatile and associate with particulate matter. Deposition of PAH particles on crops also contributes PAHs to the diet and may be of concern for agricultural sites located near major industrial areas or roadways.

In urban environments, airborne carcinogenic PAHs are predicted to increase lung cancer risk. The low molecular weight PAHs partition into the volatile fraction of air, while higher molecular weight PAHs associated with small particulates can travel deep into the lungs (Ramirez et al. 2011). PAHs are lipophilic so upon exposure, they are readily absorbed by organisms. However, they can also be metabolized, which complicates measurement of exposure, as well as their toxic effects. PAH metabolites are detected in urine, where 1-hydroxypyrene (1-OHP) is a commonly measured biomarker of PAH exposure (Hansen et al. 2008). High 1-OHP levels are detected in coke oven and aluminum smelter workers, as well as residents living near industries with high PAH emissions, such as coal fired power plants (Hu et al. 2011). Increased levels of PAH metabolites are observed in children in polluted areas. For instance, 6-7 year old children who attended an elementary school near a heavily trafficked road in Guangzhou, China had higher levels of PAH metabolites in their urine than children who attended a school farther from large roadways (Fan et al. 2012).

Reactive PAH metabolites form adducts with DNA, RNA and protein. Adduct formation is part of the toxic mechanism of many PAHs, leading to DNA damage and mutations, but can also be used as a measure of exposure (Baird et al. 2005). Human PAH exposures can be monitored by detection of PAH-DNA adducts in white blood cells and other tissues. These biomarkers of PAH exposure have been associated with various cancers and other health endpoints such as reduced fetal growth (Kriek et al. 1998; Tang et al. 2006). Many studies estimate PAH exposure by monitoring PAHs in air, either from point sources or personal air monitors. While these studies do not determine internal PAH dose, they provide exposure information for a more complete spectrum of PAHs. Background ranges of PAHs are reported at 0.02-1.2 ng/m³ in rural areas and 0.15-19.3 ng/m³ in urban air; average total exposure in the U.S. has been estimated at 3 mg/day (Mumtaz and George 1995). Much higher PAH concentrations occur in major cities, occupational settings such as petroleum and dye industries, and in homes where low-efficiency fuels are used indoors. A number of studies associate increased cancer risk with these exposures. PAHs associated with small particulate matter measured at a school in Delhi, India were predicted to cause an Incremental Lifetime Cancer Risk of 3.18×10^{-6} , which is higher than the acceptable risk level of 10^{-6} (Jyethi et al. 2013). A study of air control measures implemented during the Beijing Olympics found that controlling emissions could substantially decrease risk of

excess cancer cases (Jia et al. 2011). Few studies have directly predicted effects of reduced emissions on other health endpoints. Research suggests, however, that reducing PAH exposure may have many other positive implications, such as reduced inflammatory and vascular disease.

Emerging concerns: cardiac function and effects during development

Multiple studies have shown increased risk of cardiac dysfunction with exposure to fine (pm 2.5) particulate matter, which contains PAHs along with many other contaminants. A smaller set of studies have specifically investigated relationships between PAHs and cardiac function. Occupational exposure to PAHs in asphalt workers is associated with an increased risk of fatal ischemic heart disease (Burstyn et al. 2005). Higher 1-OHP levels were associated with decreased heart rate variability in boilermakers and coke oven workers, suggesting an acute effect of PAH exposure on cardiac autonomic function (Lee et al. 2011; Li et al. 2012). In myocardial infarction survivors, an association was observed between exposure to particulate matter and symptoms of cardiovascular disease (Kraus et al. 2011). Analysis of National Health and Nutrition Examination Survey data also identified a higher prevalence of peripheral arterial disease in subjects with greater than average fluorene and phenanthrene metabolites (Xu et al. 2013). These smaller PAHs are generally present in the gas phase of emissions, and can be more prevalent than the larger PAHs (Bostrom et al. 2002). Reducing exposure to particulate air pollution has been shown to improve cardiovascular health of patients with heart disease (Langrish et al. 2011).

While it is difficult to discern effects of PAHs from other co-occurring contaminants in combustion-related exposures, epidemiological studies collectively suggest that PAHs affect cardiac function and increase risk of cardiac-related injury. A number of studies in animals have supported these associations. BaP exposure increased atherosclerosis and disrupted gene expression in the aortas of mice, as well as altered blood pressure patterns in rats (Jules et al. 2012; Kerley-Hamilton et al. 2012). In utero exposure to BaP also caused cardiac dysfunction later in life in rats (Jules et al. 2012). PAH exposure similarly affects cardiac function in fish, and developmental exposure to PAHs causes cardiac defects in developing zebrafish (Incardona et al. 2004). While epidemiological studies suggest that smaller PAHs (2-3 rings) are associated with cardiac toxicity, few studies in mammalian models have investigated the effects of these individual compounds on heart development. Studies in

zebrafish, however, have identified structure-related differences in the mechanisms by which these compounds affect the heart (Incardona et al. 2011).

The effects of PAH exposure on vascular function and inflammation may have increased impact during embryonic development. Adverse pregnancy outcomes, such as low birth weight, are associated with living near major roadways and in other areas with high vehicle emissions (Wilhelm et al. 2012). Oxidative stress is believed to play a role in this toxicity, and was supported by a study that showed dietary vitamin C reduced risk of reduced fetal growth associated with BaP exposure (Duarte-Salles et al. 2012). PAH exposure in rodents decreases vascularization in the placenta, and studies in fish embryos demonstrate PAHs disrupt molecular pathways important for proper heart formation (Rennie et al. 2011). While neural tube defects, asthma, and learning deficits are also associated with PAH exposure in epidemiological studies, the mechanisms by which PAHs may interfere with developmental processes, and the individual PAHs responsible, remain to be elucidated (Perera et al. 2009; Ren et al. 2011).

Mechanisms of PAH toxicity: activation of the aryl hydrocarbon receptor

PAHs exhibit varied non-genotoxic activity, which can not only contribute to their carcinogenicity but also mediate multiple other toxic effects. Some PAHs, including BaP, can cause toxicity by binding the aryl hydrocarbon receptor (AHR), a ligand-activated member of the basic helix-loop-helix Per-ARNT-Sim (bHLH-PAS) family of transcription factors. Ligand binding induces dimerization with the Ah receptor nuclear translocator (ARNT), translocation to the nucleus, and alteration of gene transcription, including cytochrome P450 phase 1 (*CYP1A*, *CYP1B1*) and phase 2 (*UGT1A6*, *ALDH3A1*) metabolizing enzymes (Figure 1)(Nebert et al. 2000; Sartor et al. 2009). While parent PAHs are generally unreactive, metabolism by CYP1A and other metabolizing enzymes forms more reactive metabolites such as PAH epoxides and radical cation intermediates (Cavalieri and Rogan 1995). These reactive compounds can cause cellular damage by forming DNA and protein adducts. Additionally, they can activate redox-responsive genes containing antioxidant response elements (AREs), including phase II metabolizing enzymes (Bock 2012). Further metabolism by hydroxylases forms hydroxy-PAHs, and glucuronidases and sulfotransferases conjugate these oxygenated PAHs, facilitating their excretion. Because of this complex process involving multiple intermediates, metabolism induced by AHR

activation can increase toxicity or allow for excretion, depending on the PAH structure. In the case of BaP, carcinogenicity in mice is dependent on a functional AHR (Shimizu et al. 2000). The AHR pathway and cytochrome P450 enzymes are conserved among vertebrates. Differences exist, however, in affinity of compounds for AHRs between species, as well as within populations, which affects their carcinogenicity and potency as toxicants (Hahn 2002; Wirgin et al. 2011). The work presented in this thesis focuses on non-carcinogenic mechanisms. However, the large body of research on mechanisms by which BaP interacts with the AHR to cause cancer has contributed greatly to our understanding of AHR function. While the molecular signaling pathways by which BaP induces its diverse array of toxicological effects are not fully elucidated, BaP toxicity is known to be mediated by AHR activation in many species. Beyond this, the ability of multiple CYP enzymes, which vary between tissue types, individuals and species, to metabolize PAHs creates a complex array of toxicological profiles.

In addition to toxicological effects caused via AHR induction and the formation of reactive PAH intermediates, sustained activation of the AHR leads to a number of other adverse effects. These have been well-characterized in studies with halogenated hydrocarbons, such as 2,3,7,8-tetrachlorodibenzo-*p*-dioxin (TCDD) and polychlorinated biphenyls (PCBs), which have high affinity for the AHR but are not readily metabolized. AHR activation during development causes teratogenic effects in rodents and fish, which include malformations in the heart and jaw. AHR activation additionally causes a wide range of neurologic, immune and reproductive effects (reviewed in (White and Birnbaum 2009)). A TEF approach has been employed by the World Health Organization (WHO) to rank the potency of halogenated hydrocarbons for assessment of health risk to humans and wildlife (Van den Berg et al. 2006). In contrast to the TEFs for PAHs, which are based on carcinogenic potency, TEFs for dioxin-like compounds are determined from a variety of AHR-mediated endpoints, including chronic toxicity, enzyme induction, tumor promotion and lethality, and generally correlate with ligand affinity for the receptor.

Because AHR activation by dioxin-like compounds leads to transcriptional activation of CYP1A, the enzyme has been widely used as a biomarker of AHR activation. This tool has been particularly useful for investigating exposure to dioxin-like compounds in wild

populations (Hahn 2002; Sarkar et al. 2006; Jensen et al. 2010). As interactions of the AHR such as ligand and DNA binding have been characterized, many other assays have also been developed to identify AHR-activating compounds. Several assays screen for AHR activators using dioxin responsive elements (DREs) in promoters driving reporter genes such as luciferase or GFP. The chemical activated luciferase gene expression (CALUX) assay is widely used to screen compounds for AHR activation activity (Murk et al. 1996). Several *in silico* models of the AHR ligand binding pocket have also been created to predict binding and screen for alternative AHR ligands. For example, a chemical library screen and an *in silico* AHR molecular docking study identified leflunomide, a rheumatoid arthritis drug, as an AHR agonist, which was confirmed in human, mouse and zebrafish (O'Donnell et al. 2010). PAHs that have high affinity for the AHR induce AHR-mediated toxicological effects similar to those caused by exposure to dioxin-like compounds. Because of their structural diversity and aforementioned metabolism, however, PAHs have a wide range of additional biological activities that complicate the interpretation of CYP1A activity as a biomarker for exposure and toxic effects. Some PAHs, such as fluoranthene, inhibit CYP1A, and can lead to synergistic toxicity in fish embryos when combined with other PAHs (Billiard et al. 2006; Timme-Laragy et al. 2007). Other conditions, such as hypoxia, can also inhibit CYP1A induction (Fleming and Di Giulio 2011). Finally, CYP1A induction can be elevated by PAHs (such as chrysene) in the absence of other signs of toxicity (Incardona et al. 2006). Because of these complex interactions, AHR affinity on its own is not a sufficient predictor of PAH toxicity.

Effects of PAH exposure on fish development

PAH exposure causes developmental abnormalities in fish embryos, including pericardial and yolk sac edema, disrupted cardiac function, craniofacial and spinal malformations, anemia and reduced growth, which have been described in many studies addressing toxicity of PAH mixtures to wild fish populations (Barron et al. 2004). Many of these effects are similar to those described for planar halogenated compounds (PCBs). Fish are exposed to high levels of PAHs from events such as oil spills, from runoff, and from sites contaminated by industrial activity. Research on fish populations exposed to PAHs has contributed to our understanding of the AHR, its crosstalk with other signaling pathways and the complex mechanisms of PAH toxicity. While dioxin-like compounds are toxic to marine life, there are

several examples of fish populations adapted to live in heavily contaminated sites (Nacci et al. 2009; Bugel et al. 2010). These phenotypes provide fascinating information about interactions between pathways that facilitate adaptation to the external environment; many of the adaptive mechanisms have yet to be fully determined. A study of Atlantic tomcod in the Hudson River found that populations resistant to contaminants had a deletion in AHR2 that rendered it non-functional (Wirgin et al. 2011). Atlantic killifish from a heavily contaminated wood treatment facility site on the Elizabeth River, VA are exposed to high concentrations of PAHs and exhibit higher levels of DNA damage compared to fish from a reference site with low PAH levels (Wills et al. 2010; Jung et al. 2011). Their embryos are resistant to developmental defects induced by PAHs and PCBs, and their adaptive phenotype highlights the complexity of AHR regulation. PCB 126, a dioxin-like compound that is not readily metabolized, does not induce Cyp1a expression in these embryos, while PAHs BaP and benzo(k)fluoranthene (BkF) induce Cyp1a (though at lower levels than reference site embryos). This suggests that ligands can interact differently with the AHR and/or other transcription factors to induce Cyp1a expression both in the presence and absence of overt toxicity.

Research on the effects of crude and weathered oil in various fish species has also contributed to our understanding of biological effects of PAHs. In adult fish, narcosis has been described as a toxicological endpoint of exposure to low molecular weight PAHs, and is characterized by loss of balance, lethargy and decreased respiration which is reversible but can result in death during prolonged exposure to high concentrations (Vanwezel and Opperhuizen 1995). In fish embryos, however, three ring PAHs disrupt heart function, causing arrhythmia and eventual heart failure (Incardona et al. 2004). Studies from a number of labs have demonstrated that PAHs induce malformations in embryos via different mechanisms, depending on their structures. 3-ring PAHs induce cardiac toxicity with a suggested mechanism of ion channel disruption (Incardona et al. 2004). Many 4 and 5-ring PAHs bind the aryl hydrocarbon receptor, causing cardiac toxicity along with other effects (Incardona et al. 2006). Because of the different mechanisms, predicting toxicity of PAH mixtures remains a challenge. A need for studies that clarify the biological effects of low molecular weight PAHs has been recognized in order to better understand the effect of PAH contamination in aquatic ecosystems (Hylland 2006). Characterizing the different

mechanisms of PAH developmental toxicity is an important first step in predicting toxicity of mixtures, both in aquatic systems and human populations.

Discovering endogenous functions of the AHR

As previously discussed, the AHR pathway has been well-studied and plays a central role in the toxicological mechanisms of many PAHs. Despite over 30 years since its discovery as the receptor responsible for mediating TCDD toxicity, characterization of endogenous functions of the receptor remains a rapidly developing area of research. PAS (Per-ARNT-Sim) family transcription factors, of which the AHR is a member, are involved in a variety of physiological processes including circadian rhythms and oxygen sensing (McIntosh et al. 2010). The AHR dimerization partner required for transcriptional activation, ARNT (also known as Hif1b), is a member of the Hypoxia Inducible Factor (HIF) family of proteins. AHR binding partners such as hsp90 and p300 also interact with other transcription factors (Beischlag et al. 2008). Many studies have demonstrated AHR crosstalk with other transcriptional regulators such as NFkB, ER and GCR via direct or indirect mechanisms (Puga et al. 2009). A handful of studies have also shown AHR dimerization with other proteins, such as klf6, and activation of other downstream genes via an alternative recognition sequence (Wilson et al. 2013). This propensity to interact with other transcription factors supports the notion that AHR-mediated developmental toxicity may be, at least in part, caused by disruption of endogenous functions mediated in concert with other interacting proteins. This is supported by studies that have demonstrated that *Cyp1a* and other metabolic genes highly induced by AHR are not responsible for the toxic effects of TCDD (Antkiewicz et al. 2006). The means by which AHR activation leads to downregulation of genes, in particular, is not well-defined. A study of transcriptional binding of the AHR with and without exogenous ligand identified a large number of genes involved in developmental and vascular processes that were bound by the AHR in the absence of TCDD and BaP. Upon ligand binding, the targets shifted to genes involved in xenobiotic metabolism (Sartor et al. 2009). Along the same lines, recent studies have identified roles for the AHR in a myriad of processes, including progenitor cell expansion and differentiation (Smith et al. 2013). It would appear that many functions of the AHR in normal development have yet to be discovered.

AHR knockout mouse strains developed by three different groups illustrate the importance of the AHR in normal liver development and immune function, and continue to expand understanding of the receptor's role in both toxicological responses and normal physiology (Fernandez-Salguero et al. 1995; Schmidt et al. 1996; Lahvis et al. 2005). Because their development can be observed non-invasively, fish have provided much insight into mechanisms of AHR-mediated toxicity during development. Three AHR isoforms have been identified in zebrafish: AHR1A, AHR1B, and AHR2 (Tanguay et al. 1999; Andreassen et al. 2002; Hahn 2002; Karchner et al. 2005). Numerous studies with known AHR ligands, however, have identified AHR2 as the primary mediator of early life stage toxicological effects in zebrafish (Prasch et al. 2003; Teraoka et al. 2003; Antkiewicz et al. 2006). Other genes, including *foxq1a* and *sox9b* have been uncovered as mediators of TCDD-induced effects on jaw and heart development (Xiong et al. 2008; Planchart and Mattingly 2010; Hofsteen et al. 2013). The ability to transiently knock down genes in zebrafish has enabled study of the roles of these genes during development. Knockdown of AHR2 has also highlighted crosstalk between the AHR pathway and NRF2, which provides protection against oxidative stress induced by PAHs (Timme-Laragy et al. 2009). While AHR2 knockdown is able to rescue TCDD-induced toxicity, it does not completely prevent Ahr2 activity, and is a transient effect. An AHR2 knockout zebrafish would therefore greatly expand capability to investigate biological functions of the receptor during development and throughout the lifespan.

The zebrafish model

The zebrafish is an excellent system in which to pursue mechanisms of toxicity during development, which is rapid. By 5 days post-fertilization all organ systems are functional (Figure 2)(Kimmel et al. 1995; Sali 2012). Development external to the mother allows for non-invasive observation and imaging over the course of development. Additionally, environmental factors such as chemical exposure can be meticulously controlled. A fully sequenced genome with ever-increasing annotation allows for investigation of genetic targets of interest. Genes can be specifically targeted with antisense oligos (morpholinos) to transiently knock down expression during development. Many transgenic zebrafish lines are available for studies. The small size of zebrafish makes them adaptable to development in 96 well plates and amenable for large scale genetic screens. Forward and reverse genetic

screens have been employed to identify thousands of mutants with specific mutations and phenotypes. More recently, zinc finger and TALEN technologies have enabled the creation of targeted knockouts in zebrafish. Chemical screens can be conducted in zebrafish with amounts of chemical comparable to cell-culture studies, allowing for rapid screening of large numbers of chemicals *in vivo*. Recent development of high-throughput technology has enabled much-needed investigation of compounds that are detected in environmental samples but lack toxicity data.

Substituted PAHs: adding complexity to toxicity evaluation

PAHs in the environment exist not only as parent PAH structures, but as substituted derivatives such as oxygenated PAHs (OPAHs). Because substitutions occur via both biotic and abiotic processes, it is expected that concentrations of substituted PAHs may be higher than parent PAHs under certain conditions. As advances in detection methods allow for quantification of a wider range of compounds that constitute exposure paradigms, there is an accompanying need for toxicity data in order to assess health risks. The large number of substituted PAH structures poses a significant challenge; identifying groups of structures that behave similarly would help the prioritization of studies to determine toxicological mechanisms of these compounds, and eventually improve predictive capability for modeling toxicity of PAHs and mixtures. Our laboratory conducted a toxicity screen for developmental toxicity and Ahr activation of 38 oxygenated PAHs (OPAHs) in zebrafish embryos (Knecht et al. 2013). Embryos were statically exposed from 6 to 120 hours post fertilization (hpf) to 0.8 – 500 μ M concentrations of OPAH in embryo media, then screened for malformations. For each compound, embryos exposed to a concentration that caused ~80% malformations but not mortality were examined for Cyp1a expression with immunohistochemistry. We found that OPAHs induced toxicity at a wide range of concentrations. Some observations could be made based on structure; several quinones (1,4-naphthoquinone, phenanthrene-quinone, 1,2-naphthoquinone) had steep dose-response curves and caused mortality at concentrations < 4 μ M. Cyp1a expression was not observed at these concentrations (Knecht et al. 2013). A substantial group of compounds caused malformations such as pericardial edema and yolk sac edema at concentrations < 20 μ M. Some of these, such as benzo(a)fluorenone, phenanthrene-1,4-dione, and benz(a)anthracene-7,12-dione, induced Cyp1a expression in the vasculature. Many,

including 1,9-benz-10-anthrone and 9-hydroxybenzo(a)pyrene, induced malformations but no Cyp1a expression. A large number of PAHs did not induce malformations below 20 μ M. Of these, some induced Cyp1a expression that was specifically expressed in the liver at higher concentrations. We also observed interesting patterns of Cyp1a expression in the lateral line of zebrafish exposed to oxygenated naphthalenes. The differential Cyp1a expression patterns observed with OPAHs that were similarly toxic suggested differential involvement of the aryl hydrocarbon receptor.

Categorizing compounds, predicting PAH toxicity

In the studies presented here, I used whole genome microarrays to identify transcriptional profiles of developmental toxicity induced by three parent PAHs and two OPAHs in zebrafish. Differential proposed mechanisms of dibenzothiophene (DBT), pyrene (PYR) and benz(a)anthracene (BAA) – induced developmental toxicity in zebrafish embryos are discussed in Chapter 2. I examined PAH body burdens following exposures and found large differences in the amount of PAH in embryos. Measuring uptake was important for discerning dose-dependent differences from biological mechanisms. Expanding the investigation of different PAH structures, I chose two 4-ring OPAHs, benz(a)anthracene-7,12-dione (7,12-B[a]AQ) and 1,9-benz-10-anthrone (BEZO) from the OPAH toxicity screen conducted in our laboratory to further investigate transcriptional profiles. 7,12-B[a]AQ is an oxygenated derivative of parent PAH BAA, while BEZO is a mono-oxygenated PAH with a different ring arrangement. In Chapter 4, I investigated the role of AHR2 in mediating the toxicity of these two compounds.

A handful of other studies have compared transcriptional profiles across several PAH structures in other model systems, with a similar goal of identifying biomarkers of exposure and increasing toxicity prediction capability for this class of compounds. A study of gene expression changes induced by 3-4 ring PAHs in leukemia (THP-1) cells identified groups of PAHs that induced similar gene expression profiles. Predictor genes were identified, which included calcium binding proteins, transcription factors, immune response and genes with oxidoreductase activity (Wan et al. 2008). In a similar study in liver hepatoma cells (HepG2) gene expression profiles were determined from cells exposed to 2-5 ring PAHs (Song et al. 2012). Transcriptional signatures were compared between known carcinogens and non-carcinogens. Interestingly, clustering did not predict known carcinogenicity; however,

known carcinogens induced genes involved in oxidative stress, while non-carcinogenic PAHs such as fluoranthene did not. An interesting study of human lymphocytes identified a small number of genes that were significantly differentially expressed in PAH-exposed coke oven workers (Wu et al. 2011). These genes were involved in metal ion binding and transport, and included myosin XVB and solute carrier family 25 member 34. These studies have begun to identify biomarkers and propose mechanisms for diverse PAH structures, including the non-genotoxic PAHs. However, the majority of these studies have been carried out in cell lines, and none have explored PAH toxicity in developing embryos. Our *in vivo* approach provides a unique set of data that can be used to group PAHs based on a large set of genes that are important during early development. The availability of an annotated genome and high homology of genes between vertebrates allows us to compare biomarkers and eventually validate across species. Global transcriptional analysis of PAH exposure in multiple systems will create a powerful dataset from which to identify biological mechanisms associated with structural differences. The overarching objective of the studies presented here is to employ transcriptional profiling techniques to identify potential differential mechanisms by which PAHs induce developmental toxicity, and to further characterize the role of the aryl hydrocarbon receptor in biological pathways that are disrupted by PAH exposure.

Summary and study objectives

We hypothesized that PAHs induce developmental effects in embryos via distinct mechanisms that could be identified by comparative investigation of global changes in transcription that occur following chemical exposure. We compared the transcriptional profiles of 5 PAH structures that induce different malformation profiles in developing zebrafish (Figure 3). In Chapter 2, we used a whole genome mRNA microarray to compare parent PAHs which differentially activate the aryl hydrocarbon receptor, DBT, PYR and BAA. Using concentrations that induced malformations but not mortality, we identified genes that were differentially regulated over time and in response to the three PAH structures. PAH body burdens were analyzed at both time points, which was important for discerning dose-related differences from those that represented unique molecular mechanisms. By analyzing functional roles of misregulated genes and their predicted regulatory transcription factors, we showed that the BAA response (AHR activated) could be

distinguished from regulatory networks disrupted by DBT and PYR exposure (AHR not activated).

In chapter 3, we developed a zebrafish line with a mutation in *ahr2* to enable deeper mechanistic investigation of the role of the AHR in PAH-induced toxicity. We characterized AHR activity in the mutant line using TCDD and leflunomide as toxicological probes to investigate function, ligand binding and Cyp1a induction patterns of paralogues AHR2, AHR1A and AHR1B. In these studies, I determined that *ahr2*^{hu3335} zebrafish are functionally null. We then further explored function of the other zebrafish AHR paralogues, and demonstrated differential ligand binding and Cyp1a expression patterns mediated by the three receptors.

Because the *ahr2*^{hu3335} line was developed from a founder identified in a screen of a mutant library generated by random mutagenesis (TILLING, Targeting Induced Local Lesions In Genomes), the line required multiple generations of outcrosses to reduce background mutations. Embryo production and quality was variable over the first three outcrosses, and limited our ability to conduct reliable studies of PAH-induced toxicity in the *ahr2*^{hu3335} line. We investigated BAA, DBT and PYR-induced toxicity in *ahr2*^{hu3335} and *ahr2*⁺ zebrafish, and confirmed the differential involvement of the AHR in mediating toxicological effects (Appendix 1). Background malformations in these experiments were higher than normal, however, so we utilized an AHR2 morpholino to knock down expression in the remaining studies in this dissertation.

While BAA induced toxicity dependent on the AHR, DBT and PYR caused toxicity via other mechanisms. We conducted preliminary characterization of other phenotypes associated with these PAHs, with the goal of identifying more sensitive endpoints to assess for toxic effects. We observed a unique hyperactive phenotype in PYR-exposed embryos, and investigated this response over a wider concentration range. We also investigated whether localized inflammation could be visualized in the transgenic *mpx:gfp* zebrafish line, which expresses green fluorescent protein (driven by myeloid-specific peroxidase promoter) in neutrophils. Preliminary data from these studies are presented in Appendix 2.

In Chapter 4, We explored the role of the AHR in mediating toxicity induced by 4-ring OPAHs BEZO and 7,12-B[a]AQ. We showed that despite very different Cyp1a expression profiles, both BEZO and 7,12-B[a]AQ induced toxicity via AHR2. We used RNA-seq to compare transcriptional profiles induced by the OPAHs at 48 hpf, and identified potential novel targets of the AHR as well as intriguing mechanistic differences by which the AHR may interact with other transcription factors to differentially regulated target genes. We additionally compared sets of transcripts across both platforms (microarray and RNA-seq), and identified patterns of expression across all 5 PAH structures.

Together these studies show that PAHs act through multiple mechanisms that differentially involve the AHR to induce developmental toxicity. We identified clusters of transcripts involved in mechanisms, which can be further pursued to unravel molecular targets of PAHs, as well as be utilized as biomarkers to begin to predict effects of additional PAH structures. These studies demonstrate the power of transcriptomics approaches for comparing toxicity pathways of structurally-related compounds, identifying biomarkers of toxic effects, and generating hypotheses to further mechanistic understanding of a large family of compounds

References

- Andreasen, E. A., M. E. Hahn, et al. (2002). "The zebrafish (*Danio rerio*) aryl hydrocarbon receptor type 1 is a novel vertebrate receptor." *Mol Pharmacol* **62**(2): 234-249.
- Antkiewicz, D. S., R. E. Peterson, et al. (2006). "Blocking expression of AHR2 and ARNT1 in zebrafish larvae protects against cardiac toxicity of 2,3,7,8-tetrachlorodibenzo-p-dioxin." *Toxicol Sci* **94**(1): 175-182.
- Baird, W. M., L. A. Hooven, et al. (2005). "Carcinogenic polycyclic aromatic hydrocarbon-DNA adducts and mechanism of action." *Environ Mol Mutagen* **45**(2-3): 106-114.
- Barron, M. G., M. G. Carls, et al. (2004). "Evaluation of fish early life-stage toxicity models of chronic embryonic exposures to complex polycyclic aromatic hydrocarbon mixtures." *Toxicol Sci* **78**(1): 60-67.
- Beischlag, T. V., J. Luis Morales, et al. (2008). "The aryl hydrocarbon receptor complex and the control of gene expression." *Crit Rev Eukaryot Gene Expr* **18**(3): 207-250.
- Billiard, S. M., A. R. Timme-Laragy, et al. (2006). "The role of the aryl hydrocarbon receptor pathway in mediating synergistic developmental toxicity of polycyclic aromatic hydrocarbons to zebrafish." *Toxicol Sci* **92**(2): 526-536.
- Bock, K. W. (2012). "Ah receptor- and Nrf2-gene battery members: Modulators of quinone-mediated oxidative and endoplasmic reticulum stress." *Biochem Pharmacol* **83**(7): 833-838.

- Bostrom, C. E., P. Gerde, et al. (2002). "Cancer risk assessment, indicators, and guidelines for polycyclic aromatic hydrocarbons in the ambient air." Environ Health Perspect **110 Suppl 3**: 451-488.
- Bugel, S. M., L. A. White, et al. (2010). "Impaired reproductive health of killifish (*Fundulus heteroclitus*) inhabiting Newark Bay, NJ, a chronically contaminated estuary." Aquat Toxicol **96**(3): 182-193.
- Burstyn, I., H. Kromhout, et al. (2005). "Polycyclic aromatic hydrocarbons and fatal ischemic heart disease." Epidemiology **16**(6): 744-750.
- Cavalieri, E. L. and E. G. Rogan (1995). "Central role of radical cations in metabolic activation of polycyclic aromatic hydrocarbons." Xenobiotica **25**(7): 677-688.
- Choi, H., W. Jedrychowski, et al. (2006). "International studies of prenatal exposure to polycyclic aromatic hydrocarbons and fetal growth." Environ Health Perspect **114**(11): 1744-1750.
- Ciganek, M., J. Neca, et al. (2004). "A combined chemical and bioassay analysis of traffic-emitted polycyclic aromatic hydrocarbons." Sci Total Environ **334-335**: 141-148.
- Collins, J. F., J. P. Brown, et al. (1998). "Potency equivalency factors for some polycyclic aromatic hydrocarbons and polycyclic aromatic hydrocarbon derivatives." Regul Toxicol Pharmacol **28**(1): 45-54.
- Duarte-Salles, T., M. A. Mendez, et al. (2012). "Dietary benzo(a)pyrene and fetal growth: effect modification by vitamin C intake and glutathione S-transferase P1 polymorphism." Environ Int **45**: 1-8.
- EPA, U. (2010). Development of a relative potency factor (RPF) approach for polycyclic aromatic hydrocarbon (PAH) mixtures (External review draft). U. S. E. P. Agency. Washington, DC.
- EPA, U. (2012). "Integrated Risk Information System." from <http://www.epa.gov/iris/>.
- Fan, R., D. Wang, et al. (2012). "Preliminary study of children's exposure to PAHs and its association with 8-hydroxy-2'-deoxyguanosine in Guangzhou, China." Environ Int **42**: 53-58.
- Fernandez-Salguero, P., T. Pineau, et al. (1995). "Immune system impairment and hepatic fibrosis in mice lacking the dioxin-binding Ah receptor." Science **268**(5211): 722-726.
- Fleming, C. R. and R. T. Di Giulio (2011). "The role of CYP1A inhibition in the embryotoxic interactions between hypoxia and polycyclic aromatic hydrocarbons (PAHs) and PAH mixtures in zebrafish (*Danio rerio*)." Ecotoxicology **20**(6): 1300-1314.
- Hahn, M. E. (2002). "Aryl hydrocarbon receptors: diversity and evolution." Chem Biol Interact **141**(1-2): 131-160.
- Hahn, M. E. (2002). "Biomarkers and bioassays for detecting dioxin-like compounds in the marine environment." Sci Total Environ **289**(1-3): 49-69.
- Hansen, A. M., L. Mathiesen, et al. (2008). "Urinary 1-hydroxypyrene (1-HP) in environmental and occupational studies--a review." Int J Hyg Environ Health **211**(5-6): 471-503.
- Hertz-Picciotto, I., H. Y. Park, et al. (2008). "Prenatal exposures to persistent and non-persistent organic compounds and effects on immune system development." Basic Clin Pharmacol Toxicol **102**(2): 146-154.
- Hofsteen, P., J. Plavicki, et al. (2013). "Sox9b is Required for Epicardium Formation and Plays a Role in TCDD-induced Heart Malformation in Zebrafish." Mol Pharmacol.

- Hu, S. W., Y. J. Chan, et al. (2011). "Urinary levels of 1-hydroxypyrene in children residing near a coal-fired power plant." *Environ Res* **111**(8): 1185-1191.
- Hylland, K. (2006). "Polycyclic aromatic hydrocarbon (PAH) ecotoxicology in marine ecosystems." *J Toxicol Environ Health A* **69**(1-2): 109-123.
- Incardona, J. P., T. K. Collier, et al. (2004). "Defects in cardiac function precede morphological abnormalities in fish embryos exposed to polycyclic aromatic hydrocarbons." *Toxicol Appl Pharmacol* **196**(2): 191-205.
- Incardona, J. P., H. L. Day, et al. (2006). "Developmental toxicity of 4-ring polycyclic aromatic hydrocarbons in zebrafish is differentially dependent on AH receptor isoforms and hepatic cytochrome P4501A metabolism." *Toxicol Appl Pharmacol* **217**(3): 308-321.
- Incardona, J. P., T. L. Linbo, et al. (2011). "Cardiac toxicity of 5-ring polycyclic aromatic hydrocarbons is differentially dependent on the aryl hydrocarbon receptor 2 isoform during zebrafish development." *Toxicol Appl Pharmacol* **257**(2): 242-249.
- Jennings, A. A. (2012). "Worldwide regulatory guidance values for surface soil exposure to noncarcinogenic polycyclic aromatic hydrocarbons." *J Environ Manage* **101**: 173-190.
- Jensen, B. A., C. M. Reddy, et al. (2010). "Developing tools for risk assessment in protected species: Relative potencies inferred from competitive binding of halogenated aromatic hydrocarbons to aryl hydrocarbon receptors from beluga (*Delphinapterus leucas*) and mouse." *Aquat Toxicol* **100**(3): 238-245.
- Jia, Y., D. Stone, et al. (2011). "Estimated reduction in cancer risk due to PAH exposures if source control measures during the 2008 Beijing Olympics were sustained." *Environ Health Perspect* **119**(6): 815-820.
- Jules, G. E., S. Pratap, et al. (2012). "In utero exposure to benzo(a)pyrene predisposes offspring to cardiovascular dysfunction in later-life." *Toxicology*.
- Jung, D., C. W. Matson, et al. (2011). "Genotoxicity in Atlantic killifish (*Fundulus heteroclitus*) from a PAH-contaminated Superfund site on the Elizabeth River, Virginia." *Ecotoxicology* **20**(8): 1890-1899.
- Jyethi, D. S., P. S. Khillare, et al. (2013). "Risk assessment of inhalation exposure to polycyclic aromatic hydrocarbons in school children." *Environ Sci Pollut Res Int*.
- Karchner, S. I., D. G. Franks, et al. (2005). "AHR1B, a new functional aryl hydrocarbon receptor in zebrafish: tandem arrangement of *ahr1b* and *ahr2* genes." *Biochem J* **392**(Pt 1): 153-161.
- Kerley-Hamilton, J. S., H. W. Trask, et al. (2012). "Inherent and Benzo[a]pyrene-Induced Differential Aryl Hydrocarbon Receptor Signaling Greatly Affects Life Span, Atherosclerosis, Cardiac Gene Expression, and Body and Heart Growth in Mice." *Toxicol Sci* **126**(2): 391-404.
- Kimmel, C. B., W. W. Ballard, et al. (1995). "Stages of embryonic development of the zebrafish." *Dev Dyn* **203**(3): 253-310.
- Knecht, A. L., B. C. Goodale, et al. (2013). "Comparative developmental toxicity of environmentally relevant oxygenated PAHs." *Toxicol Appl Pharmacol*.
- Kraus, U., S. Breitner, et al. (2011). "Particle-associated organic compounds and symptoms in myocardial infarction survivors." *Inhalation Toxicology* **23**(7): 431-447.
- Kriek, E., M. Rojas, et al. (1998). "Polycyclic aromatic hydrocarbon-DNA adducts in humans: relevance as biomarkers for exposure and cancer risk." *Mutat Res* **400**(1-2): 215-231.

- Lahvis, G. P., R. W. Pyzalski, et al. (2005). "The aryl hydrocarbon receptor is required for developmental closure of the ductus venosus in the neonatal mouse." Mol Pharmacol **67**(3): 714-720.
- Langrish, J. P., X. Li, et al. (2011). "Reducing personal exposure to particulate air pollution improves cardiovascular health in patients with coronary heart disease." Environ Health Perspect **120**(3): 367-372.
- Lee, M. S., S. Magari, et al. (2011). "Cardiac autonomic dysfunction from occupational exposure to polycyclic aromatic hydrocarbons." Occup Environ Med **68**(7): 474-478.
- Li, X., Y. Feng, et al. (2012). "The dose-response decrease in heart rate variability: any association with the metabolites of polycyclic aromatic hydrocarbons in coke oven workers?" PLoS One **7**(9): e44562.
- Mahler, B. J., P. C. Van Metre, et al. (2005). "Parking lot sealcoat: an unrecognized source of urban polycyclic aromatic hydrocarbons." Environ Sci Technol **39**(15): 5560-5566.
- McIntosh, B. E., J. B. Hogenesch, et al. (2010). "Mammalian Per-Arnt-Sim proteins in environmental adaptation." Annu Rev Physiol **72**: 625-645.
- Menzie, C. A., B. B. Potocki, et al. (1992). "Exposure to Carcinogenic Pahs in the Environment." Environmental Science & Technology **26**(7): 1278-1284.
- Mumtaz, M. and J. George (1995). Toxicological profile for polycyclic aromatic hydrocarbons (PAHs). Atlanta, GA, Agency for Toxic Substances and Disease Registry, U.S. Department of Health and Human Services.
- Murk, A. J., J. Legler, et al. (1996). "Chemical-activated luciferase gene expression (CALUX): a novel in vitro bioassay for Ah receptor active compounds in sediments and pore water." Fundam Appl Toxicol **33**(1): 149-160.
- Nacci, D., M. Huber, et al. (2009). "Evolution of tolerance to PCBs and susceptibility to a bacterial pathogen (*Vibrio harveyi*) in Atlantic killifish (*Fundulus heteroclitus*) from New Bedford (MA, USA) harbor." Environ Pollut **157**(3): 857-864.
- Nebert, D. W., A. L. Roe, et al. (2000). "Role of the aromatic hydrocarbon receptor and [Ah] gene battery in the oxidative stress response, cell cycle control, and apoptosis." Biochem Pharmacol **59**(1): 65-85.
- O'Donnell, E. F., K. S. Saili, et al. (2010). "The anti-inflammatory drug leflunomide is an agonist of the aryl hydrocarbon receptor." PLoS One **5**(10).
- Perera, F., W. Y. Tang, et al. (2009). "Relation of DNA methylation of 5'-CpG island of ACSL3 to transplacental exposure to airborne polycyclic aromatic hydrocarbons and childhood asthma." PLoS One **4**(2): e4488.
- Perera, F. P., Z. Li, et al. (2009). "Prenatal Airborne Polycyclic Aromatic Hydrocarbon Exposure and Child IQ at Age 5 Years." Pediatrics.
- Planchart, A. and C. J. Mattingly (2010). "2,3,7,8-Tetrachlorodibenzo-p-dioxin upregulates FoxQ1b in zebrafish jaw primordium." Chem Res Toxicol **23**(3): 480-487.
- Polidori, A., J. Kwon, et al. (2010). "Source proximity and residential outdoor concentrations of PM(2.5), OC, EC, and PAHs." J Expo Sci Environ Epidemiol **20**(5): 457-468.
- Prasch, A. L., H. Teraoka, et al. (2003). "Aryl hydrocarbon receptor 2 mediates 2,3,7,8-tetrachlorodibenzo-p-dioxin developmental toxicity in zebrafish." Toxicol Sci **76**(1): 138-150.
- Puga, A., C. Ma, et al. (2009). "The aryl hydrocarbon receptor cross-talks with multiple signal transduction pathways." Biochem Pharmacol **77**(4): 713-722.
- Ramesh, A., S. A. Walker, et al. (2004). "Bioavailability and risk assessment of orally ingested polycyclic aromatic hydrocarbons." Int J Toxicol **23**(5): 301-333.

- Ramirez, N., A. Cuadras, et al. (2011). "Risk assessment related to atmospheric polycyclic aromatic hydrocarbons in gas and particle phases near industrial sites." Environ Health Perspect **119**(8): 1110-1116.
- Ren, A., X. Qiu, et al. (2011). "Association of selected persistent organic pollutants in the placenta with the risk of neural tube defects." Proc Natl Acad Sci U S A **108**(31): 12770-12775.
- Rennie, M. Y., J. Detmar, et al. (2011). "Vessel tortuosity and reduced vascularization in the fetoplacental arterial tree after maternal exposure to polycyclic aromatic hydrocarbons." Am J Physiol Heart Circ Physiol **300**(2): H675-684.
- Saili, K. S. (2012). Developmental neurobehavioral toxicity of bisphenol A in zebrafish (Danio rerio) [electronic resource] / by Katherine Schletz Saili. Corvallis, Or. :, Oregon State University.
- Sarkar, A., D. Ray, et al. (2006). "Molecular Biomarkers: their significance and application in marine pollution monitoring." Ecotoxicology **15**(4): 333-340.
- Sartor, M. A., M. Schnekenburger, et al. (2009). "Genomewide analysis of aryl hydrocarbon receptor binding targets reveals an extensive array of gene clusters that control morphogenetic and developmental programs." Environ Health Perspect **117**(7): 1139-1146.
- Schmidt, J. V., G. H. Su, et al. (1996). "Characterization of a murine Ahr null allele: involvement of the Ah receptor in hepatic growth and development." Proc Natl Acad Sci U S A **93**(13): 6731-6736.
- Schoeny, R. a. K. P. (1993). Provisional guidance for quantitative risk assessment of polycyclic aromatic hydrocarbons. U. S. E. P. Agency. Washington, DC.
- Shimizu, Y., Y. Nakatsuru, et al. (2000). "Benzo[a]pyrene carcinogenicity is lost in mice lacking the aryl hydrocarbon receptor." Proc Natl Acad Sci U S A **97**(2): 779-782.
- Smith, B. W., S. S. Rozelle, et al. (2013). "The aryl hydrocarbon receptor directs hematopoietic progenitor cell expansion and differentiation." Blood.
- Song, M. K., M. Song, et al. (2012). "Identification of molecular signatures predicting the carcinogenicity of polycyclic aromatic hydrocarbons (PAHs)." Toxicol Lett **212**(1): 18-28.
- Tang, D., T. Y. Li, et al. (2006). "PAH-DNA adducts in cord blood and fetal and child development in a Chinese cohort." Environ Health Perspect **114**(8): 1297-1300.
- Tanguay, R. L., C. C. Abnet, et al. (1999). "Cloning and characterization of the zebrafish (Danio rerio) aryl hydrocarbon receptor." Biochim Biophys Acta **1444**(1): 35-48.
- Teraoka, H., W. Dong, et al. (2003). "Induction of cytochrome P450 1A is required for circulation failure and edema by 2,3,7,8-tetrachlorodibenzo-p-dioxin in zebrafish." Biochem Biophys Res Commun **304**(2): 223-228.
- Timme-Laragy, A. R., C. J. Cockman, et al. (2007). "Synergistic induction of AHR regulated genes in developmental toxicity from co-exposure to two model PAHs in zebrafish." Aquat Toxicol **85**(4): 241-250.
- Timme-Laragy, A. R., L. A. Van Tiem, et al. (2009). "Antioxidant responses and NRF2 in synergistic developmental toxicity of PAHs in zebrafish." Toxicol Sci.
- Van den Berg, M., L. S. Birnbaum, et al. (2006). "The 2005 World Health Organization reevaluation of human and Mammalian toxic equivalency factors for dioxins and dioxin-like compounds." Toxicol Sci **93**(2): 223-241.
- Van Metre, P. C. and B. J. Mahler (2010). "Contribution of PAHs from coal-tar pavement sealcoat and other sources to 40 U.S. lakes." Sci Total Environ **409**(2): 334-344.

- Vanwezel, A. P. and A. Opperhuizen (1995). "Narcosis Due to Environmental-Pollutants in Aquatic Organisms - Residue-Based Toxicity, Mechanisms, and Membrane Burdens." Critical Reviews in Toxicology **25**(3): 255-279.
- Wan, B., J. W. Yarbrough, et al. (2008). "Structure-related clustering of gene expression fingerprints of thp-1 cells exposed to smaller polycyclic aromatic hydrocarbons." SAR QSAR Environ Res **19**(3-4): 351-373.
- White, S. S. and L. S. Birnbaum (2009). "An overview of the effects of dioxins and dioxin-like compounds on vertebrates, as documented in human and ecological epidemiology." J Environ Sci Health C Environ Carcinog Ecotoxicol Rev **27**(4): 197-211.
- Wilhelm, M., J. K. Ghosh, et al. (2012). "Traffic-related air toxics and term low birth weight in Los Angeles County, California." Environ Health Perspect **120**(1): 132-138.
- Wills, L. P., C. W. Matson, et al. (2010). "Characterization of the recalcitrant CYP1 phenotype found in Atlantic killifish (*Fundulus heteroclitus*) inhabiting a Superfund site on the Elizabeth River, VA." Aquat Toxicol **99**(1): 33-41.
- Wilson, S. R., A. D. Joshi, et al. (2013). "The tumor suppressor Kruppel-like factor 6 is a novel aryl hydrocarbon receptor DNA binding partner." J Pharmacol Exp Ther **345**(3): 419-429.
- Wirgin, I., N. K. Roy, et al. (2011). "Mechanistic basis of resistance to PCBs in Atlantic tomcod from the Hudson River." Science **331**(6022): 1322-1325.
- Wu, M. T., T. C. Lee, et al. (2011). "Whole genome expression in peripheral-blood samples of workers professionally exposed to polycyclic aromatic hydrocarbons." Chem Res Toxicol **24**(10): 1636-1643.
- Xiong, K. M., R. E. Peterson, et al. (2008). "Aryl hydrocarbon receptor-mediated down-regulation of sox9b causes jaw malformation in zebrafish embryos." Mol Pharmacol **74**(6): 1544-1553.
- Xu, X., H. Hu, et al. (2013). "Studying the effects of polycyclic aromatic hydrocarbons on peripheral arterial disease in the United States." Sci Total Environ **461-462C**: 341-347.

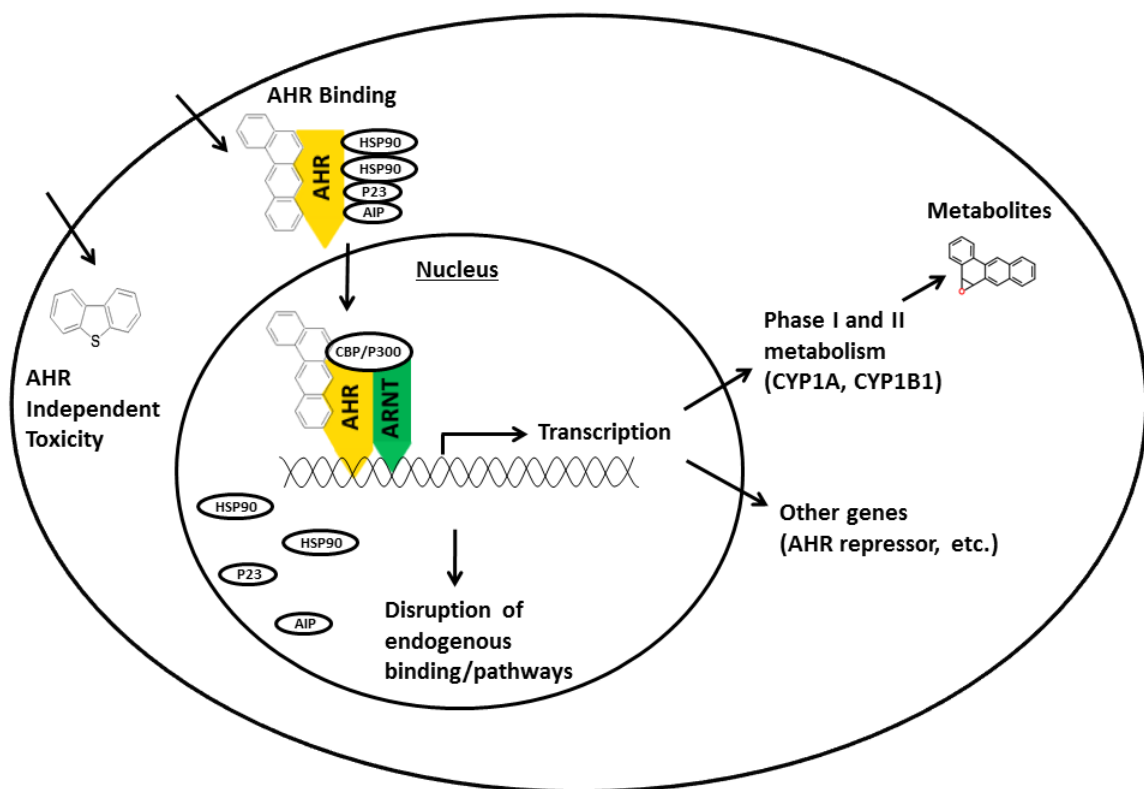


Figure 1-1 Schematic diagram of the aryl hydrocarbon receptor pathway

Upon entering the cell, some PAHs are bound by the aryl hydrocarbon receptor (AHR), which resides in the cytosol, and in its unliganded state is bound by 90 kDa heat-shock protein (HSP90), co-chaperone p23, and aryl hydrocarbon interacting protein (AIP). Upon ligand binding, the AHR translocates to the nucleus and dimerizes with the aryl hydrocarbon receptor nuclear translocator (ARNT). Together with other interacting proteins, such as CREB binding protein (CBP/P300), the AHR/ARNT heterodimer binds to aryl hydrocarbon receptor response elements (AHREs) in the genome and activates transcription of many genes. Genes directly activated by the AHR include phase I and II metabolizing enzymes such as cytochrome p4501A and 1B1 (CYP1A and CYP1B1). These enzymes metabolize PAHs to more reactive metabolites, which can be further metabolized and excreted, but can also cause toxicity by interacting with DNA and proteins. The battery of genes induced by the AHR includes the AHR repressor as well as other targets which may mediate PAH-induced toxicity. Binding of AHR to ARNT and localization to AHRE in response to ligand activation may additionally disrupt endogenous pathways, leading to toxic effects.

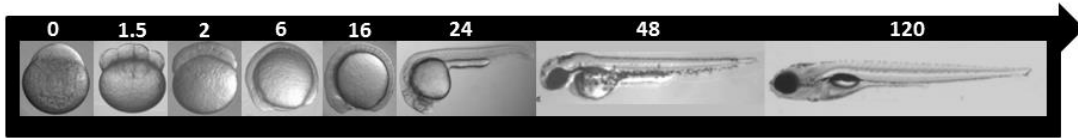


Figure 1-2 Zebrafish early development

Stages of zebrafish development from fertilization to 120 hours post fertilization (hpf) (adapted from Sali 2012).

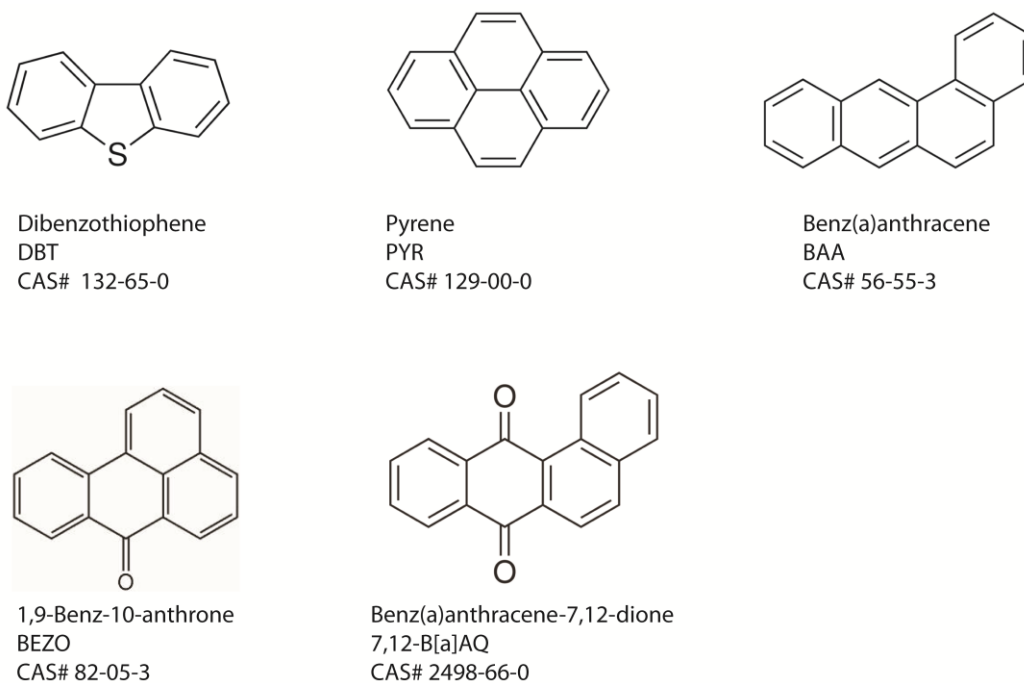


Figure 1-3 Polycyclic aromatic hydrocarbon structures

Compounds investigated in this dissertation include parent PAHs dibenzothiophene, pyrene, and benz(a)anthracene, and OPAHs 1,9-Benz-10-anthrone and benz(a)anthracene-7,12-dione.

Chapter 2 - Structurally distinct polycyclic aromatic hydrocarbons induce differential transcriptional responses in developing zebrafish

Britton C. Goodale¹, Susan C. Tilton², Margaret M. Corvi¹, Glenn R. Wilson¹, Derek B. Janszen², Kim A. Anderson¹, Katrina M. Waters² and Robert L. Tanguay^{1*}

1.Department of Environmental and Molecular Toxicology, the Environmental Health Sciences Center, Oregon State University, Corvallis, OR,

2.Computational Biology and Bioinformatics, Pacific Northwest National Laboratory

Toxicology and Applied Pharmacology

Reprinted with permission

Elsevier B.V. © 2013 All rights reserved.

Abstract

Polycyclic aromatic hydrocarbons (PAHs) are ubiquitous in the environment as components of fossil fuels and by-products of combustion. These multi-ring chemicals differentially activate the aryl hydrocarbon receptor (AHR) in a structurally dependent manner, and induce toxicity via both AHR-dependent and-independent mechanisms. PAH exposure is known to induce developmental malformations in zebrafish embryos, and recent studies have shown cardiac toxicity induced by compounds with low AHR affinity. Unraveling the potentially diverse molecular mechanisms of PAH toxicity is essential for understanding the hazard posed by complex PAH mixtures present in the environment. We analyzed transcriptional responses to PAH exposure in zebrafish embryos exposed to benz(a)anthracene (BAA), dibenzothiophene (DBT) and pyrene (PYR) at concentrations that induced developmental malformations by 120 h post-fertilization (hpf). Whole genome microarray analysis of mRNA expression at 24 and 48 hpf identified genes that were differentially regulated over time and in response to the three PAH structures. PAH body burdens were analyzed at both time points using GC-MS, and demonstrated differences in PAH uptake into the embryos. This was important for discerning dose-related differences from those that represented unique molecular mechanisms. While BAA misregulated the least number of transcripts, it caused strong induction of *cyp1a* and other genes known to be downstream of the AHR, which were not induced by the other two PAHs. Analysis of functional roles of misregulated genes and their predicted regulatory transcription factors also distinguished the BAA response from regulatory networks disrupted by DBT and PYR exposure. These results indicate that systems approaches can be used to classify the toxicity of PAHs based on the networks perturbed following exposure, and may provide a path for unraveling the toxicity of complex PAH mixtures.

Keywords: AHR; microarray; dibenzothiophene; pyrene; benz(a)anthracene; systems toxicology

Introduction

Polycyclic aromatic hydrocarbons (PAHs) are a diverse class of chemicals composed of multiple fused benzene rings, which originate from both petrogenic and pyrogenic sources and are ubiquitous in the environment. Many PAHs are biologically active, cause toxicity in a variety of organisms, and can adversely affect human health. Increasing PAH concentrations in the environment, particularly in urban areas, has been attributed to anthropogenic activities such as fossil fuel burning, automobile exhaust, oil refining and coal tar seal coating (Van Metre and Mahler 2005; Polidori et al. 2010; Van Metre and Mahler 2010). PAHs are present in the ultrafine particulate fraction as well as the gas phase of ambient air, and are considered carcinogenic components of cigarette smoke, vehicle exhaust, wood smoke and other emissions (Bostrom et al. 2002; Ramirez et al. 2011). The primary routes of human exposure are inhalation and ingestion. PAHs associated with ultrafine particulate matter can accumulate in the bronchial epithelium, while volatile PAHs are readily absorbed through the alveolar epithelium (Ramirez et al. 2011). For non-smoking individuals, ingestion via foods and unintentional consumption of household dust (of particular concern for young children) is a primary contributor to PAH exposure (Menzie et al. 1992; Ramesh et al. 2004). Seven non-substituted PAHs are considered possible carcinogens (group 2B) by the US EPA, and 16 PAHs are listed as priority pollutants because of their prevalence in urban and suburban air (EPA 2012). PAH-containing coal tar mixtures are known to be carcinogenic in humans (International Agency for Research on Cancer) (Collins et al. 1998). Human exposure to PAHs almost always occurs within complex mixtures, which may contain multiple PAHs and often include other chemicals such as halogenated hydrocarbons and metals. Because of complex exposure patterns, it is difficult to associate health effects in human populations with individual PAHs.

While the bulk of research on PAHs has focused on mutagenic and carcinogenic properties, exposure to PAH mixtures and ultrafine particulate matter is associated with an array of other health effects in humans, including immune system deficiency, cardiovascular disease and impaired development (Burstyn et al. 2005; Choi et al. 2006; Hertz-Picciotto et al. 2008; Lee et al. 2011; Ren et al. 2011). Activation of the aryl hydrocarbon receptor (AHR) and generation of reactive oxygen species (ROS) are key modes of action initiated by some PAHs, but the full extent of the molecular responses that result from exposure to this

diverse set of compounds has not been characterized. A number of PAHs, including benzo(a)pyrene (BaP) and dimethylbenz(a)anthracene (DMBA), bind the AHR and induce expression of phase I and II metabolizing genes, such as *CYP1A1*, *GSTA1*, *NQO1* and *UGT1A6*, along with many other downstream transcripts (Guengerich 2000; Nebert et al. 2000). Activation of the AHR pathway and metabolism of PAHs can result in a protective effect against PAH toxicity. In many cases, however, AHR activation and metabolism by CYP enzymes increase PAH reactivity and toxicity, which is consequential to the PAH, route of exposure, and exposure concentration (Nebert et al. 2004; Shi et al. 2010). The low molecular weight PAHs (2-3 rings) are generally poor AHR ligands and less potent carcinogens, but are often detected at higher levels in environmental samples and human urine than their higher molecular weight counterparts (Durant et al. 1996; Naumova et al. 2002; Ciganek et al. 2004; Hecht et al. 2010).

Several studies have associated PAH exposure during pregnancy with adverse birth outcomes such as reduced fetal growth and neural tube defects (Choi et al. 2006; Ren et al. 2011). In rodents, exposure to BaP and DMBA induces abnormal vasculature in the placenta and interferes with fetal growth (Detmar et al. 2008; Rennie et al. 2011). Developmental exposure to BaP also impairs cardiac function later in life (Jules et al. 2012).

In zebrafish embryos, BaP-induced cardiac toxicity is mediated by the aryl hydrocarbon receptor (AHR2) (Incardona et al. 2011). However, other PAH structures induce cardiac toxicity and developmental effects via distinct mechanisms that are not AHR-dependent (Incardona et al. 2005). Analyses of global mRNA transcriptional responses to individual PAH exposures demonstrate that structurally-distinct PAHs induce unique gene expression patterns in both human macrophage leukemia (THP-1) cells and circulating leukocytes of rats (Wan et al. 2008; Jung et al. 2011). Little is known, however, about the toxicity pathways and molecular signatures of these diverse exposures during embryonic development.

We used whole genome mRNA microarrays to investigate transcriptional responses that lead to developmental toxicity of three distinct PAHs in developing zebrafish. Dibenzothiophene (DBT), pyrene (PYR) and benz(a)anthracene (BAA) all induce developmental abnormalities by 5 days post fertilization, but have different proposed

toxicity mechanisms. DBT (3 rings) induces cardiac toxicity that is independent of the AHR (Incardona et al. 2004). BAA (4 rings) induces Cyp1a expression and developmental toxicity via activation of AHR2, while PYR (4 rings) toxicity was shown to be metabolism-dependent (Incardona et al. 2006). We determined PAH body burden and corresponding transcriptional profiles in PAH-exposed zebrafish embryos at 24 and 48 hours post-fertilization, before toxicity could be visibly identified. We found that DBT, PYR and BAA induce mRNA expression profiles that differentially implicate AHR activity, and highlight multiple pathways that can be disrupted by exposure to PAHs over the course of vertebrate development.

Methods

Zebrafish lines and embryos:

Adult wild type 5D zebrafish were housed at the Sinnhuber Aquatic Research Laboratory on a recirculating system maintained at $28\pm 1^{\circ}\text{C}$ with a 14 h light/10 h dark schedule. Embryos were collected from group spawns of adult zebrafish as described previously (Reimers et al. 2006) and all experiments were conducted with fertilized embryos according to Oregon State University Institutional Animal Care and Use Protocols.

Chemical Exposures and Developmental Toxicity Assessment:

Dibenzothiophene (>99%), pyrene (99%) and 1,2-benzanthracene (99%) were purchased from Sigma-Aldrich and dissolved in DMSO (J.T. Baker) at 50 mM, 50 mM and 25 mM concentrations, respectively. Embryos were cleaned, developmentally staged, and batch-exposed in glass vials at 6 h post fertilization (hpf) (chorions intact) to PAHs or vehicle control with 1% final DMSO concentration in E2 embryo medium (Kimmel et al. 1995). For all experiments, exposures were conducted on a rocker and embryos were protected from light until the experimental time points. For developmental toxicity experiments, PAH solutions were removed at 48 hpf and embryos were rinsed 4x and incubated in fresh embryo medium until 120 hpf, when they were assessed visually for malformations as previously described (Truong et al. 2011). Preliminary range-finding studies were conducted with each PAH and all further developmental toxicity assessments were conducted at 25 μM with 20 embryos per vial in 2 ml exposure solution. Microarray and body burden exposures were conducted with 40 embryos per vial in 4 ml solution.

Analysis of Developmental Toxicity Endpoints:

Embryos were anesthetized with tricaine methanesulfonate and visually assessed at 120 hpf for yolk sac, axis, trunk, somite, fin, cardiac, eye, snout, jaw, otic vesicle, brain and pigment malformations. Mortality and the percentage of embryos with each malformation were calculated for each treatment group with the vial (20 embryos) as the experimental unit. The experiment was repeated 3 times. A generalized linear model (binomial distribution, logit link) one-way ANOVA was performed for the 8 endpoints which were observed in at least 3 embryos across all treatment groups. If the overall p-value indicated differences among the treatment percentages, individual comparisons were conducted using Tukey's all pairwise post hoc test in R version 2.12.

Detection of PAH body burden in zebrafish embryos:

Embryos were exposed to 0, 1, 5, 10 and 25 μ M PAH (1% DMSO) solutions in glass vials as described previously, with 40 embryos per vial in 4 ml exposure solution. As with all exposures in this study, embryos were exposed at 6 hpf with chorions intact and incubated at 28°C on a rocker. Control embryos hatched just before 48 hpf; exposure to 10 and 25 μ M PAH delayed hatching by 3-4 h, but all treatment groups hatched on their own by 72 hpf. Because several exposure concentrations are above solubility for PAHs in embryo medium, PAH precipitate accumulated on the outside of the chorion. In order to measure the amount of PAH internalized by the embryos, chorions were removed immediately following exposure and before analysis as described below. For each biological replicate, 2 vials were combined after exposure.

For analysis at 24 hpf, embryos were rinsed with fish water and transferred to a clean glass petri dish. They were incubated in 82 μ g/ml pronase (Sigma-Aldrich) at room temperature, gently agitated for 3 min, then rinsed thoroughly using an automated dechorionating system as previously described (Mandrell et al. 2012). Following rinsing, embryos were placed in a 28°C incubator for 20 min, after which >95% of chorions were removed by gentle agitation of the dish.

At 48 hpf, the majority of embryos had hatched and did not require batch dechoriation. They were chilled on ice to reduce activity, PAH solution was removed, and embryos were transferred to a clean glass petri dish with cold fish water. Chorions were removed from any

remaining embryos with forceps, and embryos were gently agitated and rinsed 4x with fish water. Immediately following dechoriation, 50 embryos from each treatment group were loaded into microcentrifuge tubes with approximately 80 mg 1 mm glass beads and placed on ice for at least 10 min. Embryos were homogenized in 500 μ l ethyl acetate with a bullet blender (Next Advance, Averill Park, NY). Samples were then vortexed and incubated 15 min before centrifuging for 5 min at 16,000 RCF. 400 μ l of supernatant was stored in amber vials at 4°C until analysis.

Percent PAH recovery for this method was calculated from 4 replicates of unexposed 24 and 48 hpf embryo samples loaded into microcentrifuge tubes as above and spiked with 12.5 μ l PAH stock in DMSO. Samples were processed identically to experimental samples. Zebrafish extracts were analyzed using an Agilent 5975B Gas Chromatograph-Mass Spectrometer (GC-MS) with a DB-5MS column (30 m x 0.25 mm x 0.25 μ m) in electron impact mode (70 eV) using selective ion monitoring (SIM). The GC parameters were as follows: injection port maintained at 300 °C, 1.0 ml min⁻¹ helium flow, 70 °C initial temperature, 1 min hold, 10 °C min⁻¹ ramp to 300 °C, 4 min hold, and 10 °C min⁻¹ ramp to 310 °C, 4 min hold. The MS temperatures were operated at 150, 230 and 280 °C for the quadrupole, source and transfer line respectively. Standards for BAA, DBT and PYR (>97% purity) were purchased from AccuStandard (New Haven, CT). Isotopically labeled chrysene-D12 and acenaphthylene-D8 were purchased from C/D/N incorporated (Quebec, Canada). A nine point calibration curve (10 pg/ μ l to 10 ng/ μ l) was conducted to determine relative response ratios of PAHs to deuterated surrogate standards; chrysene-D12 was used as the deuterated surrogate for PYR (r^2 = 0.9992) and BAA (r^2 = 0.9982), acenaphthylene-D8 was used for DBT (r^2 = 0.9991).

Calibration verification standards for target analytes and surrogates were analyzed at least every 22 samples and reported values within $\pm 20\%$ of the true value were considered to meet our data quality objectives (DQO). Only results from samples run between two calibration verifications that met the DQO were accepted; the majority were within $\pm 10\%$ of the true value. PAHs in all laboratory blanks (solvent-exposed embryos) were below detection except for 5 samples in which DBT and BAA were detected. This possible contamination was <10% of the levels detected in our lowest exposure sample groups, and

deemed negligible. Body burden ($\mu\text{mol/g}$ embryo) was calculated using average embryo weights of 0.4 mg at 24 hpf and 0.3 mg at 48 hpf. Pairwise comparisons were conducted between PAH-exposed samples and time-matched controls, as well between 24 and 48 hpf at each exposure concentration with Mann-Whitney Rank Sum tests using SigmaPlot software.

Microarray analysis of mRNA expression:

Embryos batch-exposed in groups of 40 to 25 μM DBT, PYR, BAA or 1% DMSO control were homogenized in TRI Reagent (Molecular Research Center, Cincinnati, OH) at 24 and 48 hpf for RNA isolation. Four independent biological replicates were prepared for each treatment. Total RNA was isolated with phenol-chloroform extraction, and RNA was quantified and quality confirmed with a NanoDrop ND-1000 UV-Vis spectrophotometer and Agilent Bioanalyzer 2100. Microarray analysis was performed by the University of Wisconsin McArdle Laboratory of Cancer Research Microarray Facility. Briefly, cDNA was synthesized from 1.2 μg of total RNA from each sample and labeled with cy3 (experimental samples) or cy5 (pooled control sample) according to the Agilent protocol with minor modifications. Equal amounts of cy3 and cy5 labeled samples were mixed, fragmented, and hybridized to Agilent Zebrafish V2 array chips. Slides were scanned immediately with an Agilent microarray scanner (Agilent Technologies, Santa Clara, CA). Microarray files were submitted to the NCBI Gene Expression Omnibus, accession number GSE44130 <http://www.ncbi.nlm.nih.gov/geo/query/acc.cgi?acc=GSE44130>.

Microarray analysis:

Raw intensity data were processed by Agilent Feature Extraction software using Lowess normalization. Quality control analysis was performed on preprocessed data in GeneSpring v.11 (Silicon Genetics, Redwood City, CA) software using feature intensity distributions from box-whisker plots to determine interquartile range span and median intensity value across the experiment. The intra-group versus between-group comparisons were made using correlation matrix plots, followed with principle components analysis to determine potential outliers. One biological replicate from the DBT 48 hpf treatment group was removed as an outlier, resulting in an N=3 for that treatment group. Normalized data were transformed to time-specific controls and analyzed by one-way ANOVA for unequal

variances (Welch's ANOVA) with Tukey's post hoc test and 5% false discovery rate calculation (Benjamini and Hochberg 1995). Values are reported as fold change (log2) with associated Benjamini-Hochberg adjusted p value in each treatment group compared to time-matched control. Correlation analysis between treatment groups was performed by linear regression of log2 fold change values, using the union of significant genes from both groups. Based on the significant correlation between DBT and PYR treatments at both time points, these datasets were further filtered to identify the subset of genes that were significantly different between them ($p < 0.05$, 1.5-fold change). Genes that did not meet these criteria were considered similar between the DBT and PYR treatments for functional and transcription factor analysis.

Bioinformatic analysis:

Unsupervised hierarchical clustering of microarray data was performed using Euclidean distance metric and centroid linkage clustering to group gene expression patterns by similarity. The clustering algorithms, heat map visualizations and centroid calculations were performed with Multi-Experiment Viewer (Saeed et al. 2003) software based on log2 expression ratio values. For downstream bioinformatic analysis, zebrafish identifiers on the Agilent platform were converted to human orthologs using Bioinformatics Resource Manager v. 2.3 (Tilton et al. 2012). Genes that did not have human orthologs were still included in the bioinformatic analysis using their zebrafish identifier. Both MetaCore (GeneGO) and DAVID software recognize mixed identifiers (Entrez Gene ID) from human and zebrafish. Significant targets from the microarray and genes of interest are referred to by zebrafish gene identifiers, where zebrafish-derived information was available in the literature. Functional annotation and network information, however, were primarily derived from other species, and data for many genes of interest were only available in the mammalian literature; we present this information with human gene identifiers throughout the results and discussion. Functional enrichment was determined using the DAVID functional annotation tool (Huang et al. 2009), which utilizes the Fisher Exact test to measure gene enrichment in biological process Gene Ontology (GO) category terms for significant genes compared to background, which consisted of all genes on the Agilent platform. GO biological process categories from levels 3, 4, and 5 were included for enrichment calculation. Since the DAVID functional annotation tool clusters GO terms by

similarity to reduce redundancy, the biological processes are presented in the results with a representative process from each significant cluster ($p < 0.05$) that represented at least 1% of genes from the exposure group. To identify major transcriptional regulators of gene expression by PAHs, the Statistical Interactome tool was used in MetaCore to measure the interconnectedness of genes in the experimental dataset relative to all known interactions in the background dataset. Statistical significance of over-connected interactions was calculated using a hypergeometric distribution, where the p value represents the probability of a particular mapping arising by chance for experimental data compared to the background (Nikolsky et al. 2009). Networks were constructed in MetaCore for experimental data using an algorithm that identifies the shortest path to directly connect nodes in the dataset to transcription factors. Network visualizations were generated in Cytoscape (Shannon et al. 2003).

Quantitative RT-PCR

Validation of gene expression changes identified in the microarray analysis was conducted for a group of transcripts selected to represent differential regulation patterns by the three PAHs at 24 and 48 hpf. Gene-specific primers (MWG Operon) for qRT-PCR amplification are listed in Table S1. Sub aliquots of 10 μ g total RNA from the microarray analysis were reverse transcribed using Superscript III (Invitrogen) according to manufacturer instructions. All qRT-PCR assays were performed in 20 μ l reactions consisting of 10 μ l Power SYBR Green PCR master mix (Applied Biosystems), 0.4 μ l each primer, 9.2 μ l H₂O and 50 ng equivalents of cDNA. Amplification (StepOnePlus, Applied Biosystems) was performed with cycling parameters as follows: 95°C for 10 min; 40 cycles of 95°C for 15 s, 60°C for 1 min; 95°C for 15 sec and 60°C for 1 min. A melt curve was performed at 3° increments to assess for multiple products. Relative fold change values in PAH-treated samples compared to vehicle controls were calculated for genes of interest, normalized to β -actin, by the method described by Pfaffl (Pfaffl 2001). Three independent biological replicates were assessed and statistically analyzed by one-way ANOVA with Tukey's post-hoc test using SigmaPlot software.

Results and discussion

Dibenzothiophene, pyrene, and benz(a)anthracene induce developmental toxicity in zebrafish embryos.

Exposure to DBT, PYR or BAA caused a significant increase in the incidence of abnormal embryos compared to the vehicle control exposure at 120 hpf. All three compounds induced pericardial edema, snout and jaw malformations (Fig. 1). PYR and BAA exposures caused significant increases in yolk sac edema, while DBT did not. DBT, however, induced distinct axis malformations (Fig. 1B) which were not present in BAA- or PYR-exposed embryos (Tables 1, 2). Interestingly, the 25 μ M concentration of all three PAHs induced malformations in >80% of embryos by 120 hpf, while mortality was < 10%, not significantly different from control (Table 1). The phenotypes induced by these PAHs suggested different underlying pathologies. BAA induced more severe edema, while necrotic tissue was observed in PYR-exposed embryos, particularly in the anterior yolk sac, liver and digestive tract (Fig. 1C); these embryos did not survive more than a couple hours past 120 hpf. This was observed previously by Incardona et al, who demonstrated that DBT, PYR and BAA induced malformations in zebrafish that were differentially dependent on activation of the AHR and metabolism by Cyp1a (Incardona et al. 2004; Incardona et al. 2005). The differential proposed mechanisms of these PAHs presented an ideal opportunity to investigate the diversity of molecular pathways that lead to developmental effects of PAH exposure. The objective of this study was not to mimic environmental exposures, but rather to identify molecular pathways that precede morphological changes induced by different PAH structures. Based on our developmental toxicity data, 25 μ M was identified as an appropriate concentration for microarray analysis of early gene expression changes elicited by DBT, PYR and BAA exposure.

Zebrafish exposed to dibenzothiophene, pyrene and benz(a)anthracene in embryo medium accumulate differential PAH body burdens.

The internal body burden of PAH in embryos was measured after exposures as described for the microarray analysis. To allow for structure-toxicity comparisons between the three compounds, as well as to relate gene expression data to other model systems, DBT, PYR and BAA were detected by GC-MS in zebrafish embryos exposed to a range of concentrations (1-25 μ M). PAH recovery averaged between 80 and 125% (Table S2). Measured PAH values were therefore reported as detected in experimental samples, unadjusted for recovery. The

amount of PAH detected in embryos revealed stark differences between the three PAH structures. At all concentrations and time points, DBT body burden in embryos was the highest, averaging 3.4 and 5.3 $\mu\text{mol/g}$ at 24 and 48 hpf, respectively, following exposure to 25 μM DBT (Fig. 2A). DBT had the highest solubility in water, and uptake did not plateau in the range of concentrations tested here. PAH body burden of embryos exposed to 25 μM PYR averaged 1.0 and 2.9 $\mu\text{mol/g}$ at 24 hpf and 48 hpf, respectively, and uptake appeared to reach a plateau, likely because of low compound solubility in embryo medium (Fig. 2B). BAA body burden was markedly lower than the other two PAHs at all exposure concentrations. An apparent saturation was reached at 0.10 $\mu\text{mol/g}$ embryo at 24 hpf, an order of magnitude lower than PYR (Fig. 2C). Water solubility of BAA was the lowest of these PAHs, and the high concentrations employed in this study were above solubility with 1% DMSO in embryo medium. At 48 hpf, BAA concentrations averaged 0.19 $\mu\text{mol/g}$ in embryos from the 25 μM exposure group.

Studies of early-life exposure to PAHs showed that the bioconcentration factor (BCF) in fish embryos correlated with the octanol water partition coefficient (K_{ow}) (Mathew et al. 2008). The log K_{ow} values of DBT, PYR and BAA are 4.38, 4.88 and 5.79, respectively (Hansch 1995). BAA would therefore be predicted to have the highest BCF of the PAHs in our study. BCFs have primarily been calculated for larvae (post-hatch), however, and the short duration exposures employed in our study did not allow steady-states to be achieved. Steady-state PAH concentrations were similarly not attained in zebrafish eggs in a study reported by Petersen and colleagues (Petersen and Kristensen 1998). Metabolism could also explain differences in parent PAH concentration, but is expected to be low during the developmental stages chosen for gene expression analysis in this study (Petersen and Kristensen 1998). Metabolism increases upon hatching in Atlantic killifish embryos, and zebrafish exhibit greater inducibility of *cyp1a* starting at 48 hpf, the approximate time of hatching in our laboratory (Binder and Stegeman 1984; Andreassen et al. 2002). While metabolism could potentially explain the small decrease in BAA between 24 and 48 hpf at the lower concentrations, it is unlikely to explain the large difference in body burdens observed between PAH structures. Differences between PAHs in this study appear to be driven by their solubility in embryo medium, rather than their BCFs or metabolism. The 25 μM exposures for the microarray study represent an acute exposure intended to identify

mRNA expression changes that precede appearance of morphological abnormalities. While total dose and maximum exposure calculations were beyond the scope of this study, the measurement of parent PAH in the embryos at the time of gene expression analysis provided important information for mechanistic comparison between the PAHs.

mRNA expression profiles induced by PAH exposure are different at 24 and 48 h post fertilization.

Pairwise analysis of variance across all exposure groups identified significant expression changes in 1079 transcripts compared to time-matched controls (Table S3). Entrez or Ensembl IDs were identified for 935 of these in the Ensembl zebrafish genome assembly (Zv9). Unsupervised bidirectional clustering of all experimental groups indicated a strong developmental time point effect, and revealed unique gene expression patterns in response to the three PAHs. At 24 hpf, DBT and PYR exposure groups clustered closely, while BAA induced a strikingly different expression pattern (Figs. 3A, D). DBT and PYR exposure groups also clustered at 48 hpf, but with distinct separation from the 24 hpf samples and with a notably larger group of down-regulated transcripts. The expression profile induced by BAA at 48 hpf clustered more closely with 24 hpf BAA than with the other 48 hpf PAH samples (Fig. 3A). At 24 hpf, DBT, PYR and BAA exposures induced significant changes in 357, 67 and 38 transcripts, respectively. As reflected in the heatmap, more transcripts were differentially expressed at 48 hpf, but relative quantities of differentially expressed transcripts were maintained; DBT induced changes in 656, PYR in 191 and BAA in 107 transcripts (Figs. 3B-D). Fifteen genes that were significantly differentially regulated by at least one of the PAHs were selected for qRT-PCR validation of the differential regulatory patterns observed in the array. PAH- and time-dependent expression changes were confirmed for the majority of genes examined (Table S4). Fold change values were similar between the microarray and qRT-PCR for most genes, demonstrating good reliability of the microarray for identifying meaningful changes in gene expression induced by PAH exposure. *mstnb*, which was identified as a significantly decreased transcript at 24 hpf, was not decreased in BAA-exposed samples analyzed by qRT-PCR. Upon further investigation, however, we identified 5 probes on the Agilent array that target *mstnb*, only one of which identified a significant expression difference (p value 0.04). This suggested nonspecificity of that probe for *mstnb*, or potentially differential splicing. As others have reported previously,

we observed lower correlation between the microarray and qRT-PCR for down-regulated transcripts; qRT-PCR identified fewer changes that met statistical significance ($p < 0.05$), but trends in regulation were consistent (Morey et al. 2006).

For each PAH, we compared transcripts significantly differentially expressed at 24 hpf with transcripts that were significant at 48 hpf. These experimental time points encompass a period of rapid development in zebrafish, during which fin morphogenesis begins, the circulatory system forms, tactile sensitivity and swimming behavior are initiated, and pigment develops (Kimmel et al. 1995). Developmental progression is reflected in the stronger influence of time point than PAH structure in the bidirectional clustering (Fig. 3A).

While 95 transcripts were misexpressed by DBT at both 24 and 48 hpf, they represented only 27% of the 24 hpf significant gene set, and did not include the most highly misexpressed transcripts from either time point. The most differentially expressed transcripts across both time points were *acana*, *ankrd1b* and *hsqb11* (Fig. 3B). *ankrd1b* and *hsqb11* are both involved in myogenesis; *hsqb11* is specifically expressed in muscle pioneers, up-regulated by intracellular calcium, and involved in muscle fiber organization in developing zebrafish (Kluver et al. 2011; Kojic et al. 2011). Similar to DBT, the expression of only a few transcripts were significant impacted by PYR at both 24 and 48 hpf. The two genes differentially expressed >2 fold were *tnfb*, a member of the tumor necrosis factor family of proinflammatory cytokines, and *zgc:153258* (Fig. 3C). These robust responses, conserved over time, represent potential biomarkers of exposure to the individual PAHs. The transcripts with the largest fold changes, however, were not consistent over time, which suggested that separate analysis at each time point could provide better insight into mechanisms driving responses to DBT and PYR exposure.

The BAA transcriptional profile is consistent from 24 to 48 hpf, and distinct from DBT and PYR-induced changes.

In contrast to DBT and PYR, 45% of transcripts differentially expressed by BAA at 24 hpf were also significant at 48 hpf, and those with the largest fold changes were conserved between time points (Fig. 3D). The most highly misexpressed genes at 24 hpf were *cyp1a*, *cyp1b1*, *cyp1c1*, *cyp1c2*, *ahrra* and *foxq1l*. All of these genes were elevated and, along with *sult6b1* and *ctgfb*, remained elevated at 48 hpf. The *cyp1* genes and *aryl-hydrocarbon*

receptor repressor (ahrta) are well-known targets of AHR, while *sult6b1* is a recently identified sulfotransferase that could potentially be involved in BAA metabolism. Together, these genes represent a consistent signature of the transcriptional response to BAA exposure in zebrafish embryos from 24 to 48 hpf.

We conducted between-PAH comparisons separately at 24 and 48 hpf to identify significant transcripts unique to each PAH exposure. Though BAA exposure affected the smallest number of transcripts, they were highly induced and formed a distinct cluster (Fig. 3D) that overlapped minimally with the DBT and PYR transcriptional profiles. Only 7 of the significant genes in the 24 hpf BAA exposure group were similarly differentially expressed in response to DBT or PYR. At 48 hpf, the BAA expression pattern remained distinct, where only 27 of the 107 differentially expressed transcripts were similarly regulated by another PAH. In addition, we observed no correlation between the transcriptional response induced by BAA and either of the other PAHs at 24 or 48 hpf ($r^2 < 0.2$), using linear regression analysis of all significant transcripts. The entire set of significant BAA transcripts was therefore used for analysis of pathways and biological functions disrupted by BAA exposure at 24 and 48 hpf (discussed below).

DBT and PYR induce a similar dose-dependent transcriptional profile.

Common patterns in gene expression between DBT and PYR exposure groups are apparent in the heatmap in Figure 3A at both time points; however, the magnitude of the PYR-induced transcriptional response is visibly lower. This trend was reflected in the linear regression analysis of PYR vs. DBT log₂ expression values, where a strong positive correlation was observed at 24 hpf (Fig. 4A, union of DBT and PYR significant transcripts, $r^2 = 0.77$, $p < 0.001$). The regression slope, however, demonstrated that DBT-induced expression changes were on average 1.6 fold greater than PYR-induced changes in these transcripts. This apparent dose-effect suggested that solubility and uptake were the primary drivers of differential transcriptional responses between these compounds, rather than unique molecular targets. The dose-effect is supported by the body burden data; DBT body burdens were 3.4 times higher than PYR body burdens in the 25 μ M exposure cohorts at 24 hpf. This trend persisted with a similar correlation at 48 hpf ($r^2 = 0.647$, $p < 0.001$), wherein DBT on average induced 1.75-fold greater expression changes than PYR (Fig. 4B)

and DBT body burdens were 1.8 times greater than PYR. We found that comparing the PAHs following ANOVA analysis exaggerated transcriptional profile differences, because many PYR-induced changes did not reach statistical significance ($p < 0.05$ compared to control). Because of the significant correlation in responses, we employed a direct statistical comparison of DBT and PYR to better define the conserved transcriptional response, as well as identify transcripts with meaningful expression differences between the two groups.

Direct pairwise comparison of DBT and PYR log2 FC values at 24 hpf identified 343 similarly expressed transcripts, and only 42 that were significantly different ($p < 0.05$). At 48 hpf, 139 were significantly different, while 572 transcripts were similar between the two PAHs. Because of the overwhelming conservation of response, functional analysis was performed using the set of similarly expressed genes at each time point to identify biological processes disrupted by DBT and PYR exposure. We focused further mechanistic analysis on the DBT-PYR vs. the BAA responses.

Disruption of ion transport, muscle function, and metabolism by DBT and PYR at 24 hpf

Of the 343 transcripts representing the conserved DBT and PYR responses at 24 hpf, approximately 70% were under-expressed compared to control. 308 had sufficient annotation, which translated to 256 unique DAVID IDs. Fatty acid biosynthesis, ion transport, skeletal muscle contraction, steroid biosynthesis and oxoacid metabolism were the most enriched of the 12 significant biological processes identified by DAVID functional analysis, which together depict wide disruption of molecular signaling by 24 hpf (Table 4). We used the MetaCore Statistical Interactome tool to identify major transcription factors predicted to regulate significant genes in this dataset. JUN, RELA, SP1, PPARA, RXRA, ESR1, ESR2, and NR3C1 (glucocorticoid receptor) were predicted to regulate the largest sets of differentially expressed transcripts (Table S5). Transcripts were up- and down-regulated in approximately equal numbers, and there was considerable overlap of the predicted targets of these transcription factors. The extensive molecular responses to these PAHs highlighted a complex network of regulatory processes involved in normal embryo development that were unlikely to be mediated through one primary transcription factor but rather were responsive to chemical-induced perturbations such as oxidative stress, inflammation, altered metabolism and disruption of ion balance and cardiac function.

The ion transport biological process contained the largest number of misregulated transcripts at 24 hpf (Table 3) and is discussed further below as a common biological response to all PAH exposures in this study. Ion balance is important for muscle development and function, which was also significantly affected by DBT and PYR at 24 hpf. Transcripts in the skeletal muscle contraction and muscle cell development biological processes were primarily under-expressed, and included myoglobin, which is also required for angiogenesis in zebrafish (Table 3)(Vlecken et al. 2009). Members of the ion transport cluster may interact with these transcripts or themselves be important for muscle and cardiac function in the context of zebrafish development.

Genes involved in fatty acid biosynthesis, steroid biosynthesis and oxoacid metabolism were also primarily underexpressed (Table 3). A notable exception was *cholesterol 25-hydroxylase (ch25h)*, which encodes a cholesterol metabolizing enzyme involved in the inflammatory response, and was elevated >4 fold by both DBT and PYR (Park and Scott 2010). The functions of these genes and their roles during development have yet to be characterized in zebrafish, but together they implicate disruption of metabolic processes.

Transcription factors RELA and JUN are predicted to regulate renin-angiotensin system-related genes misexpressed in DBT and PYR exposed embryos.

In contrast to the previously-discussed biological processes, the majority of genes associated with negative regulation of cell proliferation (Table 3) have known roles in zebrafish development, and many are predicted downstream targets of the NF- κ B family member RELA (Table S5; *bdnf*, *tnfrsf9a*, *zgc:114127*, *agt*, *msxe*, *tnfb*) as well as JUN (Table S5; *cx43*, *smad3b*, *tnfrsf9a*, *agt*, *tnfb*). These processes are likely mediated through multiple interacting transcription factors. Of the 15 transcription factors that were significant at 24 hpf, RELA and JUN were predicted to regulate the most highly induced genes in the DBT-PYR dataset, *agt* and *tnfb*, as well as many other genes involved in the significant biological processes. The inflammatory cytokine *tnfb* is one of two *TNF* homologs in zebrafish, both of which are highly induced in larvae in response to LPS stimulation (Wiens and Glenney 2011). Angiotensinogen (AGT) is the precursor of angiotensin (ANG II), a potent regulator of blood pressure and water homeostasis in the renin-angiotensin signaling (RAS) network (Wu et al. 2011). Transcription of *AGT* is induced by glucocorticoids through the

glucocorticoid receptor, as well as by TNF and other inflammatory cytokines via activation of NF- κ B (Brasier and Li 1996). ANG II induces *AGT* transcription in a positive feedback loop involving NF- κ B, and also activates JUN via JNK signaling in cardiac myocytes and vascular smooth muscle cells (Brasier and Li 1996; Brasier et al. 2000). As an initiator of tissue inflammation, TNF activates NF- κ B, induces inflammatory and anti-apoptotic gene expression in a cell-type dependent manner, and also activates JUN via JNK (Tian et al. 2005). In this study, DBT and PYR exposure led to increased expression of *tnfb* and *complement component 7*, along with macrophage-related genes *mpeg1* and *mst1*, all of which are involved in innate inflammatory response. Both *Tnf* and *Agt* are expressed in the myocardium of rats following ischemia, remodel ATP-dependent calcium channels, and have been implicated in atherosclerosis and hypertension (Isidoro Tavares et al. 2009). In developing rat embryos, activation of angiotensin receptors with exogenous ANG II disrupts cardiac looping (Price et al. 1997). These two genes, in combination with the significant enrichment of other targets of RELA, JUN, and the glucocorticoid receptor, suggest that inflammatory response and RAS signaling may play a role in the cascade of effects observed in response to DBT and PYR exposure. Cardiovascular functions of the RAS system are conserved in teleosts (Le Mevel et al. 2008), and though not yet explored in embryonic zebrafish, the RAS system has been identified as important for fetal cardiovascular response, body fluid balance, and neuroendocrine regulation, and may be involved in fetal programming of hypertension later in life (Mao et al. 2009).

We created a map of key predicted transcription factors, including RELA and JUN, and their downstream targets that were significantly misregulated in the three PAH exposure groups at 24 or 48 hpf (Fig. 5). A substantial number of transcripts, including *TNF* and *AGT*, are predicted to be regulated by both transcription factors, but RELA is predicted to regulate the largest number of genes that were induced by DBT/PYR exposure at 24 or 48 hpf. While RELA was also identified as a significant transcriptional regulator of BAA genes (discussed below), the DBT-PYR and BAA exposure networks overlapped with only 10 RELA targets (Fig. 5, purple). Fig. 5 therefore highlights the distinct nature of RELA regulatory roles in the toxicity pathways of different PAH structures.

Developmental processes in DBT and PYR-exposed embryos are widely misregulated at 48 hpf.

By 48 hpf, 572 transcripts were differentially expressed in DBT and PYR embryos compared to controls, 478 of which were annotated. DAVID functional analysis identified 21 biological processes that were significantly affected by DBT and PYR exposure; oxoacid metabolic process was the most enriched functional cluster, but was composed of different genes than at 24 hpf (Table 4). Many of the most significant processes misregulated at 48 hpf were directly related to embryonic development, and the regionalization, neurogenesis and central nervous system development functions together highlight widespread disruption of nervous system development (Table 4). Thirty-five transcription factors were predicted to regulate significantly enriched groups of genes within this dataset; JUN, PPARA, RELA, RXRAa and SP1 were significant at both 24 and 48 hpf (Table S5). NR3C1 and ER, which were significant at 24 hpf, were no longer enriched at 48 hpf, whereas CREB1, P53, YY1 and TBP became significant with the largest numbers of misregulated downstream targets. The breadth of expression changes at 48 hpf is not restricted to a singular toxicity pathway, but rather encompasses substantial network perturbations consistent with aberrant embryonic development. These and the many other misexpressed transcripts may result from a cascade of processes downstream of the genes disrupted at 24 hpf, but also reflect the vast molecular changes that occur in a normally developing zebrafish between these two time points.

Biological functions of BAA-misregulated genes are consistent with AHR-dependent toxicity.

Human or mouse homologues were available for 29 of the 38 transcripts significantly misregulated by BAA at 24 hpf, which translated to 19 unique DAVID IDs. Several genes, including *cyp1a*, were represented by multiple probes within this significant transcript set. Functional analysis of genes misregulated by BAA at 24 hpf identified two biological processes, hormone metabolism and tissue development, that were significantly enriched within this dataset (Table 4). Metabolic process genes were up-regulated, and included well-known biomarkers of AHR activation such as *cyp1a*, as well as *si:dkey-94e7.2*, a predicted homolog of retinol dehydrogenase 11 (*RDH11*). Expression of genes involved in tissue development was also primarily increased (Table 3), likely via AHR signaling. A *foxq1* homolog was induced by BAA, and based on the probe sequence we identified the transcript as *foxq1b*, an AHR-dependent TCDD-inducible gene expressed in zebrafish jaw primordium (Planchart and Mattingly 2010). Tissue development genes *ptn* and *ctgfb* (Table 3) are not

known to be directly regulated by the AHR, but may be important mediators of AHR-dependent developmental toxicity; *ctgfb* was also induced in developing jaws of zebrafish exposed to TCDD (Xiong et al. 2008).

Transcription factor prediction identified AHR as significant at 24 hpf, along with its dimerization partner, ARNT, and C/EBP δ (Table S5). The large fold changes in a relatively small number of significant transcripts suggest that BAA interacts with one primary transcription factor at 24 hpf, and the transcriptional profile supports previous demonstration of AHR-dependent toxicity induced by BAA (Incardona et al. 2006).

BAA transcriptional response indicates oxidative and metabolic stress at 48 hpf

The BAA transcriptional response expanded to 107 misexpressed transcripts at 48 hpf, 99 of which were sufficiently annotated. Though the *cyp1* genes remained the most strongly elevated, they were joined by *ahr*, *wfikk1*, and *cathepsin L.1 (ctsl.1)*, which was elevated 4-fold. *Ctsl.1* encodes a widely expressed protease important for blood pressure regulation, and was recently identified as dioxin-responsive (Mbewe-Campbell et al. 2012). DAVID functional annotation clustering of the 70 unique targets identified eight significantly enriched biological functions (Table 4). Genes involved in hormone metabolism again formed a significant cluster, which included two phase 2 metabolizing enzymes, *ugt1b5* and *ugt1b7*, along with the *cyp1* transcripts. Transcripts associated with cation transport, in contrast, were not known AHR targets, and are discussed further within the ion transport response common to all three PAHs. The cellular homeostasis transcript group was composed of antioxidant-related genes (*gsr*, *prdx1*, and *zgc:92066*, a homolog of *FTMT*), and transcripts involved in blood pressure regulation and chemokine signaling that are not known to be direct targets of AHR (Table 4).

Vascular development genes are misexpressed in BAA-exposed embryos.

Genes involved in vasculature development were over-represented among transcripts affected by BAA at 48 hpf. They included chemokine receptor *cxcr4a*, which had increased expression, and its ligand, *cxcl12b*, which was under-expressed. Interestingly, this expression pattern was also observed in a microarray analysis of TCDD-induced transcriptional changes in zebrafish jaw, suggesting misregulated chemokine signaling may indeed be involved in AHR-mediated toxicity in the developing embryo (Xiong et al. 2008).

cxc4a is required for arterial-venous network formation and is expressed in response to low blood flow and in unperfused blood vessels in developing zebrafish (Bussmann et al. 2011). Other vasculature development genes included *connexin 39.4* (*cx39.4*), *connective tissue growth factor b* (*ctgfb*), *c-fos induced growth factor* (*figf*, previously *vegfd*) and *TCDD-inducible poly(ADP-ribose) polymerase* (*tiparp*) (Table 4). *atp2a2a* (reduced expression) is not annotated as a vascular development gene, but is required for heart looping in zebrafish (Ebert et al. 2005). Together these transcriptional changes convey disruption of vascular development and circulatory system function. This is in agreement with blood pressure misregulation and endothelial dysfunction in rats developmentally exposed to benzo(a)pyrene, another PAH known to induce AHR signaling (Jules et al. 2012).

RELA is a significant transcription factor in the BAA regulatory network

Transcription factor analysis at 48 hpf predicted involvement of multiple transcription factors (Table S5). AHR was interestingly no longer significant, though its dimerization partner ARNT was predicted to regulate a significantly enriched cluster of genes. SP1, TP53, CREB1 and RELA were upstream of the largest number of genes misregulated by BAA at 48 hpf (Table S5). RELA interacts directly with AHR and is an important regulator of inflammatory immune and oxidative stress responses (Tian et al. 1999). The RELA and AHR regulatory networks are displayed in Figure 5, which shows that the AHR regulates a set of genes that were distinct to the BAA exposures and were not predicted to be under direct regulation by RELA. The large number of genes downstream of RELA, however, which includes some of the most highly misexpressed genes such as *CTGF* and *CTSL1*, suggests RELA may play an important role in the BAA toxicity pathway (Figure 5).

Differential affinities for the AHR result in few transcripts common to PAH exposure

The few genes similarly misregulated by all three PAHs represent potential general biomarkers of PAH exposure. At 24 hpf, only 5 transcripts were similarly affected by all 3 PAHs. The most highly elevated probes (approximately 3-fold for all PAHs), A_15_P477220 and A_15_P247256, both target ESTs that are not yet annotated in the zebrafish V9 genome. Decreased transcripts at 24 hpf included *slco5a1*, a solute carrier organic transporter family member, and a non-specific probe. By 48 hpf, 23 transcripts were similarly expressed in response to all three PAHs. The most elevated genes across all three PAHs were *cyp1a*,

cyp1b1, *wfikkn1*, *LOC794658* (similar to *chrn3*), *s100z* and *cxcr4a*. The largest decreases were observed in *g0s2*, *kif20a*, *cfdl*, and two uncharacterized genes, *zgc:171318* and *zgc:153311*. Though the molecular toxicity pathways of BAA and DBT/PYR are, on the whole, very different, these genes highlight some commonalities.

The most commonly used biomarker of AHR activation, *cyp1a*, was elevated by all three PAHs at 48 hpf. However, DBT and PYR only induced 1.2 and 2.1 fold changes, respectively, whereas BAA induced *cyp1a* 34.5-fold. The minimal and delayed *cyp1a* induction suggests that it occurs via metabolites or very weak AHR activation by DBT and PYR. Barron and colleagues reported the potency of BAA as an AHR agonist as 519 times greater than PYR, and though DBT was not analyzed, 3-ring PAHs included in the study were less potent than PYR or were inactive in assay systems (Barron et al. 2004). Though Cyp1a protein expression is induced by PYR exposure in zebrafish embryos, Incardona et al. reported a markedly different expression pattern than was observed with BAA, and suggested Cyp1a metabolism and hepatic toxicity were drivers of the developmental effects (Incardona et al. 2006). DBT, in contrast, has been reported to induce developmental toxicity via disruption of early cardiac function, as well as act as a Cyp1a inhibitor (Incardona et al. 2004; Wassenberg et al. 2005). In light of these proposed different mechanisms of action, the overlap of transcripts misregulated by DBT and PYR at both 24 and 48 hpf in this study is striking. Indeed, the different malformations observed in DBT and PYR-treated embryos, despite similar molecular response profiles, may be a result of metabolic processes that are more active after the 48 hpf time point employed in this study. The marked effects of DBT exposure on axis formation, which were not observed in response to PYR, could also be explained by the dramatic differences in PAH body burden at these equivalent exposure concentrations. Signaling that directs axis formation occurs early in development; the uptake of DBT was relatively rapid, whereas the lower solubility and uptake of PYR potentially did not achieve a threshold concentration to induce such effects.

Disruption of ion transport and calcium signaling is common across all PAHs

Ion transport and homeostatic processes were misregulated by all three PAHs in this study, though the significant transcripts in the DBT-PYR response are largely different from those affected by BAA. All three exposures induced differential expression of genes involved in

calcium homeostasis, suggesting that calcium signaling plays a role in PAH-induced developmental toxicity, as has been shown previously in dioxin-exposed zebrafish at 48 hpf (Alexeyenko et al. 2010). In a separate study of TCDD effects on heart development, transcriptional changes related to calcium homeostasis preceded the development of cardiac malformations in zebrafish, suggesting that they may be causal for malformations rather than simply a result of reduced blood flow (Carney et al. 2006). Though early calcium influx is a well-known response to several AHR ligands, the dependence of this response on AHR binding and the consequence within the developmental context are unknown.

PAHs have previously been shown to increase intracellular calcium through protein tyrosine kinases, inhibiting SERCA activity, and activating RYR receptors, though the intensity and duration of the response is dependent on PAH and cell type (Archuleta et al. 1993; Krieger et al. 1995; Gao et al. 2005). All three PAHs in our study increased transcription of calcium binding protein *s100z*. The S100 family of EF-hand calcium binding proteins regulates a diverse range of cellular functions in a calcium-dependent manner, and is associated with many pathological conditions including inflammation, atherosclerosis, diabetes, and neurodegeneration (Hermann et al. 2012). Future investigation of the dependence of these transcriptional changes on AHR signaling will provide insight into whether they represent a common mechanism, or are induced via different molecular responses to the PAHs in our study

Differential AHR activation results in distinct RELA regulatory responses to PAH exposures

RELA was a predicted transcriptional regulator of both the BAA and DBT-PYR toxicological responses. Despite this, there was little overlap in the transcriptional networks (Figure 5). Differential AHR activation can explain the AHR gene battery that was uniquely induced by BAA at 24 hpf. However, a large portion of the RELA network expressed in response to DBT and PYR was not affected by BAA exposure (Figure 5). This difference could potentially be explained by dose. BAA is the least soluble in water, and body burden was an order of magnitude lower than the other PAHs. We therefore cannot exclude the possibility that BAA would activate the DBT-PYR transcriptional network at an equivalent internal concentration. Body burdens of DBT and PYR-exposed embryos are within the range reported to induce toxicity through mechanisms classified under “nonpolar narcosis”, such

as interference with lipid fluidity and membrane function (Vanwezel and Opperhuizen 1995). The general pattern of narcotic response, including lost sense of balance, response to stimuli, and reduced ventilation frequency, is not applicable to the early developmental stages of embryos analyzed in this study. However, DBT concentrations in embryos averaged 3.4 $\mu\text{mol/g}$ at 24 hpf, and PYR reached 2.9 $\mu\text{mol/g}$ by 48 hpf following exposure to 25 μM waterborne concentrations. Toxicity from nonpolar narcosis has been reported to occur at 2-8 $\mu\text{mol/g}$ body weight, depending on the compound and organism (Vanwezel and Opperhuizen 1995). The data presented here characterize the extensive molecular response to these relatively high internal concentrations, and our analysis identified RELA as a significant mediator in the DBT-PYR transcriptional network. Interestingly, though BAA toxicity was induced by a lower body burden concentration of 0.12 $\mu\text{mol/g}$ at 48 hpf, network analysis also identified RELA as a significant regulator of BAA-induced transcriptional changes. This suggests that RELA involvement in PAH toxicity is modulated by both AHR activation and PAH concentration. Future studies with multiple PAHs would be useful for identifying whether transcriptional networks identified here are differentially induced by diverse PAH structures.

Transcriptional responses to PAH exposures are conserved across species

We compared the profiles of genes differentially regulated by three PAHs in the developing zebrafish embryo and identified disrupted biological processes that overlap notably with studies in other model systems. The genes differentially regulated by BAA were consistent with previous reports of AHR activation by this PAH, and many of them were identified in array studies with other known AHR ligands in zebrafish. All three PAHs misregulated genes important in vasculature development and cardiac function. This has been observed in BaP-exposed rats, as well as in previous studies of fish exposed to a number of PAHs (Incardona et al. 2009; Incardona et al. 2011; Huang et al. 2012; Jules et al. 2012). Oxidative stress was a component of the toxic response, as has also been reported previously, and we observed differential regulation of immune-related genes, particularly by DBT and PYR. Though fewer studies have examined PAHs that are not strong AHR agonists, PAHs that do not induce CYP1A have similarly been observed to induce inflammatory cytokines in cells in culture (Suresh et al. 2009; Ovrevik et al. 2010). PAHs are known immunotoxicants in fish, with well-established effects on lymphocytes (Krieger et al. 1994; Reynaud and Deschaux

2006). The gene expression changes observed in this study, however, primarily represent innate immune responses, as the adaptive immune system is not mature until weeks 4-6 of development (Meeker and Trede 2008). We therefore would not expect to see substantial overlap between the genes observed in this study and others conducted with tissues from adult organisms. Nevertheless, calcium binding and immune response were identified as important differentially expressed gene clusters in human macrophage leukemia cells exposed to diverse PAHs in vitro, and metal ion binding and transport were the most significant biological processes associated with occupational PAH exposure in peripheral blood of coke-oven workers (Wan et al. 2008; Wu et al. 2011). Chronic PAH exposure in coke-oven workers has also been associated with altered immunological parameters, including increased TNF α in serum, as well increased markers of lipid peroxidation and oxidative stress (Jeng et al. 2011). Increased malondialdehyde and decreased reduced glutathione were similarly observed in bronchial asthma patients, and correlated with blood phenanthrene levels, providing further evidence of PAH-induced oxidative stress in human populations (Suresh et al. 2009).

We identified multiple potential biomarkers of individual PAHs over time, as well as genes commonly misregulated by PAHs with differential AHR affinity. Many of the significant biological processes disrupted in this study, such as ion homeostasis, have been observed previously in other models, and provide insight into fundamental molecular pathways that are sensitive to PAH exposure and conserved between organ systems and species. Further investigation of these pathways in response to more structurally diverse PAHs in the environment will be invaluable to understanding the hazard potential of PAH exposure during development.

Acknowledgements

We are grateful to Cari Buchner, Carrie Barton and the staff at the Sinnhuber Aquatic Research Laboratory for fish husbandry expertise. Bradley Stewart processed the microarrays at the University of Wisconsin McArdle Laboratory of Cancer Research Microarray Facility. We would also like to thank Tanguay laboratory members, in particular Jane La Du, Michael Simonich and Sean Bugel, for their feedback and critical review of the manuscript. This work was supported by the NIEHS Superfund Research Program P42 ES016465, Core Center Grant P30 ES000210 and the NIEHS Training Grant T32 ES007060.

Pacific Northwest National Laboratory is a multi-program national laboratory operated by Battelle Memorial Institute for the DOE under contract number DE-AC05-76RL01830.

References

- Alexeyenko, A., D. M. Wassenberg, et al. (2010). "Dynamic zebrafish interactome reveals transcriptional mechanisms of dioxin toxicity." PLoS One **5**(5): e10465.
- Andreasen, E. A., J. M. Spitsbergen, et al. (2002). "Tissue-specific expression of AHR2, ARNT2, and CYP1A in zebrafish embryos and larvae: effects of developmental stage and 2,3,7,8-tetrachlorodibenzo-p-dioxin exposure." Toxicol Sci **68**(2): 403-419.
- Archuleta, M. M., G. L. Schieven, et al. (1993). "7,12-Dimethylbenz[a]anthracene activates protein-tyrosine kinases Fyn and Lck in the HPB-ALL human T-cell line and increases tyrosine phosphorylation of phospholipase C-gamma 1, formation of inositol 1,4,5-trisphosphate, and mobilization of intracellular calcium." Proc Natl Acad Sci U S A **90**(13): 6105-6109.
- Barron, M. G., R. Heintz, et al. (2004). "Relative potency of PAHs and heterocycles as aryl hydrocarbon receptor agonists in fish." Mar Environ Res **58**(2-5): 95-100.
- Benjamini, Y. and Y. Hochberg (1995). "Controlling the False Discovery Rate - a Practical and Powerful Approach to Multiple Testing." Journal of the Royal Statistical Society Series B-Methodological **57**(1): 289-300.
- Binder, R. L. and J. J. Stegeman (1984). "Microsomal electron transport and xenobiotic monooxygenase activities during the embryonic period of development in the killifish, *Fundulus heteroclitus*." Toxicol Appl Pharmacol **73**(3): 432-443.
- Bostrom, C. E., P. Gerde, et al. (2002). "Cancer risk assessment, indicators, and guidelines for polycyclic aromatic hydrocarbons in the ambient air." Environ Health Perspect **110 Suppl 3**: 451-488.
- Brasier, A. R., M. Jamaluddin, et al. (2000). "Angiotensin II induces gene transcription through cell-type-dependent effects on the nuclear factor-kappaB (NF-kappaB) transcription factor." Mol Cell Biochem **212**(1-2): 155-169.
- Brasier, A. R. and J. Li (1996). "Mechanisms for inducible control of angiotensinogen gene transcription." Hypertension **27**(3 Pt 2): 465-475.
- Burstyn, I., H. Kromhout, et al. (2005). "Polycyclic aromatic hydrocarbons and fatal ischemic heart disease." Epidemiology **16**(6): 744-750.
- Bussmann, J., S. A. Wolfe, et al. (2011). "Arterial-venous network formation during brain vascularization involves hemodynamic regulation of chemokine signaling." Development **138**(9): 1717-1726.
- Carney, S. A., J. Chen, et al. (2006). "Aryl hydrocarbon receptor activation produces heart-specific transcriptional and toxic responses in developing zebrafish." Mol Pharmacol **70**(2): 549-561.
- Choi, H., W. Jedrychowski, et al. (2006). "International studies of prenatal exposure to polycyclic aromatic hydrocarbons and fetal growth." Environ Health Perspect **114**(11): 1744-1750.
- Ciganek, M., J. Neca, et al. (2004). "A combined chemical and bioassay analysis of traffic-emitted polycyclic aromatic hydrocarbons." Sci Total Environ **334-335**: 141-148.
- Collins, J. F., J. P. Brown, et al. (1998). "Potency equivalency factors for some polycyclic aromatic hydrocarbons and polycyclic aromatic hydrocarbon derivatives." Regul Toxicol Pharmacol **28**(1): 45-54.

- Detmar, J., M. Y. Rennie, et al. (2008). "Fetal growth restriction triggered by polycyclic aromatic hydrocarbons is associated with altered placental vasculature and AhR-dependent changes in cell death." *Am J Physiol Endocrinol Metab* **295**(2): E519-530.
- Durant, J. L., W. F. Busby, Jr., et al. (1996). "Human cell mutagenicity of oxygenated, nitrated and unsubstituted polycyclic aromatic hydrocarbons associated with urban aerosols." *Mutat Res* **371**(3-4): 123-157.
- Ebert, A. M., G. L. Hume, et al. (2005). "Calcium extrusion is critical for cardiac morphogenesis and rhythm in embryonic zebrafish hearts." *Proc Natl Acad Sci U S A* **102**(49): 17705-17710.
- EPA, U. (2012). "Integrated Risk Information System." from <http://www.epa.gov/iris/>.
- Gao, J., A. A. Voss, et al. (2005). "Ryanodine receptor-mediated rapid increase in intracellular calcium induced by 7,8-benzo(a)pyrene quinone in human and murine leukocytes." *Toxicol Sci* **87**(2): 419-426.
- Guengerich, F. P. (2000). "Metabolism of chemical carcinogens." *Carcinogenesis* **21**(3): 345-351.
- Hansch, C., Albert, L., Hoekman, D. (1995). *Exploring QSAR: Volume 2: Hydrophobic, Electronic, and Steric Constants*, American Chemical Society.
- Hecht, S. S., S. G. Carmella, et al. (2010). "Analysis of phenanthrene and benzo[a]pyrene tetraol enantiomers in human urine: relevance to the bay region diol epoxide hypothesis of benzo[a]pyrene carcinogenesis and to biomarker studies." *Chem Res Toxicol* **23**(5): 900-908.
- Hermann, A., R. Donato, et al. (2012). "S100 calcium binding proteins and ion channels." *Front Pharmacol* **3**: 67.
- Hertz-Picciotto, I., H. Y. Park, et al. (2008). "Prenatal exposures to persistent and non-persistent organic compounds and effects on immune system development." *Basic Clin Pharmacol Toxicol* **102**(2): 146-154.
- Huang da, W., B. T. Sherman, et al. (2009). "Systematic and integrative analysis of large gene lists using DAVID bioinformatics resources." *Nat Protoc* **4**(1): 44-57.
- Huang, L., C. Wang, et al. (2012). "Benzo[a]pyrene exposure influences the cardiac development and the expression of cardiovascular relative genes in zebrafish (Daniorerio) embryos." *Chemosphere* **87**(4): 369-375.
- Incardona, J. P., M. G. Carls, et al. (2009). "Cardiac arrhythmia is the primary response of embryonic Pacific herring (*Clupea pallasii*) exposed to crude oil during weathering." *Environ Sci Technol* **43**(1): 201-207.
- Incardona, J. P., M. G. Carls, et al. (2005). "Aryl hydrocarbon receptor-independent toxicity of weathered crude oil during fish development." *Environ Health Perspect* **113**(12): 1755-1762.
- Incardona, J. P., T. K. Collier, et al. (2004). "Defects in cardiac function precede morphological abnormalities in fish embryos exposed to polycyclic aromatic hydrocarbons." *Toxicol Appl Pharmacol* **196**(2): 191-205.
- Incardona, J. P., H. L. Day, et al. (2006). "Developmental toxicity of 4-ring polycyclic aromatic hydrocarbons in zebrafish is differentially dependent on AH receptor isoforms and hepatic cytochrome P4501A metabolism." *Toxicol Appl Pharmacol* **217**(3): 308-321.
- Incardona, J. P., T. L. Linbo, et al. (2011). "Cardiac toxicity of 5-ring polycyclic aromatic hydrocarbons is differentially dependent on the aryl hydrocarbon receptor 2 isoform during zebrafish development." *Toxicol Appl Pharmacol* **257**(2): 242-249.

- Isidoro Tavares, N., P. Philip-Couderc, et al. (2009). "Angiotensin II and tumour necrosis factor alpha as mediators of ATP-dependent potassium channel remodelling in post-infarction heart failure." Cardiovasc Res **83**(4): 726-736.
- Jeng, H. A., C. H. Pan, et al. (2011). "Polycyclic aromatic hydrocarbon-induced oxidative stress and lipid peroxidation in relation to immunological alteration." Occup Environ Med **68**(9): 653-658.
- Jules, G. E., S. Pratap, et al. (2012). "In utero exposure to benzo(a)pyrene predisposes offspring to cardiovascular dysfunction in later-life." Toxicology.
- Jung, K. H., J. H. Noh, et al. (2011). "Molecular signature for early detection and prediction of polycyclic aromatic hydrocarbons in peripheral blood." Environ Sci Technol **45**(1): 300-306.
- Kimmel, C. B., W. W. Ballard, et al. (1995). "Stages of embryonic development of the zebrafish." Dev Dyn **203**(3): 253-310.
- Kluver, N., L. Yang, et al. (2011). "Transcriptional response of zebrafish embryos exposed to neurotoxic compounds reveals a muscle activity dependent hspb11 expression." PLoS One **6**(12): e29063.
- Kojic, S., D. Radojkovic, et al. (2011). "Muscle ankyrin repeat proteins: their role in striated muscle function in health and disease." Crit Rev Clin Lab Sci **48**(5-6): 269-294.
- Krieger, J. A., J. L. Born, et al. (1994). "Persistence of calcium elevation in the HPB-ALL human T cell line correlates with immunosuppressive properties of polycyclic aromatic hydrocarbons." Toxicol Appl Pharmacol **127**(2): 268-274.
- Krieger, J. A., D. R. Davila, et al. (1995). "Inhibition of sarcoplasmic/endoplasmic reticulum calcium ATPases (SERCA) by polycyclic aromatic hydrocarbons in HPB-ALL human T cells and other tissues." Toxicol Appl Pharmacol **133**(1): 102-108.
- Le Mevel, J. C., F. Lancien, et al. (2008). "Central cardiovascular actions of angiotensin II in trout." Gen Comp Endocrinol **157**(1): 27-34.
- Lee, M. S., S. Magari, et al. (2011). "Cardiac autonomic dysfunction from occupational exposure to polycyclic aromatic hydrocarbons." Occup Environ Med **68**(7): 474-478.
- Mandrell, D., L. Truong, et al. (2012). "Automated zebrafish chorion removal and single embryo placement: optimizing throughput of zebrafish developmental toxicity screens." J Lab Autom **17**(1): 66-74.
- Mao, C., L. Shi, et al. (2009). "Development of fetal brain renin-angiotensin system and hypertension programmed in fetal origins." Prog Neurobiol **87**(4): 252-263.
- Mathew, R., J. A. McGrath, et al. (2008). "Modeling polycyclic aromatic hydrocarbon bioaccumulation and metabolism in time-variable early life-stage exposures." Environ Toxicol Chem **27**(7): 1515-1525.
- Mbewe-Campbell, N., Z. Wei, et al. (2012). "Genes and environment: novel, functional polymorphism in the human cathepsin L (CTSL1) promoter disrupts a xenobiotic response element (XRE) to alter transcription and blood pressure." J Hypertens.
- Meeker, N. D. and N. S. Trede (2008). "Immunology and zebrafish: spawning new models of human disease." Dev Comp Immunol **32**(7): 745-757.
- Menzie, C. A., B. B. Potocki, et al. (1992). "Exposure to Carcinogenic Pahs in the Environment." Environmental Science & Technology **26**(7): 1278-1284.
- Morey, J. S., J. C. Ryan, et al. (2006). "Microarray validation: factors influencing correlation between oligonucleotide microarrays and real-time PCR." Biol Proced Online **8**: 175-193.

- Naumova, Y. Y., S. J. Eisenreich, et al. (2002). "Polycyclic aromatic hydrocarbons in the indoor and outdoor air of three cities in the U.S." Environ Sci Technol **36**(12): 2552-2559.
- Nebert, D. W., T. P. Dalton, et al. (2004). "Role of aryl hydrocarbon receptor-mediated induction of the CYP1 enzymes in environmental toxicity and cancer." J Biol Chem **279**(23): 23847-23850.
- Nebert, D. W., A. L. Roe, et al. (2000). "Role of the aromatic hydrocarbon receptor and [Ah] gene battery in the oxidative stress response, cell cycle control, and apoptosis." Biochem Pharmacol **59**(1): 65-85.
- Nikolsky, Y., E. Kirillov, et al. (2009). "Functional analysis of OMICs data and small molecule compounds in an integrated "knowledge-based" platform." Methods Mol Biol **563**: 177-196.
- Ovrevik, J., V. M. Arlt, et al. (2010). "Differential effects of nitro-PAHs and amino-PAHs on cytokine and chemokine responses in human bronchial epithelial BEAS-2B cells." Toxicol Appl Pharmacol **242**(3): 270-280.
- Park, K. and A. L. Scott (2010). "Cholesterol 25-hydroxylase production by dendritic cells and macrophages is regulated by type I interferons." J Leukoc Biol **88**(6): 1081-1087.
- Petersen, G. I. and P. Kristensen (1998). "Bioaccumulation of lipophilic substances in fish early life stages." Environmental Toxicology and Chemistry **17**(7): 1385-1395.
- Pfaffl, M. W. (2001). "A new mathematical model for relative quantification in real-time RT-PCR." Nucleic Acids Res **29**(9): e45.
- Planchart, A. and C. J. Mattingly (2010). "2,3,7,8-Tetrachlorodibenzo-p-dioxin upregulates FoxQ1b in zebrafish jaw primordium." Chem Res Toxicol **23**(3): 480-487.
- Polidori, A., J. Kwon, et al. (2010). "Source proximity and residential outdoor concentrations of PM(2.5), OC, EC, and PAHs." J Expo Sci Environ Epidemiol **20**(5): 457-468.
- Price, R. L., W. Carver, et al. (1997). "The effects of angiotensin II and specific angiotensin receptor blockers on embryonic cardiac development and looping patterns." Dev Biol **192**(2): 572-584.
- Ramesh, A., S. A. Walker, et al. (2004). "Bioavailability and risk assessment of orally ingested polycyclic aromatic hydrocarbons." Int J Toxicol **23**(5): 301-333.
- Ramirez, N., A. Cuadras, et al. (2011). "Risk assessment related to atmospheric polycyclic aromatic hydrocarbons in gas and particle phases near industrial sites." Environ Health Perspect **119**(8): 1110-1116.
- Reimers, M. J., J. K. La Du, et al. (2006). "Ethanol-dependent toxicity in zebrafish is partially attenuated by antioxidants." Neurotoxicol Teratol **28**(4): 497-508.
- Ren, A., X. Qiu, et al. (2011). "Association of selected persistent organic pollutants in the placenta with the risk of neural tube defects." Proc Natl Acad Sci U S A **108**(31): 12770-12775.
- Rennie, M. Y., J. Detmar, et al. (2011). "Vessel tortuosity and reduced vascularization in the fetoplacental arterial tree after maternal exposure to polycyclic aromatic hydrocarbons." Am J Physiol Heart Circ Physiol **300**(2): H675-684.
- Reynaud, S. and P. Deschaux (2006). "The effects of polycyclic aromatic hydrocarbons on the immune system of fish: a review." Aquat Toxicol **77**(2): 229-238.
- Saeed, A. I., V. Sharov, et al. (2003). "TM4: a free, open-source system for microarray data management and analysis." Biotechniques **34**(2): 374-378.

- Shannon, P., A. Markiel, et al. (2003). "Cytoscape: a software environment for integrated models of biomolecular interaction networks." Genome Res **13**(11): 2498-2504.
- Shi, Z., N. Dragin, et al. (2010). "Organ-specific roles of CYP1A1 during detoxication of dietary benzo[a]pyrene." Mol Pharmacol **78**(1): 46-57.
- Suresh, R., A. Shally, et al. (2009). "Assessment of association of exposure to polycyclic aromatic hydrocarbons with bronchial asthma and oxidative stress in children: A case control study." Indian J Occup Environ Med **13**(1): 33-37.
- Tian, B., D. E. Nowak, et al. (2005). "A TNF-induced gene expression program under oscillatory NF-kappaB control." BMC Genomics **6**: 137.
- Tian, Y., S. Ke, et al. (1999). "Ah receptor and NF-kappaB interactions, a potential mechanism for dioxin toxicity." J Biol Chem **274**(1): 510-515.
- Tilton, S. C., T. L. Tal, et al. (2012). "Bioinformatics resource manager v2.3: an integrated software environment for systems biology with microRNA and cross-species analysis tools." BMC Bioinformatics **13**(1): 311.
- Truong, L., S. L. Harper, et al. (2011). "Evaluation of embryotoxicity using the zebrafish model." Methods Mol Biol **691**: 271-279.
- Van Metre, P. C. and B. J. Mahler (2005). "Trends in hydrophobic organic contaminants in urban and reference lake sediments across the United States, 1970-2001." Environ Sci Technol **39**(15): 5567-5574.
- Van Metre, P. C. and B. J. Mahler (2010). "Contribution of PAHs from coal-tar pavement sealcoat and other sources to 40 U.S. lakes." Sci Total Environ **409**(2): 334-344.
- Vanwezel, A. P. and A. Opperhuizen (1995). "Narcosis Due to Environmental-Pollutants in Aquatic Organisms - Residue-Based Toxicity, Mechanisms, and Membrane Burdens." Critical Reviews in Toxicology **25**(3): 255-279.
- Vlecken, D. H., J. Testerink, et al. (2009). "A critical role for myoglobin in zebrafish development." Int J Dev Biol **53**(4): 517-524.
- Wan, B., J. W. Yarbrough, et al. (2008). "Structure-related clustering of gene expression fingerprints of thp-1 cells exposed to smaller polycyclic aromatic hydrocarbons." SAR QSAR Environ Res **19**(3-4): 351-373.
- Wassenberg, D. M., A. L. Nerlinger, et al. (2005). "Effects of the polycyclic aromatic hydrocarbon heterocycles, carbazole and dibenzothiophene, on in vivo and in vitro CYP1A activity and polycyclic aromatic hydrocarbon-derived embryonic deformities." Environ Toxicol Chem **24**(10): 2526-2532.
- Wiens, G. D. and G. W. Glenney (2011). "Origin and evolution of TNF and TNF receptor superfamilies." Dev Comp Immunol **35**(12): 1324-1335.
- Wu, C., H. Lu, et al. (2011). "Molecular and Pathophysiological Features of Angiotensinogen: A Mini Review." N Am J Med Sci (Boston) **4**(4): 183-190.
- Wu, M. T., T. C. Lee, et al. (2011). "Whole genome expression in peripheral-blood samples of workers professionally exposed to polycyclic aromatic hydrocarbons." Chem Res Toxicol **24**(10): 1636-1643.
- Xiong, K. M., R. E. Peterson, et al. (2008). "Aryl hydrocarbon receptor-mediated down-regulation of sox9b causes jaw malformation in zebrafish embryos." Mol Pharmacol **74**(6): 1544-1553.

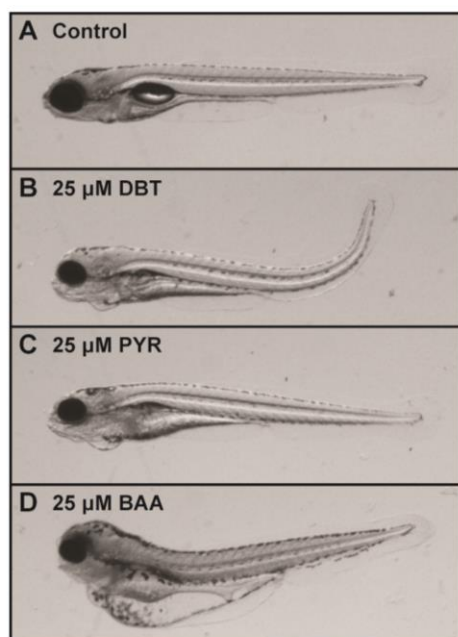


Figure 2-1 PAHs induce abnormalities in developing zebrafish

Representative images of 120 hpf larvae after exposure to (A) 1% DMSO control, (B) 25 μ M DBT, (C) 25 μ M PYR, and (D) 25 μ M BAA from 6 to 48 hpf.

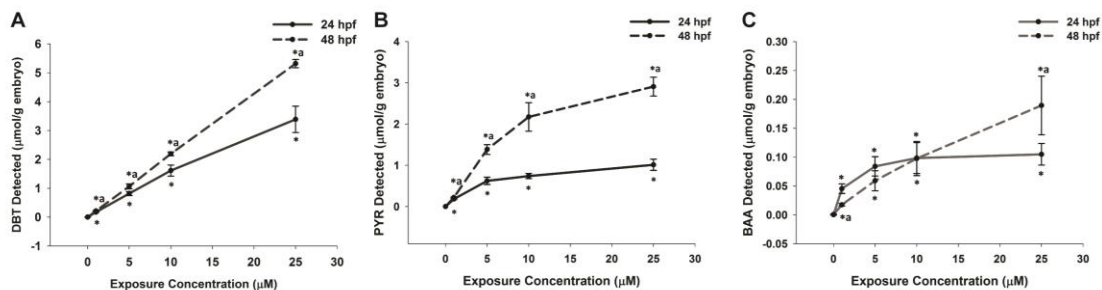


Figure 2-2 Body burdens of PAH detected in embryos

PAH was detected in embryos exposed to (A) DBT, (B) PYR, and (C) BAA from 6 to 24 (solid lines) or 48 (dashed lines) hpf. *Significantly different than time-matched DMSO control (Mann-Whitney rank sum test, $p < 0.05$). ^aSignificant difference between 48 and 24 hpf samples at the same exposure concentration (Mann-Whitney rank sum test, $p < 0.05$).

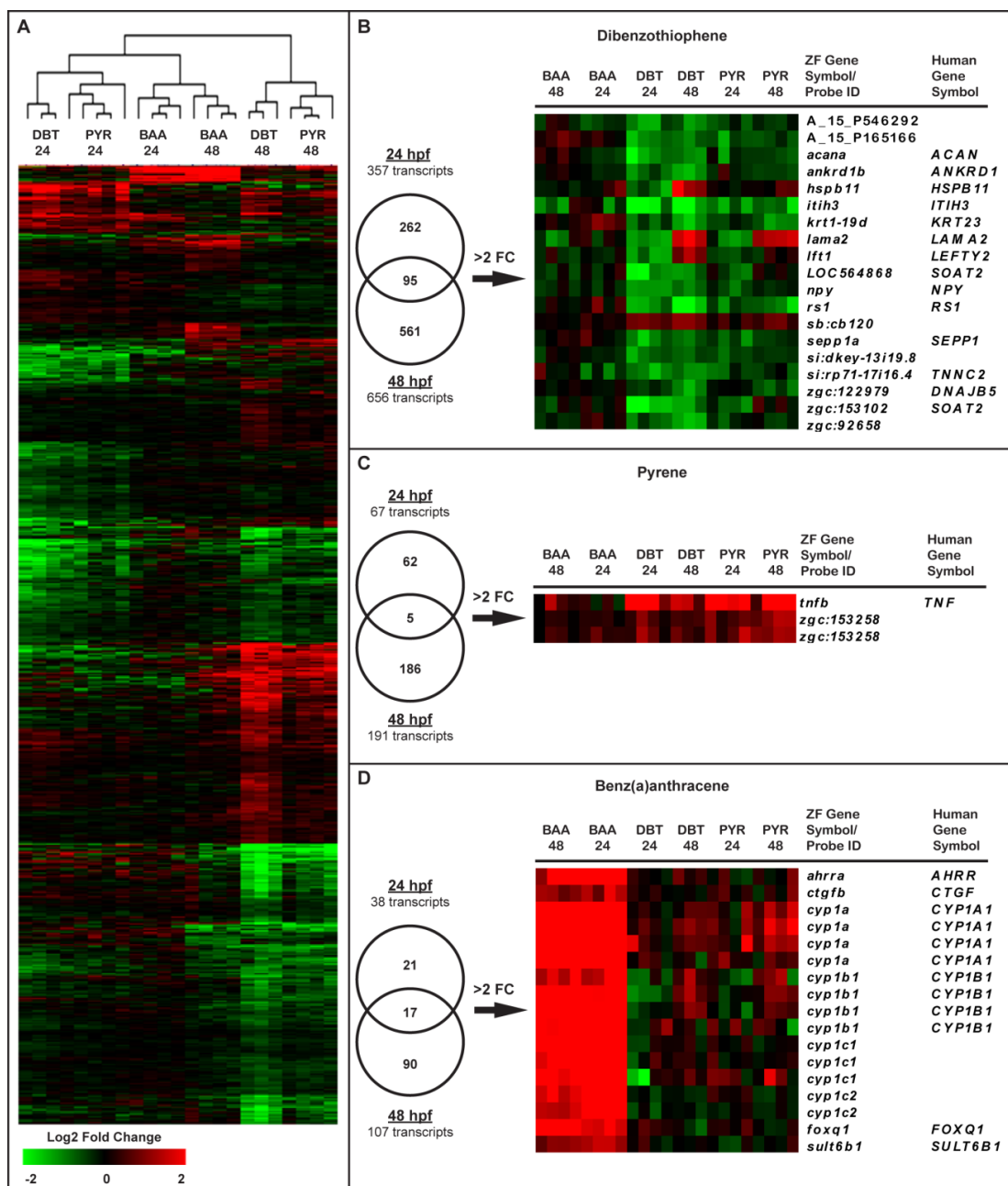


Figure 2-3 Differentially expressed transcripts in PAH-exposed embryos

A) Bidirectional hierarchical clustering heatmap of log2 fold change (FC) values of all 1079 genes significantly differentially expressed compared to control (One-way ANOVA with 5% FDR, adjusted p value < 0.05). Comparison of significant genes between 24 and 48 hpf for (B) DBT, (C) PYR and (D) BAA exposure groups is shown by Venn diagram. Heatmap enlargements show transcripts differentially expressed (adjusted p value < 0.05, >2-FC) at both time points for each PAH.

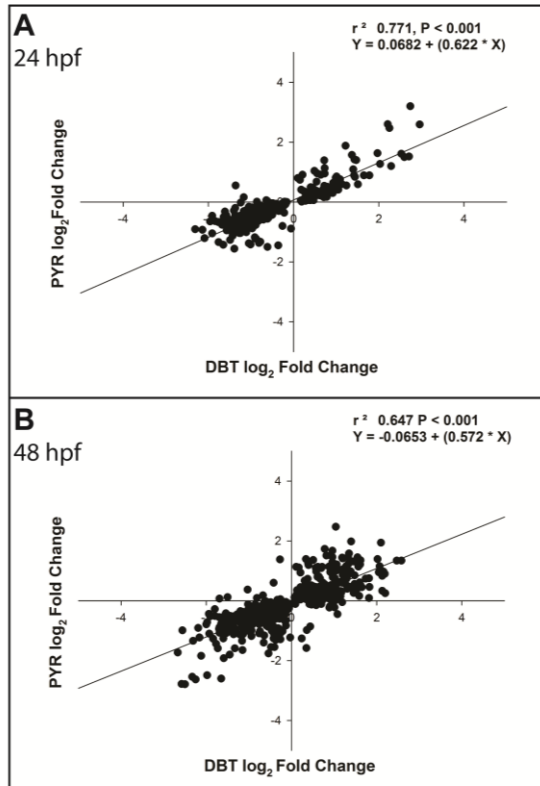


Figure 2-4 Direct comparison of PYR and DBT expression values

Comparison of gene expression between PYR and DBT treatment groups at 24 and 48 hpf. Linear regressions of \log_2 FC values for the union of transcripts significantly ($p < 0.05$) misregulated by DBT or PYR compared to control ($n = 712$). Linear associations at (A) 24 hpf and (B) 48 hpf were both significant ($p < 0.001$).

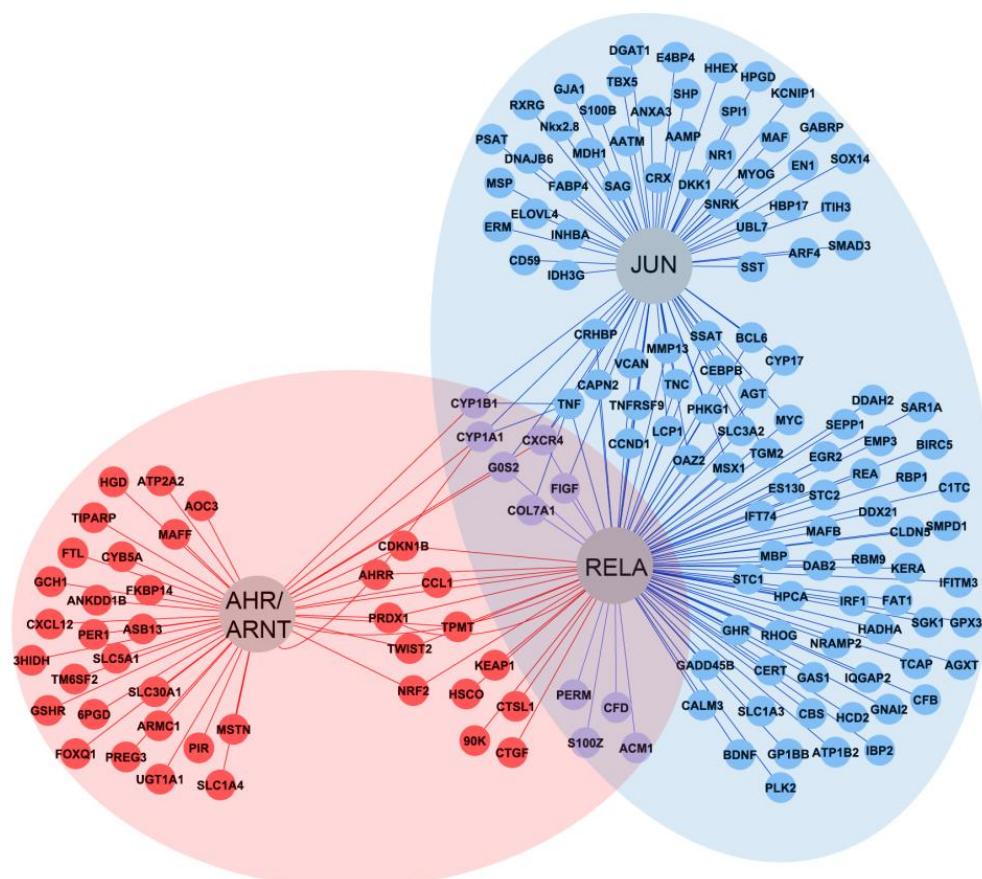


Figure 2-5 Comparison of AHR, RELA and JUN regulatory networks

Networks of transcripts under regulatory control of AHR, RELA and JUN, that were misregulated in response to BAA (red), or DBT/PYR (blue) exposure. Transcripts that overlapped between the two PAH networks are represented in purple. Significant transcripts ($p < 0.05$) from both the 24 and 48 hpf time points were combined to create the regulatory network.

Table 2-1 Developmental abnormalities in PAH-exposed embryos

Mean percentage of embryos (95 percentile) with malformations observed at 120 hpf following exposure to 25 µM BAA, DBT, PYR or DMSO control from 6 to 48 hpf. * Significantly different than DMSO Control, p < 0.05, one-way ANOVA with Dunnett's post hoc test.

Effect								
Treatment	Mortality	Axis	Eye	Jaw	Pericardial Edema	Snout	Yolk Sac	Any Malformation
Control	4 (1, 13)	3.1 (1, 10)	4.2 (1, 16)	7.3 (2, 21)	4.2 (1, 13)	4.2 (1, 15)	4.2 (1, 15)	11 (5, 22)
DBT	3.3 (0, 58)	44.8 (9, 87)*	15.5 (1, 78)	75.9 (21, 97)*	55.2 (12, 92)*	19 (2, 76)*	15.5 (1, 75)	83.3 (39, 97)*
PYR	5 (0, 57)	12.3 (1, 61)	5.3 (0, 72)	98.3 (33, 100)*	68.4 (19, 95)*	22.8 (2, 79)*	36.8 (4, 88)*	98.3 (33, 100)*
BAA	1.7 (0, 67)	8.5 (1, 55)	10.2 (0, 74)	81.4 (25, 98)*	74.6 (23, 97)*	32.2 (4, 85)*	54.2 (9, 94)*	85 (41, 98)*

Table 2-2 Comparison of malformations induced by PAH treatments

P values of Tukey's all pairwise post hoc test are displayed for each comparison, malformations that were significantly different between treatment groups are shaded ($p < 0.05$).

Test	Effect							
	Mortality	Axis	Eye	Jaw	Pericardial Edema	Snout	Yolk Sac	Any Malformation
DBT v Control	8.53E-01	4.30E-06	1.41E-01	2.70E-06	2.50E-06	4.66E-02	1.01E-01	7.20E-09
PYR v Control	7.09E-01	6.02E-02	6.53E-01	1.50E-04	3.10E-08	2.22E-02	1.87E-03	2.10E-05
BAA v Control	9.47E-01	1.83E-01	3.31E-01	8.20E-07	4.60E-09	3.44E-03	3.10E-05	6.10E-09
DBT v PYR	9.31E-01	1.91E-03	4.84E-01	1.75E-01	4.63E-01	9.27E-01	1.67E-01	1.85E-01
BAA v DBT	8.93E-01	5.10E-04	8.34E-01	8.83E-01	1.80E-01	4.59E-01	8.26E-03	9.80E-01
BAA v PYR	7.23E-01	8.07E-01	7.93E-01	2.58E-01	8.22E-01	6.87E-01	3.78E-01	2.21E-01

Table 2-3 Biological functions affected by PAH exposure at 24 hpf

Significantly enriched biological functions identified by DAVID analysis of all transcripts differentially regulated (adjusted p value < 0.05) by BAA exposure or by DBT and PYR at 24 hpf. E score: overall cluster enrichment score, %: percentage of total gene list involved in functional cluster, p-values determined by modified Fischer's Exact test (EASE score).

	Biological Process	GO Term	Downregulated genes	Upregulated genes	E Score	%	P Value
BAA	hormone metabolic process	GO:0042445		<i>cyp1a, cyp1b1, cyp1c1, cyp1c2, si:dkey-94e7.2</i>	2.06	15.79	5.12E-03
	tissue development	GO:0009888	<i>mstnb</i>	<i>foxq1l, ptn, ctgfb</i>	1.21	21.05	2.77E-02
DBT and PYR	fatty acid biosynthetic process	GO:0006633	<i>elovl6, fads2, ptgds, si:ch73-131e21.5, tpi1b</i>	<i>ch25h, elovl7a</i>	2.67	3.02	6.10E-04
	ion transport	GO:0006811	<i>atp2a1l, cpt1b, gabra1, grin1b, KCNAB1, kcnip1b, kcnip3, LOC100004247, rhbg, sfxn4, si:ch211-195b13.1, si:ch211-221p4.4, slc24a5, zgc:101827, zgc:113361, zgc:158296</i>	<i>LOC571584, si:ch211-244h7.4, slc22a18, slc31a1, tmem38b, zgc:162356, zgc:162495</i>	2.32	8.30	7.86E-03
	skeletal muscle contraction	GO:0003009	<i>homer1, mb, si:rp71-17i16.4, tnni2b.2</i>		2.18	1.51	1.10E-03
	steroid biosynthetic process	GO:0006694	<i>cyp17a1, hmgcs1, hsd17b7, lss, nsdhl, rdh8l</i>	<i>ch25h, dhcr7</i>	2.14	3.02	9.43E-04
	oxoacid metabolic process	GO:0043436	<i>acsf3, cpt1b, elovl6, fabp11b, fads2, ghra, hibadhb, mdh1b, ptgds, rbp1a, rnpep, si:ch73-131e21.5, tpi1b, tyrp1b, zgc:113076, zgc:154046</i>	<i>ch25h, elovl7a, mthfd1</i>	1.93	7.17	1.27E-02
	intermediate filament organization	GO:0045109	<i>dnajb6b, krt1-19d, krt23, nefm</i>		1.80	1.13	6.71E-03
	negative regulation of cell proliferation	GO:0008285	<i>bdnf, cd9a, cx43, smad3b, tnfrsf9a, wfad1, zgc:114127, zgc:158296</i>	<i>agt, msxe, notch2, tbx16, tnfb</i>	1.77	4.91	1.67E-02
	muscle cell development	GO:0055001	<i>homer1, LOC796577, myoz1a, zgc:158296</i>	<i>myog</i>	1.71	1.89	1.89E-02
	sterol biosynthetic process	GO:0016126	<i>hmgcs1, lss, nsdhl</i>	<i>ch25h, dhcr7</i>	1.56	1.89	5.49E-03

Table 2-3 (Continued)

	Biological Process	GO Term	Downregulated genes	Upregulated genes	E Score	%	P Value
DBT and PYR	cellular amide metabolic process	GO:0043603	<i>ghra, hibadhb, mdh1b, tpi1b, zgc:113076</i>		1.41	1.89	2.64E-02
	monosaccharide catabolic process	GO:0046365	<i>hibadhb, mdh1b, pfkma, tpi1b, zgc:162337</i>		1.28	1.89	3.16E-02
	regulation of erythrocyte differentiation	GO:0045646		<i>inhbaa, mafba, spi1l</i>	1.09	1.13	4.65E-02

Table 2-4 Biological functions affected by PAH exposure at 48 hpf

Significantly enriched biological functions identified by DAVID analysis of all transcripts differentially regulated (adjusted p value < 0.05) in BAA exposed embryos, and common transcripts disrupted by DBT and PYR at 48 hpf. E score: overall cluster enrichment score, %: percentage of total gene list involved in functional cluster, p-values determined by modified Fischer's Exact test (EASE score).

	Biological Process	GO Term	Downregulated Genes	Upregulated Genes	E Score	%	P Value
BAA	cellular homeostasis	GO:0019725	<i>edn2, cxcl12b, atp2a2a</i>	<i>slc30a1, cxcr4a, zgc:92066, gsr, prdx1, ccl1, ccr9a</i>	2.75	14.29	4.50E-04
	chemotaxis	GO:0006935	<i>cxcl12b, edn2</i>	<i>ccr9a, cxcr4a, ccl1</i>	2.50	7.14	2.18E-03
	hormone met. process	GO:0042445	<i>lrata</i>	<i>ugt1b5, ugt1b7, cyp1b1, cyp1c2, cyp1a, cyp1c1</i>	2.16	5.71	1.26E-02
	tetrapyrrole met. process	GO:0033013	-	<i>zgc:77234, ugt1b5, ugt1b7, cyp1a</i>	1.92	4.29	1.25E-02
	vasculature development	GO:0001944	<i>cx39.4, cxcl12b</i>	<i>ctgfb, cxcr4a, figf, tiparp</i>	1.89	8.57	1.01E-02
	H ₂ O ₂ met. process	GO:0042743	-	<i>cyp1a, prdx1</i>	1.59	4.29	5.65E-03
	cation transport	GO:0006812	<i>armc1l, atp2a2a, cx39.4, slc5a1</i>	<i>cdkn1bl, slc30a1, zgc:92066</i>	1.32	10.00	3.83E-02
DBT and PYR	organ development	GO:0048513	<i>atp2a2a, col7a1, cx39.4, cxcl12b, edn2, prl, slc5a1</i>	<i>cdkn1bl, ctgfb, cxcr4a, cyp1a, figf, foxq1, foxf2a, tiparp, ved</i>	1.29	21.43	4.12E-02
	oxoacid metabolic process	GO:0043436	<i>acaa1, acadl, adipor1a, adipor1b, agxt2l1, agxta, agxtb, amt, cpt1b, elovl4b, glsa, got2a, hadha, hadhb, idh3b, LOC565975, lta4h, mdh1b, padi2, rbp2b, rnpep, sc5dl, sgpl1, zgc:113076, zgc:136850, zgc:154046</i>	<i>aspg, cbsb, cyp1a, cyp26c1, glc, npc1, phgdh, ppat, psat1, slc1a3a</i>	4.72	8.35	2.66E-05
	embryonic development ending in birth or egg hatching	GO:0009792	<i>ift52, ric8a, zfp2m2b</i>	<i>capn2b, cebpb, col4a3bp, cyp1a, eng1b, evx1, foxa, gas1b, gata2a, hoxa2b, hoxa4a, hoxb2a, hoxc1a, hoxc6b, msxe, nkx2.7, pax1a, phgdh, si:ch211-204c21.1, tcap, tgfb1a</i>	3.61	5.90	1.01E-04
	regionalization	GO:0003002	<i>egr2b, ift52, neurod</i>	<i>cyp26c1, egr2a, eng1b, evx1, foxa, gas1b, hhex, hoxa2b, hoxa4a, hoxb2a, hoxc4a, hoxc6b, pax1a, tcap, tgfb1a</i>	3.38	4.18	2.75E-04

Table 2-4 (Continued)

DBT and PYR	Biological Process	GO Term	Downregulated Genes	Upregulated Genes	E Score	%	P Value
	neurogenesis	GO:0022008	<i>bdnf, clic5, crx, egr2b, gnao1b, LOC799290, mbp, mbpa, neurod, otx5, rab3aa, rnd1, spon2b, vcanb</i>	<i>ascl1a, btg4, cebpb, cxcr4a, egr2a, eng1b, epha2, evx1, foxa, gas1b, gata2a, gdf7, her15.1, hoxa2b, mag, nr2f6b, phgdh, slc1a3a, tgfb1a, unc5b, uts1</i>	2.77	7.62	3.27E-03
	embryonic organ development	GO:0048568	<i>clic5, neurod, zfp2b</i>	<i>cebpb, gas1b, gata2a, hoxa2b, hoxa4a, hoxb2a, hoxc4a, myca, otop1, tcap, tgfb1a</i>	2.43	3.44	2.40E-03
	positive regulation of macromolecule metabolic process	GO:0010604	<i>crx, egr2b, fkb1ab, ift52, klf2a, LOC570917, maf, neurod, npas4, otx5, psmd4b, psmd7, psmd8, rxrga, tnai2b.2, zfp2b, zgc:110116</i>	<i>ascl1a, cask, cebpb, cebpg, egr2a, evx1, foxa, gata2a, gdf7, her15.1, hhex, hoxa2b, im:7162084, irf11, myca, pth1a, sox19a, tgfb1a, tnfb, uts1, vgl2b, zgc:158781</i>	2.35	9.34	2.19E-03
	negative regulation of cell communication	GO:0010648	<i>gnai2, hcrt, rgs11, zgc:136569, bcl6ab</i>	<i>cyp26c1, dkk1b, gas1b, hhex, im:7162084, npc1, oncut1, rgs4</i>	1.99	3.44	1.01E-02
	cellular component morphogenesis	GO:0032989	<i>bbs7, bdnf, clic5, cryaa, egr2b, rab3aa, spon2b, vcanb</i>	<i>bcl6ab, col4a3bp, cxcr4a, egr2a, gas1b, gdf7, hoxa2b, LOC796577, oncut1, sfrp5, si:ch211-204c21.1, slc1a3a, tcap, unc5b</i>	1.93	5.16	9.16E-03
	central nervous system development	GO:0007417	<i>egr2b, faim2, gnao1b, LOC799290, mbpa, mbpa, neurod, sepp1a, sh3gl2</i>	<i>ascl1a, cxcr4a, cyp26c1, dkk1b, egr2a, eng1b, evx1, foxa, gas1b, gata2a, hhex, hoxa2b, hoxb2a, msxe, nkx2.7, phgdh</i>	1.87	5.41	1.27E-02
	hormone met. process	GO:0042445	<i>lrta, rbp2b</i>	<i>crhbp, cyp1a, cyp1b1, cyp26c1, scarb1,</i>	1.82	1.97	1.51E-02
	organ morphogenesis	GO:0009887	<i>agc1, bbs7, clic5, crx, cryaa, cryaa, fkb1ab, ift52, neurod, otx5, sgpl1, six6a</i>	<i>cmlc1, gas1b, hhex, hoxa2b, hoxa4a, hoxb2a, hoxc4a, im:7162084, msxe, myca, otop1, tcap, tgfb1a, tnfb, zgc:158781</i>	1.79	6.39	1.62E-02
	fatty acid oxidation	GO:0019395	<i>acaa1, adipor1a, adipor1b, cpt1b, hadha, hadhb, zgc:154046</i>		1.66	1.47	7.21E-03

Table 2-4 (Continued)

DBT and PYR	Biological Process	GO Term	Downregulated Genes	Upregulated Genes	E Score	%	P Value
	muscle tissue dev.	GO:0060537	<i>fkbp1ab, LOC100536295, rxrga, zfp2m2b</i>	<i>cmlc1, LOC796577, nkx2.7, tcap, vgl2b</i>	1.65	2.21	2.45E-02
	reg. of transmission of nerve impulse	GO:0051969	<i>bdnf, cspg5b, egr2b, gnai2, hcrt, rab3aa, zgc:136569</i>	<i>egr2a, slc1a3a, tnfb, uts1</i>	1.58	2.46	2.56E-02
	pos. reg. of cellular process	GO:0048522	<i>bdnf, crx, egr2b, fkbp1ab, gnai2, hcrt, ift52, klf2a, LOC556700, LOC570917, maf, mfge8a, neurod, npas4, otx5, pnp4b, psmd4b, psmd7, psmd8, rxrga, si:ch211-135f11.1, tnni2b.2, trim35, zfp2m2b, zgc:100906, zgc:110116, zgc:110680</i>	<i>ascl1a, bcl6ab, cask, cebpb, cebpg, cyp1a, egf, egr2a, evx1, flt4, foxa, GAS1 (3 of 3), gas1b, gata2a, gdf7, her15.1, hhex, hoxa2b, im:7162084, irf11, LOC794658, myca, ncs1a, nkx2.7, oncut1, plk2b, pth1a, scarb1, si:dkey-24p1.4, slc1a3a, sox19a, sst1.1, tgfb1a, tnfb, uts1, vgl2b, zgc:154093, zgc:158781, zgc:85939</i>	1.57	15.5	2.29E-02
	oxidoreduction coenzyme met. process	GO:0006733	<i>coq3, idh3b, idh3g, itgb1bp3, mdh1b, pgls, pnp4b, zgc:113076</i>		1.55	1.72	3.73E-03
	pos. reg. of catalytic activity	GO:0043085	<i>gadd45bb, gnai2, gnao1b, gng13b, hcrt, psmd4b, psmd7, psmd8, ptplad1, rgn, si:ch211-135f11.1, zgc:110116</i>	<i>cmlc1, cxcr4a, egf, LOC794658, myca, npr3, pth1a, scarb1, slc11a2, tgfb1a, tnfb</i>	1.52	5.9	2.22E-02
	pyridine nucleotide metabolic process	GO:0019362	<i>idh3b, itgb1bp3, mdh1b, pgls, pnp4b, zgc:113076</i>		1.44	1.47	9.14E-03
	cellular amino acid metabolic process	GO:0006520	<i>agxt2l1, agxta, agxtb, amt, glsa, got2a, padi2</i>	<i>aspg, cbsb, gldc, phgdh, ppat, psat1, slc1a3a</i>	1.43	3.19	2.33E-02
	cell morph. involved in differentiation	GO:0000904	<i>bdnf, clic5, cryaa, egr2b, rab3aa, spon2b, vcanb</i>	<i>cxcr4a, egr2a, gas1b, gdf7, hoxa2b, si:ch211-204c21.1, slc1a3a, unc5b</i>	1.38	3.44	3.54E-02
	ear development	GO:0043583	<i>bdnf, clic5</i>	<i>gas1b, her15.1, hoxa2b, myca, otop1, tcap</i>	1.35	1.97	2.53E-02

Table 2-S1 Primer sequences used for qRT-PCR

Ensembl Transcript ID	Zebrafish Gene Symbol	Forward primer	Reverse Primer
ENSDART00000010918	<i>agt</i>	TGACGGACACACAGTTTAC	GTTGCTTCAGGTTGAAATGC
ENSDART00000105896	<i>atp2a1l</i>	AGCAGTTCATTGTTACCTG	AGAACAACCAGCCAGAAATC
ENSDART00000077511	<i>ccr9a</i>	GCATGTTGGTATTTGAAGCC	CTGTGTCCGACATAACAGAG
ENSDART00000066439	<i>ch25h</i>	ACCACAAATACACATCCACC	TCATTCAAAGTGCAAGTGTCC
ENSDART00000017756	<i>ctsl.1</i>	GGACTCCTACCCCTATGAAG	ATAACCAACAGCCAGAACAC
ENSDART00000038200	<i>cyp1a</i>	TGCCGATTTTCATCCCTTTCC	AGAGCCGTGCTGATAGTGTC
ENSDART00000099870	<i>cyp1b1</i>	CTGCATTGATTTCCGAGACGTG	CACACTCCGTGTTGACAGC
ENSDART00000019953	<i>cyp1c1</i>	AGTGGCACAGTCTACTTTGAGAG	TCGTCCATCAGCACTCAG
ENSDART00000016487	<i>cyp1c2</i>	GTGGTGGAGCACAGACTAAG	TTCAGTATGAGCCTCAGTCAAAC
ENSDART00000103784	<i>edn2</i>	CCAGGATCAGCTAGAGAGAG	ATTTCACTGGTGTGGAAGAG
ENSDART00000109464	<i>g0s2</i>	ATAACCACCGACAAACAAGG	AGCATGTCAAAGTCTGGTTC
ENSDART00000100386	<i>mstnb</i>	AAGAGGACGATGAACATGC	GATCGTATTCGGTGTCTTCC
ENSDART00000025669	<i>slc16a9b</i>	TCCCTGTCACCAAGAACTAC	TGAAGTAAAACGCCAGATCG
ENSDART00000130131	<i>sult6b1</i>	GTGGGTTTAACTGGATGGTG	GAGACCACTGTGTCTTTCG
ENSDART00000017569	<i>tnfb</i>	GTCTACAGCACCATTACC	ATTCAGTGCACAACTCTCAC

Table 2-S2 Percent recovery by GC-MS for PAH body burden studies

Percent recovery GC-MS method of PAH detection in zebrafish embryos, calculated from laboratory control samples spiked with BAA, DBT or PYR in DMSO.

Spike (nmoles)	Average Detected (nmoles)	Percent Recovery	Standard Deviation
BAA 24 hpf			
5	4.5	89.1	3.7
25	22.1	88.6	5.6
50	47.2	94.4	3.8
125	118.6	94.8	4.9
DBT 24 hpf			
5	5.1	101.4	2.5
25	25.0	100.1	1.7
50	49.9	99.9	3.8
125	134.5	107.6	2.6
PYR 24 hpf			
5	5.5	109.7	4.0
25	29.1	116.4	10.3
50	61.6	123.1	5.2
125	156.7	125.4	10.6
BAA 48 hpf			
5	4.6	91.1	1.1
25	20.1	80.3	1.5
50	44.1	88.2	3.0
125	111.3	89.0	2.5
DBT 48 hpf			
5	5.3	105.7	3.1
25	26.0	103.8	3.3
50	51.2	102.4	4.7
125	136.17	108.94	2.94
PYR 48 hpf			
5	5.1	102.3	6.1
25	25.8	103.4	3.7
50	56.0	111.9	4.2
125	144.7	115.8	5.2

Table 2-S4 Gene expression values detected by microarray and qRT-PCR

Mean log2 fold change and B-H adjusted p-values of differentially regulated transcripts from the microarray, compared with log2 fold change (mean \pm SD) detected with qRT-PCR. ^aSignificantly different from vehicle control (One-way ANOVA with Tukey's post hoc test and 5% FDR, $p < 0.05$) ^bSignificantly different from vehicle control (One-way ANOVA with Tukey's post hoc test, $p < 0.05$).

Zebrafish Gene Symbol	Human Gene Symbol	24 hpf								48 hpf									
		DBT Array log ₂ FC	DBT log ₂ FC	QPCR log ₂ FC	PYR Array log ₂ FC	PYR log ₂ FC	QPCR log ₂ FC	BAA Array log ₂ FC	BAA log ₂ FC	QPCR log ₂ FC	DBT Array log ₂ FC	DBT log ₂ FC	QPCR log ₂ FC	PYR Array log ₂ FC	PYR log ₂ FC	QPCR log ₂ FC	BAA Array log ₂ FC	BAA log ₂ FC	QPCR log ₂ FC
agt	AGT	2.6 ^a	2.7 ± 0.7 ^b	1.5	2.1 ± 1.3	-0.0	0.1 ± 0.9	---	---	---	---	---	---	---	---	---	---	---	---
atp2a1l	ATP2A1	-1.1 ^a	-1.8 ± 0.7	-0.6	-0.9 ± 0.8	-0.1	0.1 ± 0.9	---	---	---	---	---	---	---	---	---	---	---	---
ccr9a	CCR9	0.04	0.4 ± 1.0	0.2	0.8 ± 0.5	0.7	1.7 ± 0.5	-0.2	0.2 ± 0.5	-0.1	-0.2 ± 0.5	1.8 ^a	1.3 ± 0.3 ^a	---	---	---	---	---	---
ch25h	CH25H	2.2	2.7 ± 1.3 ^b	2.6 ^a	3.0 ± 1.1 ^b	0.1	1.0 ± 0.5	---	---	---	---	---	---	---	---	---	---	---	---
ctsl1	CTSL1	---	---	---	---	---	---	0.5	-0.2 ± 0.4	-0.1	-0.4 ± 0.1	2.1 ^a	1.7 ± 0.2 ^b	---	---	---	---	---	---
cyp1a	CYP1A1	0.6	-0.0 ± 0.5	0.7	0.5 ± 0.5	4.1 ^a	4.8 ± 0.4 ^b	0.3	0.8 ± 0.2	1.1	1.4 ± 0.5 ^b	5.1 ^a	6.6 ± 0.3 ^b	---	---	---	---	---	---
cyp1b1	CYP1B1	0.2	-0.8 ± 0.2	0.3	-0.5 ± 0.5	2.8 ^a	2.4 ± 0.3 ^b	-0.2	0.6 ± 0.3	0.0	0.1 ± 0.6	2.5 ^a	2.6 ± 0.3 ^b	---	---	---	---	---	---
cyp1c1	---	-0.8	-0.3 ± 0.4	0.5	-0.1 ± 0.5	2.5 ^a	2.2 ± 0.4 ^b	0.2	-0.2 ± 0.2	0.7	-0.2 ± 0.3	4.7 ^a	4.1 ± 0.4 ^b	---	---	---	---	---	---
cyp1c2	---	-0.2	-0.3 ± 0.2	0.3	0 ± 0.2	1.7 ^a	1.6 ± 0.3 ^b	-0.4	-0.2 ± 0.3	-0.2	-0.3 ± 0.3	2.5 ^a	3.1 ± 0.3 ^b	---	---	---	---	---	---
g0s2	G0S2	-1.3 ^a	-1.6 ± 0.4 ^b	-0.8	-0.5 ± 0.3	-0.2	0.1 ± 0.2	-0.2	-0.4 ± 0.5	-1.0 ^a	-0.8 ± 0.4	-1.1 ^a	-0.6 ± 0.2	---	---	---	---	---	---
mstnb	MSTN	-1.8 ^a	-0.7 ± 0.1	-0.6	-0.2 ± 0.3	-1.5 ^a	-0.3 ± 0.2	---	---	---	---	---	---	---	---	---	---	---	---
si:ch211-202b2.2	EDN2	---	---	---	---	---	---	-0.0	-0.0 ± 0.1	-0.3	0.0 ± 0.3	-0.9 ^a	-0.8 ± 0.2 ^b	---	---	---	---	---	---
slc16a9b	SLC16A9	3.0 ^a	3.3 ± 0.3 ^b	2.6 ^a	2.9 ± 0.4 ^b	0.2	0.3 ± 0.8	---	---	---	---	---	---	---	---	---	---	---	---
sult6b1	SULT6B1	0.1	0.1 ± 0.1	-0.2	0.2 ± 0.3	1.0 ^a	1.0 ± 0.2	0.0	-0.3 ± 0.3	0.0	-0.3 ± 0.2	1.4 ^a	1.0 ± 0.2 ^b	---	---	---	---	---	---
tnfb	TNF	2.7 ^a	2.9 ± 1.0 ^b	3.2 ^a	3.2 ± 0.6 ^b	0.6	0.0 ± 0.2	1.0	0.8 ± 0.2	2.5 ^a	2.3 ± 0.7 ^b	0.1	-0.2 ± 0.2	---	---	---	---	---	---

Table 2-S5 Predicted transcription factors for PAH responses

Transcription factors identified as significantly over-connected ($p < 0.05$) to genes differentially expressed ($p < 0.05$) in response to PAH exposure at 24 and 48 hpf. Significance was calculated by hypergeometric distribution in MetaCore. Actual: Number of genes in the dataset that interact with the transcription factor, Expected: Number of genes in the dataset predicted to interact with the transcription factor based on total number of interactions on the Agilent platform calculated as mean value for hypergeometric distribution, Ratio: Connectivity ratio (Actual/Expected), p-value: Probability to have the given value of Actual or higher (FDR adjusted p-value < 0.05)

Network Object Name	24 hpf								48 hpf							
	BAA Actual	BAA Expected	BAA Ratio	BAA p-value	DBT-PYR Actual	DBT-PYR Expected	DBT-PYR Ratio	DBT-PYR p-value	BAA Actual	BAA Expected	BAA Ratio	BAA p-value	DBT-PYR Actual	DBT-PYR Expected	DBT-PYR Ratio	DBT-PYR p-value
AHR	4.00	0.51	7.78	1.53E-03					10.00	2.65	3.77	2.81E-04				
TFAP2A									5.00	0.69	7.29	6.08E-04				
ARNT	4.00	0.13	30.03	8.38E-06					6.00	0.95	6.31	3.66E-04				
CEBPD	3.00	0.19	15.68	8.74E-04									25.00	13.87	1.80	3.29E-03
JUN					19.00	9.07	2.09	1.95E-03	14.00	5.14	2.73	4.69E-04	55.00	30.53	1.80	1.31E-05
CREB1									6.00	0.60	9.97	2.95E-05				
CUX1													9.00	3.10	2.90	3.81E-03
EGR2																
EN1					4.00	0.33	12.21	2.58E-04					8.00	1.38	5.81	5.67E-05
ERG																
ESR1					37.00	19.46	1.90	1.12E-04								
ESR2					11.00	2.89	3.81	1.51E-04								
FOXO1													15.00	3.91	3.83	8.20E-06
FOSL2													6.00	1.13	5.32	7.97E-04
NR3C1					26.00	12.96	2.01	5.73E-04	10.00	3.09	3.24	9.31E-04				
GLI1													7.00	1.50	4.66	6.80E-04
HBP1													3.00	0.19	15.97	5.68E-04
HES1					6.00	1.19	5.05	1.16E-03								
HOXB1													3.00	0.19	15.97	5.68E-04
IRF4													6.00	1.44	4.17	2.95E-03
JUND													12.00	3.82	3.14	4.38E-04
KLF4													14.00	5.54	2.53	1.35E-03
KLF5													6.00	0.81	7.37	1.23E-04
NR1H3													9.00	2.69	3.34	1.45E-03
MYEF2													2.00	0.06	31.94	9.78E-04

Table 2-S5 (Continued)

Network Object Name	24 hpf								48 hpf							
	BAA Actual	BAA Expected	BAA Ratio	BAA p-value	DBT- PYR Actual	DBT-PYR Expected	DBT- PYR Ratio	DBT- PYR p- value	BAA Actual	BAA Expected	BAA Ratio	BAA p-value	DBT- PYR Actual	DBT-PYR Expected	DBT- PYR Ratio	DBT- PYR p- value
NFATC4					4.00	0.45	8.88	9.40E-04								
NFE2L2									7.00	1.19	5.89	1.77E-04				
REST													20.00	9.99	2.00	2.55E-03
NR4A2					5.00	0.76	6.60	8.84E-04								
OTX2													6.00	1.38	4.36	2.34E-03
TP53													42.00	27.11	1.55	3.05E-03
PITX2													8.00	1.66	4.82	2.22E-04
PPARA					13.00	2.50	5.20	1.25E-06					13.00	3.82	3.40	1.14E-04
PKNOX1													3.00	0.28	10.65	2.22E-03
PGR													17.00	6.07	2.80	1.28E-04
RARA													10.00	3.69	2.71	3.90E-03
RELA					24.00	11.39	2.11	4.65E-04	16.00	3.81	4.20	7.49E-07	35.00	17.41	2.01	6.65E-05
RORA					10.00	2.46	4.07	1.76E-04								
RXRA					10.00	2.68	3.73	3.59E-04					11.00	4.10	2.68	2.71E-03
SF1													9.00	2.38	3.78	5.89E-04
SIX1					5.00	0.53	9.39	1.60E-04								
SIX4					3.00	0.20	14.65	9.16E-04								
SOX5													11.00	3.29	3.35	4.39E-04
SOX6													5.00	0.72	6.94	6.19E-04
SP1					74.00	48.31	1.53	5.79E-05	24.00	11.95	2.01	3.48E-04	112.00	73.86	1.52	1.38E-06
SP3									9.00	1.97	4.56	1.45E-04				
STAT5A													13.00	4.10	3.17	2.34E-04
TBP													27.00	15.03	1.80	2.40E-03
TCF7L2													17.00	6.67	2.55	3.88E-04
TWIST2													2.00	0.06	31.94	9.78E-04
UBTF													2.00	0.06	31.94	9.78E-04
YY1													30.00	15.56	1.93	4.52E-04

Chapter 3 - AHR2 mutant reveals functional diversity of aryl hydrocarbon receptors in zebrafish

Britton C. Goodale¹, Jane K. La Du¹, William H. Bisson², Derek B. Janszen³, Katrina M. Waters³ and Robert L. Tanguay^{1*}

1. Department of Environmental and Molecular Toxicology, the Environmental Health Sciences Center, Oregon State University, Corvallis, OR, USA

2. Pharmaceutical Biochemistry Group, School of Pharmaceutical Sciences, University of Geneva, Geneva, Switzerland

3. Computational Biology and Bioinformatics Group, Pacific Northwest National Laboratory, Richland, WA, USA

Published in PLOS ONE

7(1): e29346. doi:10.1371/journal.pone.0029346

Open access article distributed under the terms of the Creative Commons Attribution License

Abstract

The aryl hydrocarbon receptor (AHR) is well known for mediating the toxic effects of TCDD and has been a subject of intense research for over 30 years. Current investigations continue to uncover its endogenous and regulatory roles in a wide variety of cellular and molecular signaling processes. A zebrafish line with a mutation in *ahr2* (*ahr2*^{hu3335}), encoding the AHR paralogue responsible for mediating TCDD toxicity in zebrafish, was developed via Targeting Induced Local Lesions IN Genomes (TILLING) and predicted to express a non-functional AHR2 protein. We characterized AHR activity in the mutant line using TCDD and leflunomide as toxicological probes to investigate function, ligand binding and CYP1A induction patterns of paralogues AHR2, AHR1A and AHR1B. By evaluating TCDD-induced developmental toxicity, mRNA expression changes and CYP1A protein in the AHR2 mutant line, we determined that *ahr2*^{hu3335} zebrafish are functionally null. *In silico* modeling predicted differential binding of TCDD and leflunomide to the AHR paralogues. AHR1A is considered a non-functional pseudogene as it does not bind TCDD or mediate *in vivo* TCDD toxicity. Homology modeling, however, predicted a ligand binding conformation of AHR1A with leflunomide. AHR1A-dependent CYP1A immunohistochemical expression in the liver provided *in vivo* confirmation of the *in silico* docking studies. The *ahr2*^{hu3335} functional knockout line expands the experimental power of zebrafish to unravel the role of the AHR during development, as well as highlights potential activity of the other AHR paralogues in ligand-specific toxicological responses.

Introduction

The aryl hydrocarbon receptor (AHR), while best known for its role as an environmental sensor and mediator of 2,3,7,8-tetrachlorodibenzo-*p*-dioxin (TCDD) toxicity, has captured attention in recent years with a growing body of research elucidating its endogenous functions. As a member of the bHLH-per-ARNT-sim(PAS) family of proteins, the AHR is a transcriptional regulator containing two evolutionarily-conserved domains: a basic helix-loop-helix (bHLH) domain, which enables binding to aromatic hydrocarbon-responsive elements (AHREs), and a PAS domain, consisting of two 51- amino acid imperfect repeats (PAS-A and PAS-B), responsible for dimerization, ligand binding and interaction with other proteins (Fukunaga et al. 1995; Fukunaga and Hankinson 1996). Originally discovered for its role in modulating TCDD sensitivity in mice, the AHR binds a wide variety of ligand structures, including polycyclic and halogenated aromatic hydrocarbons (PAH and HAHs). Ligand binding induces disassociation from a cytoplasmic protein complex and translocation to the nucleus where the AHR heterodimerizes with the aryl hydrocarbon nuclear translocator (ARNT) (Nebert et al. 1975; Schmidt and Bradfield 1996; Denison and Nagy 2003). The AHR-ARNT heterodimer, along with other transcriptional enhancers, binds to AHREs and activates transcription of CYP1A, as well as NQO1, ALHD3A1, UGT1A6 and many other genes involved in metabolism, oxidative stress response and cell signaling (Nebert et al. 2000; Sartor et al. 2009). The role of the AHR in mediating toxicity of environmental contaminant exposure has been extensively studied (reviewed in (Gu et al. 2000; Nebert et al. 2004; Kerkvliet 2009)), and mechanism of action in immune, reproductive, developmental and other toxicological responses remain active areas of investigation. The diversity of physiological systems impacted by AHR activation and its crosstalk with other regulatory pathways support the notion that endogenous functions for the receptor likely preceded its role as an environmental sensor (Puga et al. 2009).

TCDD binding activity of the AHR is conserved among vertebrates. Substitutions in critical residues produce variation in ligand affinity, which underlies differences in TCDD sensitivity between species, inbred mouse strains, and wild fish populations (Nebert et al. 1975; Ema et al. 1994; Hahn 2002; Wirgin et al.). Structural comparisons of receptors provide information necessary for risk assessment extrapolation between species, as well as insight into receptor evolution (Hahn et al. 2006). In addition, *in silico* modeling of the

AHR has emerged as a powerful screening tool for potential AHR ligands (Bisson et al. 2009; Murray et al.).

Developing fish embryos are extremely sensitive to AHR-mediated planar hydrocarbon toxicity and hold a number of experimental advantages including development external to the mother, ease of observation, and genetic tractability. As such, zebrafish are a valuable model for investigation of developmental signaling processes in the context of xenobiotic exposures (Billiard et al. 2002; Carney et al. 2006). In teleosts, genome-wide duplication events have resulted in co-orthologs for many mammalian genes. While some gene duplicates have become non-functional, others have been evolutionarily conserved via the partitioning of functions between paralogues (Postlethwait et al. 2004). Three AHR isoforms have been identified in zebrafish: AHR1A, AHR1B, and AHR2 (Tanguay et al. 1999; Andreasen et al. 2002; Hahn 2002; Karchner et al. 2005). Numerous studies with known AHR ligands, however, have identified AHR2 as the primary mediator of early life stage toxicological effects in zebrafish (Prasch et al. 2003; Teraoka et al. 2003; Antkiewicz et al. 2006). Antisense oligonucleotide (morpholino) knockdown of AHR2 affords almost complete resistance to TCDD-induced developmental toxicity, and prevents the inhibitory effects of AHR ligands on epimorphic regeneration (Prasch et al. 2003; Mathew et al. 2006). Toxicity of many other HAHs and PAHs is also primarily dependent on AHR2. While AHR1B does bind TCDD, it is less sensitive to activation by TCDD than AHR2 (Karchner et al. 2005; Antkiewicz et al. 2006; Billiard et al. 2006). In contrast, AHR1A does not bind TCDD and is deficient in transactivation activity (Andreasen et al. 2002; Karchner et al. 2005). Beyond functioning as xenobiotic sensors, the zebrafish AHR paralogues are proposed to serve endogenous functions that have yet to be elucidated.

Recent studies have highlighted endogenous roles for the AHR in a complex array of immune system, cell cycle regulatory, reproductive and developmental processes (Peterson et al. 1993; Hernandez-Ochoa et al. 2009; Kerkvliet 2009; Matsumura et al. 2009; Singh et al. 2009). AHR knockout mouse strains developed by three different groups illustrate the importance of the AHR in normal liver development and immune function, and continue to expand understanding of the receptor's role in both toxicological responses and normal physiology (Fernandez-Salguero et al. 1995; Schmidt et al. 1996; Lahvis et al. 2005). A

functional zebrafish AHR2 knockout line will allow for investigation of the biological functions of the receptor throughout the zebrafish lifespan, and will eliminate the concern of incomplete knockdown that can occur with morpholinos. Complete loss of AHR2 activity in a zebrafish line will also enable functional analysis of the other two receptors, which has to date been experimentally difficult. As the primary mediator of TCDD toxicity, we proposed AHR2 as a target of great value to the zebrafish community for Targeting Induced Local Lesions IN Genomes (TILLING). Here we describe characterization of AHR function in the first TILLING-identified AHR2 mutant zebrafish. We report loss of AHR2 function in a mutant AHR2 line, and present evidence of ligand- and tissue-specific activation and function of AHR1A and AHR1B.

Results

Generation of a functionally null AHR2 zebrafish line

The *ahr2*^{hu3335} line was established, upon request, by the Hubrecht institute from a TILLING-identified founder with a TTG to TAG point mutation in residue Leu534, resulting in a premature stop codon in the transactivation domain of AHR2 (Figure 1). While the bHLH and PAS domains are predicted to remain intact in the truncated protein, the transactivation domain of zebrafish AHR2 is required for transcriptional activation (Andreasen et al. 2002). In addition, the premature stop codon location is > 55 nucleotides upstream of an exon-exon boundary, likely rendering the mutant AHR2 mRNA a target of nonsense-mediated mRNA decay, which will be further discussed below (Wittkopp et al. 2009).

ahr2^{hu3335} zebrafish survived to adulthood with no consistently observed abnormalities during development. Jaw, gill and fin malformations were observed in adult fish, but did not appear to cause significant morbidity or mortality (Figure 2). The fins of *ahr2*^{hu3335} adult zebrafish are damaged compared to their *ahr2*⁺ clutch mates, a characteristic which persisted in the offspring of wild-type 5D-outcrossed *ahr2*^{hu3335/+} zebrafish (Figure 2A, B). Visible jaw malformations in *ahr2*^{hu3335} adults prompted us to investigate bone structure using non-destructive microCt scanning. MicroCt imaging revealed structural differences in the neurocrania of an *ahr2*^{hu3335} and an aged-matched wild-type strain 5D adult zebrafish, including a striking extension of the ethmoid and mandibular regions (Figure 2C, D)

(Cubbage and Mabee 1996). Further, the dentary, maxilla and premaxilla of the *ahr2^{hu3335}* zebrafish had notably different structure, creating an extended mandible. Other bones, such as the orbitals and supraorbitals, appeared smaller in the *ahr2^{hu3335}* zebrafish, which may be an artifact of scanning reduced bone thickness compared to the wild type (Cubbage and Mabee 1996).

In comparison to their *ahr⁺* and *ahr⁺/hu3335* siblings, spawning activity of *ahr2^{hu3335}* homozygous crosses was less robust and egg fertilization rates were low (50-75%). As is discussed further in regard to developmental toxicity assays, pericardial edema and jaw malformations occurred with higher incidence in some of the *ahr2^{hu3335}* clutches. Sporadic spawning activity of *ahr2^{hu3335}* homozygous crosses and successful in vitro fertilization demonstrated that the *ahr2^{hu3335}* mutation does not prevent reproductive function in this line. Irregular spawning, however, suggests deficits in reproductive physiology or behavior.

ahr2^{hu3335} embryos are resistant to TCDD-induced developmental toxicity

To assess AHR2 function in the *ahr2^{hu3335}* strain, we compared developmental toxicity of TCDD in the *ahr2^{hu3335}* mutants to *ahr2⁺* embryos. Exposure to 0.1, 1 or 10 nM TCDD resulted in a concentration-dependent increase in axis malformations and pericardial edema observed at 120 hpf in the *ahr2⁺* embryos (Figure 3A, C). Of the fifteen endpoints evaluated, TCDD concentration was significantly correlated with increases in yolk sac and pericardial edemas, and axis, eye, snout, jaw and trunk malformations (Table 2). Mortality, touch response, fin, pigment, brain, circulatory, somite and otic malformations were not significant responses in either fish line. *ahr2^{hu3335}* embryos were resistant to TCDD-dependent malformations, and the responses of *ahr2⁺* and *ahr2^{hu3335}* embryos to TCDD exposure were significantly different from each other (Table 2). Background pericardial edema and jaw malformations were observed in *ahr2^{hu3335}* embryos but were not TCDD-dependent.

mRNA expression indicates the ahr2^{hu3335} mutation abrogates AHR2 function

We evaluated mRNA expression to further assess AHR2 function, and observed a 16-fold difference in AHR2 transcript abundance between *ahr2⁺* and *ahr2^{hu3335}* embryos (Figure 4A). This supports the hypothesis that AHR2 mRNA is degraded in the *ahr2^{hu3335}* line. We next examined AHR2-dependent gene expression to determine whether the point mutation

perturbs expression of downstream transcriptional targets. Expression of CYP1A, CYP1B1, CYP1C1, CYP1C2, AHR1A and AHR1B transcripts were not significantly different between *ahr2*^{hu3335} and *ahr2*⁺ embryos (Figure 4A).

To further confirm the lack of AHR2 functionality, we investigated mRNA expression changes in response to TCDD, which induces AHR2-dependent expression of a number of mRNAs at 48 hpf (Jonsson et al. 2007). Developmental TCDD exposure induced robust expression of CYP1A, CYP1C1 and CYP1C2 mRNA at 48 hpf in *ahr2*⁺ embryos relative to vehicle-treated controls (Figure 4B). As expected in the absence of a functional AHR2, mRNA expression was not significantly elevated in *ahr2*^{hu3335} embryos exposed to TCDD.

AHR1A predicted to bind leflunomide but not TCDD

We recently reported a homology model that has been used to predict binding affinity of potential ligands to the human, mouse and zebrafish AHRs (O'Donnell et al.). In order to investigate differential function of the zebrafish AHR paralogues, we tested TCDD and a known AHR ligand with a non-classical structure, leflunomide, in a series of molecular docking studies. Sequence alignment of the mouse and zebrafish AHR-PASB domains produced identities of 65.1% (zfAHR1A), 78.5% (zfAHR1B) and 70.5 % (zfAHR2). High similarity between the three isoforms at the primary and predicted tertiary structural levels was also noted, with 74.3% (AHR2/1B) and 69.9% (AHR1B/1A) identity. TCDD and leflunomide were docked into zebrafish AHR1A-, AHR1B-, and AHR2-LBD homology models. TCDD docked in AHR2 and AHR1B with predicted binding energies of -3.97 kcal/mol and -4.86 kcal/mol, respectively, but was unable to dock in AHR1A (Table 3, Figure 5A-B). Leflunomide was also able dock in AHR2 and AHR1B, with predicted binding energies of -2.13 kcal/mol and -1.97 kcal/mol, respectively (Table 3). Interestingly, in contrast to TCDD, leflunomide docked into AHR1A, but in a unique orientation (Bisson et al. 2009) (Table 3, Figure 5E).

AHR1A possesses specific residues that play potential roles in TCDD insensitivity (Karchner et al. 2005). Key residues characterized in the mouse AHR-LBD influencing TCDD binding are conserved in zebrafish AHR2 and AHR1B, which are both TCDD sensitive (Pandini et al. 2007; Bisson et al. 2009; Pandini et al. 2009). In AHR1A, residues His296, Ala386 and Gln388 have been substituted with Tyr296, Thr386 and His388 (Karchner et al. 2005). The

side chains of these residues cause both decreased volume and altered polarity of the AHR1A binding pocket, in comparison to AHR2, AHR1B, as well as mouse and human AHRs (26). TCDD docking is consequently not possible in AHR1A, which has been confirmed both *in vitro* and *in vivo* (Andreasen et al. 2002; Karchner et al. 2005). Homology modeling predicted that leflunomide, however, is able to dock in AHR1A with a unique orientation not found in human, mouse, or zebrafish AHR1B and AHR2 isoforms (O'Donnell et al.). As shown previously, leflunomide docks in AHR2 and AHR1B with a hydrogen bond (HB) interaction between the nitrogen atom of the isoxazole ring of the ligand and the OH of the side chain of Thr294 ((O'Donnell et al.), Figure 5C, D). Here we employed the homology model to examine AHR1A interaction with leflunomide for the first time, and discovered that the leflunomide docking position is flipped and a double HB interaction between the nitrogen and oxygen of the isoxazole ring of the ligand and the side chain of Thr354 is formed (Figure 5E). A binding energy of -2.19 kcal/mol was predicted which is in the range calculated for the other two isoforms (Table 3). Based on these data, we predicted that leflunomide would be a functional AHR1A ligand.

CYP1A protein induction patterns are ligand- and AHR isoform-dependent

We used immunohistochemical analysis of CYP1A protein expression as a biomarker of AHR activation to investigate *in vivo* AHR ligand binding patterns in TCDD and leflunomide-exposed larvae. Exposure to 1 nM TCDD from 6-24 hpf induces AHR2-dependent CYP1A expression in a number of tissues, including the heart, liver and enteric tract, with the predominant expression in the vascular endothelium of larvae (Figure 6A) (Andreasen et al. 2002). We focused our evaluation of AHR function on the most robust CYP1A induction patterns, which were observed in vasculature and liver (Andreasen et al. 2002; Carney et al. 2004). As predicted by the qRT-PCR results, CYP1A protein expression in TCDD-exposed *ahr2*^{hu3335} larvae was limited to faint vascular expression, just above background, in all embryos examined (Figure 6B). Exposure to 10 nM TCDD, which induced severe malformations and robust CYP1A expression in wild-type embryos, did not notably increase CYP1A expression in *ahr2*^{hu3335} larvae (data not shown).

To confirm the predicted binding of leflunomide to all three zebrafish AHRs *in vivo*, we examined CYP1A induction in *ahr2*^{hu3335} larvae exposed to 10 μ M leflunomide from 48-72

hpf. In comparison to wild type larvae, vascular CYP1A expression was drastically reduced in leflunomide-exposed *ahr2*^{hu3335} larvae (Figure 6C, D). In contrast to TCDD exposure, however, AHR2-independent CYP1A expression was observed in the developing livers of leflunomide-exposed *ahr2*^{hu3335} larvae (Figure 6D). This expression pattern persisted in larvae exposed until 120 hpf, with vascular expression remaining low and liver expression increasing, likely due to growth that occurs from 72-120 hpf (data not shown).

Based on molecular docking studies (Figure 5), we hypothesized that leflunomide induced CYP1A in *ahr2*^{hu3335} larvae via activation of the other AHR homologs, and utilized splice-blocking morpholinos to transiently knock down AHR1A and AHR1B separately and in combination. We conducted immunohistochemical analysis of CYP1A expression at 72 hpf to capture the window of morpholino efficacy, which was confirmed with PCR using primers flanking the target sites (Supplemental Figure 1). As the liver is small at 72 hpf, we employed double-staining with a hepatocyte nuclear factor 4 α (HNF4 α) antibody to confirm the presence of hepatocytes (Dong et al. 2007) (data not shown). CYP1A expression in AHR1B morpholino-injected *ahr2*^{hu3335} larvae persisted in the liver (Figure 6E), but was notably absent in the vasculature. In contrast, injection of the AHR1A morpholino in *ahr2*^{hu3335} embryos blocked leflunomide-induced expression of CYP1A in the liver, while faint vascular expression remained. When co-injected, the AHR1A and AHR1B morpholinos blocked all CYP1A expression in leflunomide-exposed *ahr2*^{hu3335} larvae (Figure 6F). When expression of all 3 AHR isoforms was eliminated, CYP1A expression in leflunomide-exposed embryos was indistinguishable from vehicle-exposed controls (Figure 6G).

Discussion

ahr2^{hu3335} zebrafish, homozygous for a point mutation in *ahr2*, survive to adulthood and are functional AHR2 knockouts by all measures tested. The premature stop codon in residue 534 is predicted to result in a non-functional protein due to its truncated transactivation domain. Though we cannot exclude the possibility that some biological activity of a potential cryptic protein remains, we saw no evidence to support its presence. Analysis of *ahr2*^{hu3335} mRNA levels suggests that the mutant AHR2 transcript is at least partially degraded and the truncated protein may be present only at very low levels, if at all.

The *ahr2*^{hu3335} adult zebrafish exhibit notable fin and skeletal differences compared to wild type. We also observed a higher background of developmental abnormalities in *ahr2*^{hu3335} larvae. These phenotypes may not necessarily be due to the mutation; reduced spawning and small clutch sizes of *ahr2*^{hu3335} zebrafish limited the selection of embryos for experiments, whereas large wild type clutches allow for precise selection of high-quality embryos. Studies in both AHR-deficient and AHR ligand-treated mice provide strong evidence of an endogenous role of the receptor in female reproductive physiology. Deficiencies in maintaining pregnancy and surviving lactation have been reported in AHR knockout mice (Abbott et al. 1999), and disruption of AHR function alters ovarian development, folliculogenesis, steroid hormone synthesis, ovulation and possibly reproductive senescence (Hernandez-Ochoa et al. 2009). In keeping with AHR knockout mouse models, *ahr2*^{hu3335} zebrafish are capable of producing viable embryos, but exhibit decreased reproductive success. It is important to note, however, that other ENU-induced mutations throughout the genome of this fish line could be responsible for observed phenotypic abnormalities. Zebrafish TILLING mutants require multiple outcrosses to reduce undesired mutations to background levels. Because outcrosses of the *ahr2*^{hu3335} line were in progress at the time of this study, it is premature to attribute all phenotypic abnormalities observed in *ahr2*^{hu3335} homozygotes to the mutation in *ahr2*. Decreased reproductive capacity of homozygous mutants, as well as fin and jaw abnormalities may represent interesting models of endogenous AHR function and certainly warrant further investigation if they persist in the mutant line following further outcrosses.

In the present study, we used TCDD as a tool to investigate AHR2 function in the *ahr2*^{hu3335} line. We found that *ahr2*^{hu3335} embryos were resistant to TCDD-induced developmental toxicity at concentrations that cause severe malformations in *ahr2*⁺ embryos. *ahr2*^{hu3335} embryos treated with 10nM TCDD showed few signs of morbidity at 120 hpf. Transient AHR2 knockdown delays, but does not prevent, TCDD-induced mortality (Prasch et al. 2003). Therefore it would be interesting to examine longer-term effects of TCDD exposure in future experiments with the *ahr2*^{hu3335} line.

The most well-known biomarker of AHR activation is the induction of CYP1A expression. Among the suite of cytochrome P450 metabolizing enzymes in zebrafish, CYP1A, CYP1B1,

CYP1C1 and CYP1C2 are elevated in response to AHR agonist exposure (Jonsson et al. 2007). In agreement with our developmental toxicity data, no elevation in CYP1A, CYP1C1 or CYP1C2 expression was observed in TCDD-exposed *ahr2*^{hu3335} embryos. Taken together, these data support the concept that AHR2 is not functional in this line. The notable, but statistically insignificant, increase in CYP1A expression following TCDD treatment in *ahr2*^{hu3335} embryos is likely due to TCDD activation of AHR1B, as further discussed below.

While the dependence of CYP1A activation by TCDD on AHR2 is well-established, studies with PAHs in zebrafish embryos have revealed diverse CYP1A expression patterns dependent on other AHR isoforms (Incardona et al. 2005; Incardona et al. 2006). This study represents the first time that an *in silico*-based modeling approach was utilized to investigate ligand binding by all three receptors. Molecular docking with TCDD predicted that both AHR1B and AHR2, but not AHR1A, would bind TCDD due to substitutions in the binding pocket. In contrast to TCDD, *in silico* modeling with leflunomide predicts favorable binding energies for all three zebrafish AHR isoforms. Interestingly, leflunomide docked into AHR1A with a different predicted conformation than in the other two receptors, but with equivalent affinity. This finding is particularly intriguing, as AHR1A is incapable of binding classical AHR ligands (Karchner et al. 2005), is deficient in transactivation activity (Andreasen et al. 2002), and therefore was once considered non-functional.

We confirmed the AHR modeling results *in vivo* using CYP1A protein expression as a biomarker of AHR activation. In keeping with our mRNA expression and *in silico* modeling studies, TCDD-exposed *ahr2*^{hu3335} larvae were largely devoid of CYP1A protein expression observed in TCDD-exposed *ahr2*⁺ larvae. Leflunomide also induces strong vascular CYP1A protein expression in *ahr2*⁺ larvae, but unlike with TCDD, the *ahr2*^{hu3335} embryos exhibited striking leflunomide-induced CYP1A expression in the liver. This finding is in agreement with the modeling results. To tease apart AHR isoform-dependence of the residual CYP1A expression, we transiently knocked down the receptors individually and in combination in *ahr2*^{hu3335} larvae. We found AHR1B-dependent vascular induction and AHR1A-dependent liver induction of CYP1A expression. Knockdown of AHR1A and AHR1B in combination prevented all CYP1A induction. Taken together, these data suggest that, contrary to

previous observations with TCDD, all three AHR isoforms are involved in leflunomide-induced CYP1A expression in zebrafish larvae.

These data demonstrate that there are concrete differences in ligand binding activity of the zebrafish AHRs, and that AHR1A is not a pseudogene as previously proposed, but rather has affinity for different ligand structures. While residual CYP1A expression has been observed in TCDD-treated AHR2-morphants, it was faint and vascular in nature, attributable to incomplete knockdown (Prasch et al. 2003). Our immunohistochemical results with the *ahr2*^{hu3335} line suggest that mild vascular expression of CYP1A is induced via AHR1B, and can be effectively knocked down to background with morpholino injection. AHR1A-dependent CYP1A expression is seemingly incongruous with previous investigation of AHR1A function *in vitro*, but the lack of a known AHR1A ligand limited previous efforts. The AHR1A-dependent CYP1A expression pattern we observed here is consistent with the reported AHR1A mRNA expression in the liver (Andreasen et al. 2002).

Putative AHR1A ligands could be identified with further *in silico* modeling; work by Incardona and colleagues also offers clues with several PAHs that induce CYP1A expression independently of AHR2 (Incardona et al. 2005; Incardona et al. 2006; Incardona et al.). Pyrene induced liver expression of CYP1A in an AHR1A-dependent manner (Incardona et al. 2006), and more recently retene-induced CYP1A expression was shown to be incompletely dependent on AHR2 (Scott et al.). Here, we offer further evidence that AHR1A is a functional receptor *in vivo*, though the transactivation requirements for this receptor remain to be elucidated. *In vitro* data with AHR chimera proteins suggest that transactivation requirements of AHR1A differ from those of AHR2 (Andreasen et al. 2002).

The presence of three apparently functional aryl hydrocarbon receptors in zebrafish raises several interesting questions: How do these receptors differ? What functions have led to their evolutionary conservation? And to what extent do the AHR1 receptors need to be considered in toxicological studies in zebrafish? While the presence of multiple AHRs certainly complicates study of receptor function in fish, subfunction partitioning among isoforms presents a unique opportunity to unravel the many physiological functions of the AHR that are conserved among vertebrates (Postlethwait et al. 2004). As summarized in Table 4, the studies presented here add to a body of research demonstrating significant

differences in receptor expression, ligand binding, and mRNA induction activity. With respect to transcript localization, AHR2 is widely distributed through most organs investigated in adult zebrafish, while AHR1A is mainly expressed in the liver, and to a lesser extent in the heart, kidney and swim bladder (Andreasen et al. 2002). AHR1B expression has yet to be fully characterized, but our CYP1A IHC results suggest that the isoform is widely distributed, but is expressed at much lower levels than AHR2. The subfunction partitioning of these receptors is not strictly locational. Overlapping expression of AHR2 and AHR1A has been previously described, and we also noted overlap in AHR2- and AHR1-dependent CYP1A expression patterns (Andreasen et al. 2002; Karchner et al. 2005). A cell or tissue-level analysis may reveal more subtle localization differences, as has been implied in differential PAH-induced CYP1A patterns in endocardial and myocardial tissue (Incardona et al. 2006; Incardona et al.). Little is yet known about the endogenous function of these receptors and their downstream transcriptional targets. If expression of AHR1A and AHR1B is limited, it may be difficult to detect significant changes in their transcriptional targets in whole embryo homogenate. As we have shown here, however, the *ahr2*^{hu3335} line will ease the study of the other two receptors by removing the overpowering transcriptional changes induced through AHR2. The three receptors together present an intriguing opportunity to unravel multiple regulatory functions that may be conserved in the mammalian AHR.

This is the first report of CYP1A induction dependent on all three of the zebrafish AHRs. However, toxicity mediated through the AHR1 receptors has not, as of yet, been documented. Pyrene liver toxicity was reduced with AHR1A knockdown, but AHR2 knockdown prevented the majority of the chemical's developmental effects (Incardona et al. 2006). In the case of TCDD and other similarly-structured HAHs, the small binding pocket of AHR1A prevents it from having a role in ligand-induced toxicological effects. AHR1A and AHR1B receptors may hold little importance in toxicological studies with these compounds. Indeed the studies presented here support the large body of previous research indicating that TCDD-induced early life stage toxicity is mediated through AHR2. Though some CYP1A and other downstream target induction may occur via AHR1B, any developmental abnormalities caused by this pathway are more subtle than those investigated to date. The possibility remains, however, that AHR1B may play a role in later life stage impacts of

TCDD. These data warrant further investigation of the AHR isoforms with structurally diverse, less-well studied compounds. Ultimately, further bioinformatic and modeling efforts with zebrafish and mammalian AHRs could help determine the best model for human AHR activity, taking into account both ligand binding and receptor expression characteristics.

This was the first time that all three AHR isoforms were knocked down in developing zebrafish. Our findings suggest that, consistent with mammalian literature, AHR function is not required to complete development (Schmidt et al. 1996; Gonzalez and Fernandez-Salguero 1998). Without full histological evaluations of the AHR1Amo/AHR1Bmo/*ahr2*^{hu3335} larvae at 120hpf, we cannot exclude non-lethal malformations, particularly hepatic abnormalities, which have been reported in AHR knockout mice (Schmidt et al. 1996; Lahvis et al. 2005). It may not be possible to fully answer the question of whether the AHR paralogues are required for hepatic development in zebrafish with the tools employed here, as the liver undergoes significant development after 72hpf, when morpholino efficacy is in decline. We therefore present the *ahr2*^{hu3335} line as a valuable resource available to the zebrafish research community, and suggest that development of both AHR1A and AHR1B (already requested by the research community) mutant lines would further extend the power of this model for investigating both the endogenous and ligand-mediated roles of the AHR in developing vertebrates.

Materials and Methods

Zebrafish lines and embryos

Adult zebrafish were housed according to Institutional Animal Care and Use Committee protocols at Oregon State University on a recirculating system with water temperature of 28±1°C and a 14 h light/10 h dark schedule. Zebrafish embryos carrying a point mutation in *ahr2* (*ahr2*^{hu3335} strain) were requested and generously provided by the Hubrecht Institute. The *ahr2*^{hu3335} line was identified from a library of *N*-ethyl-*N*-nitrosourea (ENU)-mutagenized zebrafish using the TILLING method as previously described (Wienholds et al. 2003). Offspring of heterozygous *ahr2*^{hu3335} carriers were raised to adulthood at the Sinnhuber Aquatic Research Laboratory, and genotyped for the *ahr2*^{hu3335} point mutation with DNA isolated from fin clips (Wienholds et al. 2003). PCR amplification was performed

with genomic DNA and *ahr2* gene-specific primers (Table 1), the product was purified using a QIAquick PCR purification kit (Qiagen) and sequenced with an ABI 3730 capillary sequencer at the Center for Genome Research and Biocomputing at Oregon State University. Homozygous carriers of the T → A point mutation in residue 534 (Figure 1) were identified to create an *ahr2*^{hu3335} population. Because the TILLING method relies on random mutagenesis, mutant lines of interest carry other mutations throughout the genome. F1 fish are predicted to carry 3000-6000 mutations and multiple outcrosses are necessary to reduce off-target mutations (Moens et al. 2008). *ahr2*^{hu3335} carriers were outcrossed to the wild type 5D (*ahr2*^{+/+}) line, and homozygous mutants were identified from an incross of their progeny. The *ahr2*^{hu3335} mutant line has been maintained with subsequent outcrosses on the wild type 5D background, which was also used for all *ahr2*⁺ control experiments in our laboratory.

All developmental toxicity experiments were conducted with fertilized embryos obtained from group spawns of adult zebrafish as described previously (Reimers et al. 2006). Embryos used in experiments are defined as homozygous (*ahr2*^{hu3335}), heterozygous (*ahr2*^{hu3335/+}) or wild-type (*ahr2*⁺) for the point mutation in AHR2.

MicroCt imaging

Micro computed tomography (μCT) was used for nondestructive three-dimensional imaging of zebrafish heads. The fish were scanned using a Scanco μCT40 scanner (Scanco Medical AG, Basserdorf, Switzerland) at 45 kVp, 177 mA, and a voxel size of 12 x 12 x 12 μm. The heads were imaged at threshold settings of 140 (scale 0 – 1000).

Homology modeling, molecular docking and binding energy calculations

Molecular Modeling of zebrafish AHR2, AHR1B and AHR1A isoforms was conducted as described previously (17). Briefly, the homology models of mouse, human, rat and zebrafish AHR-LBD (ligand binding domains) were built using the NMR resolved structure of the PAS domain of human hypoxia-inducible-factor 2α as the 3D-template. Models were then refined in the internal coordinates with Molsoft ICM v3.5-1p. Molecular docking of TCDD and Leflunomide ligands and binding energy calculation were performed as reported (Bisson et al. 2009).

Chemical exposures and developmental toxicity assessment

TCDD (99.2% purity in DMSO, Cambridge Isotope Laboratories) and leflunomide (Sigma-Aldrich) were dissolved in DMSO. All exposures were conducted in E2 embryo medium with staged embryos (Kimmel et al. 1995). Embryos were batch exposed to 0.1, 1, 10 nM TCDD or 0.1% DMSO vehicle control in 2 mL embryo medium in glass vials from 6-24 hours post fertilization (hpf). Embryos were then rinsed 4X with embryo media and transferred to plastic dishes to develop until the indicated experimental time points. Embryo homogenate for mRNA expression analysis was collected at 48 hpf, and developmental toxicity of TCDD exposure was assessed by visually inspecting embryos at 120 hpf for malformations as previously described (Truong et al.) with three biological replicates. Developmental toxicity assay data were analyzed by fitting a 2 parameter logistic regression model to the concentration-response data for each malformation. Significance of the TCDD concentration-response curve was calculated for each fish line. Differential responses were assessed with a t-test to compare the parameters from the *ahr2*⁺ model to those from the *ahr2*^{hu3335} model. No adjustment for multiplicity was made. R software v12.0 (2010) was used for these analyses.

For leflunomide exposures, embryos were transferred into individual wells of a 96-well plate and exposed to 10 μ M leflunomide or 0.1% DMSO control in 100 μ L embryo medium from 48-72 hpf, when they were humanely euthanized and fixed for immunohistochemistry analysis.

Total RNA isolation and reverse transcription

For qRT-PCR studies, 20 embryos per treatment group were homogenized in TRIzol (Invitrogen) and stored at -80°C until use. Total RNA was isolated via phenol/guanidine isothiocyanate/chloroform separation. For morpholino splice-blocking confirmation, 15 embryos were homogenized in RNazol (Molecular Research Center) for total RNA isolation. RNA was quantified using a SynergyMx microplate reader (Biotek) with the Gen5 Take3 module to calculate 260/280 O.D. ratios. Superscript III First-Strand Synthesis (Invitrogen) was used with oligo(dT) primer to reverse transcribe cDNA from total RNA.

Quantitative RT-PCR

Relative abundance of AHR1A, AHR1B, AHR2, CYP1A, CYP1B1, CYP1C1 and CYP1C2 mRNA transcripts were assessed in whole embryo homogenate. Gene-specific primers (MWG Operon) are listed in Table 1. All qRT-PCR assays were performed in 20 μ l reactions consisting of 10 μ l Power SYBR Green PCR master mix (Applied Biosystems), 0.4 μ l each primer, 9.2 μ l H₂O and 50 ng equivalents of cDNA. Amplification (Step One Plus, Applied Biosystems) was performed with cycling parameters as follows: 95°C for 10 min; 40 cycles of 95°C for 15 s, 60°C for 1 min; 95°C for 15 sec and 60°C for 1 min. A melt curve was performed at 3° increments to assess for multiple products.

qRT-PCR analysis was performed with StepOne Software v2.1 (Applied Biosystems) using the $\Delta\Delta$ Ct method with genes of interest normalized to β -actin (Livak and Schmittgen 2001). Three independent biological replicates were assessed and statistically analyzed by comparing *ahr2*^{hu3335} to *ahr2*⁺ or TCDD-treated to control with a Student's t-test using Graphpad Prism 5.01 software (Graphpad Software Inc. La Jolla, CA).

Morpholino injection

Splice-blocking morpholinos designed against AHR1A and AHR1B were purchased from Gene Tools (Philomath, OR). The AHR1A splice-blocking morpholino (AHR1A_{mo}, 5' CTTTTGAAGTGACTTTTGGCCCGCA 3') was described previously (Incardona et al. 2006) and was tagged on the 3' end with fluorescein. We designed a morpholino to target the exon7/intron7 boundary of AHR1B (AHR1B_{mo}, 5' ACACAGTCGTCCATGATTACTTTGC 3'). A standard control morpholino from Gene Tools (c_{mo}, 5' CCTCTTACCTCAGTTACAATTTATA 3') was used as a negative control. *ahr2*^{hu3335} embryos were injected at the 1-2 cell stage with approximately 2 nl of 1.5 mM morpholino dissolved in ultrapure water with 0.5% phenol red. For AHR1A_{mo} +AHR1B_{mo} co-injections, the final concentration of each morpholino was 0.83 mM. Embryos were allowed to develop in fish water and screened for successful morpholino incorporation with fluorescein visualization at 24 hpf. mRNA mis-splice was confirmed with PCR primers flanking the target sites at 24 and 72 hpf (AHR1A and AHR1B-mo primers Table 1).

Immunohistochemistry (IHC)

Wild-type strain 5D and *ahr2*^{hu3335} embryos treated with 1nM TCDD (or 0.1% DMSO control) from 6-24 hpf were fixed at 120 hpf in 4% paraformaldehyde (J.T. Baker) overnight

at 4°C. Leflunomide treated embryos (48-72 hpf) were fixed at 72 hpf to capture the window of morpholino efficacy. Mouse α fish CYP1A monoclonal (1:500 dilution, Biosense laboratories) and goat α human HNF4 α polyclonal (1:100 dilution, Santa Cruz Biotechnology) primary antibodies were used. Secondary antibodies consisted of Alexafluor® 546 rabbit α mouse IgG (H+L) (1:1000) and Alexafluor® 488 donkey α goat IgG (H+L) (1:1000) (Molecular Probes, Eugene, OR). Immunohistochemistry was performed as previously described (Mathew et al. 2006). Briefly, whole fixed embryos were permeabilized with 0.005% trypsin on ice for 10 min, washed 3X with PBST and post-fixed in 4% paraformaldehyde for 10 min. Samples were blocked for 1h in 10% normal goat serum (single labeling) or BlockAid (double labeling) (Invitrogen). Samples were incubated with primary antibodies overnight at 4°C, followed by 4 30min washes in PBST and incubation with secondary antibody overnight at 4°C. At least 8 embryos per treatment group were imaged by epi-fluorescence microscopy using a Zeiss Axiovert 200M microscope with 5X and 10X objectives.

Acknowledgments

This work was supported by the NIEHS Environmental Health Sciences SRP grant Project #3 P42 ES016465, Core Center Grant P30 ES00210 and the NIEHS Training Grant T32 ES7060 to RLT. We gratefully acknowledge Edwin Cuppen at the Hubrecht Institute for the *ahr2*^{hu3335} line and the European Commission Consortium Integrated Project “ZF-MODELS-Zebrafish Models for Human Development and Disease”, Contract No. LSHG-CT-2003-503496. We would like to thank the Skeletal Biology Laboratory at OSU for the microCt analysis, and the Center for Genome Research and Biocomputing at OSU for sequencing support. We are grateful to Cari Buchner, Carrie Barton, Brittany McCauslin, Jessika Dobson and the staff at the Sinnhuber Aquatic Research Laboratory for fish husbandry expertise and to members of the Tanguay laboratory for their helpful feedback and critical review of the manuscript.

References

(2010). R: A language and environment for statistical computing. R. D. C. Team. Vienna, Austria.

- Abbott, B. D., J. E. Schmid, et al. (1999). "Adverse reproductive outcomes in the transgenic Ah receptor-deficient mouse." *Toxicol Appl Pharmacol* **155**(1): 62-70.
- Andreasen, E. A., M. E. Hahn, et al. (2002). "The zebrafish (*Danio rerio*) aryl hydrocarbon receptor type 1 is a novel vertebrate receptor." *Mol Pharmacol* **62**(2): 234-249.
- Andreasen, E. A., J. M. Spitsbergen, et al. (2002). "Tissue-specific expression of AHR2, ARNT2, and CYP1A in zebrafish embryos and larvae: effects of developmental stage and 2,3,7,8-tetrachlorodibenzo-p-dioxin exposure." *Toxicol Sci* **68**(2): 403-419.
- Antkiewicz, D. S., R. E. Peterson, et al. (2006). "Blocking expression of AHR2 and ARNT1 in zebrafish larvae protects against cardiac toxicity of 2,3,7,8-tetrachlorodibenzo-p-dioxin." *Toxicol Sci* **94**(1): 175-182.
- Billiard, S. M., M. E. Hahn, et al. (2002). "Binding of polycyclic aromatic hydrocarbons (PAHs) to teleost aryl hydrocarbon receptors (AHRs)." *Comp Biochem Physiol B Biochem Mol Biol* **133**(1): 55-68.
- Billiard, S. M., A. R. Timme-Laragy, et al. (2006). "The role of the aryl hydrocarbon receptor pathway in mediating synergistic developmental toxicity of polycyclic aromatic hydrocarbons to zebrafish." *Toxicol Sci* **92**(2): 526-536.
- Bisson, W. H., D. C. Koch, et al. (2009). "Modeling of the aryl hydrocarbon receptor (AhR) ligand binding domain and its utility in virtual ligand screening to predict new AhR ligands." *J Med Chem* **52**(18): 5635-5641.
- Carney, S. A., R. E. Peterson, et al. (2004). "2,3,7,8-Tetrachlorodibenzo-p-dioxin activation of the aryl hydrocarbon receptor/aryl hydrocarbon receptor nuclear translocator pathway causes developmental toxicity through a CYP1A-independent mechanism in zebrafish." *Mol Pharmacol* **66**(3): 512-521.
- Carney, S. A., A. L. Prasch, et al. (2006). "Understanding dioxin developmental toxicity using the zebrafish model." *Birth Defects Res A Clin Mol Teratol* **76**(1): 7-18.
- Cubbage, C. C. and P. M. Mabee (1996). "Development of the cranium and paired fins in the zebrafish *Danio rerio* (Ostariophysi, cyprinidae)." *Journal of Morphology* **229**(2): 121-160.
- Denison, M. S. and S. R. Nagy (2003). "Activation of the aryl hydrocarbon receptor by structurally diverse exogenous and endogenous chemicals." *Annu Rev Pharmacol Toxicol* **43**: 309-334.
- Dong, P. D., C. A. Munson, et al. (2007). "Fgf10 regulates hepatopancreatic ductal system patterning and differentiation." *Nat Genet* **39**(3): 397-402.
- Ema, M., N. Ohe, et al. (1994). "Dioxin binding activities of polymorphic forms of mouse and human arylhydrocarbon receptors." *J Biol Chem* **269**(44): 27337-27343.
- Fernandez-Salguero, P., T. Pineau, et al. (1995). "Immune system impairment and hepatic fibrosis in mice lacking the dioxin-binding Ah receptor." *Science* **268**(5211): 722-726.
- Fukunaga, B. N. and O. Hankinson (1996). "Identification of a novel domain in the aryl hydrocarbon receptor required for DNA binding." *J Biol Chem* **271**(7): 3743-3749.
- Fukunaga, B. N., M. R. Probst, et al. (1995). "Identification of functional domains of the aryl hydrocarbon receptor." *J Biol Chem* **270**(49): 29270-29278.
- Gonzalez, F. J. and P. Fernandez-Salguero (1998). "The aryl hydrocarbon receptor: studies using the AHR-null mice." *Drug Metab Dispos* **26**(12): 1194-1198.
- Gu, Y. Z., J. B. Hogenesch, et al. (2000). "The PAS superfamily: sensors of environmental and developmental signals." *Annu Rev Pharmacol Toxicol* **40**: 519-561.

- Hahn, M. E. (2002). "Aryl hydrocarbon receptors: diversity and evolution." Chem Biol Interact **141**(1-2): 131-160.
- Hahn, M. E., S. I. Karchner, et al. (2006). "Unexpected diversity of aryl hydrocarbon receptors in non-mammalian vertebrates: insights from comparative genomics." J Exp Zool A Comp Exp Biol **305**(9): 693-706.
- Hernandez-Ochoa, I., B. N. Karman, et al. (2009). "The role of the aryl hydrocarbon receptor in the female reproductive system." Biochem Pharmacol **77**(4): 547-559.
- Incardona, J. P., M. G. Carls, et al. (2005). "Aryl hydrocarbon receptor-independent toxicity of weathered crude oil during fish development." Environ Health Perspect **113**(12): 1755-1762.
- Incardona, J. P., H. L. Day, et al. (2006). "Developmental toxicity of 4-ring polycyclic aromatic hydrocarbons in zebrafish is differentially dependent on AH receptor isoforms and hepatic cytochrome P4501A metabolism." Toxicol Appl Pharmacol **217**(3): 308-321.
- Incardona, J. P., T. L. Linbo, et al. (2011). "Cardiac toxicity of 5-ring polycyclic aromatic hydrocarbons is differentially dependent on the aryl hydrocarbon receptor 2 isoform during zebrafish development." Toxicol Appl Pharmacol **257**(2): 242-249.
- Jonsson, M. E., M. J. Jenny, et al. (2007). "Role of AHR2 in the expression of novel cytochrome P450 1 family genes, cell cycle genes, and morphological defects in developing zebra fish exposed to 3,3',4,4',5-pentachlorobiphenyl or 2,3,7,8-tetrachlorodibenzo-p-dioxin." Toxicol Sci **100**(1): 180-193.
- Karchner, S. I., D. G. Franks, et al. (2005). "AHR1B, a new functional aryl hydrocarbon receptor in zebrafish: tandem arrangement of ahr1b and ahr2 genes." Biochem J **392**(Pt 1): 153-161.
- Kerkvliet, N. I. (2009). "AHR-mediated immunomodulation: the role of altered gene transcription." Biochem Pharmacol **77**(4): 746-760.
- Kimmel, C. B., W. W. Ballard, et al. (1995). "Stages of embryonic development of the zebrafish." Dev Dyn **203**(3): 253-310.
- Lahvis, G. P., R. W. Pyzalski, et al. (2005). "The aryl hydrocarbon receptor is required for developmental closure of the ductus venosus in the neonatal mouse." Mol Pharmacol **67**(3): 714-720.
- Livak, K. J. and T. D. Schmittgen (2001). "Analysis of relative gene expression data using real-time quantitative PCR and the 2(-Delta Delta C(T)) Method." Methods **25**(4): 402-408.
- Mathew, L. K., E. A. Andreasen, et al. (2006). "Aryl hydrocarbon receptor activation inhibits regenerative growth." Mol Pharmacol **69**(1): 257-265.
- Matsumura, F., A. Puga, et al. (2009). "Biological functions of the arylhydrocarbon receptor: beyond induction of cytochrome P450s. Introduction to this special issue." Biochem Pharmacol **77**(4): 473.
- Moens, C. B., T. M. Donn, et al. (2008). "Reverse genetics in zebrafish by TILLING." Brief Funct Genomic Proteomic **7**(6): 454-459.
- Murray, I. A., C. A. Flaveny, et al. (2011). "Suppression of cytokine-mediated complement factor gene expression through selective activation of the Ah receptor with 3',4'-dimethoxy-alpha-naphthoflavone." Mol Pharmacol **79**(3): 508-519.
- Nebert, D. W., T. P. Dalton, et al. (2004). "Role of aryl hydrocarbon receptor-mediated induction of the CYP1 enzymes in environmental toxicity and cancer." J Biol Chem **279**(23): 23847-23850.

- Nebert, D. W., J. R. Robinson, et al. (1975). "Genetic expression of aryl hydrocarbon hydroxylase activity in the mouse." *J Cell Physiol* **85**(2 Pt 2 Suppl 1): 393-414.
- Nebert, D. W., A. L. Roe, et al. (2000). "Role of the aromatic hydrocarbon receptor and [Ah] gene battery in the oxidative stress response, cell cycle control, and apoptosis." *Biochem Pharmacol* **59**(1): 65-85.
- O'Donnell, E. F., K. S. Saili, et al. (2010). "The anti-inflammatory drug leflunomide is an agonist of the aryl hydrocarbon receptor." *PLoS One* **5**(10).
- Pandini, A., M. S. Denison, et al. (2007). "Structural and functional characterization of the aryl hydrocarbon receptor ligand binding domain by homology modeling and mutational analysis." *Biochemistry* **46**(3): 696-708.
- Pandini, A., A. A. Soshilov, et al. (2009). "Detection of the TCDD binding-fingerprint within the Ah receptor ligand binding domain by structurally driven mutagenesis and functional analysis." *Biochemistry* **48**(25): 5972-5983.
- Peterson, R. E., H. M. Theobald, et al. (1993). "Developmental and reproductive toxicity of dioxins and related compounds: cross-species comparisons." *Crit Rev Toxicol* **23**(3): 283-335.
- Postlethwait, J., A. Amores, et al. (2004). "Subfunction partitioning, the teleost radiation and the annotation of the human genome." *Trends Genet* **20**(10): 481-490.
- Prasch, A. L., H. Teraoka, et al. (2003). "Aryl hydrocarbon receptor 2 mediates 2,3,7,8-tetrachlorodibenzo-p-dioxin developmental toxicity in zebrafish." *Toxicol Sci* **76**(1): 138-150.
- Puga, A., C. Ma, et al. (2009). "The aryl hydrocarbon receptor cross-talks with multiple signal transduction pathways." *Biochem Pharmacol* **77**(4): 713-722.
- Reimers, M. J., J. K. La Du, et al. (2006). "Ethanol-dependent toxicity in zebrafish is partially attenuated by antioxidants." *Neurotoxicol Teratol* **28**(4): 497-508.
- Sartor, M. A., M. Schnekenburger, et al. (2009). "Genomewide analysis of aryl hydrocarbon receptor binding targets reveals an extensive array of gene clusters that control morphogenetic and developmental programs." *Environ Health Perspect* **117**(7): 1139-1146.
- Schmidt, J. V. and C. A. Bradfield (1996). "Ah receptor signaling pathways." *Annu Rev Cell Dev Biol* **12**: 55-89.
- Schmidt, J. V., G. H. Su, et al. (1996). "Characterization of a murine Ahr null allele: involvement of the Ah receptor in hepatic growth and development." *Proc Natl Acad Sci U S A* **93**(13): 6731-6736.
- Scott, J. A., J. P. Incardona, et al. (2011). "AhR2-mediated, CYP1A-independent cardiovascular toxicity in zebrafish (*Danio rerio*) embryos exposed to retene." *Aquat Toxicol* **101**(1): 165-174.
- Singh, K. P., F. L. Casado, et al. (2009). "The aryl hydrocarbon receptor has a normal function in the regulation of hematopoietic and other stem/progenitor cell populations." *Biochem Pharmacol* **77**(4): 577-587.
- Tanguay, R. L., C. C. Abnet, et al. (1999). "Cloning and characterization of the zebrafish (*Danio rerio*) aryl hydrocarbon receptor." *Biochim Biophys Acta* **1444**(1): 35-48.
- Teraoka, H., W. Dong, et al. (2003). "Induction of cytochrome P450 1A is required for circulation failure and edema by 2,3,7,8-tetrachlorodibenzo-p-dioxin in zebrafish." *Biochem Biophys Res Commun* **304**(2): 223-228.
- Truong, L., S. L. Harper, et al. (2011). "Evaluation of embryotoxicity using the zebrafish model." *Methods Mol Biol* **691**: 271-279.

- Wienholds, E., F. van Eeden, et al. (2003). "Efficient target-selected mutagenesis in zebrafish." Genome Res **13**(12): 2700-2707.
- Wirgin, I., N. K. Roy, et al. (2011). "Mechanistic basis of resistance to PCBs in Atlantic tomcod from the Hudson River." Science **331**(6022): 1322-1325.
- Wittkopp, N., E. Huntzinger, et al. (2009). "Nonsense-mediated mRNA decay effectors are essential for zebrafish embryonic development and survival." Mol Cell Biol **29**(13): 3517-3528.

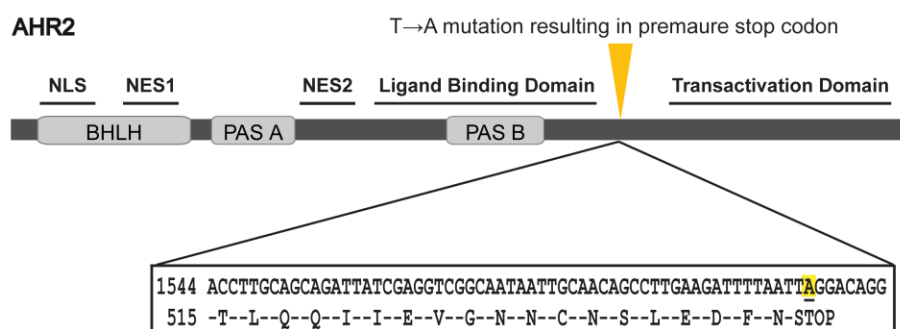


Figure 3-1 Schematic diagram of predicted AHR2 protein in *ahr2*^{hu3335} zebrafish

The *ahr2*^{hu3335} zebrafish line has a T → A point mutation in residue 534, resulting in a premature stop codon in the transactivation domain of the protein. The predicted truncated protein contains the ligand binding, DNA binding and ARNT binding domains, but lacks the transactivation domain previously shown to be essential for a functional AHR2 protein (Hahn 1998; Andreassen et al. 2002). NLS: nuclear localization signal, NES1: nuclear export signal 1, NES2: nuclear export signal 2.

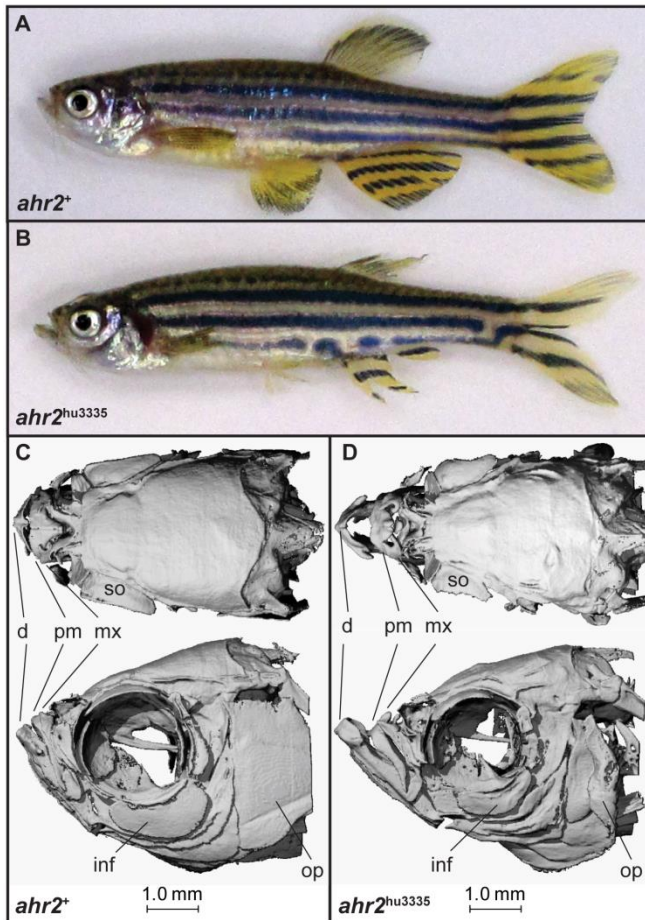


Figure 3-2 Fin and skeletal abnormalities in *ahr2*^{hu3335} zebrafish

A-B) Brightfield and **(C-D)** microCt imaging of adult *ahr2*⁺ and *ahr2*^{hu3335} zebrafish. Notable differences were observed in the dentate (d), premaxilla (pm), maxilla (mx), supraorbital (so), infraorbital 3 (inf) and operculum (op).

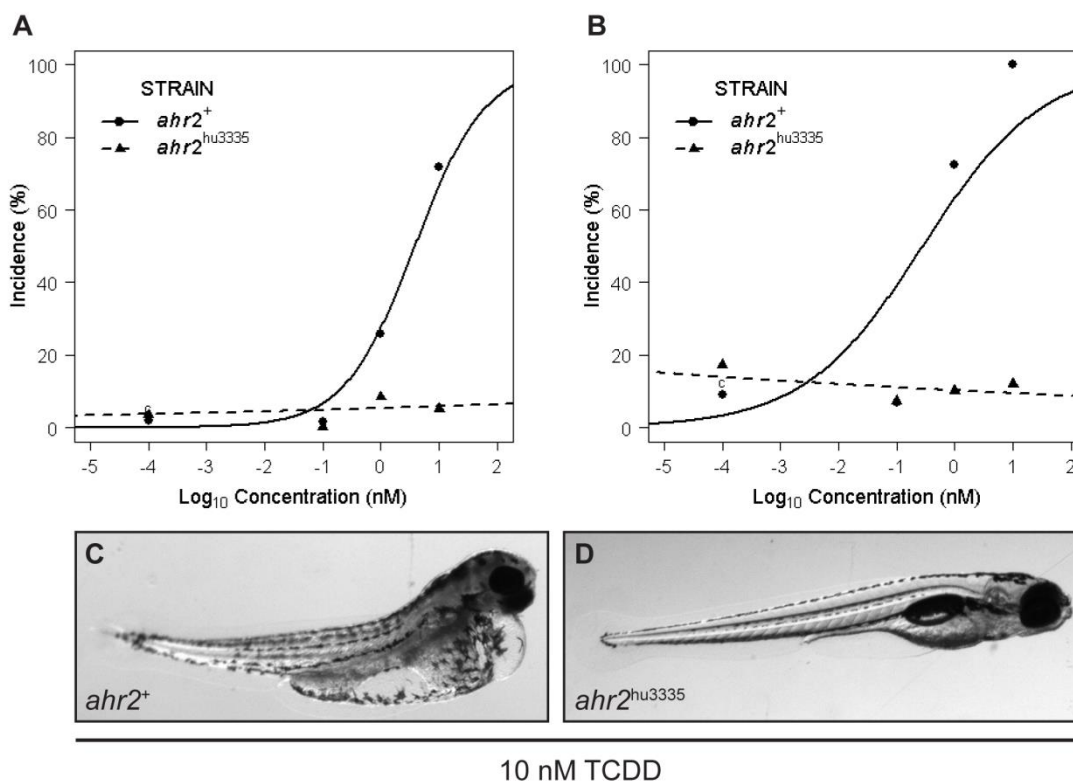


Figure 3-3 *ahr2*^{hu3335} embryos are resistant to TCDD developmental abnormalities

A) Percent of embryos with axis malformations and **B)** percent incidence pericardial edema at 120 hpf in embryos treated with 0, 0.1, 1 or 10 nM TCDD from 6-24 hpf. Vehicle control groups (c, 0.1% DMSO) are displayed at 10⁻⁴ for graphing purposes. Data represent three independent experiments with 20 embryos per treatment group. **C)** Representative image of *ahr2*⁺ and **(D)** *ahr2*^{hu3335} embryos developmentally exposed to 10 nM TCDD at 120 hpf.

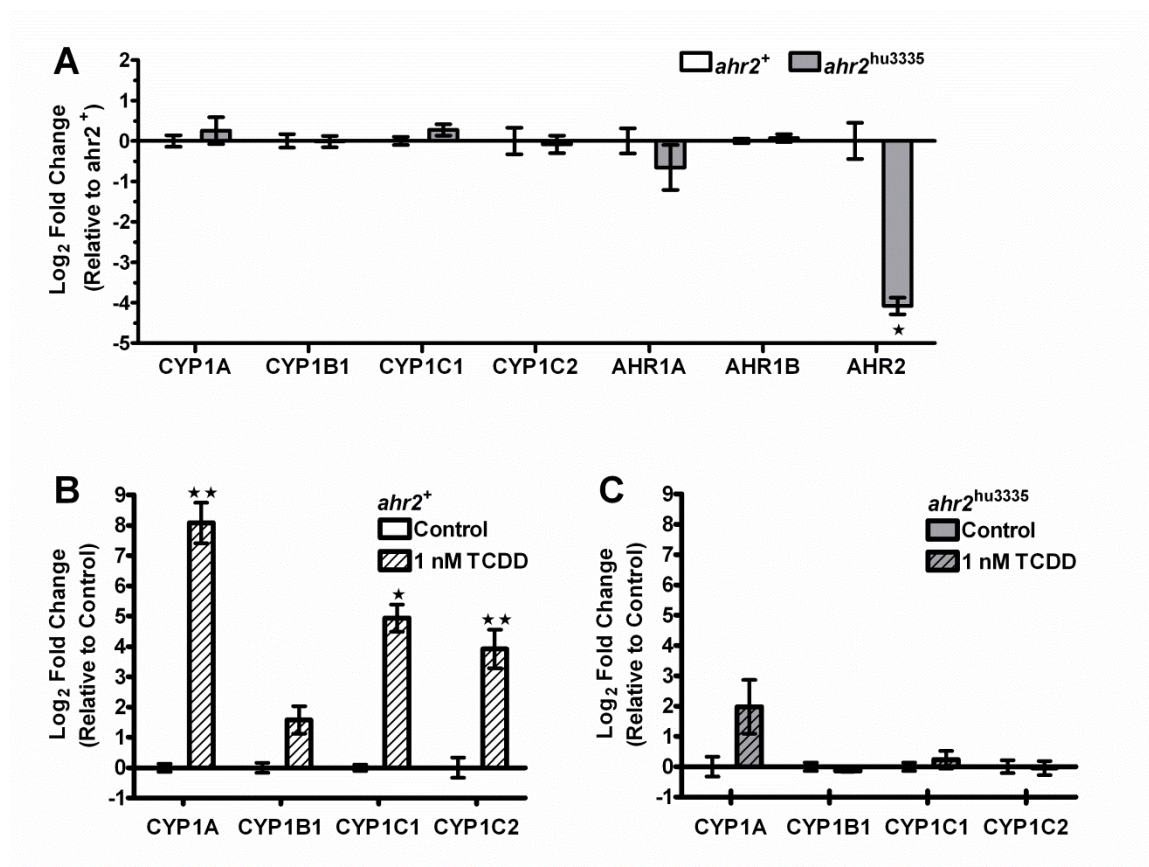


Figure 3-4 *ahr2*^{hu3335} embryos are resistant to TCDD-induced CYP induction

A) Comparative analysis of AHR1A, AHR1B, CYP1A, CYP1B, CYP1C1 and CYP1C2 mRNA expression in wild-type 5D and *ahr2*^{hu3335} mutant embryos at 48hpf. $\Delta\Delta Ct$ values were calculated by comparing sample ΔCt values (normalized to β -actin) to the mean *ahr2*⁺ ΔCt for each gene. Data were analyzed by paired student's t-test, * $p < .05$. **B)** Developmental exposure (6-24 hpf) to 1nM TCDD induced significant CYP1A, CYP1C1 and CYP1C2 expression at 48 hpf in *ahr2*⁺ embryos. Data is shown normalized to vehicle-treated controls and was analyzed with paired student's t-test, * $p < .05$, ** $p < .01$. **C)** Developmental exposure to 1nM TCDD did not induce significant mRNA expression changes in *ahr2*^{hu3335} embryos. While CYP1A was elevated, the difference was not significant (paired student's t-test treated vs. vehicle control).

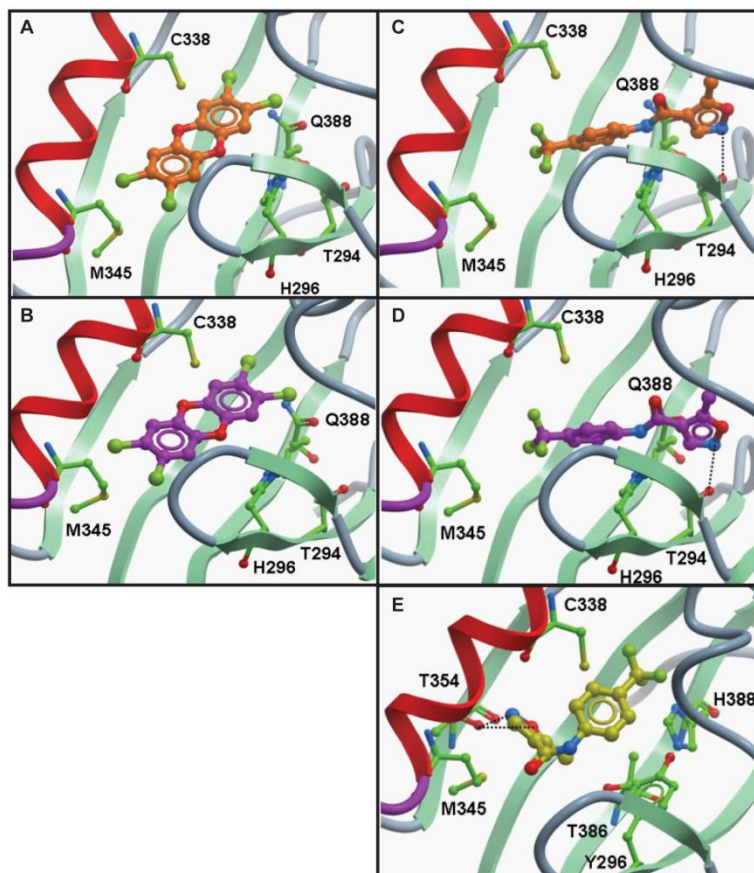


Figure 3-5 Molecular docking of TCDD and Leflunomide in zebrafish AHR isoforms

A) TCDD docking orientation in zebrafish AHR2- and **B)** AHR1B-LBD homology model binding pocket (ICM v3.5-1n, Molsoft). **C)** Leflunomide docking orientation into AHR2-, **D)** AHR1B- and **E)** AHR1A homology model binding pockets. The residues are displayed as sticks and colored by atom type with the carbon atoms in green. The protein backbone is displayed as ribbon and colored by secondary structure. The ligand is displayed as sticks and colored by atom

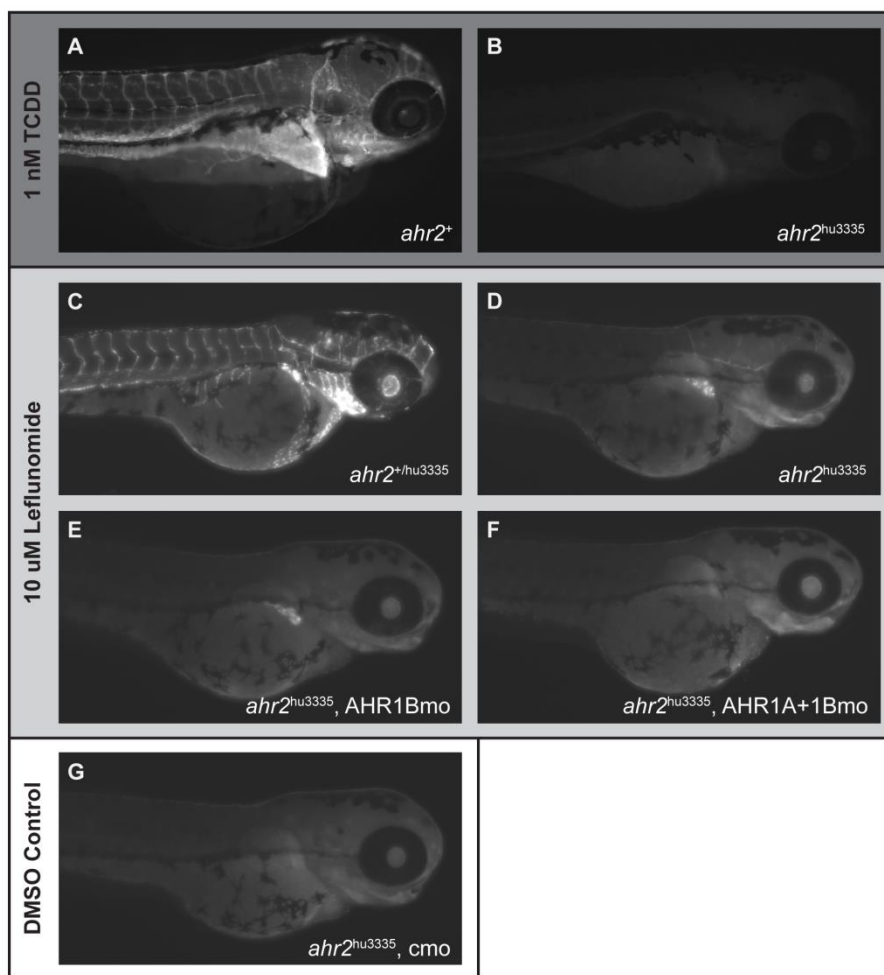


Figure 3-6 CYP1A protein expression patterns

CYP1A expression at 120 hpf in **(A)** *ahr2*⁺ and **(B)** *ahr2*^{hu3335} larvae following exposure to 1 nM TCDD from 6-24 hpf. **(C)** Leflunomide-induced CYP1A expression at 72 hpf in wild-type and **(D)** *ahr2*^{hu3335} mutants. **(E)** Leflunomide-induced CYP1A expression in AHR1B-morphant *ahr2*^{hu3335} larvae and **(F)** larvae co-injected with AHR1A and AHR1B of morpholinos. **(G)** DMSO control. TCDD-exposed embryos were IHC processed side-by-side and imaged at 120 hpf using the same exposure settings and a single focal plane. Leflunomide-exposed embryos and DMSO control were processed side-by-side and imaged at 72 hpf using the same exposure times; images were created from a z-stack of 10 15.4uM slices centered on the liver.

Table 3-1 Primer sequences for PCR experiments**mo**- morpholino mis-splice detection **mut**- mutant point mutation detection

Target	Forward Primer (5'- 3')	Reverse Primer (5'- 3')
<i>AHR1A</i>	CGCAAAAGGAGGAAACCTGTC	CCTGTAGCAAAAATTCCCCCT
<i>AHR1B</i>	GGTTTGTGTCGTCAAACAACAGTAACCACG	CCACCAACACAAAGCCATTAAGAGCCTG
<i>AHR1B-mo</i>	CTTTGTGTGTCGTTTCCGATGCC	GCACAGTAGAGCATATCAGCTGC
<i>AHR2</i>	TGGACTAGATCAGACAACCC	GAAGAGGGAGAGTCATTGTG
<i>AHR2-mut</i>	TATTGCTAGGCAGAGAGCAC	GATGTCTTCTGTGATGATTTTCG
<i>CYP1A</i>	TGCCGATTTTCATCCCTTTCC	AGAGCCGTGCTGATAGTGTC
<i>CYP1B1</i>	CTGCATTGATTTCGAGACGTG	CACACTCCGTGTTGACAGC
<i>CYP1C1</i>	AGTGGCACAGTCTACTTTGAGAG	TCGTCCATCAGCACTCAG
<i>CYP1C2</i>	GTGGTGGAGCACAGACTAAG	TTCAGTATGAGCCTCAGTCAAAC
<i>β-ACTIN</i>	AAGCAGGAGTACGATGAGTC	TGGAGTCCTCAGATGCATTG

Table 3-2 Concentration responses for developmental effects

Effect	p-value of <i>ahr2</i> ⁺ TCDD concentration-response	p-value of <i>ahr2</i> ^{hu3335} TCDD concentration-response	p- value of <i>ahr2</i> ⁺ <i>ahr2</i> ^{hu3335} differential response
yolk sac edema	< 0.0001	0.7181	0.0004
axis	< 0.0001	0.2754	0.0006
eye	< 0.0001	1.0000	0.0005
snout	< 0.0001	0.6706	0.0004
jaw	< 0.0001	0.8632	0.0011
pericardial edema	< 0.0001	0.0848	0.0002

Table 3-3 Predicted binding energy values for zebrafish AHR2, AHR1B and AHR1A
(kcal/mol), ND – unable to dock

	AHR2	AHR1B	AHR1A
TCDD	-3.97	-4.86	ND
Leflunomide	-2.13	-1.97	-2.19

Table 3-4 Summary of zebrafish AHR ligand binding, activity and expression

Receptor	Receptor mRNA expression in adult zebrafish	In vitro TCDD binding and activity	Homology model predicted ligand binding		Dominant receptor-dependent CYP1A protein induction pattern (larval)
			<i>TCDD</i>	<i>Leflunomide</i>	
AHR1A	heart, swimbladder, liver, kidney(Andreasen et al. 2002)	N(Andreasen et al. 2002; Karchner et al. 2005)	N	Y	liver
AHR1B	NA	Y(Karchner et al. 2005)	Y	Y	vasculature
AHR2	brain, heart, muscle, swimbladder, liver, gill, skin, eye, kidney, fin(Andreasen et al. 2002)	Y(Andreasen et al. 2002; Karchner et al. 2005)	Y	Y	liver, vasculature

Chapter 4 - Ahr-dependent developmental toxicity and differential transcriptional profiles induced by 4-ring oxygenated PAHs

Goodale, B.C.¹, Tilton, S.C.², Sullivan, C.M.^{1,3}, Waters, K.M.² and Tanguay, R.L.¹.

1. Department of Environmental and Molecular Toxicology, the Environmental Health Sciences Center, Oregon State University, Corvallis, OR,

2. Computational Biology and Bioinformatics, Pacific Northwest National Laboratory, Richland, WA

3. Center for Genome Research and Biocomputing, Oregon State University, Corvallis, OR

Abstract

Polycyclic aromatic hydrocarbons (PAHs) are common air pollutants and combustion byproducts that exhibit diverse mutagenic, carcinogenic, proinflammatory and teratogenic properties. Unsubstituted (parent) PAHs are defined by three or more fused benzene rings; oxygen-substituted PAHs (OPAHs) are also formed during combustion, as well as via phototoxidation and biological degradation of parent PAHs. Despite their prevalence both in contaminated industrial sites and in urban air, their mechanisms of action in biological systems are relatively understudied. Like parent PAHs, OPAHs exhibit structure-dependent mutagenic activities and differential activation of the aryl hydrocarbon receptor (AHR). In the canonical AHR signaling pathway, the AHR translocates to the nucleus upon ligand binding, dimerizes with the aryl hydrocarbon receptor nuclear translocator (ARNT), and binds to DNA response elements to activate transcription of a suite of downstream genes that include cytochrome p450 phase 1 metabolizing enzymes (CYP1A, CYP1B1). In a screen of diverse OPAHs for developmental toxicity in zebrafish, 4-ring OPAHs benzo[a]anthracene (BEZO) and benzo[a]anthracene-7,12-dione (7,12-B[a]AQ) induced similar morphological aberrations and markers of oxidative stress, but only 7,12-B[a]AQ significantly induced *cyp1a* expression. We investigated the role of the AHR in mediating the toxicity of BEZO and 7,12-B[a]AQ, and found that knockdown of *ahr2* rescued developmental effects caused by both compounds. Using comparative RNA-seq, we show that BEZO induces expression of xenobiotic metabolizing genes directly regulated by AHR with distinctively lower potency than 7,12-B[a]AQ. The much larger majority of significantly-induced transcripts, including genes that regulated redox-homeostasis, were affected similarly by these two OPAHs. Biological functions and transcription factors predicted to regulate the genes significantly misexpressed by BEZO and 7,12-B[a]AQ suggest that the AHR interacts differentially with other transcription factors and coactivators to mediate the developmental toxicity caused by these compounds.

Introduction

Polycyclic aromatic hydrocarbons (PAHs) are major components of combustion emissions and contaminants at hazardous waste sites. Automobiles, wood burning, coal-based energy production and other combustion processes produce both parent (unsubstituted) PAHs, consisting of multiple fused carbon rings, as well as a variety of substituted derivatives. PAHs are associated with both the gaseous and ultrafine particulate fractions of urban air, can accumulate in the lungs when inhaled, and are considered major carcinogenic components of combustion emissions (Bostrom et al. 2002; Ramirez et al. 2011). Oxygenated, nitrated, and methylated PAHs also form from parent PAHs through photo-oxidation (via ozone and hydroxyl radical) reactions as well as biotic metabolism in the environment (Yu 2002; Lundstedt et al. 2007). The EPA has identified 16 PAHs on its priority pollutant list, based on their prevalence at Superfund sites and potential health effects (EPA 2012). Parent PAHs are routinely measured in order to estimate total PAH contamination levels and potential hazard, but degradation products, such as oxygenated PAHs (OPAHs) are less frequently accounted for. As detection methods have improved and standards are more widely available, recent studies showed that OPAHs are present in PAH-contaminated environmental samples, and it is expected that they may be present at higher concentrations than parent PAHs (Lundstedt et al. 2006; Layshock et al. 2010; Walgraeve et al. 2010). Despite this, little data is available about their toxicity. Like a number of parent PAHs, some OPAHs are mutagenic (Durant et al. 1996; Gurbani et al. 2013). Based on the varied and structure-dependent toxicological effects of unsubstituted PAHs, which include developmental toxicity mediated by the aryl hydrocarbon receptor (AHR), as well as cardiac toxicity and immune effects, substituted PAH structures are likely to also induce non-cancer toxic effects. A screen of OPAH toxicity in developing zebrafish demonstrated that OPAHs cause developmental effects at a wide range of waterborne concentrations, and different structural elements likely explain their differential induction of a variety of morphological abnormalities (Knecht et al. 2013). Like unsubstituted PAHs, OPAHs differentially induce expression of known targets of the aryl hydrocarbon receptor, such as *cyp1a*. They also induce expression of genes involved in redox homeostasis, suggesting that oxidative stress also plays a role in their toxicity. Because of their ubiquity, and potential greater prevalence in some environmental situations than parent PAHs, there is a need to understand

mechanisms by which OPAHs cause toxicity, and how these mechanisms are related to, or distinct from, those identified for parent PAHs.

Here we compare the transcriptional signatures and proposed toxicological mechanisms of two structurally-related OPAHs, 1,9 benz-10-anthrone (BEZO) and benz(a)anthracene-7,12-dione (7,12-B[a]AQ) during embryonic development. These 4-ring OPAHs, which are detected in environmental samples, differ in their ring arrangement and oxygenation pattern. BEZO is detected in air samples associated with high traffic emissions, but is also an important intermediate used in production of dyes (Nielsen et al. 1999; Wei et al. 2012). Exposure has been associated with hepatic and dermal lesions in workers, as well as ascorbic acid depletion in animal models (Singh et al. 2003). 7,12-B[a]AQ is also detected in air and at industrial waste sites, and was among the most abundant OPAHs detected in urban air in Beijing (Wang et al. 2011; Wei et al. 2012). 7,12-B[a]AQ can be formed from benz(a)anthracene (BAA), an EPA priority pollutant PAH which is mutagenic and induces developmental toxicity via the AHR (Incardona et al. 2006). Both compounds were identified in a zebrafish toxicity screen to disrupt normal development, while differentially inducing *cyp1a* expression, suggesting distinct modes of action. We investigated the role of Ahr2 in mediating developmental toxicity. We used whole genome mRNA sequencing to investigate global differences in transcription induced by these compounds. Despite their differential *cyp1a* activation and early morphology profiles, we found that developmental toxicity of both BEZO and 7,12-B[a]AQ was dependent on *ahr2*. Transcriptional profiling with RNA-seq showed largely similar gene expression between the compounds, with cellular redox homeostasis genes playing a large role in the toxicological response. The large difference in *cyp1a* expression, coupled with more subtle differences in the expression of interacting transcription factors, highlights the ability of the AHR to mediate toxicity via alternate pathways in a ligand-dependent manner. Understanding the multitude of AHR interactions is important for assessing and predicting health risk posed by OPAHs. Comparative transcriptional profiling additionally sheds light on conserved mechanisms and biomarkers that may be more appropriate than *cyp1a* for inferring exposure and AHR activation by this class of emerging contaminants.

Materials and Methods

Fish Husbandry

All experiments were conducted with wild-type 5D zebrafish. Adult zebrafish were maintained at the Sinnhuber Aquatic Research Laboratory on a recirculating system with a water temperature of $28 \pm 1^\circ\text{C}$, and a 14 hr light: 10 hr dark photoperiod. All experiments were conducted with embryos collected in the morning from multiple adult zebrafish set up for group spawning as described previously (Reimers et al. 2006). Adult care and reproductive techniques were conducted according to Institutional Animal Care and Use Committee protocols at Oregon State University.

Chemicals

Analytical grade (> 98% purity) 1,9-benz-10-anthrone (BEZO) was purchased from Fluka, and benz(a)anthracene-7,12-dione (7,12-B[a]AQ) was purchased from Sigma-Aldrich. Compounds were dissolved to 10 mM in dimethyl sulfoxide (DMSO). Stocks were sonicated in a bath sonicator for 15 min before each use. For embryo exposures, BEZO and 7,12-B[a]AQ stocks in 100% DMSO were dissolved in embryo media to a final concentration of 1% DMSO.

Developmental toxicity

Embryos were cleaned, developmentally staged and batch-exposed in glass vials at 6 hours post fertilization (hpf) to 5, 7.5 and 10 μM concentrations of OPAH or 1% DMSO vehicle control, 20 embryos per vial in 2 mL exposure solution (Kimmel et al. 1995). Vials were protected from light and incubated on a rocker at 28°C for the duration of the exposure. Embryos were collected at 48 hpf for RNA and immunohistochemical analysis. For developmental toxicity evaluations, embryos remained in solution until 72 hpf, when they were rinsed 3 times, transferred to individual wells of a 96-well plate, and incubated in fresh embryo media until evaluation at 120 hpf. Embryos were then euthanized with MS-222 (tricaine methanesulfonate) and evaluated for yolk sac, axis, trunk, somite, fin, cardiac, eye, snout, jaw, otic vesicle, brain and pigment malformations. Mortality and the percentage of embryos with each malformation were calculated for each treatment group with the vial (20 embryos) as the experimental unit. Representative larvae were imaged at 48 and 120 hpf with a Nikon Coolpix 5000 digital camera. Experiments were repeated in triplicate, and percent incidence data across replicates was analyzed for significance using SigmaPlot

software. Data were analyzed for morpholino and treatment effects by two-way ANOVA with Tukey's all pairwise post hoc test for each endpoint.

Morpholino injection

Embryos were injected at the single cell stage with a fluorescein-tagged translation-blocking morpholinos targeting *ahr2* (*ahr2*-MO, 5' TGTACCGATACCCGCCGACATGGTT 3'), or a standard nonsense control (control-MO, 5' cctcttacctcagttacaatttata 3') purchased from Gene Tools (Philomath, OR) at a concentration of 0.75mM. Injection volume was ~2nL. Fertilized, normally developing embryos were screened for morpholino incorporation at 4 hpf by fluorescence microscopy. Three independent replicates were conducted.

RNA isolation

Groups of 20 embryos were homogenized at 48 hpf in RNazol (Molecular Research Center, Cincinnati, OH) using a bullet blender with 0.5 mM zirconium oxide beads (Next Advance, Averill Park, NY). Samples were stored at -80°C until RNA isolation via phenol guanidine extraction. RNA was quantified and quality assessed using a SynergyMx microplate reader with the Gen5 Take3 module to calculate O.D. 260/280 ratios. Quality of RNA samples for sequencing was additionally assessed with an Agilent Bioanalyzer 2100. cDNA was synthesized from 1 µg (confirmation with RNA from sequencing samples) or 2 µg of RNA using the ABI high capacity cDNA synthesis kit. cDNA was diluted and 50 ng equivalents of RNA were used for QPCR reactions. 3-4 biological replicates were collected per treatment group.

Quantitative RT-PCR

Gene-specific primers (MWG Operon) for qRT-PCR amplification are listed in Table S1. All qRT-PCR assays were performed in 20 µl reactions consisting of 10 µl Power SYBR Green PCR master mix (Applied Biosystems), 0.4 µl each primer, 9.2 µl H₂O and 50 ng equivalents of cDNA. Amplification (Step One Plus, Applied Biosystems) was performed with cycling parameters as follows: 95°C for 10 min; 40 cycles of 95°C for 15 s, 60°C for 1 min; 95°C for 15 sec and 60°C for 1 min. A melt curve was performed at 3° increments to assess for multiple products. Relative fold change values in PAH-treated samples compared to vehicle controls were calculated for genes of interest, normalized to β-actin, by the method

described by Pfaffl (Pfaffl 2001). Four biological replicates were assessed and statistically analyzed by Two-way ANOVA with Tukey's post-hoc test using Sigmaplot software.

Immunohistochemistry

Whole embryos were fixed at 48 hpf in 4% paraformaldehyde at 4°C overnight. Mouse α fish CYP1A monoclonal (1:500 dilution, Biosense laboratories) primary antibody and Alexafluor® 594 goat α mouse IgG (H+L) (1:1000 dilution, Molecular Probes, Eugene, OR) secondary antibody were used for immunofluorescent labeling of Cyp1a as described by Svoboda et al (Svoboda et al. 2001). Briefly, embryos were washed in phosphate-buffered saline containing 0.1% Tween-20 (PBST), permeabilized by a 1 h incubation in distilled H₂O followed by 20 min in cold acetone and 30 min incubation in 1 mg/ml collagenase. Embryos were blocked for 1h in PBST with 10% normal goat serum, incubated with 1° antibody in 10% NGS overnight at 4°C, washed in PBST, and incubated in 2° antibody 4 h at RT. Embryos were imaged by epi-fluorescence microscopy using a Zeiss Axiovert 200M microscope with 5X objective. Merged images were created from z-stacks of 5 20uM slices captured under identical exposure conditions. Two overlapping frames were spliced to capture the entire length of each larva.

Paired-end mRNA sequencing

mRNA was isolated from total RNA samples, fractionated and libraries prepared with custom barcodes for sequencing at the University of Oregon Genomics Core Facility. 50 bp paired-end sequencing was conducted with an Illumina HiSeq 2000 sequencer; sequence (fastq) files were transferred to the Oregon State University Center for Genome Research and Biocomputing for analysis. Sequences were filtered based on Illumina quality scores and analyzed for quality using FastQC analytical software (Babraham Bioinformatics). Reads were trimmed to exclude low quality sequences at the end of reads.

Sequence mapping, transcriptome assembly and statistical analysis

Paired-end sequence reads were aligned with TopHat version 2.0.7 (Trapnell et al. 2009) to *Danio rerio* genome assembly Zv9.70 using the following parameters: 50 bp minimum intron length, 10000 bp maximum intron length, 200 mate pair inner distance, 150 bp mate pair inner distance stdev, --no-mixed option (only paired alignments). Transcripts were

assembled using Cufflinks, and merged with Cuffmerge using Zv9.70 as a guide to create a GTF file with all transcripts assembled from our data (Trapnell et al. 2012). Differentially expressed transcripts, first including novel transcripts from our dataset, were identified with Cuffdiff by comparing BEZO and 7,12 B[a]AQ exposed samples to the 1% DMSO control. Upper quartile normalization and bias correction using Zv9.70 were performed, and an FDR of 0.01 was applied. Differentially expressed genes with an adjusted p value of <0.05 were considered significant. We conducted a second statistical analysis in Cuffdiff, using only the Zv9.70 transcriptome (no novel transcripts), to identify significant gene lists with better annotation for analysis of biological functions for each BEZO and 7,12-B[a]AQ, using an FDR of 0.05. Log₂ fold change (log₂FC) values were calculated by comparing each sample FPKM value to the mean control FPKM value. For comparisons with microarray PAH data, log₂FC values based on fluorescence intensity values were used, microarray data is available in the NCBI GEO omnibus Accession: GSE44130 (Goodale et al. 2013). Hierarchical clustering and heatmap visualizations were conducted with Multiexperiment Viewer (MeV) (Saeed et al. 2003).

Pathway analysis

Go Rilla (Gene Ontology enRichment anaLysis and visualization) tool was used to identify enriched gene ontology (GO) terms from clusters of genes in the BEZO-7,12-B[a]AQ heatmap (Eden et al. 2009). Official gene symbols were used, with the background of official gene symbols for all transcripts identified in the dataset. GO Rilla recognized 15,768 zebrafish gene symbols provided from our combined GTF file. GO terms with p values <0.001 were considered significant.

The Bioinformatics Resource Manager v 2.3 (BRM) was used to identify Entrez IDs and human homologs of significant genes identified in our statistical comparison using the Zv9 transcriptome (Tilton et al. 2012). We used Metacore GeneGo software to identify enriched biological processes, GO terms, and predicted transcription factors from the BEZO and 7,12-B[a]AQ significant gene lists ($p < 0.05$). Statistical significance of over-connected interactions was calculated using a hypergeometric distribution, where the P value represents the probability of a particular mapping arising by chance for experimental data compared to the background (Nikolsky et al. 2009). Networks were constructed in

MetaCore for experimental data using an algorithm that identifies the shortest path to directly connect nodes in the dataset to transcription factors. Network visualizations were generated in Cytoscape (Shannon et al. 2003). MetaCore processes, GO terms, and predicted transcription factors were filtered to include only those associated with at least 10 genes in the dataset. For MetaCore processes, a statistical cutoff of $P < 0.005$ was used. GO terms with associated P values < 0.001 were considered significant, and the 20 most significant GO terms for each OPAH were reported. Transcription factors with statistical overconnectedness P values < 0.001 were considered significant.

Results

AHR2 morphants are resistant to BEZO and 7,12-B[a]AQ induced developmental toxicity

We investigated the role of AHR2 in developmental toxicity of 7,12-B[a]AQ and BEZO by exposing control and *ahr2* morpholino-injected (morphant) zebrafish embryos to 0, 5, 7.5 and 10 μM concentrations of OPAH and observing morphological changes at 120 hpf. Both 7,12-B[a]AQ and BEZO induced a concentration-dependent increase in the percentage of control -injected embryos with pericardial edema (Figure 2A and B, dark circles, F and G). Interestingly, neither 7,12-B[a]AQ nor BEZO caused a significant increase in pericardial edema in *ahr2* morphants (Figure 2A and B, light circles, I and J). BEZO and 7,12-B[a]AQ-exposed control morphants also had significant jaw, eye and axis malformations, which were not significantly increased in *ahr2* morphants (two way ANOVA, $P < 0.05$). While a slight increase in embryos exhibiting at least one malformation was observed in *ahr2* morphants exposed to 7,12-B[a]AQ or BEZO, the increases were not significant. As observed previously, 7,12-B[a]AQ and BEZO induced similar malformation profiles, which also included significant increases in jaw, yolk sac edema, and to a lesser extent curved body axis (Figure 2F, G). The compounds induced a similar concentration response, with the 7.5 μM exposure eliciting a response in nearly 100% of embryos.

BEZO and 7,12-B[a]AQ induce distinct malformations and cytochrome P450 phase 1 metabolizing enzyme expression at 48 hpf

To further compare the developmental toxicity of these 4-ring OPAHs, we focused on the earlier 48 hpf developmental time point, when robust Cyp1a expression can be visualized by immunohistochemistry following ligand exposure, but the liver and its metabolic activity

are not yet functional. We examined *cyp1a* and *cyp1b1* mRNA expression in control and *ahr2* morphant embryos exposed to 7.5 μ M 7,12-B[a]AQ or BEZO, compared to vehicle control. As is expected for an Ahr2 agonist, 7,12 B[a]AQ exposure induced a robust, 197-fold average increase in *cyp1a* expression in control-injected embryos (Figure 3A). The *ahr2* morpholino caused a 64% reduction, with *cyp1a* induced 61-fold in *ahr2* morphants exposed to 7,12 B[a]AQ. *Cyp1b1* expression was also induced by 7,12-B[a]AQ exposure, with an average 17-fold change in control-injected embryos (Figure 3A). *cyp1b1* induction was 96% prevented with the *ahr2* morpholino; basal expression was significantly (albeit only 1.8 fold) higher in *ahr2* morphants compared to control morphants, and was not significantly induced by 7,12 B[a]AQ exposure. 7,12-B[a]AQ induced malformations, including pooling of blood ventral to the developing heart, slight curved body axis and reduced size, which were apparent by 48 hpf (Figure 3E, compared to 3C vehicle control). Cyp1a protein, visualized by whole-mount immunohistochemistry, was robustly expressed throughout the trunk and brain vasculature, as well as the developing heart (Figure 3K, compared to 3I control). The *ahr2* morpholino completely prevented all of the morphological effects observed (Figure 3F, compared to 3C,D controls). Cyp1a protein expression was largely prevented, with some remaining vascular expression in the eye, brain, and trunk (Figure 3L). This expression is in agreement with the 61-fold change in *cyp1a* mRNA in the *ahr2* morphants. The incomplete block of *cyp1a* expression by morpholino is in line with previous studies, and may be due to incomplete morpholino efficacy or induction via one of the other zebrafish AHR isoforms. It is important to note, however, that it does not correspond with any observable malformations at 48 or 120 hpf.

In contrast to the strong *cyp1a* induction observed with 7,12-B[a]AQ, exposure to 7.5 μ M BEZO induced a 4.5-fold increase in *cyp1a* in control morphants (Figure 3B). While statistically significant, this *cyp1a* induction is only ~2% of the 7,12-B[a]AQ response. Knockdown of *ahr2* resulted in a 42% rescue of the *cyp1a* induction by BEZO. *Cyp1b1* was induced 1.8-fold by BEZO exposure. This expression level was similar to that in *ahr2* morphants, which showed no difference in *cyp1b1* expression between treatment groups. While *cyp1a* and *cyp1b1* induction was minimal, BEZO induced distinct physiological abnormalities by 48hpf. Severe edema was consistently observed surrounding the developing heart (Figure 3G). Compared to the 120 hpf time point, the BEZO and 7,12

B[a]AQ phenotypes could be readily distinguished at 48 hpf, where BEZO-exposed embryos had more pronounced pericardial edema, but did not exhibit the axis and shorter trunk length induced by 7,12-B[a]AQ (Figure 3G compared to 3E). BEZO-induced malformations were not accompanied with any Cyp1a protein expression detectable by whole-mount immunohistochemistry (Figure 3M). This was consistent with the very low *cyp1a* mRNA induction. In agreement with the 120 hpf malformation data, however, knockdown of AHR2 completely rescued the BEZO-induced developmental abnormalities at 48 hpf (Figure 3H).

Comparison of mRNA expression profiles with mRNA-seq

The large difference in *cyp1a* mRNA expression at an EC100 concentration for malformations suggested differences in transcriptional regulation between BEZO and B[a]AQ. We used whole genome mRNA expression profiling (mRNA-seq) to identify global mRNA expression changes induced by these two OPAHs at 48 hpf. Paired-end 50bp RNA-seq was conducted on embryos exposed to 10 μ M 7,12-B[a]AQ, 10 μ M BEZO or 1% DMSO control from 6-48 hpf. Three biological replicates of pooled RNA from 20 embryos were sequenced for each exposure group. An average of 48.2 ± 7.9 (stdev) million paired sequence reads passing Illumina QC were obtained per sample. Alignment to Sanger zebrafish genome build Zv9.70 resulted in 36.2 ± 6.1 million mapped reads per sample (75%). Of these, an average of 28.8 ± 5.3 million paired reads per sample (~80%) mapped uniquely to one location in the genome (Table S2). Transcripts were assembled with cufflinks and merged with the Zv9.70 transcriptome to obtain a combined transcript file with 32,432 Ensembl genes and 13,478 novel transcripts. Comparison of each treatment with the DMSO control using CuffDiff identified 964 differentially expressed transcripts in the 7,12-B[a]AQ group and 696 in the BEZO group ($p < 0.05$ with a FDR of 0.01). The union of significant transcripts was 1351.

Are transcripts misexpressed in embryos exposed to the parent PAH BAA similarly affected by OPAHs?

We previously identified transcripts misexpressed in response to three parent PAHs, dibenzothiophene (DBT), pyrene (PYR), and benz(a)anthracene (BAA) using the Agilent mRNA microarray platform (Goodale et al. 2013). BAA is a previously-identified AHR agonist, while the other two PAHs do not induce AHR-dependent toxicity. We hypothesized

that the genes significantly misexpressed by BAA would respond similarly to 7,12-B[a]AQ, because of their identical ring structures (Figure 1). We examined the expression of these genes across 7,12-B[a]AQ and BEZO, in comparison to the parent PAHs, in order to better refine a set of genes distinct to PAHs that induce toxicity via the AHR. We also sought to discern any differences between the three putative AHR ligands, and to identify misexpressed transcripts common to all PAH exposures. Ensembl IDs and corresponding transcripts were identified in the RNA-seq dataset for 57 transcripts that were significantly misexpressed by BAA at 48 hpf in the microarray study (Goodale et al. 2013). Of these transcripts, 32 were significant for 7,12-B[a]AQ and 17 for BEZO. Caution is necessary for comparison across studies on different platforms; the magnitude of fold change values detected by microarray vs. RNA-seq have been shown to be different, and the platforms can differ in their sensitivity (van Delft et al. 2012). Comparison of significant gene lists in particular is problematic because of the different background sets and statistical methods employed. We have found heatmaps useful for visualizing patterns in expression across PAHs and identifying clusters of similarly expressed transcripts for further analysis. A heatmap of the BAA significant transcripts was created using log2FC values for each sample compared to the average control (1% DMSO) value on its platform (Fluorescence intensity for microarray, FPKM value for RNA-seq). Bidirectional hierarchical clustering was conducted in the MultiExperiment Viewer to identify clusters of differentially expressed transcripts (Figure 4). Replicates of each PAH treatment group clustered together; no platform-based clustering was observed among the controls. 7,12-B[a]AQ samples were the most distant from controls, and clustered closely with BAA. As expected for compounds lacking AHR activity, DBT and PYR clustered most closely with the control samples. The BEZO cluster grouped between the BAA-7,12-B[a]AQ cluster and the other PAHs, with less robust expression than 7,12-B[a]AQ and BAA, but also notably different than PYR and DBT. Expression patterns on the whole were similar across BEZO, BAA and 7,12-B[a]AQ, but differed in magnitude, suggesting that differences between the PAHs for this set of transcripts lie in dose, potency, or platform, rather than mechanism. No directional differences were observed that would suggest distinct regulatory mechanisms between these PAHs. Several distinct clusters of genes were identified by the bidirectional hierarchical clustering. The genes in the top cluster, *cyp1a*, *cyp1c1*, *wfikk1*, *ahrrrb*, *cyp1c2*

and *cyp1b1* were the most highly induced by BAA and 7,12-B[a]AQ, with mean FC values reaching 230 for *cyp1a*. They were also induced by BEZO, but to a lower extent (4-fold or less), in agreement with our previous data for *cyp1a*. A large group of genes below the top cluster were only mildly induced by BAA, and were more variable for the rest of the PAHs. A small cluster of genes in the middle of the heatmap, *s100z*, *cxc4a*, *slc1a4* and *psat1*, were consistently induced by all 5 PAH exposures. *Cxr4a* and *s100z* were previously identified in the microarray study among the most highly elevated transcripts across the three parent PAH structures (Goodale et al. 2013). The cluster below this consisted of transcripts that were robustly elevated by BEZO, B[a]AQ and BAA, such as *ctsl.1*, *sult6b1* and *gsr*, but were not increased in DBT and PYR samples. Finally, the bottom cluster of the heatmap consisted of transcripts generally repressed by all 5 PAHs. This transcript set had subtle differences in expression levels between the AHR-activating vs AHR-independent PAHs. In order to investigate whether log₂FC values in the heatmap accurately portrayed expression trends across compounds that were tested on different platforms, we validated expression of genes from multiple clusters with qRT-PCR across all 5 PAHs (Table 1). Log₂FC values of *cyp1a*, *ctsl.1*, *sult6b1*, and *cxc4a* were very consistent between q-RT-PCR and both genome-wide platforms. Expression patterns of *ctgfb* and *s100z*, which were not as highly induced by any of the PAHs, were consistent in the qRT-PCR, but statistical significance was more variable across platforms (Table 1). Statistical analysis methods employed (ANOVA across treatment groups vs. pairwise with control, multiple testing corrections) were different between qRT-PCR, microarray, and RNA-seq. Significant gene list comparisons may therefore result in erroneous conclusions with this data. Our qRT-PCR analysis supports the idea, however, that clustering based on gene expression values may be a useful way to identify meaningful differences between PAHs using data from these two platforms. Based on the clustering analysis presented here with the AHR-related transcript list, we might predict BEZO to be an AHR agonist with lower potency than BAA and 7,12-B[a]AQ.

Novel BEZO and 7,12-B[a]AQ-induced transcripts identified with RNA-seq

mRNA-seq data provides a rich resource to compare expression across the entire genome, including novel transcripts not yet annotated in the current assembly. In order to identify transcriptional differences between BEZO and 7,12-B[a]AQ that might explain morphological and apparent potency differences for inducing AHR-related targets, we used

Cuffdiff to compare each OPAH treatment group to the 1% DMSO control. In our primary analysis, we employed a transcript set that included all transcripts in the zebrafish genome (Zv9) as well as novel transcripts identified in our dataset.

Comparison of the significant gene lists ($p < 0.05$, 0.01 FDR) revealed 309 transcripts that were significantly misexpressed in response to both PAHs. 387 transcripts were unique to BEZO, and 655 were unique to BaAQ. 366 of the significant transcripts had a fold change > 2 (Figure 5A). Of these, 125 transcripts were unique to BEZO, while 171 were unique to 7,12-B[a]AQ. 70 transcripts were similarly expressed between the two OPAHs, and the numbers of over- vs under-expressed transcripts were nearly equivalent. 10 of the transcripts similarly expressed in the BEZO and 7,12-B[a]AQ groups were not annotated in Zv9 (novel to our dataset). BEZO and 7,12-B[a]AQ uniquely induced changes in 22 and 33 novel transcripts, respectively. Annotation of the zebrafish genome has undergone rapid improvement in recent years; experimentally identified transcripts from RNA-seq studies, however, have yet to be fully incorporated into the transcriptome. While “novel” transcripts may result from sequencing errors, repeats, or incorrect assembly, they may also represent as-of-yet unidentified genes that could be involved in mechanisms of toxicity, which are not yet fully elucidated for the AHR. We examined novel transcripts that had the largest fold changes between treatment groups using both Gbrowse, to examine coverage across our samples, as well as with the Ensembl genome browser to view predicted transcripts from publicly available RNA-seq data. Many of our “novel” transcripts corresponded with regions of high transcriptional coverage in other datasets, but were not annotated as transcripts in publicly available databases. Novel transcript XLOC_030523 was one of the most highly induced transcripts in the 7,12-B[a]AQ treatment groups (9.7 fold, $p < 0.05$). The genomic context of this predicted transcript (Chromosome 3: 63102008-63105155) is displayed in Figure 5B (top). The pooled RNA-seq alignment track shows a long region of moderate coverage upstream of *sox9b* on the -1 strand, and a predicted transcript based on this RNA-seq data (5 dpf exon track). There are no Ensembl/Havana annotated transcripts within this region. The Gbrowse view (Figure 5B, bottom) shows the predicted transcript from our dataset, along with neighboring transcripts that were likely predicted as separate because of the low coverage. The control samples all had very low coverage of this region, while the 7,12-B[a]AQ samples had much higher coverage. This supports the Cufflinks-Cuffdiff

identification of this as an overexpressed transcript in the 7,12-B[a]AQ -exposed embryos. Several of the neighboring predicted transcripts were also significantly increased by 7,12-B[a]AQ, but not by BEZO. By visualizing our data alongside a set of recently-identified long intergenic non-coding RNAs (lincRNAs) we discovered that several of our predicted “novel” transcripts are part of a leader-like lincRNA (Chew et al. 2013). Its location near *sox9b* is particularly intriguing, given the important role of *sox9b* in mediating AHR-dependent effects of TCDD on tissue regeneration, jaw and heart development (Andreasen et al. 2006; Xiong et al. 2008; Hofsteen et al. 2013). The mechanism by which AHR activation results in decreased *sox9b* expression is not known. In our dataset *sox9b* was decreased by 7,12-B[a]AQ, though not significantly, perhaps because RNA was from whole embryo rather than specific tissue types. Novel transcripts identified within this dataset will require additional validation. Examination of the genomic context, as demonstrated in Figure 5B, suggested that many are not sequencing artifacts but rather have not yet been annotated in Zv9, and should be included in our comparison of BEZO and 7,12-B[a]AQ.

We performed hierarchical clustering on the union of BEZO and 7,12-B[a]AQ significantly misexpressed transcripts with FC >2, and identified clusters of transcripts with different expression patterns (Figure 5C). Considering now the entire set of misexpressed transcripts, rather than the AHR agonist-associated transcripts discussed earlier, a set of genes underexpressed in BEZO and 7,12-B[a]AQ-exposed embryos was notable. Few genes were identified in the microarray as down-regulated by BAA. This could potentially reflect a difference in the platforms used; we nevertheless compared expression of the BEZO and 7,12-B[a]AQ significant transcripts from Figure 5C across all 5 PAHs (Figure S3). The genes down-regulated by the OPAHs were generally not affected by BAA. Many, however, were similarly misregulated by DBT and PYR. There was also a notable group of transcripts induced by the OPAHs, including *gstp1*, which were not strongly affected by the parent PAHs. Differences between the OPAHs remained subtle, however. No oppositely expressed gene clusters were apparent between BEZO and 7,12-B[a]AQ.

We used GO rilla Gene Ontology enrichment analysis to investigate biological processes associated with differentially expressed gene clusters (Figure 5C). Because significant transcripts were identified from our merged transcriptome, many did not have sufficient

annotation for ontology analysis (novel transcripts and transcripts lacking official gene names); biological processes were only identified for 5 of the clusters. The significant ($P < 0.001$) GO process for cluster 12, which contained the previously-discussed *cyp1* genes, was Response to Chemical Stimulus (GO:0042221, Figure 5C bottom). The only significant term identified for the large group of transcripts overexpressed in both BEZO and 7,12-B[a]AQ was Oxidation-reduction Process (GO:0055114). Cluster 8, expressed more highly in BEZO-exposed embryos, was enriched for Cell-cycle Arrest (GO:0007050). Phototransduction (GO:0007602) was significant for the very small but prominent cluster 7, which was underexpressed in BEZO-exposed embryos and contained *opn1lw2*, *opn1sw1* (opsin isoforms) and *crygm2d11* (gamma D crystallin). Another group of genes in cluster 5, containing *rs1* (retinoschisin) and *arr3a* (retinal arrestin) were enriched for Visual Perception (GO:0007601). No significant biological processes were identified for the remaining clusters of misexpressed transcripts.

Ahr2 knockdown prevents induction of transcripts unique to BEZO and 7,12-B[a]AQ toxicity profiles

Knockdown of AHR2 prevented induction of morphological defects by BEZO and 7,12-B[a]AQ. AHR binding for these compounds, however, has not been determined. It is feasible that some transcriptional changes observed are not dependent on AHR2, particularly if AHR-dependent toxicity is mediated via an intermediate (endogenous ligand or metabolite) following an upstream interaction of the OPAH with another target. We selected a set of differentially expressed transcripts from the RNA-seq dataset and investigated their expression in *ahr2* morphants with qRT-PCR. We focused on lesser-known transcripts since AHR2-dependence of known AHR targets (Cyp1 enzymes) was previously established. *wfikkn1*, a top BAA target identified in the microarray analysis, was induced 5.5 fold by 7,12-B[a]AQ (Figure 6A), but not by BEZO. No significant induction was observed in the *ahr2* morphants. *Glutathione S-transferase pi 2* (*gstp2*), by contrast, is a redox responsive gene and was significantly induced by both 7,12-B[a]AQ (4.8 fold) and BEZO (3.1 fold). Again no significant induction was observed in *ahr2* morphants (Figure 6B). *Arginase 2* (*arg2*) was one of the few genes significantly induced by BEZO but unchanged by 7,12-B[a]AQ (Figure 5C cluster 8). This differential expression was confirmed by qRT-PCR in the control morphants, and AHR2 knockdown prevented *arg2* induction by BEZO (Figure 6C).

We also confirmed induction of *insulin-like growth factor binding protein 1a (igfbp1a)*, one of the transcripts most highly induced by BEZO, and *plac-8 onzin related like 4 (ponzr4)*, one of the transcripts most reduced by OPAH exposure in the RNA-seq dataset (Figure 6D,E). Comparative expression levels detected by qRT-PCR between BEZO and 7,12-B[a]AQ were consistent with those observed with RNA-seq, and AHR2 knockdown prevented misexpression of both of these genes (Figure 6D,E striped bars). Finally, we investigated *p53* expression, as a master regulator that was induced by BEZO in the RNA-seq dataset. A very slight (1.2 fold) induction was detected by qRT-PCR, with no significant difference between 7,12-B[a]AQ and BEZO. *ahr2* morphants had slightly higher *p53* expression than control morphants, which was not affected by OPAH exposure (Figure 6F).

Predicted transcription factors and biological processes affected by BEZO and 7,12-B[a]AQ

To better understand biological processes affected by exposure to BEZO and 7,12-B[a]AQ during development, we analyzed the entire sets of genes significantly affected by each OPAH for statistically enriched biological processes. For this analysis, we used significant genes identified by CuffDiff analysis across transcripts annotated in the zebrafish (Zv9) transcriptome (novel transcripts were not included). Significant transcripts for 7,12-B[a]AQ and BEZO exposures are listed in Tables S3 and S4, respectively. When compared to the previous analysis, which included novel transcripts, we observed good overlap in the significant gene lists; 337(93%) and 317(83%) of genes significant for 7,12-B[a]AQ and BEZO, respectively, were previously identified as significant. Entrez IDs (human homolog preferred) were identified for 587 of the 600 significant genes. Metacore GeneGo software was used to identify significant biological processes, gene ontology terms, and transcriptional regulators associated with the significant gene lists. The most significant process invoked by both OPAHs was Hypoxia and Oxidative Stress Response (Figure 7A). As suggested by the heatmap clustering (Figure 5C), Visual Perception was highly affected by BEZO, but not 7,12-B[a]AQ. Immune-Related Processes Involving the Complement and Kallikrein-Kinin Systems, as well as Inflammation (Phagocytosis) and Cell Cycle were affected by 7,12-B[a]AQ. The significant gene ontology terms agreed with these processes, and provide more insight into affected molecular mechanisms. Metabolic processes and response to chemical stimulus were the most significantly enriched GO terms, and involved over 150 genes (Table 2). The majority of the most enriched GO terms for each OPAH were

significant for both ($p < 0.001$). Notably, Tissue Development and Oxidation-reduction Processes were less significant in BEZO, while Visual Perception and Sensory Perception of Light Stimulus were not significant for 7,12-B[a]AQ. The decreased expression of eye-related genes (opsins, crystallins, *visual system homeobox 1*, *retina and anterior neural fold homeobox 1*) was also reflected in the transcription factors (TFs) predicted to be important in the BEZO response. NR2E3 nuclear receptor subfamily 2, group E, member 3 (also known as PNR, photoreceptor-specific nuclear receptor) and Maf (v-maf avian muscloponeurotic fibrosarcoma oncogene homolog) were among the most significant, and are both important in eye development. Other top predicted TFs for BEZO were C/EBPbeta and SP1. Among the most significant TFs predicted for 7,12-B[a]AQ were C/EBPbeta, ATF-2, RELA and c-Jun (Table 2). Both OPAHs were predicted to regulate networks involving HIF1A, C/EBPalpha, c-Myc and NRF2. Many of these TFs interact, and tightly coordinate responses to oxidative stress/redox homeostasis as well as many other cellular functions. The enriched biological processes and transcription factors highlight the prominent role of oxidative stress and hypoxia-related signaling for both of these oxygenated PAHs, while other processes, such as visual perception and AHR-mediated metabolic/chemical response processes, represent potential structure-dependent differences in toxicological mechanisms.

While AHR was significant ($P < 4.26E-04$ and $2.49E-03$ for 7,12-B[a]AQ and BEZO, respectively), it was not as significant as other TFs. The number of genes predicted with high confidence to interact with AHR was also much lower. Because we experimentally determined that both BEZO and 7,12-B[a]AQ-induced developmental toxicity depended on AHR2, we were interested to identify known interactors of AHR that were misexpressed in BEZO and 7,12-B[a]AQ-exposed embryos. Significantly misexpressed genes that have been shown to interact with the AHR (including both high and low confidence interactions) are displayed in Figure 6B. BEZO (blue) and 7,12-B[a]AQ (yellow) significant genes had some overlap, which included overexpressed TFs NFE2L1 (homolog of antioxidant regulator NRF, which shares highest similarity with *nrf2b* in zebrafish) and CITED2 (Cbp/p300-interacting transactivator), among others (Timme-Laragy et al. 2012). Though a large group of AHR-interacting genes were unique to 7,12-B[a]AQ (Figure 7B, yellow), the only TF was FOXQ1 (Forkead box Q1) which mediates TCDD-induced jaw malformations (Planchart and Mattingly 2010). AHR-interacting genes unique to BEZO included TFs P53, C/EBPbeta, and

CXCR4. While these were induced by both OPAHs, they were induced more strongly (and significantly) by BEZO, and could potentially contribute to the severe developmental toxicity of BEZO despite its weak induction of canonical AHR target genes.

Discussion

We found that BEZO and 7,12-B[a]AQ caused morphological abnormalities in developing zebrafish, including disrupted heart development, craniofacial abnormalities, eye defects and edema, at similar waterborne exposure concentrations. Their disparate induction of *cyp1a* mRNA and protein expression, which was identified previously and confirmed in this study, led us to predict differential involvement of the AHR in the toxicity mechanisms of these environmentally relevant OPAHs (Knecht et al. 2013). Despite the practically negligible induction of *cyp1a* and lack of *cyp1b1* induction by BEZO, the BEZO-induced toxicological endpoints evaluated in this study were dependent on AHR2. Cyp1a expression and metabolic activity are both widely used as biomarkers of AHR activation, particularly for environmental monitoring studies. For dioxin-like compounds, Cyp1a has been demonstrated to correlate well with ligand affinity for the receptor as well as AHR-associated toxicological effects in a plethora of organisms (Safe 1998; Billiard et al. 2002). AHR activation and Cyp1a expression are also associated with toxicity of many PAHs, such as benzo(a)pyrene. However, the structural diversity of the parent compounds, not to mention their substituted derivatives and propensity for metabolism, complicates prediction and interpretation of AHR interactions for this chemical class. This has been previously shown in zebrafish, where 4- and 5-ring PAH structures differentially interact with AHRs, resulting in tissue-specific Cyp1a expression patterns as well as a range of morphological effects (Incardona et al. 2006; Incardona et al. 2011; Knecht et al. 2013). Fluoranthene and dibenzothiophene inhibit Cyp1a activity, though the mechanism by which these PAHs act as inhibitors remains unknown (Willett et al. 2001; Wassenberg et al. 2005). Studies with AHR agonists and alternative AHR ligands, both in cell culture and animal models, have recently highlighted how ligands can differentially mediate a multitude of AHR-dependent biological processes (Patel et al. 2009; Murray et al. 2011; Narayanan et al. 2012). Adding to the complexity are reports of AHR-mediated responses in the absence of a xenobiotic ligand, including both *cyp1a* induction in hyperoxia, as well as decreased *cyp1a* expression resulting from oxidative stress (Barker et al. 1994; Couroucli et al. 2002) In this

context, an environmentally-relevant OPAH that induces AHR-dependent developmental toxicity in the absence of strong Cyp1a expression should perhaps not be entirely unexpected.

Because of its use in dye manufacture and associated reports of dermal lesions and decreased liver function in exposed workers, a number of studies have investigated BEZO toxicity in rodents. Exposure to high concentrations of BEZO causes decreased ascorbic acid associated with liver, kidney, and testis histopathological changes in guinea pigs, which could be attenuated with ascorbic acid supplementation (Das et al. 1994). In agreement with our study, Singh et al. observed decreased cytochrome P-450 phase 1 enzymes and ethoxyresorufin-O-deethylase (EROD) activity in guinea pigs exposed to BEZO (2003). Both in that study and others, BEZO caused a decrease in glutathione (GSH), and an increase in cytochrome P-450 phase 2 enzymes including glutathione peroxidase and glutathione reductase (Dwivedi et al. 2001). To our knowledge, involvement of the AHR in these effects awaits investigation.

Using mRNA sequencing, we compared the global transcriptional profile of BEZO with that of Cyp1a-inducer 7,12-B[a]AQ, as well as parent PAHs previously investigated via microarray. Because of the 60-fold difference in *cyp1a* expression at concentrations that induce comparable toxicity, we anticipated that other genes associated with AHR activation would be differentially regulated by BEZO and 7,12-B[a]AQ, helping to elucidate alternate toxicity mechanisms. We previously identified a set of transcripts differentially expressed in zebrafish embryos exposed to BAA, the unsubstituted parent PAH of 7,12-B[a]AQ, which induces AHR2-dependent morphological abnormalities in zebrafish, and toxicity in a variety of model systems (Incardona et al. 2006; Jennings 2012). Few of the BAA-induced transcripts were similarly regulated by other parent PAHs that exert AHR-independent toxic effects. We identified differential regulation of this specific set of AHR-interacting transcripts by examining their fold change values in BEZO and 7,12-B[a]AQ exposed embryos (compared to controls). In addition to *cyp1a*, *cyp1c1*, *cyp1c2*, *cyp1b1*, *ahrrb* and *wfikkn1* were more highly expressed in 7,12-B[a]AQ than BEZO. With the exception of *wfikkn1*, these transcripts are all known targets of the AHR (Baba et al. 2001; Jonsson et al. 2007). Other transcripts associated with AHR activation, such as oxidative stress and phase

2 metabolizing enzymes *gsr*, *prdx1*, and *sult6b1*, were induced at comparable levels by BEZO, 7,12-B[a]AQ and BAA. None of the BAA transcripts were oppositely expressed in response to BEZO vs. 7,12-B[a]AQ and BAA. While expression of the phase 1 metabolizing enzymes implies a potency, dose, or metabolism difference between these 4-ring PAHs, the consistency of expression for the rest of the transcripts across all three compounds perhaps suggests that the majority of transcriptional responses are not directly mediated by AHR, but rather by the network of transcription factors, such as NRF2, NFkB subunit RELA, CEBPB that are known to interact with AHR (Tian et al. 1999; Vogel et al. 2004; Timme-Laragy et al. 2009).

Examination of all identified transcripts that were significantly misexpressed in response to BEZO or 7,12-B[a]AQ supported the notion that these and multiple other TFs mediate the web of transcriptional changes that result from exposure to OPAHs. Many interacting and tightly regulated mechanisms coordinate to respond to stimuli such as xenobiotic exposure, hypoxia, UV irradiation and endogenous (hormone) signaling. Crosstalk between the AHR and other transcription factors has been widely reported. As a member of the PAS family of transcription factors, the AHR interacts with other PAS proteins and shares the requirement of ARNT for dimerization and transcriptional activation with HIF1A (Gu et al. 2000). AHR crosstalk via other binding partners and coactivators, including *p300* (CREB binding protein), HSP90, and the AHR repressor (AHRR) have been reported (Beischlag et al. 2008; Evans et al. 2008). We identified 366 transcripts that were significantly differentially expressed 2 fold or greater in response to OPAH exposure. Despite the fact that only 19% of these were significant in both OPAH exposure groups, we did not identify any clusters of transcripts with strong evidence of opposite (down vs. up) regulation between BEZO and 7,12-B[a]AQ. Rather, we observed clusters with more subtle differences in the degree of regulation. Phase 1 enzymes, as discussed previously, were more robustly induced by 7,12-B[a]AQ. BEZO, on the other hand, induced striking decreased expression of a cluster of genes involved in photoreception, which were relatively unaffected by 7,12-B[a]AQ. The largest clusters of significant transcripts in the BEZO/7,12-B[a]AQ comparison (Figure 5C) had similar levels of expression, however. The observation that relatively few of these transcripts were similarly disrupted in embryos exposed to the parent PAH BAA (Figure S1) suggests that perhaps the bulk of the transcriptional response to OPAHs is not mediated by

direct ligand activation of the AHR. These more reactive PAHs likely interact with cells in a multitude of other ways, causing oxidative stress, DNA and/or protein damage. It is important to keep in mind that a global transcriptional analysis does not discern between adaptive and harmful responses; indeed many of the pathways induced by these PAHs, such as NRF2-mediated antioxidant activity, likely protect the embryo from damage rather than mediate toxic effects (Van Tiem and Di Giulio 2011; Garner and Di Giulio 2012).

By comparing the BEZO and 7,12-B[a]AQ-induced transcripts across all PAHs, we identified clusters of transcripts that are differentially expressed in response to diverse PAH structures. We found that many of the transcripts misexpressed in response to the OPAHs followed similar expression patterns in DBT and PYR-exposed embryos. Inflammatory signaling via NFkB and CEBPB was significant for both OPAHs as well as DBT and PYR in the microarray analysis (Goodale et al. 2013); these pathways may be similarly involved in responding to PAH exposure via a mechanism that can be activated by a broad range of structures. We compared transcript expression across all 5 PAHs at concentrations that induced malformations, and were able to identify genes more consistently expressed than the *cyp1* transcripts, which may be useful to predict AHR-independent biological effects for mixtures containing multiple PAHs. Of all PAHs investigated, BAA induced expression of the smallest number of significant genes, a pattern which is supported in the heatmap (Figure S1). We attributed some of this difference to uptake, which was much lower for BAA than the other two parent PAHs. The toxicity of BAA demonstrated, for the parent PAHs, that a PAH with affinity for the AHR can induce toxicity at a much lower body burden than PAHs that do not induce AHR activity. Without body burden data we cannot definitively discern uptake vs. mechanistic differences between the OPAHs. Based on the similar log Kows of BEZO and 7,12-B[a]AQ (4.81 and 4.4, respectively), however, we would not predict large uptake differences (Meylan and Howard 1995). The similarity of expression among transcripts (in exception of the canonical AHR targets), as well as transcriptional clusters that were more strongly misexpressed by BEZO than 7,12-B[a]AQ, additionally suggests that the difference between these compounds is more complex than uptake. Further exploration of differential AHR-mediated pathways will be necessary to identify true mechanistic differences.

The relative insignificance of AHR in the predicted biological functions and transcription factors for BEZO and 7,12-B[a]AQ raises the question of why AHR2 knockdown offers pronounced protection against these compounds. For 7,12-B[a]AQ and parent PAH BAA, we might predict that following the initial binding to the AHR, a cascade of effects mediated by both the AHR response complex and metabolites leads to the wide array of transcriptional changes. For BEZO, however, the mechanism is less clear; is BEZO binding the AHR directly? If so, why isn't Cyp1a robustly expressed? We investigated *ahr2* dependence of transcripts that were highly misexpressed by BEZO, but are not known to be associated with AHR. If BEZO was affecting other pathways, and perhaps activating the AHR via a crosstalk mechanism, we would expect some transcripts to be induced in the absence of AHR2. In the small set of transcripts investigated here, however, we saw no evidence of AHR2-independent regulation. Rather, we identified *arg2*, and *igfbp1a*, AHR2-dependent transcripts induced more strongly by BEZO than 7,12-B[a]AQ.

The subtle differences in gene expression that correspond with distinct morphologies at 48 hpf in our study suggest differential interactions of the AHR with other TFs or co-activators. Regulation of TFs often occurs post-transcriptionally, so we would not necessarily expect large changes in TF transcripts themselves. A predicted network from the distinct cluster of genes associated with visual perception in BEZO-exposed embryos predicted the involvement of p53, which has been previously demonstrated to be involved in disrupted eye development in zebrafish (Kim et al. 2013). P53 was significantly induced 1.5 fold by BEZO, but only 1.1 fold (not significantly) by 7,12-B[a]AQ in the RNA-seq analysis. We saw no difference, however, between BEZO and 7,12-B[a]AQ with qRT-PCR, and expression of p53 was actually increased slightly in *ahr2* mutants. Interestingly, *arg2*, which is induced by hypoxia and involved in endothelial dysfunction/reduced NO signaling, has also recently been implicated in retinopathy (Durante 2013). *Arg2* deficient mice are resistant to retinal degeneration induced in oxygen induced retinopathy (Narayanan et al. 2011). While the mechanism of AHR2-dependent *arg2* induction remains unknown, it may be a mediator of eye-specific effects observed with BEZO. Another transcription factor, CCAAT/enhancer binding protein beta (CEBPB), was also significantly induced by BEZO 1.7 fold, but not by 7,12-B[a]AQ. CEBPB is a mediator of the acute phase response, and AHR activation by TCDD

was shown to decrease C/EBPB presence on the promoter of acute phase gene *Saa3* (Patel et al. 2009).

Further studies are needed to elucidate the involvement of other predicted transcription factors and interacting proteins, such as ARNT and CEBPB, in the toxicological effects mediated by these OPAHs. Several selective AHR modulators (SAhRMs), which bind to the AHR and repress inflammatory signaling via a mechanism that does not involve binding to AHR response elements, have been identified in cell culture (Patel et al. 2009). SAhRMs do not induce canonical AHR signaling such as CYP1A expression, and it is hypothesized that repressive activity occurs via AHR interaction with coactivators /repressors (Narayanan et al. 2012). We observed reductions in acute phase response genes (*c3*, *c4*, *cfdl*) in response to OPAH exposure, which suggests that these alternate mechanisms could also explain some of the *ahr2*-dependent gene regulation observed in our study. There is evidence of cell-type specific activities of the AHR, however. Interactions observed in a particular cell line may therefore not translate to the same transcriptional relationships in the whole animal context. Further investigation will be necessary to elucidate non-canonical AHR2 signaling pathways in the developing embryo. Comparative transcriptional profiling of PAHs demonstrates that PAHs likely mediate toxicity via a suite of mechanisms, including both canonical and non-canonical AHR signaling, depending on structure. We have identified clusters of transcripts associated with structures that induced AHR-dependent and AHR-independent toxicity; further elucidation of the complex web of AHR interactions will catalyze predictive capability for this diverse group of environmentally pertinent chemicals.

Acknowledgements

The authors would like to thank Cari Buchner, Carrie Barton and the staff at the Sinnhuber Aquatic Research Laboratory for their excellent fish husbandry and expertise. Jason Carriere processed the RNA samples and conducted mRNA sequencing at the University of Oregon Genomics Core Facility, Eugene, OR. We would also like to thank Tanguay laboratory members, in particular Lisa Truong, Derik Haggard and Jill Franzosa for their advice with RNA-seq analysis and critical review of the manuscript. We are grateful to OSU Superfund Research Program Core D/Anderson Laboratory for their analytical support, advice, and providing OPAHs. This work was supported by the NIEHS Superfund Research Program P42 ES016465, Core Center Grant P30 ES000210 and the NIEHS Training Grant T32 ES007060.

Pacific Northwest National Laboratory is a multi-program national laboratory operated by Battelle Memorial Institute for the DOE under contract number DE-AC05-76RL01830.

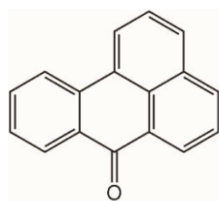
References

- Andreasen, E. A., M. E. Hahn, et al. (2002). "The zebrafish (*Danio rerio*) aryl hydrocarbon receptor type 1 is a novel vertebrate receptor." *Mol Pharmacol* **62**(2): 234-249.
- Andreasen, E. A., L. K. Mathew, et al. (2006). "Regenerative growth is impacted by TCDD: gene expression analysis reveals extracellular matrix modulation." *Toxicol Sci* **92**(1): 254-269.
- Baba, T., J. Mimura, et al. (2001). "Structure and expression of the Ah receptor repressor gene." *J Biol Chem* **276**(35): 33101-33110.
- Barker, C. W., J. B. Fagan, et al. (1994). "Down-regulation of P4501A1 and P4501A2 mRNA expression in isolated hepatocytes by oxidative stress." *J Biol Chem* **269**(6): 3985-3990.
- Beischlag, T. V., J. Luis Morales, et al. (2008). "The aryl hydrocarbon receptor complex and the control of gene expression." *Crit Rev Eukaryot Gene Expr* **18**(3): 207-250.
- Billiard, S. M., M. E. Hahn, et al. (2002). "Binding of polycyclic aromatic hydrocarbons (PAHs) to teleost aryl hydrocarbon receptors (AHRs)." *Comp Biochem Physiol B Biochem Mol Biol* **133**(1): 55-68.
- Bostrom, C. E., P. Gerde, et al. (2002). "Cancer risk assessment, indicators, and guidelines for polycyclic aromatic hydrocarbons in the ambient air." *Environ Health Perspect* **110 Suppl 3**: 451-488.
- Chew, G. L., A. Pauli, et al. (2013). "Ribosome profiling reveals resemblance between long non-coding RNAs and 5' leaders of coding RNAs." *Development* **140**(13): 2828-2834.
- Couroucli, X. I., S. E. Welty, et al. (2002). "Regulation of pulmonary and hepatic cytochrome P4501A expression in the rat by hyperoxia: implications for hyperoxic lung injury." *Mol Pharmacol* **61**(3): 507-515.
- Das, M., K. Garg, et al. (1994). "Attenuation of benzanthrone toxicity by ascorbic acid in guinea pigs." *Fundam Appl Toxicol* **22**(3): 447-456.
- Durant, J. L., W. F. Busby, Jr., et al. (1996). "Human cell mutagenicity of oxygenated, nitrated and unsubstituted polycyclic aromatic hydrocarbons associated with urban aerosols." *Mutat Res* **371**(3-4): 123-157.
- Durante, W. (2013). "Role of arginase in vessel wall remodeling." *Front Immunol* **4**: 111.
- Dwivedi, N., M. Das, et al. (2001). "Role of biological antioxidants in benzanthrone toxicity." *Archives of Toxicology* **75**(4): 221-226.
- Eden, E., R. Navon, et al. (2009). "GORilla: a tool for discovery and visualization of enriched GO terms in ranked gene lists." *BMC Bioinformatics* **10**: 48.
- EPA, U. (2012). "Integrated Risk Information System." from <http://www.epa.gov/iris/>.
- Evans, B. R., S. I. Karchner, et al. (2008). "Repression of aryl hydrocarbon receptor (AHR) signaling by AHR repressor: role of DNA binding and competition for AHR nuclear translocator." *Mol Pharmacol* **73**(2): 387-398.

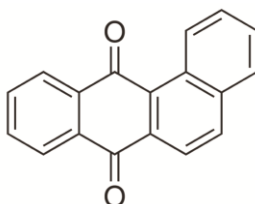
- Garner, L. V. and R. T. Di Giulio (2012). "Glutathione transferase pi class 2 (GSTp2) protects against the cardiac deformities caused by exposure to PAHs but not PCB-126 in zebrafish embryos." Comp Biochem Physiol C Toxicol Pharmacol **155**(4): 573-579.
- Goodale, B. C., S. C. Tilton, et al. (2013). "Structurally distinct polycyclic aromatic hydrocarbons induce differential transcriptional responses in developing zebrafish." Toxicol Appl Pharmacol.
- Gu, Y. Z., J. B. Hogenesch, et al. (2000). "The PAS superfamily: sensors of environmental and developmental signals." Annu Rev Pharmacol Toxicol **40**: 519-561.
- Gurbani, D., S. K. Bharti, et al. (2013). "Polycyclic aromatic hydrocarbons and their quinones modulate the metabolic profile and induce DNA damage in human alveolar and bronchiolar cells." Int J Hyg Environ Health.
- Hahn, M. E. (1998). "The aryl hydrocarbon receptor: a comparative perspective." Comp Biochem Physiol C Pharmacol Toxicol Endocrinol **121**(1-3): 23-53.
- Hofsteen, P., J. Plavicki, et al. (2013). "Sox9b is Required for Epicardium Formation and Plays a Role in TCDD-induced Heart Malformation in Zebrafish." Mol Pharmacol.
- Incardona, J. P., H. L. Day, et al. (2006). "Developmental toxicity of 4-ring polycyclic aromatic hydrocarbons in zebrafish is differentially dependent on AH receptor isoforms and hepatic cytochrome P4501A metabolism." Toxicol Appl Pharmacol **217**(3): 308-321.
- Incardona, J. P., T. L. Linbo, et al. (2011). "Cardiac toxicity of 5-ring polycyclic aromatic hydrocarbons is differentially dependent on the aryl hydrocarbon receptor 2 isoform during zebrafish development." Toxicol Appl Pharmacol **257**(2): 242-249.
- Jennings, A. A. (2012). "Worldwide regulatory guidance values for surface soil exposure to carcinogenic or mutagenic polycyclic aromatic hydrocarbons." J Environ Manage **110**: 82-102.
- Jonsson, M. E., M. J. Jenny, et al. (2007). "Role of AHR2 in the expression of novel cytochrome P450 1 family genes, cell cycle genes, and morphological defects in developing zebra fish exposed to 3,3',4,4',5-pentachlorobiphenyl or 2,3,7,8-tetrachlorodibenzo-p-dioxin." Toxicol Sci **100**(1): 180-193.
- Karchner, S. I., D. G. Franks, et al. (2005). "AHR1B, a new functional aryl hydrocarbon receptor in zebrafish: tandem arrangement of ahr1b and ahr2 genes." Biochem J **392**(Pt 1): 153-161.
- Kim, K. T., T. Zaikova, et al. (2013). "Gold nanoparticles disrupt zebrafish eye development and pigmentation." Toxicol Sci **133**(2): 275-288.
- Kimmel, C. B., W. W. Ballard, et al. (1995). "Stages of embryonic development of the zebrafish." Dev Dyn **203**(3): 253-310.
- Knecht, A. L., B. C. Goodale, et al. (2013). "Comparative developmental toxicity of environmentally relevant oxygenated PAHs." Toxicol Appl Pharmacol.
- Layshock, J. A., G. Wilson, et al. (2010). "Ketone and Quinone-Substituted Polycyclic Aromatic Hydrocarbons in Mussel Tissue, Sediment, Urban Dust, and Diesel Particulate Matrices." Environmental Toxicology and Chemistry **29**(11): 2450-2460.
- Lundstedt, S., Y. Persson, et al. (2006). Transformation of PAHs during ethanol-Fenton treatment of an aged gasworks' soil. Chemosphere. England. **65**: 1288-1294.
- Lundstedt, S., P. A. White, et al. (2007). "Sources, fate, and toxic hazards of oxygenated polycyclic aromatic hydrocarbons (PAHs) at PAH-contaminated sites." Ambio **36**(6): 475-485.

- Meylan, W. M. and P. H. Howard (1995). "Atom Fragment Contribution Method for Estimating Octanol-Water Partition-Coefficients." Journal of Pharmaceutical Sciences **84**(1): 83-92.
- Murray, I. A., C. A. Flaveny, et al. (2011). "Suppression of cytokine-mediated complement factor gene expression through selective activation of the Ah receptor with 3',4'-dimethoxy-alpha-naphthoflavone." Mol Pharmacol **79**(3): 508-519.
- Narayanan, G. A., I. A. Murray, et al. (2012). "Selective aryl hydrocarbon receptor modulator-mediated repression of CD55 expression induced by cytokine exposure." J Pharmacol Exp Ther **342**(2): 345-355.
- Narayanan, S. P., J. Suwanpradid, et al. (2011). "Arginase 2 deletion reduces neuro-glial injury and improves retinal function in a model of retinopathy of prematurity." PLoS One **6**(7): e22460.
- Nielsen, T., A. Feilberg, et al. (1999). "The variation of street air levels of PAH and other mutagenic PAC in relation to regulations of traffic emissions and the impact of atmospheric processes." Environmental Science and Pollution Research **6**(3): 133-137.
- Nikolsky, Y., E. Kirillov, et al. (2009). "Functional analysis of OMICs data and small molecule compounds in an integrated "knowledge-based" platform." Methods Mol Biol **563**: 177-196.
- Patel, R. D., I. A. Murray, et al. (2009). "Ah receptor represses acute-phase response gene expression without binding to its cognate response element." Lab Invest **89**(6): 695-707.
- Pfaffl, M. W. (2001). "A new mathematical model for relative quantification in real-time RT-PCR." Nucleic Acids Res **29**(9): e45.
- Planchart, A. and C. J. Mattingly (2010). "2,3,7,8-Tetrachlorodibenzo-p-dioxin upregulates FoxQ1b in zebrafish jaw primordium." Chem Res Toxicol **23**(3): 480-487.
- Ramirez, N., A. Cuadras, et al. (2011). "Risk assessment related to atmospheric polycyclic aromatic hydrocarbons in gas and particle phases near industrial sites." Environ Health Perspect **119**(8): 1110-1116.
- Reimers, M. J., J. K. La Du, et al. (2006). "Ethanol-dependent toxicity in zebrafish is partially attenuated by antioxidants." Neurotoxicol Teratol **28**(4): 497-508.
- Saeed, A. I., V. Sharov, et al. (2003). "TM4: a free, open-source system for microarray data management and analysis." Biotechniques **34**(2): 374-378.
- Safe, S. H. (1998). "Development validation and problems with the toxic equivalency factor approach for risk assessment of dioxins and related compounds." J Anim Sci **76**(1): 134-141.
- Shannon, P., A. Markiel, et al. (2003). "Cytoscape: a software environment for integrated models of biomolecular interaction networks." Genome Res **13**(11): 2498-2504.
- Singh, R. P., R. Khanna, et al. (2003). "Comparative effect of benzanthrone and 3-bromobenzanthrone on hepatic xenobiotic metabolism and anti-oxidative defense system in guinea pigs." Archives of Toxicology **77**(2): 94-99.
- Svoboda, K. R., A. E. Linares, et al. (2001). "Activity regulates programmed cell death of zebrafish Rohon-Beard neurons." Development **128**(18): 3511-3520.
- Tian, Y., S. Ke, et al. (1999). "Ah receptor and NF-kappaB interactions, a potential mechanism for dioxin toxicity." J Biol Chem **274**(1): 510-515.

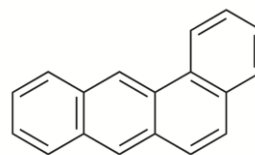
- Tilton, S. C., T. L. Tal, et al. (2012). "Bioinformatics resource manager v2.3: an integrated software environment for systems biology with microRNA and cross-species analysis tools." *BMC Bioinformatics* **13**(1): 311.
- Timme-Laragy, A. R., S. I. Karchner, et al. (2012). "Nrf2b, novel zebrafish paralog of oxidant-responsive transcription factor NF-E2-related factor 2 (NRF2)." *J Biol Chem* **287**(7): 4609-4627.
- Timme-Laragy, A. R., L. A. Van Tiem, et al. (2009). "Antioxidant responses and NRF2 in synergistic developmental toxicity of PAHs in zebrafish." *Toxicol Sci*.
- Trapnell, C., L. Pachter, et al. (2009). "TopHat: discovering splice junctions with RNA-Seq." *Bioinformatics* **25**(9): 1105-1111.
- Trapnell, C., A. Roberts, et al. (2012). "Differential gene and transcript expression analysis of RNA-seq experiments with TopHat and Cufflinks." *Nat Protoc* **7**(3): 562-578.
- van Delft, J., S. Gaj, et al. (2012). "RNA-Seq provides new insights in the transcriptome responses induced by the carcinogen benzo[a]pyrene." *Toxicol Sci* **130**(2): 427-439.
- Van Tiem, L. A. and R. T. Di Giulio (2011). "AHR2 knockdown prevents PAH-mediated cardiac toxicity and XRE- and ARE-associated gene induction in zebrafish (*Danio rerio*)." *Toxicol Appl Pharmacol* **254**(3): 280-287.
- Vogel, C. F., E. Sciallo, et al. (2004). "Dioxin increases C/EBPbeta transcription by activating cAMP/protein kinase A." *J Biol Chem* **279**(10): 8886-8894.
- Walgraeve, C., K. Demeestere, et al. (2010). "Oxygenated polycyclic aromatic hydrocarbons in atmospheric particulate matter: Molecular characterization and occurrence." *Atmospheric Environment* **44**(15): 1831-1846.
- Wang, W., N. Jariyasopit, et al. (2011). "Concentration and photochemistry of PAHs, NPAHs, and OPAHs and toxicity of PM2.5 during the Beijing Olympic Games." *Environ Sci Technol* **45**(16): 6887-6895.
- Wassenberg, D. M., A. L. Nerlinger, et al. (2005). "Effects of the polycyclic aromatic hydrocarbon heterocycles, carbazole and dibenzothiophene, on in vivo and in vitro CYP1A activity and polycyclic aromatic hydrocarbon-derived embryonic deformities." *Environ Toxicol Chem* **24**(10): 2526-2532.
- Wei, S. L., B. Huang, et al. (2012). "Characterization of PM2.5-bound nitrated and oxygenated PAHs in two industrial sites of South China." *Atmospheric Research* **109**: 76-83.
- Willett, K. L., D. Wassenberg, et al. (2001). "In vivo and in vitro inhibition of CYP1A-dependent activity in *Fundulus heteroclitus* by the polynuclear aromatic hydrocarbon fluoranthene." *Toxicol Appl Pharmacol* **177**(3): 264-271.
- Xiong, K. M., R. E. Peterson, et al. (2008). "Aryl hydrocarbon receptor-mediated down-regulation of sox9b causes jaw malformation in zebrafish embryos." *Mol Pharmacol* **74**(6): 1544-1553.
- Yu, H. (2002). "Environmental carcinogenic polycyclic aromatic hydrocarbons: photochemistry and phototoxicity." *J Environ Sci Health C Environ Carcinog Ecotoxicol Rev* **20**(2): 149-183.



1,9-benz-10-anthrone
BEZO
CAS# 82-05-3



benz(a)anthracene-7,12-dione
7,12-B[a]AQ
CAS# 2498-66-0



benz(a)anthracene
BAA
CAS# 56-55-3

Figure 4-1 Structures of BEZO, 7,12-B[a]AQ and BAA

BEZO and 7,12-B[a]AQ, both oxygenated 4-ring PAHs, are compared with 4-ring parent PAH BAA.

Figure 4-2 Developmental toxicity of 7,12-B[a]AQ and BEZO at 120 hpf

(A) Exposure from 6-72 hpf to 5, 7.5 and 10 μ M 7,12-B[a]AQ caused concentration-dependent increases in the percent of control morpholino(MO)-injected larvae with pericardial edema (dark circles). 7,12-B[a]AQ exposure did not cause significant pericardial edema above control levels in *ahr2*-MO injected embryos (light circles) (B) BEZO exposure induced pericardial edema at 5, 7.5 and 10 μ M in control-MO injected embryos (dark circles), *ahr2* morphants showed no significant increase (light circles). The percentage of embryos with at least 1 malformation was significantly increased by both 7,12-B[a]AQ(C) and BEZO (D) in control-MO injected embryos (dark circles), while *ahr2* morphants had no significant increase in the percentage of malformed embryos (light circles). Data represent 3 independent replicates analyzed by one-way ANOVA with Tukey's pairwise posthoc test. ^asignificantly different than control ^bsignificantly different than control and 5 μ M, $p < 0.05$. (E, F, G) Representative images of control-MO injected embryos exposed to 1% DMSO vehicle control, 10 μ M 7,12-B[a]AQ, and 10 μ M BEZO, respectively. Severe malformations including pericardial edema, yolk sac edema, craniofacial malformations and eye defects can be observed in F and G. (H, I, J) Representative images of *ahr2*-MO injected embryos exposed to 1% DMSO vehicle control, 10 μ M 7,12-B[a]AQ, and 10 μ M BEZO, respectively show rescue of morphological abnormalities.

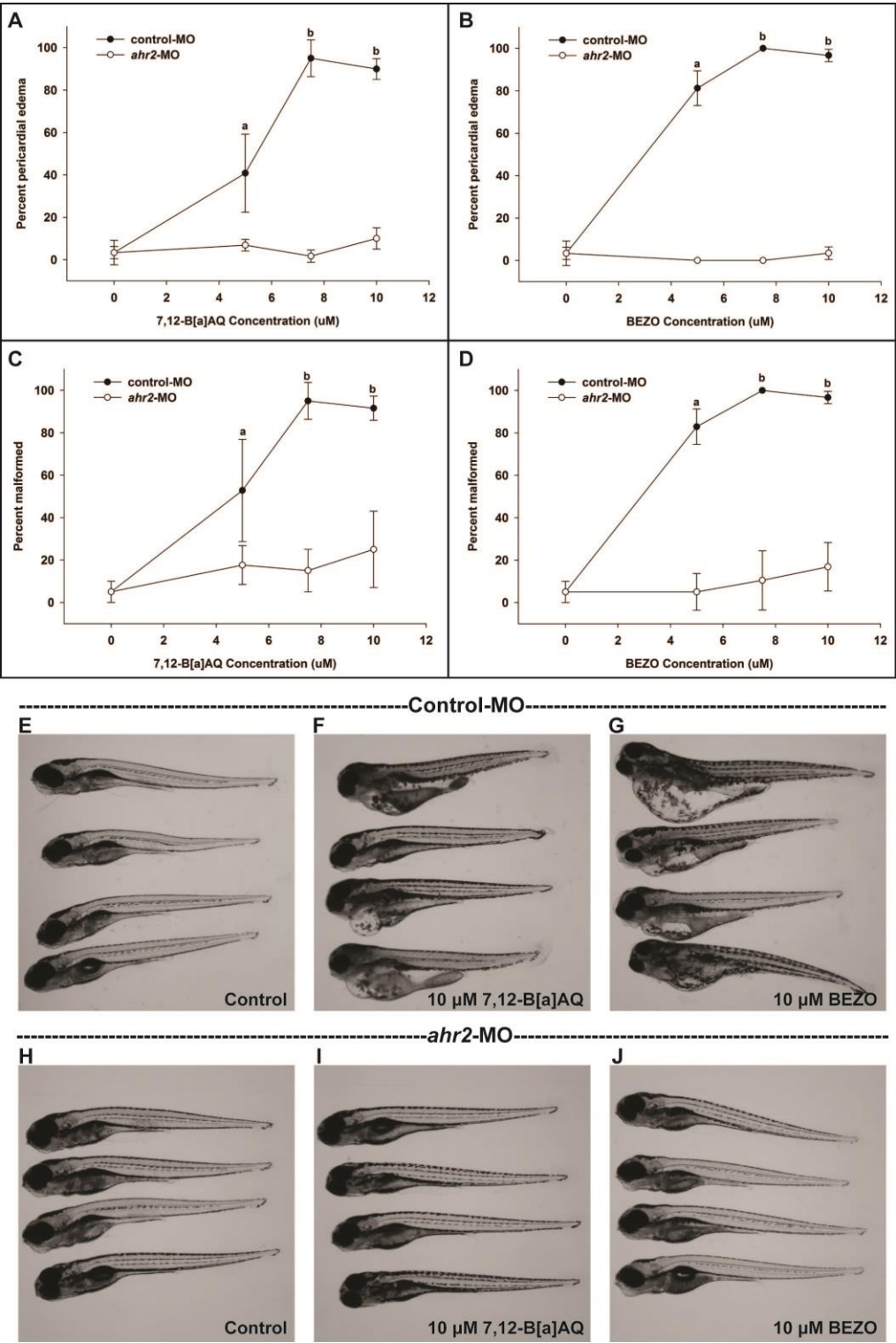


Figure 4-2

Figure 4-3 Cyp1 expression and morphology in OPAH-exposed embryos at 48 hpf

A) Exposure to 7.5 μ M 7,12-B[a]AQ induced differential expression of *cyp1a* and *cyp1b1* detected by qRT-PCR in control morpholino injected (c-MO) and *ahr2*-MO injected embryos compared to DMSO controls. B) Exposure to 7.5 μ M BEZO induced differential expression of *cyp1a* and *cyp1b1* in c-MO and *ahr2*-MO injected embryos compared to DMSO controls, but with much smaller fold change values than 7,12-B[a]AQ. Note different scale compare to Figure A. Data represent 4 biological replicates analyzed by two-way ANOVA with Tukey's posthoc test. Treatment groups not sharing a letter are statistically different ($p < 0.05$).

C, D) Representative light microscope images of 48 hpf control-MO and *ahr2*-MO injected embryos exposed to 1% DMSO vehicle control. E, F) 48 hpf control-MO and *ahr2*-MO injected embryos exposed to 7.5 μ M 7,12-B[a]AQ. Pooling of blood is apparent in E (arrow). G, H) 48 hpf control-MO and *ahr2*-MO injected embryos exposed to 7.5 μ M BEZO. Pericardial edema is apparent in G (arrow). I, J) Immunofluorescent labeling of Cyp1a protein in 48 hpf control-MO and *ahr2*-MO injected embryos exposed to 1% DMSO vehicle control. K, L) Cyp1a protein expression in 48 hpf control-MO and *ahr2*-MO injected embryos exposed to 7.5 μ M 7,12-B[a]AQ, c-MO injected embryos showed strong fluorescence throughout the vasculature (K). BEZO exposed embryos showed no Cyp1a protein expression (M, N).

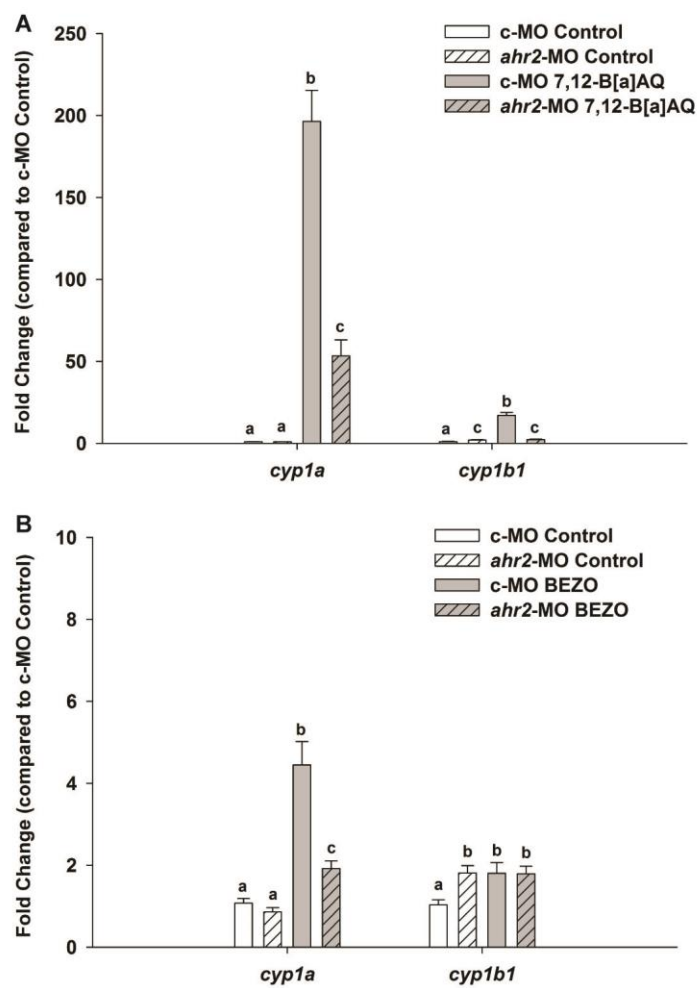
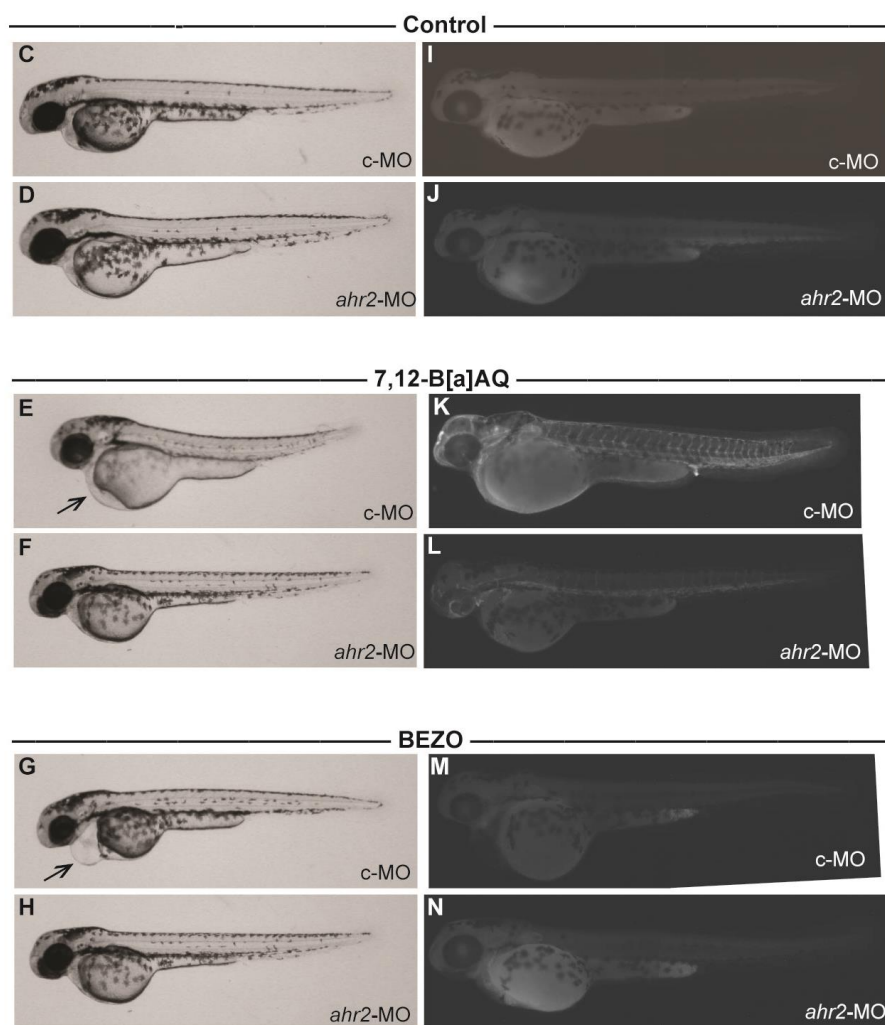


Figure 4-3

**Figure 4-3 (Continued)**

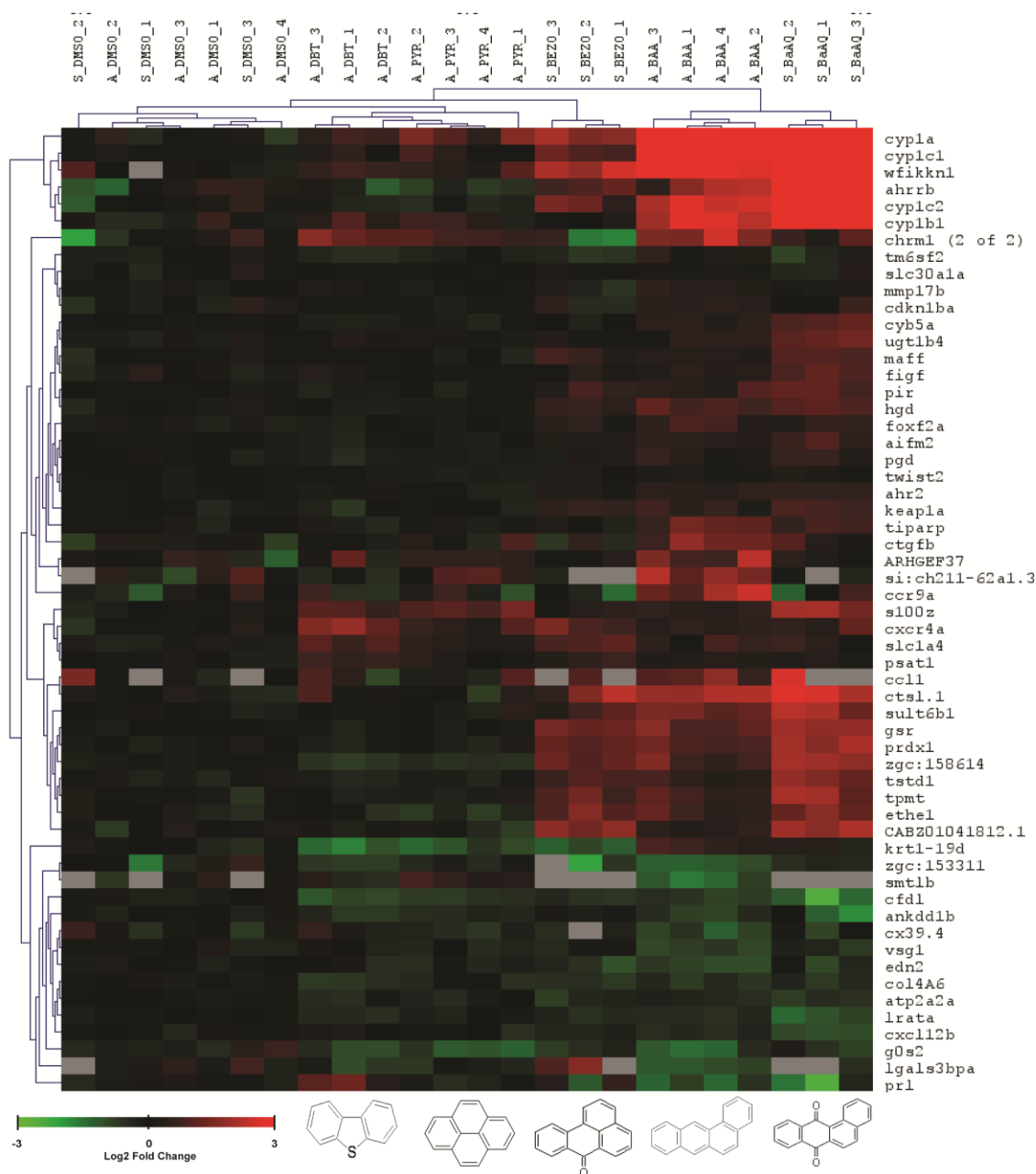


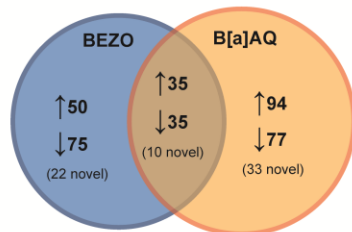
Figure 4-4 Heatmap of transcripts significantly induced by BAA exposure at 48 hpf.

Log2FC values were cluster using birectional hierarchical clustering. Individual samples are normalized to respective platform mean control value. A= array, fluorescence intensity values. S=mRNA-seq FPKM values). Insufficient data is represented in gray.

Figure 4-5 Comparison of transcripts induced by BEZO and 7,12-B[a]AQ exposure

A) Venn comparison of significant gene lists identified in mRNA-seq analysis of BEZO and 7,12-B[a]AQ with fold change >2 compared to control. **B)** novel transcript underexpressed in both BEZO and 7,12-B[a]AQ exposed samples occurs in a region with high transcriptional coverage but no annotation in Zv9 (top). Visualization of individual sample transcript reads across the predicted transcripts shows consistency within treatments (bottom). **C)** Bidirectional hierarchical clustering of all 366 transcripts significantly induced > 2 fold by BEZO or 7,12-B[a]AQ. Biological functions that were significantly enriched in clusters of transcripts are noted.

A Comparison of significant transcripts with >2 fold change
(p <0.05, 1%FDR)



B Novel transcript significantly induced by 7,12-B[a]AQ

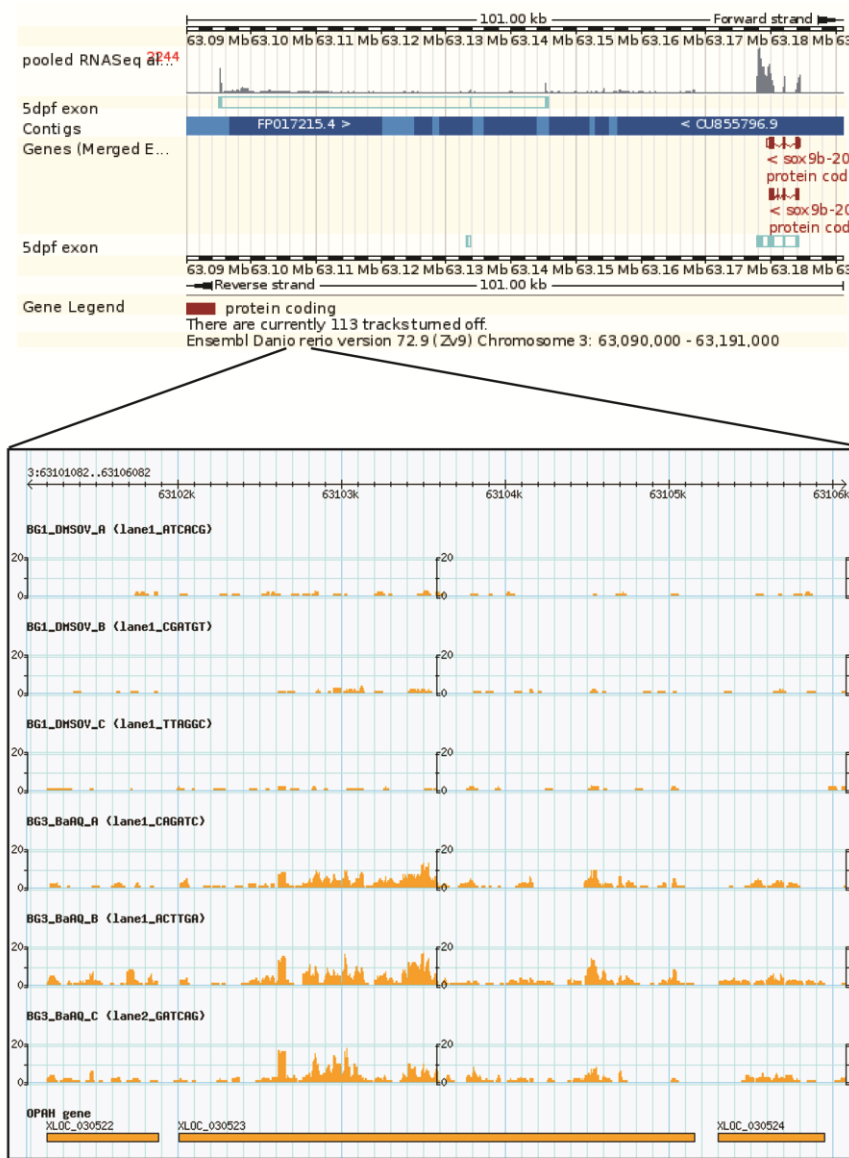


Figure 4-5

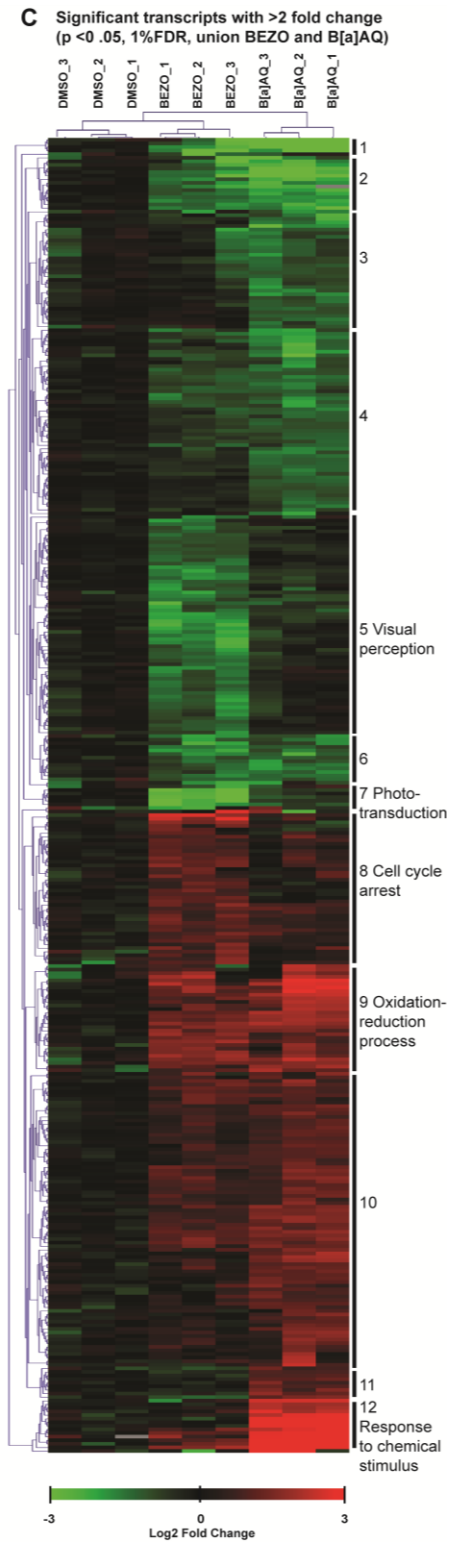


Figure 4-5 (Continued)

Figure 4-6 qRT-PCR analysis of OPAH targets in control and AHR2 morphants

Exposure to 7.5 μ M 7,12-B[a]AQ or BEZO induced differential expression of *wfikk1* (A), *gstp2* (B), *arg2* (C), *igfbp1a* (D), *ponzr4* (E) and *p53* (F) detected by qRT-PCR in c-MO and *ahr2*-MO injected embryos compared to DMSO controls. Data represent 4 biological replicates analyzed by two-way ANOVA with Tukey's posthoc test. Significantly different induction is designated with different letters ($p < 0.05$).

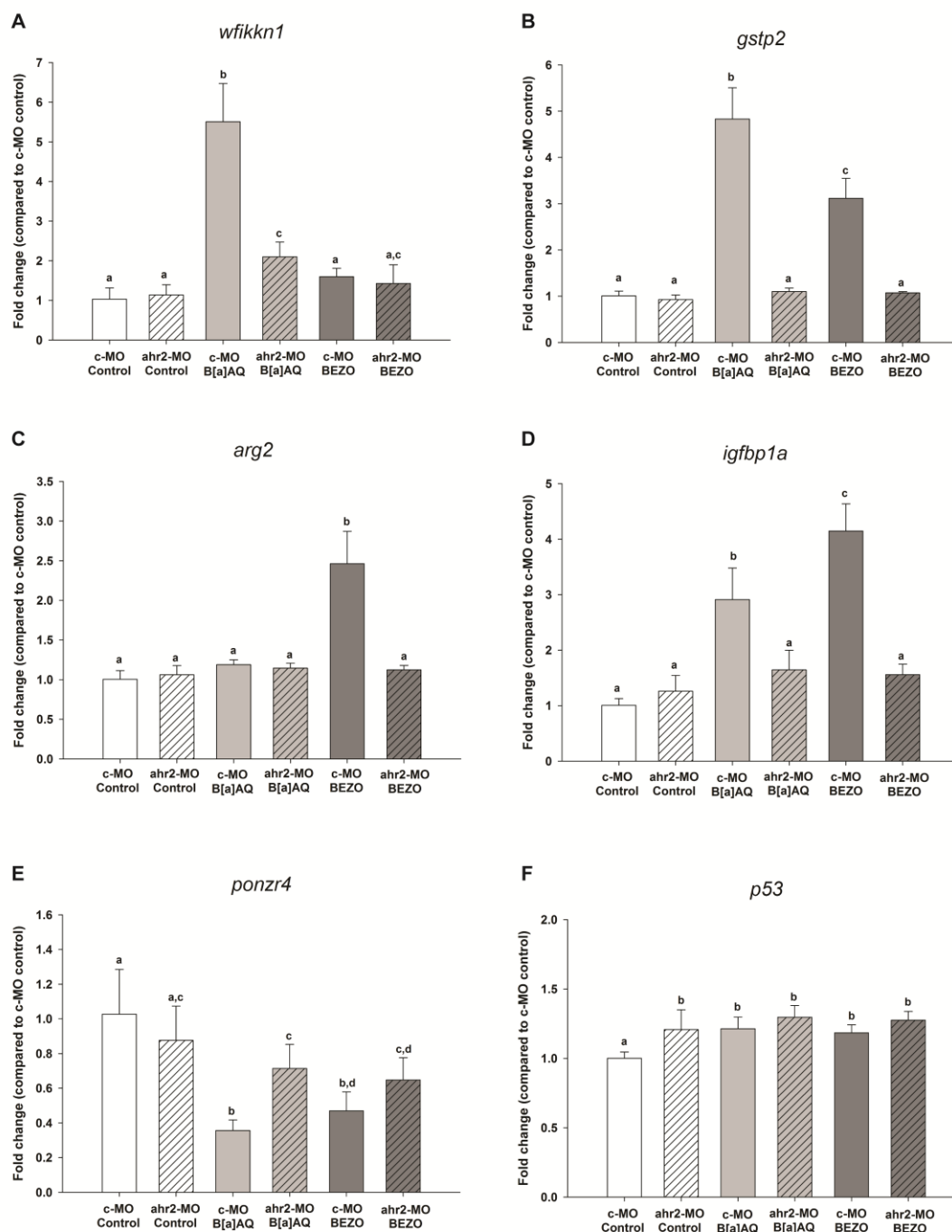


Figure 4-6

Figure 4-7 Biological processes affected by BEZO and 7,12-B[a]AQ exposure

A) MetaCore processes significantly over-represented among transcripts misexpressed by BEZO and 7,12-B[a]AQ. **B)** Predicted interactions between the AHR and transcripts differentially expressed in BEZO (blue) and 7,12-B[a]AQ (yellow) exposed embryos. Interactions were predicted using the Metacore statistical interactome tool. Color of circles represents expression of transcript compared to control (red = increased, blue = decreased). Symbols designating network object classes

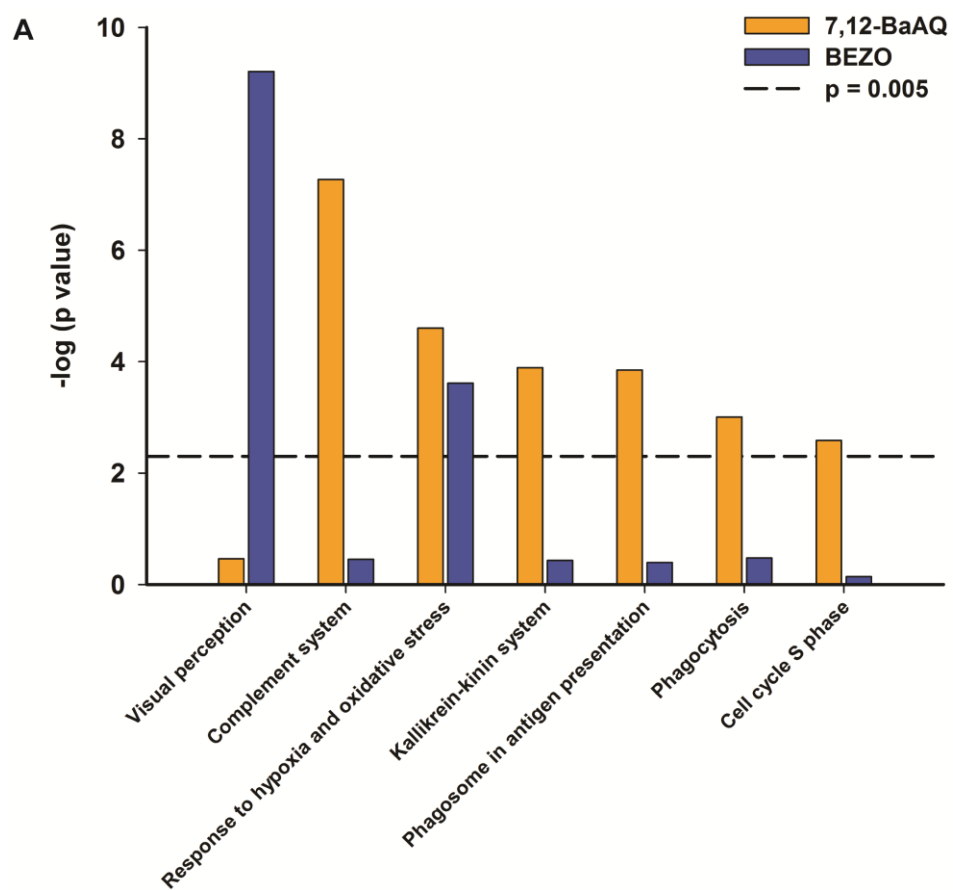
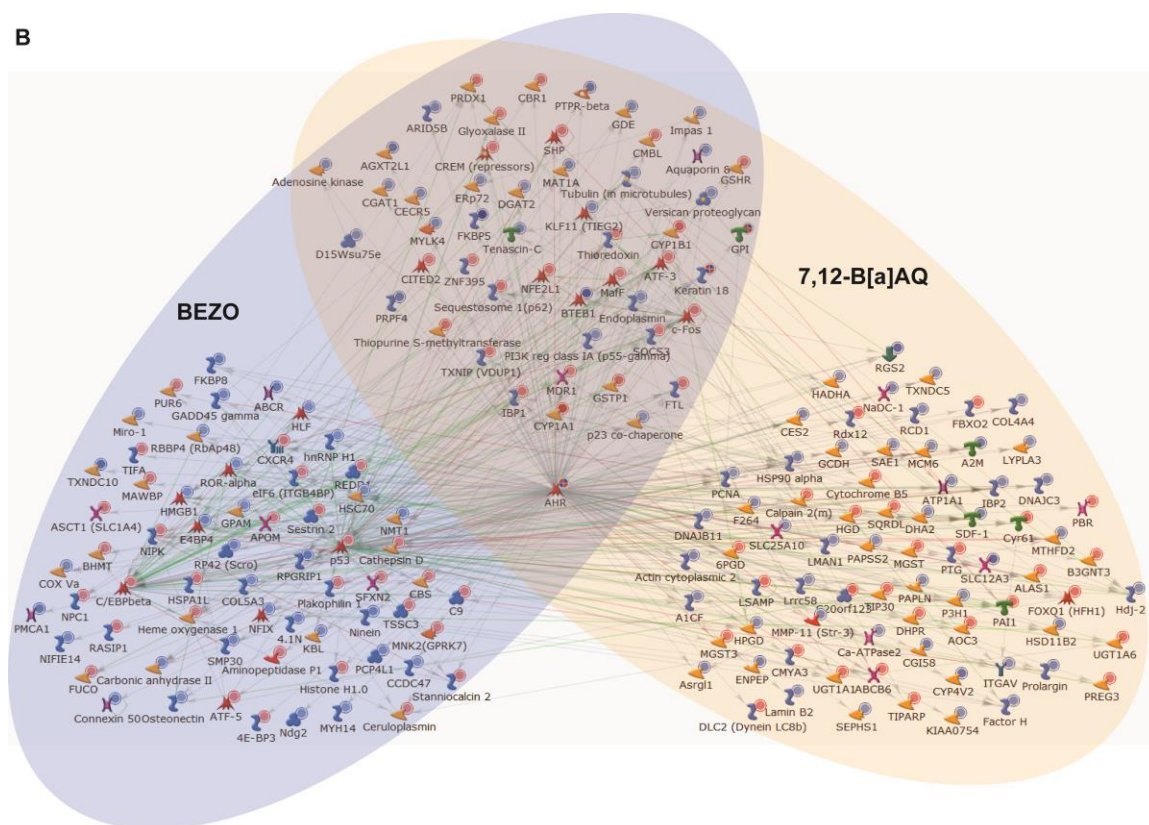


Figure 4-7


































Enzymes		Generic Classes	
 Generic enzyme		 Receptor ligand	
KINASE  Generic kinase  Protein kinase  Lipid kinase	PHOSPHATASE  Generic phosphatase  Protein phosphatase  Lipid phosphatase	 Transcription factor  Protein  Compound  Predicted metabolite or user's structure  Inorganic ion	
PHOSPHOLIPASE  Generic phospholipase		 Reaction	
PROTEASE  Generic protease  Metalloprotease	GTPase  G-alpha  RAS - superfamily	 DNA  RNA  Generic binding protein	
Channels/Transporters  Generic channel  Ligand-gated ion channel  Voltage-gated ion channel  Transporter	Receptors  Generic  GPCR  Receptors with kinase activity	G protein Adaptor/Regulators  G beta/gamma  Regulators (GDI, GAP, GEF, etc.)	

Figure 4-7 (Continued)

Table 4-1 Cross-platform comparison of expression data for genes differentially induced by PAHs

Log2 fold change values of PAH-treated samples compared to 1% DMSO control detected by microarray fluorescence intensity (DBT, PYR and BAA, previous study) or RNA-seq FPKM values (BEZO and 7,12-B[a]AQ, this study) compared to qRT-PCR log2FC values. *Significantly different than control, one-way ANOVA with Tukey's all pairwise posthoc test, $p < 0.05$ † At least one probe significantly different than control, one-way ANOVA with Tukey's all pairwise posthoc test, 0.05 FDR, adjusted p value < 0.05 . ‡ Significantly different than control, Cuffdiff pairwise comparison, 0.01 FDR, adjusted p value < 0.05)

Gene	DBT		PYR		BEZO		BAA		7,12-B[a]AQ	
	Microarray	QPCR	Microarray	QPCR	RNA-seq	QPCR	Microarray	QPCR	RNA-seq	QPCR
<i>cyp1a</i>	0.7 ± 0.21	0.81 ± 0.23	$1.24 \pm 0.54^{\ddagger}$	$1.43 \pm 0.47^*$	$1.84 \pm 0.29^{\dagger}$	$1.61 \pm 0.15^*$	$4.56 \pm 0.14^{\ddagger}$	$6.63 \pm 0.32^*$	$7.85 \pm 0.25^{\dagger}$	$7.24 \pm 0.09^*$
<i>ctsl.1</i>	0.46 ± 0.5	-0.17 ± 0.35	-0.08 ± 0.49	-0.39 ± 0.09	$1.53 \pm 0.88^{\dagger}$	$1.63 \pm 0.16^*$	$2.08 \pm 0.2^{\ddagger}$	$1.68 \pm 0.16^*$	$2.51 \pm 0.31^{\dagger}$	$2.32 \pm 0.23^*$
<i>sult6b1</i>	0.03 ± 0.1	-0.27 ± 0.26	0.04 ± 0.33	-0.28 ± 0.18	$0.8 \pm 0.42^{\dagger}$	$0.87 \pm 0.33^*$	$1.42 \pm 0.2^{\ddagger}$	$1.03 \pm 0.24^*$	$1.94 \pm 0.5^{\dagger}$	$2.42 \pm 0.26^*$
<i>cxcr4a</i>	$1.61 \pm 0.33^{\ddagger}$	$1.19 \pm 0.13^*$	$0.63 \pm 0.36^{\ddagger}$	0.28 ± 0.33	$1.14 \pm 0.42^{\dagger}$	$0.83 \pm 0.22^*$	$0.5 \pm 0.11^{\ddagger}$	0.21 ± 0.38	$0.77 \pm 0.46^{\dagger}$	$0.74 \pm 0.09^*$
<i>ctgfb</i>	-0.05 ± 0.13	-0.73 ± 0.23	0.25 ± 0.61	-0.56 ± 0.21	-0.13 ± 0.67	-0.02 ± 0.06	$1.37 \pm 0.46^{\ddagger}$	$1.23 \pm 0.17^*$	0.56 ± 0.48	$1.25 \pm 0.07^*$
<i>s100z</i>	$0.96 \pm 0.27^{\ddagger}$	0.33 ± 0.17	$1.17 \pm 0.25^{\ddagger}$	0.51 ± 0.16	0.34 ± 0.22	$0.91 \pm 0.08^*$	$0.52 \pm 0.12^{\ddagger}$	0.06 ± 0.25	$1.89 \pm 0.36^{\dagger}$	$2 \pm 0.12^*$

Table 4-2 Biological processes misregulated by OPAHs

Gene ontology terms over-represented in BEZO and 7,12-B[a]AQ significant gene lists. The 20 most significant GO terms for each OPAH are listed (Metacore GeneGO, $p < 0.001$, shading according to degree of significance).

GO term	BEZO	7,12-BaAQ	# of genes/total in process
single-organism metabolic process	6.22E-13	1.76E-20	184/2713
small molecule metabolic process	1.40E-13	3.96E-16	156/2169
response to chemical stimulus	5.70E-09	6.98E-16	164/2599
response to organic substance	6.54E-09	4.83E-14	129/1889
response to lipid	5.69E-08	2.08E-13	67/718
organ development	1.24E-12	2.40E-11	155/2420
organic acid metabolic process	1.25E-06	1.70E-12	75/839
response to hormone stimulus	6.90E-08	1.78E-12	73/840
response to organic cyclic compound	8.57E-09	4.81E-12	68/754
developmental process	9.87E-10	9.06E-12	219/4138
tissue development	4.37E-04	3.26E-11	81/1261
metabolic process	7.02E-06	4.38E-11	332/7643
response to endogenous stimulus	1.34E-08	6.01E-11	89/1187
system development	8.77E-11	2.04E-10	189/3339
oxidation-reduction process	4.98E-05	8.80E-11	67/846
response to oxygen-containing compound	4.57E-09	1.17E-10	73/881
visual perception	1.18E-10	7.67E-02	26/203
sensory perception of light stimulus	1.30E-10	7.84E-02	26/204
multicellular organismal development	5.17E-10	5.07E-10	205/3781
anatomical structure development	1.14E-09	1.13E-09	199/3744

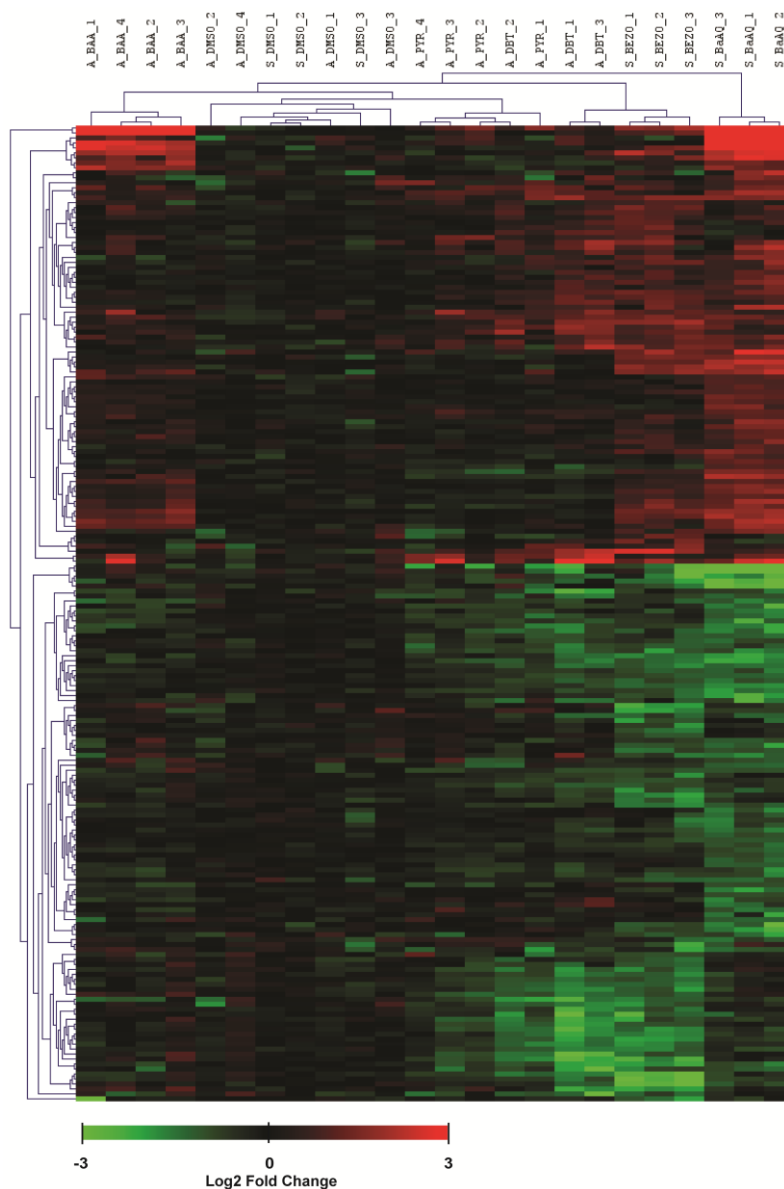


Figure 4-S1 Comparative expression across 5 PAH structures

Bidirectional hierarchically clustered heatmap of log₂FC values of transcripts significantly induced by BEZO or 7,12-B[a]AQ exposure, for which probes were identified on the Agilent zebrafish microarray platform. Individual samples are normalized to respective platform mean control value. A= array, fluorescence intensity values. S=mRNA-seq FPKM values.

Table 4-S1 Primers used for qRT-PCR analysis

Gene	Ensembl ID	Forward Primer (5'- 3')	Reverse Primer (5'- 3')
<i>arg2</i>	ENSDARG00000039269	AACGGCGGACTGACCTAC	CCAGAGCGGATGCAACTA
<i>β-actin</i>	ENSDARG00000037746	AAGCAGGAGTACGATGAGTC	TGGAGTCCTCAGATGCATTG
<i>cyp1a</i>	ENSDARG00000026039	TGCCGATTTTCATCCCTTTCC	AGAGCCGTGCTGATAGTGTC
<i>cyp1b1</i>	ENSDARG00000068934	CTGCATTGATTTCCGAGACGTG	CACACTCCGTGTTGACAGC
<i>ctgfb</i>	ENSDARG00000070586	TGTAACCAATGACAATGAGC	CATCCAGACAACTCGAAACG
<i>ctsl.1</i>	ENSDARG00000003902	GGACTCCTACCCCTATGAAG	ATAACCAACAGCCAGAACAC
<i>cxcr4a</i>	ENSDARG00000057633	ACACGGTAAACTTGTACAGC	ATGTGACAAACGAGTCCTG
<i>gstp2</i>	ENSDARG00000057338	TCTGGACTCTTTCCCGTCTCTCAA	ATTCACTGTTTGCCGTTGCCGT
<i>igfbpa</i>	ENSDARG00000014947	AAGCGGTGTGCACCGAGAGC	CCCGGTCACGAACACGGTGG
<i>ponzr4</i>	ENSDARG00000087440	GCTGTATTCTCCAATCACG	CCTTGCCCTTCATCTCTCGTC
<i>p53</i>	ENSDARG00000035559	CTCTCCCACCAACATCCACT	ACGTCCACCACCATTGTAAC
<i>s100z</i>	ENSDARG00000038729	GATCACCGTCTTCCACAAC	GTCTTCTGAGACATGAGG
<i>wfikkn1</i>	ENSDARG00000044671	TATGCACACACAGTCAACAC	GGACTCATTTACCTGTGCGAG

Table 4-S2 Sequencing mapping

Summary of total counts and mapping statistics of reads that passed Illumina CASAVA QC for RNA-seq samples in this study. Reads were mapped to genome assembly Zv9.

Sample Name	Total paired reads (Illumina QC ok)	Reads mapped to genome (Zv9)	% reads mapped	Reads mapped uniquely	% reads uniquely mapped	Reads mapped to two locations	Reads mapped to 3 or more locations	Total hits (only paired accepted)
DMSO_A	41,403,566	31,136,272	75.2	25,206,504	81	1,681,278	4,248,490	40,196,648
DMSO_B	59,745,304	45,224,497	75.7	37,320,636	82.5	2,876,464	5,027,397	59,347,598
DMSO_C	59,035,420	44,516,465	75.4	36,303,716	81.6	2,424,866	5,787,883	59,634,276
BEZO_A	51,837,910	38,800,129	74.8	31,274,174	80.6	2,056,482	5,469,473	51,499,242
BEZO_B	46,499,422	35,095,720	75.5	25,391,954	72.4	1,827,628	7,876,138	46,369,830
BEZO_C	41,818,250	31,305,119	74.9	25,532,988	81.6	1,664,374	4,107,757	39,621,128
BaAQ_A	49,416,290	37,181,558	75.2	29,973,554	80.6	1,953,912	5,254,092	50,418,194
BaAQ_B	36,241,038	26,888,497	74.2	21,517,188	80	1,372,508	3,998,801	35,143,112
BaAQ_C	47,733,496	35,477,524	74.3	27,090,316	76.4	1,971,892	6,415,316	51,354,196

Table 4-S3 7,12-B[a]AQ significantly misexpressed transcripts

Zebrafish genome assembly Zv9 transcripts identified by Cuffdiff as significantly differentially expressed in 7,12-B[a]AQ-exposed embryos compared to control (1% FDR, $q < 0.05$).). Log₂ fold change values represent mean BEZO-exposed compared to control.

Gene ID	Gene	Log2(fold_change)	q_value
ENSDARG00000026039	cyp1a	7.81	0.00E+00
ENSDARG00000058980	cyp1c1	4.81	0.00E+00
ENSDARG00000018298	cyp1c2	4.41	0.00E+00
ENSDARG00000059387	fgf7	3.82	4.35E-03
ENSDARG00000068934	cyp1b1	3.57	0.00E+00
ENSDARG00000076534	si:ch211-14a17.10	3.11	1.29E-02
ENSDARG00000057338	gstp2	2.69	1.32E-02
ENSDARG00000003902	ctsl.1	2.44	1.22E-05
ENSDARG00000015355	fosl1a	2.31	4.96E-03
ENSDARG00000005039	gstp1	2.27	0.00E+00
ENSDARG00000007344	tcap	2.25	0.00E+00
ENSDARG00000022139	ocstamp	2.06	7.57E-03
ENSDARG00000074971	DHRS13 (2 of 5)	2.00	1.93E-07
ENSDARG00000061481	CABZ01041812.1	1.96	0.00E+00
ENSDARG00000058734	prdx1	1.92	0.00E+00
ENSDARG00000086826	sult6b1	1.92	0.00E+00
ENSDARG00000061634	zgc:158614	1.90	1.87E-13
ENSDARG00000055974	TPMT (1 of 2)	1.86	2.88E-08
ENSDARG00000038729	s100z	1.84	5.98E-03
ENSDARG00000016713	dhhs13l1	1.83	5.80E-06
ENSDARG00000031683	fos	1.80	2.23E-10
ENSDARG00000086047	CABZ01067657.1	1.75	0.00E+00
ENSDARG00000019236	gsr	1.74	8.45E-11
ENSDARG00000075014	sqstm1	1.73	2.90E-02
ENSDARG00000073695	mamdc2b	1.70	1.40E-03
ENSDARG00000021149	cbr1l	1.69	0.00E+00
ENSDARG00000056638	pir	1.68	1.85E-11
ENSDARG00000044685	nr0b2a	1.59	9.65E-12
ENSDARG00000091715	CR926130.2	1.58	1.61E-12
ENSDARG00000071567	TSTD1	1.58	3.77E-08
ENSDARG00000067652	im:7150988	1.57	0.00E+00
ENSDARG00000089936	sepw2b	1.53	3.96E-08
ENSDARG00000089697	si:dkey-3d18.4	1.52	3.59E-03
ENSDARG00000035422	cyr61l1	1.48	1.71E-02
ENSDARG00000033285	gstp2	1.47	1.14E-07
ENSDARG00000002204	hsqb11	1.46	2.23E-10
ENSDARG00000030896	foxq1a	1.44	3.00E-02
ENSDARG00000005713	ethe1	1.41	3.30E-07
ENSDARG00000034852	nt5c2l1	1.39	8.31E-04
ENSDARG00000089507	ugt1b4	1.34	2.43E-11
ENSDARG00000089586	AL844567.2	1.33	2.45E-03
ENSDARG00000063223	arl14	1.32	4.60E-02
ENSDARG00000044935	hpdh	1.29	7.05E-07
ENSDARG00000075524	CYLC2	1.29	5.53E-11
ENSDARG00000056795	serpine1	1.28	6.52E-03

Gene ID	Gene	Log2(fold_change)	q_value
ENSDARG00000014646	AOC2	1.25	1.93E-07
ENSDARG00000090375	ALPK3 (2 of 2)	1.24	1.22E-03
ENSDARG00000002405	si:ch211-225b11.1	1.22	4.78E-04
ENSDARG00000053136	b2m	1.22	1.68E-02
ENSDARG00000070000	txnipb	1.18	1.49E-08
ENSDARG00000043442	MAL (2 of 3)	1.18	5.20E-06
ENSDARG00000007823	atf3	1.16	5.80E-06
ENSDARG00000079938	zgc:173594	1.16	4.00E-03
ENSDARG00000061081	arpp21	1.15	1.04E-04
ENSDARG00000025122	abhd4	1.15	2.02E-02
ENSDARG00000006220	ugt1ab	1.14	3.76E-02
ENSDARG00000073786	cmb1	1.13	3.07E-05
ENSDARG00000094719	si:dkeyp-1h4.9	1.12	2.89E-04
ENSDARG00000058005	hgd	1.09	9.84E-04
ENSDARG00000018566	CU302436.1	1.09	5.51E-11
ENSDARG00000022165	MGST1 (1 of 2)	1.08	4.73E-02
ENSDARG00000055643	cyb5a	1.08	9.57E-07
ENSDARG00000067701	myoz3a	1.07	1.54E-03
ENSDARG00000071005	ppp1r3ca	1.06	2.34E-05
ENSDARG00000014947	igfbp1a	1.06	8.85E-03
ENSDARG00000078674	hsbp9	1.05	2.07E-08
ENSDARG00000023217	CREM	1.04	4.35E-02
ENSDARG00000028386	htatip2	1.02	8.05E-03
ENSDARG00000091116	pkhd1l1	1.01	8.62E-07
ENSDARG00000032496	zgc:91887	1.00	2.93E-04
ENSDARG00000063297	abcb6	0.99	1.24E-02
ENSDARG00000039232	DUSP8 (2 of 2)	0.94	1.84E-03
ENSDARG00000031776	zgc:92066	0.94	2.09E-05
ENSDARG00000061120	slc43a2b	0.93	4.75E-04
ENSDARG00000092379	si:dkeyp-51b9.3	0.92	2.81E-02
ENSDARG00000093494	si:ch211-217k17.9	0.92	3.25E-06
ENSDARG00000093584	zgc:193505	0.91	3.97E-05
ENSDARG00000028957	maff	0.90	1.53E-05
ENSDARG00000070020	cyp2aa9	0.90	9.84E-04
ENSDARG00000026611	socs3b	0.86	1.54E-03
ENSDARG00000055510	ypel3	0.86	3.59E-03
ENSDARG00000016132	keap1a	0.85	3.98E-03
ENSDARG00000090014	CAPN2 (1 of 4)	0.85	6.87E-03
ENSDARG00000061841	tiparp	0.84	2.07E-02
ENSDARG00000017034	sqr1l	0.84	7.79E-03
ENSDARG00000074634	keap1b	0.82	5.94E-03
ENSDARG00000093521	B3GNT3 (2 of 4)	0.82	3.77E-02
ENSDARG00000087093	si:ch211-157c3.4	0.82	4.33E-02
ENSDARG00000060315	si:dkey-193b15.6	0.81	5.36E-03
ENSDARG00000095434	si:ch211-217k17.8	0.79	7.76E-03
ENSDARG00000033364	zgc:158387	0.79	8.80E-06
ENSDARG00000089046	-	0.79	2.93E-02
ENSDARG00000055045	casp3b	0.77	3.57E-02
ENSDARG00000036457	cacng6a	0.76	1.33E-02

Gene ID	Gene	Log2(fold_change)	q_value
ENSDARG00000060113	znf395a	0.75	1.99E-03
ENSDARG00000042310	blvrb	0.75	5.20E-03
ENSDARG00000094300	si:ch211-160e1.5	0.75	4.91E-04
ENSDARG00000030722	xirp1	0.75	2.05E-03
ENSDARG00000026655	tspo	0.74	6.60E-03
ENSDARG00000006982	msxd	0.73	2.91E-02
ENSDARG00000077549	AIFM2	0.73	5.72E-03
ENSDARG00000089920	MLIP	0.73	7.09E-05
ENSDARG00000040190	qdpra	0.73	2.90E-02
ENSDARG00000030905	cited2	0.72	3.67E-03
ENSDARG00000091996	si:ch211-117m20.5	0.72	3.46E-04
ENSDARG00000094557	nupr1	0.70	1.19E-02
ENSDARG00000059914	SDR42E2	0.70	3.45E-02
ENSDARG00000069559	si:ch211-239f4.7	0.69	1.64E-03
ENSDARG00000021787	abcb5	0.69	9.22E-04
ENSDARG00000028106	glrx	0.69	2.61E-02
ENSDARG00000038147	hbbe3	0.67	5.46E-03
ENSDARG00000079634	FILIP1 (1 of 2)	0.66	3.56E-02
ENSDARG00000019646	twist3	0.64	4.35E-02
ENSDARG00000035810	rgcc	0.64	5.36E-03
ENSDARG00000079119	CR848759.2	0.64	4.17E-02
ENSDARG00000013968	psap	0.59	4.32E-03
ENSDARG00000021059	alas1	0.59	5.20E-03
ENSDARG00000044212	CR385063.1	0.59	5.87E-03
ENSDARG00000089358	CABZ01035189.1	0.59	1.63E-02
ENSDARG00000011245	esrp1	0.58	1.06E-02
ENSDARG00000021833	ahr2	0.57	4.57E-03
ENSDARG00000021366	fbp1a	0.57	1.66E-02
ENSDARG00000070355	FBXO2	0.56	6.89E-03
ENSDARG00000025338	hagh	0.56	4.13E-02
ENSDARG00000070047	rgs4	0.54	2.46E-02
ENSDARG00000071601	pvalb9	0.54	2.19E-02
ENSDARG00000036107	txnipa	0.54	1.16E-02
ENSDARG00000015343	pgd	0.53	2.22E-02
ENSDARG00000038643	alas2	0.53	2.46E-02
ENSDARG00000044125	txn	0.52	3.05E-02
ENSDARG00000035519	histh1l	0.51	2.46E-02
ENSDARG00000007216	abce1	-0.46	4.73E-02
ENSDARG00000006008	dct	-0.46	4.73E-02
ENSDARG00000039578	pa2g4a	-0.48	3.13E-02
ENSDARG00000005122	atp2a2b	-0.49	3.29E-02
ENSDARG00000014179	pfkma	-0.50	2.91E-02
ENSDARG00000030913	zgc:152873	-0.51	4.67E-02
ENSDARG00000061375	sgpl1	-0.51	3.55E-02
ENSDARG00000000212	KRT23 (1 of 15)	-0.51	1.89E-02
ENSDARG00000060594	hadhab	-0.51	2.44E-02
ENSDARG00000068076	psmd7	-0.51	2.02E-02
ENSDARG00000007697	fabp7a	-0.51	2.64E-02
ENSDARG00000030972	dnaja1l	-0.52	4.73E-02

Gene ID	Gene	Log2(fold_change)	q_value
ENSDARG00000010571	ezh2	-0.53	4.03E-02
ENSDARG00000017568	HNRNPAB (2 of 2)	-0.53	3.55E-02
ENSDARG00000056248	wu:fb15e04	-0.53	1.39E-02
ENSDARG00000012234	psme3	-0.53	4.33E-02
ENSDARG00000054155	pcna	-0.53	1.10E-02
ENSDARG00000056314	a2ml	-0.53	1.16E-02
ENSDARG00000037284	ptges3a	-0.54	3.73E-02
ENSDARG00000059357	SARNP	-0.54	1.80E-02
ENSDARG00000063631	ch1073-291c23.1	-0.54	4.91E-02
ENSDARG00000036371	acta1a	-0.54	2.19E-02
ENSDARG00000063509	lrrc58b	-0.55	4.76E-02
ENSDARG00000095268	si:dkey-261h17.1	-0.55	1.21E-02
ENSDARG00000033760	pmelb	-0.55	1.44E-02
ENSDARG00000037057	gcdh	-0.55	2.90E-02
ENSDARG00000037116	cxcl12a	-0.55	1.70E-02
ENSDARG00000071353	AL929007.1	-0.55	7.82E-03
ENSDARG00000007354	pdia3	-0.55	1.63E-02
ENSDARG00000076790	si:ch211-55g3.6	-0.56	2.91E-02
ENSDARG00000006314	itgav	-0.56	1.15E-02
ENSDARG00000090495	pla2g15	-0.56	3.25E-02
ENSDARG00000026829	cotl1	-0.57	5.84E-03
ENSDARG00000012729	hcls1	-0.57	1.73E-02
ENSDARG00000054259	nat10	-0.57	4.02E-02
ENSDARG00000058292	sephs1	-0.57	4.59E-02
ENSDARG00000012694	c3a	-0.57	2.01E-02
ENSDARG00000060041	LIG1	-0.57	6.44E-03
ENSDARG00000037997	tubb5	-0.57	2.64E-02
ENSDARG00000016235	rbp1a	-0.57	1.50E-02
ENSDARG00000012066	dcn	-0.57	2.01E-02
ENSDARG00000070651	PRKCD (1 of 2)	-0.57	3.36E-02
ENSDARG00000017261	gdpd1	-0.58	3.48E-02
ENSDARG00000056600	papss2b	-0.58	1.10E-02
ENSDARG00000009342	txndc5	-0.58	3.98E-03
ENSDARG00000045367	tuba1	-0.58	1.74E-02
ENSDARG00000070050	sfrp2	-0.58	3.41E-02
ENSDARG00000037845	col9a3	-0.58	4.13E-03
ENSDARG00000021720	COL4A6	-0.59	8.75E-03
ENSDARG00000001057	bysl	-0.59	3.12E-02
ENSDARG00000008732	zgc:66479	-0.59	3.59E-03
ENSDARG00000045297	phb2	-0.60	1.80E-02
ENSDARG00000088514	and1	-0.60	2.79E-03
ENSDARG00000061124	srpr	-0.60	7.79E-03
ENSDARG00000091792	BX088649.1	-0.60	3.45E-02
ENSDARG00000040041	mcm4	-0.60	5.44E-03
ENSDARG00000087055	BX842614.2	-0.61	1.10E-02
ENSDARG00000036700	si:ch211-114n24.6	-0.62	1.14E-03
ENSDARG00000053493	aldh1a2	-0.63	5.44E-03
ENSDARG00000054807	sec13	-0.63	8.60E-03
ENSDARG00000038056	FGFBP2 (1 of 2)	-0.63	1.87E-03

Gene ID	Gene	Log2(fold_change)	q_value
ENSDARG00000011404	fen1	-0.63	1.01E-02
ENSDARG00000039345	drg1	-0.63	7.20E-03
ENSDARG00000043276	calr	-0.63	1.42E-03
ENSDARG00000086370	apoea	-0.63	2.27E-03
ENSDARG00000020956	pck2	-0.63	2.04E-03
ENSDARG00000009001	pdip5	-0.64	9.24E-04
ENSDARG00000071212	lepre1	-0.64	2.85E-03
ENSDARG00000056767	itgb3a	-0.65	3.01E-03
ENSDARG00000009401	vcanb	-0.65	2.81E-03
ENSDARG00000014091	osr1	-0.66	3.62E-02
ENSDARG00000005023	fkbp9	-0.66	2.87E-02
ENSDARG00000010962	fkbp7	-0.66	4.09E-02
ENSDARG00000042021	mapk12a	-0.66	2.19E-02
ENSDARG00000038768	mrpl12	-0.66	6.56E-03
ENSDARG00000010487	sae1	-0.66	5.24E-03
ENSDARG00000092467	si:ch73-46j18.5	-0.66	2.88E-03
ENSDARG00000057683	mcm6	-0.67	6.51E-04
ENSDARG00000018846	dgat2	-0.67	2.42E-02
ENSDARG00000037158	rcc1	-0.67	3.94E-02
ENSDARG00000001993	myhb	-0.67	3.74E-02
ENSDARG00000015088	dnajb11	-0.68	2.19E-02
ENSDARG00000055945	asph	-0.68	2.19E-02
ENSDARG00000037846	hm13	-0.68	6.32E-04
ENSDARG00000005161	gpib	-0.68	2.79E-03
ENSDARG00000020103	calrl	-0.68	1.96E-04
ENSDARG00000033855	rqcd1	-0.69	1.54E-02
ENSDARG00000015911	mcm2	-0.69	1.45E-03
ENSDARG00000021004	c5	-0.69	6.70E-03
ENSDARG00000019507	mcm5	-0.69	1.12E-03
ENSDARG00000000796	nr4a1	-0.69	1.32E-02
ENSDARG00000037961	rcn3	-0.70	1.14E-03
ENSDARG00000074908	col6a1	-0.70	1.67E-04
ENSDARG00000027495	elovl4b	-0.70	2.19E-02
ENSDARG00000039131	atp1a1a.3	-0.71	1.68E-02
ENSDARG00000010640	SLC12A2 (6 of 6)	-0.71	4.65E-03
ENSDARG00000039041	sfrp5	-0.71	4.00E-02
ENSDARG00000044975	KRT23 (9 of 15)	-0.72	2.88E-03
ENSDARG00000044261	si:ch211-243g18.2	-0.72	2.51E-02
ENSDARG00000040535	CSGALNACT1 (1 of 2)	-0.73	3.93E-02
ENSDARG00000079233	E2F2	-0.73	2.67E-02
ENSDARG00000002968	a1cf	-0.73	3.38E-02
ENSDARG00000075016	APOB (3 of 3)	-0.73	5.84E-03
ENSDARG00000012016	HPGD	-0.73	2.91E-02
ENSDARG00000069116	timmm10	-0.73	1.16E-02
ENSDARG00000092155	apoc2	-0.73	3.84E-04
ENSDARG00000060797	pfkmb	-0.74	8.38E-04
ENSDARG00000002071	adss	-0.74	6.29E-04
ENSDARG00000062688	gpnmb	-0.74	3.49E-03
ENSDARG00000069415	col17a1a	-0.75	9.61E-05

Gene ID	Gene	Log2(fold_change)	q_value
ENSDARG00000055493	hic1	-0.75	4.05E-02
ENSDARG00000069980	lman1	-0.75	5.98E-03
ENSDARG00000015495	klf3	-0.76	2.61E-04
ENSDARG00000002831	col4a4	-0.77	4.57E-02
ENSDARG00000071219	pik3r3a	-0.77	3.11E-03
ENSDARG00000038153	lgals2b	-0.77	4.62E-02
ENSDARG00000014594	anxa1b	-0.77	6.94E-04
ENSDARG00000069823	PROCA1	-0.78	1.16E-02
ENSDARG00000057738	hells	-0.78	6.94E-04
ENSDARG00000024928	ITIH4	-0.78	9.58E-03
ENSDARG00000035652	sat1a	-0.78	1.37E-02
ENSDARG00000007221	pbk	-0.79	4.10E-02
ENSDARG00000063177	manf	-0.79	3.48E-03
ENSDARG00000056778	cfhl2	-0.79	2.78E-02
ENSDARG00000069048	serpinf1	-0.79	1.53E-04
ENSDARG00000012366	fbp2	-0.79	4.34E-03
ENSDARG00000079370	utp18	-0.79	3.40E-02
ENSDARG00000052039	caspb	-0.80	2.38E-03
ENSDARG00000069261	metap2a	-0.80	4.35E-02
ENSDARG00000055278	cfb	-0.80	1.93E-05
ENSDARG00000069706	prmt6	-0.81	4.73E-02
ENSDARG00000091397	-	-0.82	1.99E-02
ENSDARG00000018258	ADK (2 of 2)	-0.82	9.14E-03
ENSDARG00000076624	ptprb	-0.82	2.12E-02
ENSDARG00000027867	PAPLN (1 of 2)	-0.82	8.10E-03
ENSDARG00000007377	odc1	-0.83	1.24E-03
ENSDARG00000018266	mthfd1a	-0.83	5.67E-03
ENSDARG00000052470	igfbp2a	-0.83	3.72E-04
ENSDARG00000090468	PPP1R3A (2 of 2)	-0.83	4.34E-03
ENSDARG00000090802	MCM3 (2 of 2)	-0.83	1.77E-02
ENSDARG00000033140	desi1a	-0.84	6.28E-04
ENSDARG00000042641	cyp51	-0.84	1.19E-02
ENSDARG00000004665	hspa5	-0.84	1.86E-06
ENSDARG00000045141	aqp8a.1	-0.84	4.61E-02
ENSDARG00000029075	pfkfb4l	-0.84	1.87E-04
ENSDARG00000056938	kera	-0.85	5.80E-06
ENSDARG00000045843	apex1	-0.85	1.59E-03
ENSDARG00000073928	mrc1a	-0.85	1.48E-04
ENSDARG00000009782	myh11a	-0.85	3.55E-02
ENSDARG00000035891	acana	-0.85	3.45E-02
ENSDARG00000041110	dnajc3	-0.87	3.51E-02
ENSDARG00000004282	zgc:77375	-0.88	2.07E-02
ENSDARG00000029204	TYRP1 (2 of 2)	-0.88	1.87E-05
ENSDARG00000052738	hmgcs1	-0.89	3.84E-04
ENSDARG00000018491	pdia4	-0.90	8.75E-08
ENSDARG00000001975	hsd11b2	-0.90	3.62E-04
ENSDARG00000003820	nr1d2a	-0.90	3.49E-02
ENSDARG00000057575	pnp4a	-0.90	2.28E-04
ENSDARG00000003570	hsp90b1	-0.91	2.70E-07

Gene ID	Gene	Log2(fold_change)	q_value
ENSDARG00000014488	ca2	-0.92	2.62E-08
ENSDARG00000090467	CABZ01074130.1	-0.92	2.53E-08
ENSDARG00000016491	aglb	-0.93	2.23E-06
ENSDARG00000016718	mmp11b	-0.94	4.33E-02
ENSDARG00000073699	-	-0.94	2.44E-08
ENSDARG00000079111	zgc:86725	-0.95	4.68E-04
ENSDARG00000013670	hyou1	-0.96	1.50E-02
ENSDARG00000060345	apod	-0.96	1.78E-04
ENSDARG00000069827	crygm2d11	-0.97	1.88E-04
ENSDARG00000041595	ces3	-0.98	2.37E-05
ENSDARG00000070597	prelp	-0.98	7.57E-03
ENSDARG00000018351	hpda	-0.98	1.79E-02
ENSDARG00000055172	BX470254.2	-0.98	1.04E-07
ENSDARG00000055100	cxcl12b	-0.99	1.30E-05
ENSDARG00000053853	slc13a2	-1.00	2.37E-05
ENSDARG00000076357	CABZ01102039.1	-1.01	3.40E-02
ENSDARG00000010478	hsp90aa1.1	-1.03	2.90E-10
ENSDARG00000090268	KRT23 (12 of 15)	-1.03	4.81E-08
ENSDARG00000039462	CABZ01076094.1	-1.03	2.73E-08
ENSDARG00000042780	APOB (1 of 3)	-1.03	8.62E-07
ENSDARG00000026771	tmem41ab	-1.04	3.45E-02
ENSDARG00000052917	im:7154842	-1.04	3.51E-09
ENSDARG00000091260	MYLK4 (1 of 2)	-1.04	1.63E-04
ENSDARG00000035914	tmem167a	-1.05	3.05E-06
ENSDARG00000038785	abcf2a	-1.06	8.08E-10
ENSDARG00000090623	CR392352.1	-1.07	5.51E-03
ENSDARG00000007480	rpe65a	-1.07	2.48E-05
ENSDARG00000036840	krt15	-1.09	1.68E-05
ENSDARG00000069988	ARID5A (2 of 2)	-1.09	4.51E-02
ENSDARG00000043806	postna	-1.10	6.50E-04
ENSDARG00000045180	acta2	-1.11	3.40E-02
ENSDARG00000039605	mat1a	-1.11	2.39E-12
ENSDARG00000037278	lrata	-1.11	2.81E-02
ENSDARG00000075161	defbl1	-1.13	4.37E-08
ENSDARG00000093774	rbp2b	-1.14	3.05E-06
ENSDARG00000030215	matn1	-1.14	1.05E-04
ENSDARG00000045808	rlbp1b	-1.16	2.91E-02
ENSDARG00000054753	col10a1	-1.17	2.44E-11
ENSDARG00000057064	enpep	-1.20	2.46E-02
ENSDARG00000023324	rab11bb	-1.23	7.79E-03
ENSDARG00000001760	tnxb	-1.23	2.55E-09
ENSDARG00000095321	si:dkey-9l20.3	-1.26	0.00E+00
ENSDARG00000038424	C4A	-1.26	1.62E-07
ENSDARG00000035309	entpd3	-1.28	2.33E-09
ENSDARG00000055118	mylipb	-1.32	1.63E-02
ENSDARG00000077872	CR626907.1	-1.33	2.88E-03
ENSDARG00000095239	si:dkeyp-106c3.1	-1.35	2.28E-02
ENSDARG00000009018	rhbg	-1.36	0.00E+00
ENSDARG00000076874	abhd5	-1.37	1.33E-02

Gene ID	Gene	Log2(fold_change)	q_value
ENSDARG00000016412	agt	-1.37	2.44E-08
ENSDARG00000079302	and2	-1.40	0.00E+00
ENSDARG00000076192	ankrd1b	-1.43	2.23E-10
ENSDARG00000041685	BX663520.1	-1.47	1.07E-03
ENSDARG00000087345	CABZ01059415.2	-1.57	7.28E-07
ENSDARG00000088636	wu:fa03e10	-1.64	0.00E+00
ENSDARG00000052631	thbs4a	-1.69	1.61E-07
ENSDARG00000030604	phkg1a	-1.70	2.90E-03
ENSDARG00000062132	cyp4v8	-1.76	2.64E-02
ENSDARG00000052207	c3c	-1.76	0.00E+00
ENSDARG00000067639	prpf4	-1.78	7.68E-04
ENSDARG00000002311	fabp11b	-1.81	0.00E+00
ENSDARG00000079933	SLC46A3 (1 of 2)	-1.84	6.91E-05
ENSDARG00000031952	mb	-1.84	0.00E+00
ENSDARG00000035544	agxt2l1	-1.91	1.42E-02
ENSDARG00000042379	zgc:103681	-2.02	4.35E-02
ENSDARG00000056875	rgs2	-2.19	1.28E-02
ENSDARG00000071173	slc12a10.2	-2.22	1.48E-04
ENSDARG00000087359	c3b	-2.26	1.58E-04
ENSDARG00000056587	cyp2r1	-2.29	2.15E-03
ENSDARG00000007024	uox	-2.94	4.67E-02
ENSDARG00000068194	klf9	-3.13	4.33E-06
ENSDARG00000088589	ponzr3	-3.41	7.93E-10
ENSDARG00000028396	fkbp5	-4.23	0.00E+00
ENSDARG00000087440	ponzr4	-4.42	3.80E-09

Table 4-S4 BEZO significantly misexpressed transcripts

Zebrafish genome assembly Zv9 transcripts identified by Cuffdiff as significantly differentially expressed in BEZO-exposed embryos compared to control (1% FDR, $q < 0.05$). Log₂ fold change values represent mean BEZO-exposed compared to control.

Gene ID	Gene	Log2(fold_change)	q_value
ENSDARG00000069375	zgc:162608	1.94	9.06E-09
ENSDARG00000014947	igfbp1a	1.91	0.00E+00
ENSDARG00000026039	cyp1a	1.83	1.27E-12
ENSDARG00000086047	CABZ01067657.1	1.72	0.00E+00
ENSDARG00000061481	CABZ01041812.1	1.72	0.00E+00
ENSDARG00000074971	DHRS13 (2 of 5)	1.68	1.43E-05
ENSDARG00000003902	ctsl.1	1.63	2.46E-02
ENSDARG00000044685	nr0b2a	1.53	1.36E-13
ENSDARG00000038025	cbx7a	1.49	1.21E-04
ENSDARG00000076221	zgc:198419	1.43	1.09E-02
ENSDARG00000007344	tcap	1.42	2.93E-12
ENSDARG00000091047	CABZ01045617.2	1.39	6.79E-08
ENSDARG00000070012	sesn2	1.36	5.73E-08
ENSDARG00000075524	CYLC2	1.35	0.00E+00
ENSDARG00000019236	gsr	1.33	1.45E-07
ENSDARG00000005713	ethe1	1.29	2.50E-07
ENSDARG00000037121	mat2ab	1.26	6.22E-06
ENSDARG00000023217	CREM	1.25	4.36E-04
ENSDARG00000005039	gstp1	1.25	0.00E+00
ENSDARG00000007823	atf3	1.23	6.38E-09
ENSDARG00000061120	slc43a2b	1.23	0.00E+00
ENSDARG00000061634	zgc:158614	1.22	2.65E-06
ENSDARG00000021149	cbr1l	1.21	0.00E+00
ENSDARG000000058734	prdx1	1.21	0.00E+00
ENSDARG00000089697	si:dkey-3d18.4	1.18	4.96E-02
ENSDARG00000094719	si:dkeyp-1h4.9	1.18	2.65E-06
ENSDARG00000057633	cxcr4a	1.18	2.51E-03
ENSDARG00000030872	cetp	1.17	2.12E-05
ENSDARG00000059914	SDR42E2	1.15	6.40E-09
ENSDARG00000078878	METTL21C (1 of 2)	1.14	2.06E-04
ENSDARG00000058980	cyp1c1	1.11	7.89E-11
ENSDARG00000051956	isca1	1.11	5.54E-10
ENSDARG00000060189	ESM1	1.09	4.13E-02
ENSDARG00000055974	TPMT (1 of 2)	1.07	1.12E-02
ENSDARG00000067857	pmt	1.04	5.14E-04
ENSDARG00000056638	pir	1.03	1.15E-04
ENSDARG00000000551	slc1a4	1.03	4.71E-12
ENSDARG00000091871	si:ch211-13o20.3	1.00	2.35E-06
ENSDARG00000039269	arg2	0.99	5.73E-08
ENSDARG00000031683	fos	0.98	4.03E-03
ENSDARG00000045708	adm2a	0.98	8.88E-03
ENSDARG00000002405	si:ch211-225b11.1	0.97	7.03E-04
ENSDARG00000056680	stc2a	0.96	8.50E-08
ENSDARG00000058476	stc1l	0.94	2.70E-02
ENSDARG00000052694	micall2a	0.94	1.55E-03

Gene ID	Gene	Log2(fold_change)	q_value
ENSDARG00000016457	irf9	0.93	2.62E-03
ENSDARG00000071567	TSTD1	0.91	9.14E-03
ENSDARG00000055723	hsp70l	0.90	4.12E-04
ENSDARG00000078882	CR407583.2	0.89	9.16E-06
ENSDARG00000077559	NCOA7 (2 of 2)	0.89	4.17E-03
ENSDARG00000061081	arpp21	0.88	2.90E-03
ENSDARG00000021242	mvp	0.88	6.92E-08
ENSDARG00000079938	zgc:173594	0.88	4.80E-02
ENSDARG00000076386	epdl1	0.88	3.93E-03
ENSDARG00000070020	cyp2aa9	0.88	7.92E-05
ENSDARG00000031776	zgc:92066	0.85	1.49E-06
ENSDARG00000020645	slc7a3a	0.85	5.98E-08
ENSDARG00000086826	sult6b1	0.83	1.04E-07
ENSDARG00000074829	RASIP1	0.83	4.21E-02
ENSDARG000000091111	TIFA	0.83	4.69E-04
ENSDARG00000033539	paics	0.83	7.89E-11
ENSDARG00000077785	ATF5 (2 of 2)	0.81	1.59E-05
ENSDARG00000075014	sqstm1	0.80	2.15E-04
ENSDARG00000073786	cmbl	0.80	4.80E-03
ENSDARG00000052148	ptgs1	0.80	1.64E-02
ENSDARG00000057121	C7 (1 of 2)	0.79	2.19E-02
ENSDARG00000019274	rasd1	0.79	8.98E-05
ENSDARG00000054058	h1fx	0.79	1.22E-11
ENSDARG00000042725	cebpb	0.78	9.16E-06
ENSDARG00000035602	dao.1	0.78	2.70E-03
ENSDARG00000025338	hagh	0.77	1.26E-05
ENSDARG00000093156	si:ch73-21g5.7	0.76	8.39E-03
ENSDARG00000040907	gcgb	0.76	1.85E-02
ENSDARG00000030905	cited2	0.73	1.05E-04
ENSDARG00000092337	gas5	0.73	1.41E-05
ENSDARG00000094557	nupr1	0.72	4.72E-04
ENSDARG00000026359	PBLD (2 of 2)	0.70	1.40E-02
ENSDARG00000091350	MYO18B	0.69	3.57E-02
ENSDARG00000045568	bcat1	0.69	3.77E-02
ENSDARG00000045976	sidt2	0.68	3.41E-04
ENSDARG00000027529	hmox1	0.68	3.18E-04
ENSDARG00000032496	zgc:91887	0.68	2.40E-02
ENSDARG00000070000	txnipb	0.68	1.89E-03
ENSDARG00000060113	znf395a	0.66	1.40E-04
ENSDARG00000001873	phgdh	0.65	1.93E-06
ENSDARG00000056379	si:ch211-154o6.6	0.65	1.85E-02
ENSDARG00000060315	si:dkey-193b15.6	0.65	1.86E-02
ENSDARG00000035559	tp53	0.64	2.83E-02
ENSDARG00000026611	socs3b	0.64	1.81E-02
ENSDARG00000038559	h1f0	0.63	7.48E-08
ENSDARG00000068096	ATF5 (1 of 2)	0.63	1.47E-03
ENSDARG00000035519	histh1l	0.63	9.62E-08
ENSDARG00000090552	wu:fb12e11	0.62	9.72E-03
ENSDARG00000059202	TSPAN2 (2 of 2)	0.62	1.53E-02
ENSDARG00000020742	NAGA	0.61	2.59E-02

Gene ID	Gene	Log2(fold_change)	q_value
ENSDARG00000021787	abcb5	0.61	7.61E-05
ENSDARG00000088885	PHGR1	0.61	1.02E-02
ENSDARG00000006019	tkf	0.60	5.66E-04
ENSDARG00000042874	phlda2	0.59	2.59E-02
ENSDARG00000070426	chac1	0.59	1.14E-06
ENSDARG00000016733	psat1	0.58	7.23E-06
ENSDARG00000035890	fuca1	0.58	1.17E-04
ENSDARG00000076838	APOM	0.57	6.17E-03
ENSDARG00000095147	KRT23 (2 of 15)	0.57	4.93E-02
ENSDARG00000033666	pi4k2a	0.56	1.03E-02
ENSDARG00000038147	hbbe3	0.56	3.51E-03
ENSDARG00000017388	gstt1b	0.56	1.82E-02
ENSDARG00000091816	CABZ01088039.1	0.56	3.58E-03
ENSDARG00000029011	xpnpep1	0.55	1.56E-02
ENSDARG00000052705	pkp1	0.55	3.21E-02
ENSDARG00000067652	im:7150988	0.54	1.92E-03
ENSDARG00000028618	KRT18 (2 of 3)	0.54	1.54E-04
ENSDARG00000041607	elf4ebp3l	0.53	1.26E-02
ENSDARG00000020232	elf6	0.53	4.29E-02
ENSDARG00000070047	rgs4	0.53	1.22E-03
ENSDARG00000018566	CU302436.1	0.53	1.78E-04
ENSDARG00000012987	gpia	0.53	9.23E-04
ENSDARG00000015164	mknk2b	0.52	3.54E-04
ENSDARG00000041394	dnajb1b	0.51	2.59E-02
ENSDARG00000007955	iars	0.51	5.19E-04
ENSDARG00000010312	cp	0.50	2.37E-04
ENSDARG00000016319	c9	0.50	1.02E-02
ENSDARG00000013968	psap	0.49	1.05E-04
ENSDARG00000036107	txnipa	0.49	1.49E-04
ENSDARG00000028957	maff	0.49	3.41E-02
ENSDARG00000094300	si:ch211-160e1.5	0.49	1.92E-02
ENSDARG00000016200	trib3	0.48	2.52E-02
ENSDARG00000056395	oncut3	0.48	2.13E-02
ENSDARG00000013430	bhmt	0.48	3.62E-03
ENSDARG00000089920	MLIP	0.48	1.22E-03
ENSDARG00000076667	ccng1	0.47	1.24E-03
ENSDARG00000017960	sfxn2	0.46	1.96E-02
ENSDARG00000054030	hoxb5b	0.46	2.17E-02
ENSDARG00000010946	cbsb	0.45	2.66E-02
ENSDARG00000069142	aars	0.45	3.18E-03
ENSDARG00000037910	FILIP1L (2 of 2)	0.44	3.98E-02
ENSDARG00000033609	map1lc3a	0.44	3.75E-02
ENSDARG00000071082	p4ha1b	0.44	1.13E-02
ENSDARG00000091996	si:ch211-117m20.5	0.43	2.01E-03
ENSDARG00000017180	npc1	0.42	3.47E-03
ENSDARG00000042934	ctgfa	0.41	1.49E-02
ENSDARG00000037618	ddit4	0.41	4.21E-02
ENSDARG00000076241	txlnbb	0.41	2.27E-02
ENSDARG00000044125	txn	0.38	4.93E-02
ENSDARG00000061100	nars	0.36	4.21E-02

Gene ID	Gene	Log2(fold_change)	q_value
ENSDARG00000057698	ctsd	0.36	3.48E-02
ENSDARG00000058656	desma	0.35	4.67E-02
ENSDARG00000079745	si:ch211-166a6.5	0.34	3.72E-02
ENSDARG00000041811	rps25	0.34	4.95E-02
ENSDARG00000026726	anxa1a	0.33	4.81E-02
ENSDARG00000042245	MYL4	-0.34	4.67E-02
ENSDARG00000057052	DSCAML1	-0.34	4.29E-02
ENSDARG00000018259	atp1a3a	-0.34	4.83E-02
ENSDARG00000019566	neurod	-0.35	3.21E-02
ENSDARG00000055216	tuba1l	-0.35	2.82E-02
ENSDARG00000009001	pdip5	-0.35	4.21E-02
ENSDARG00000074908	col6a1	-0.35	3.82E-02
ENSDARG00000017568	HNRNPAB (2 of 2)	-0.36	4.37E-02
ENSDARG00000056151	tyrp1b	-0.36	2.55E-02
ENSDARG00000073732	myh14	-0.36	4.58E-02
ENSDARG00000029058	rbb4	-0.36	3.10E-02
ENSDARG00000005551	hnrnph1l	-0.37	2.96E-02
ENSDARG00000056725	hmgb3a	-0.37	3.37E-02
ENSDARG00000019353	sparc	-0.37	4.57E-02
ENSDARG00000037846	hm13	-0.37	4.64E-02
ENSDARG00000079772	hmgb1a	-0.38	1.49E-02
ENSDARG00000090268	KRT23 (12 of 15)	-0.38	3.91E-02
ENSDARG00000068507	crybb1	-0.39	4.82E-02
ENSDARG00000004665	hspa5	-0.40	7.57E-03
ENSDARG00000071353	AL929007.1	-0.40	1.04E-02
ENSDARG00000028524	col5a3b	-0.40	5.37E-03
ENSDARG00000086222	NAT16	-0.40	1.81E-02
ENSDARG00000020103	calrl	-0.40	5.12E-03
ENSDARG00000027355	slc25a4	-0.40	5.12E-03
ENSDARG00000013963	mipb	-0.40	6.08E-03
ENSDARG00000016235	rbp1a	-0.40	4.21E-02
ENSDARG00000003570	hsp90b1	-0.41	6.65E-03
ENSDARG00000088514	and1	-0.42	2.84E-03
ENSDARG00000054362	ccdc47	-0.42	4.46E-03
ENSDARG00000069737	pou4f2	-0.42	1.47E-02
ENSDARG00000031100	ivns1abpa	-0.43	1.53E-02
ENSDARG00000063914	mt-nd3	-0.43	2.18E-03
ENSDARG00000008732	zgc:66479	-0.43	4.85E-03
ENSDARG00000058117	snap25b	-0.43	3.78E-02
ENSDARG00000061124	srpr	-0.43	1.60E-02
ENSDARG00000056292	vsx1	-0.44	1.45E-02
ENSDARG00000037284	ptges3a	-0.44	1.45E-02
ENSDARG00000062688	gpnmb	-0.44	4.90E-02
ENSDARG00000054807	sec13	-0.44	2.75E-02
ENSDARG00000076768	REPS2	-0.45	3.42E-02
ENSDARG00000018491	pdia4	-0.45	1.40E-03
ENSDARG00000011125	snrpb	-0.45	3.08E-02
ENSDARG00000014179	pfkma	-0.46	1.77E-03
ENSDARG00000037285	mipa	-0.46	1.78E-03
ENSDARG00000039913	tmem147	-0.46	4.67E-02

Gene ID	Gene	Log2(fold_change)	q_value
ENSDARG00000074169	GPAM	-0.47	1.28E-02
ENSDARG00000030411	crygn2	-0.47	3.72E-04
ENSDARG00000090467	CABZ01074130.1	-0.48	2.73E-04
ENSDARG00000001889	tuba1l2	-0.48	2.55E-04
ENSDARG00000045843	apex1	-0.48	4.29E-02
ENSDARG00000092467	si:ch73-46j18.5	-0.48	7.23E-03
ENSDARG00000036840	krt15	-0.48	4.83E-02
ENSDARG00000012381	zgc:63663	-0.49	1.01E-03
ENSDARG00000018130	rhot1a	-0.49	4.61E-02
ENSDARG00000056248	wu:fb15e04	-0.50	1.14E-04
ENSDARG00000045143	hbbe2	-0.50	4.25E-03
ENSDARG00000043257	ckbb	-0.50	1.26E-02
ENSDARG00000073699	-	-0.51	2.07E-04
ENSDARG00000071219	pik3r3a	-0.51	3.64E-02
ENSDARG00000057738	hells	-0.51	1.08E-02
ENSDARG00000002071	adss	-0.51	3.61E-03
ENSDARG00000007576	crybb1l1	-0.51	1.03E-04
ENSDARG00000038056	FGFBP2 (1 of 2)	-0.51	3.55E-04
ENSDARG00000042780	APOB (1 of 3)	-0.51	2.40E-03
ENSDARG00000005161	gpib	-0.52	4.36E-03
ENSDARG00000074752	hlfa	-0.52	1.92E-03
ENSDARG00000063631	ch1073-291c23.1	-0.52	5.49E-03
ENSDARG00000053875	cryba1b	-0.52	1.49E-04
ENSDARG00000001910	rorab	-0.53	4.63E-04
ENSDARG00000042021	mapk12a	-0.53	3.35E-02
ENSDARG00000018119	cox5ab	-0.53	1.30E-02
ENSDARG00000053502	cryaa	-0.53	4.55E-03
ENSDARG00000059357	SARNP	-0.53	2.78E-04
ENSDARG00000044562	cycsb	-0.54	2.37E-05
ENSDARG00000005643	gcat	-0.54	4.60E-02
ENSDARG00000087765	si:ch211-212n6.17	-0.54	2.44E-04
ENSDARG00000057575	pnp4a	-0.55	1.76E-02
ENSDARG00000031316	six6b	-0.55	6.48E-03
ENSDARG00000086030	PCBP3 (2 of 2)	-0.55	4.67E-02
ENSDARG00000038785	abcf2a	-0.55	8.56E-05
ENSDARG00000090468	PPP1R3A (2 of 2)	-0.56	4.64E-02
ENSDARG00000015495	klf3	-0.56	8.15E-04
ENSDARG00000037997	tubb5	-0.57	3.80E-05
ENSDARG00000036344	calb2b	-0.57	2.31E-04
ENSDARG00000024548	cryba4	-0.58	2.77E-05
ENSDARG00000070386	KRTCAP2	-0.58	2.52E-02
ENSDARG00000061836	nfixb	-0.59	2.33E-03
ENSDARG00000037588	bhlhe23	-0.59	4.51E-02
ENSDARG00000007697	fabp7a	-0.60	1.38E-06
ENSDARG00000054804	anp32e	-0.60	4.49E-04
ENSDARG00000044975	KRT23 (9 of 15)	-0.61	1.30E-03
ENSDARG00000077341	PPP1R14C (1 of 2)	-0.61	3.55E-02
ENSDARG00000007715	lgsm	-0.61	2.13E-04
ENSDARG00000009401	vcanb	-0.63	1.46E-05
ENSDARG00000036058	gnao1b	-0.63	5.90E-05

Gene ID	Gene	Log2(fold_change)	q_value
ENSDARG00000010717	chchd10	-0.63	1.66E-02
ENSDARG00000032929	cryba1l	-0.64	7.06E-08
ENSDARG00000021720	COL4A6	-0.65	1.11E-05
ENSDARG00000039605	mat1a	-0.65	4.51E-08
ENSDARG00000056938	kera	-0.65	8.98E-05
ENSDARG00000093774	rbp2b	-0.66	1.97E-03
ENSDARG00000033760	pmelb	-0.66	3.90E-06
ENSDARG00000011166	cahz	-0.66	4.72E-04
ENSDARG00000087324	crygm2d1	-0.66	1.72E-04
ENSDARG00000030349	cryba2a	-0.66	5.73E-08
ENSDARG00000018846	dgat2	-0.67	6.40E-04
ENSDARG00000069415	col17a1a	-0.67	1.21E-07
ENSDARG00000075161	defbl1	-0.67	1.12E-04
ENSDARG00000029689	TKT	-0.67	1.05E-05
ENSDARG00000069823	PROCA1	-0.68	7.87E-03
ENSDARG00000032200	rgn	-0.68	4.67E-02
ENSDARG00000095863	zgc:161979	-0.68	1.24E-08
ENSDARG00000014488	ca2	-0.69	7.78E-09
ENSDARG00000023181	pcp4l1	-0.69	1.96E-02
ENSDARG00000029019	epb41b	-0.69	4.43E-03
ENSDARG00000086917	si:ch211-212n6.18	-0.71	1.14E-02
ENSDARG00000094760	si:dkey-125i10.3	-0.72	6.00E-03
ENSDARG00000004282	zgc:77375	-0.72	3.64E-02
ENSDARG00000076693	si:ch211-212n6.8	-0.74	5.29E-05
ENSDARG00000018258	ADK (2 of 2)	-0.74	3.67E-03
ENSDARG00000012366	fbp2	-0.75	5.15E-04
ENSDARG00000014594	anxa1b	-0.76	5.45E-06
ENSDARG00000011989	crx	-0.76	4.71E-11
ENSDARG00000086658	si:ch211-212n6.16	-0.76	9.16E-06
ENSDARG00000079302	and2	-0.76	2.12E-11
ENSDARG00000040535	CSGALNACT1 (1 of 2)	-0.77	3.95E-03
ENSDARG00000003820	nr1d2a	-0.77	2.40E-03
ENSDARG00000052700	si:dkey-162b23.4	-0.77	2.33E-03
ENSDARG00000091260	MYLK4 (1 of 2)	-0.78	1.15E-03
ENSDARG00000086281	zgc:112992	-0.78	1.37E-03
ENSDARG00000052039	caspb	-0.78	1.56E-04
ENSDARG00000002193	rho	-0.78	8.72E-04
ENSDARG00000074001	crygmxl2	-0.78	5.07E-10
ENSDARG00000045685	cntn1b	-0.78	4.64E-02
ENSDARG00000002311	fabp11b	-0.78	9.38E-05
ENSDARG00000019417	gadd45g	-0.78	6.00E-03
ENSDARG00000090689	si:busm1-118j2.5	-0.79	2.41E-07
ENSDARG00000042641	cyp51	-0.79	3.32E-03
ENSDARG00000075270	CU896655.3	-0.80	3.42E-02
ENSDARG00000033140	desi1a	-0.80	2.48E-05
ENSDARG00000060345	apod	-0.82	9.09E-05
ENSDARG00000057206	nmt1b	-0.82	3.28E-02
ENSDARG00000038643	alas2	-0.83	1.61E-08
ENSDARG00000016491	aglb	-0.84	3.05E-08
ENSDARG00000087164	crygm2d4	-0.85	1.93E-06

Gene ID	Gene	Log2(fold_change)	q_value
ENSDARG00000071488	AGL (3 of 3)	-0.86	2.38E-02
ENSDARG00000052917	im:7154842	-0.86	5.59E-11
ENSDARG00000087390	hbbe1.1	-0.87	0.00E+00
ENSDARG00000015076	cx44.1	-0.87	2.78E-04
ENSDARG00000089963	hbbe1.1	-0.87	2.54E-13
ENSDARG00000043961	BX957322.1	-0.88	1.62E-04
ENSDARG00000087188	nfil3-6	-0.90	1.14E-03
ENSDARG00000088823	crygm2d3	-0.91	2.16E-05
ENSDARG00000045141	aqp8a.1	-0.91	6.26E-03
ENSDARG00000079305	hbae3	-0.94	2.54E-13
ENSDARG00000037371	dcun1d1	-0.94	3.88E-02
ENSDARG00000023537	ahr1b	-0.97	5.06E-08
ENSDARG00000057460	crygm2d13	-0.98	1.22E-11
ENSDARG00000069792	crygm2d5	-0.98	1.92E-05
ENSDARG00000052631	thbs4a	-0.98	3.93E-04
ENSDARG00000035309	entpd3	-0.98	1.27E-07
ENSDARG00000007655	crybb1l3	-0.98	2.41E-02
ENSDARG00000023082	krt1-19d	-0.99	5.84E-03
ENSDARG00000069801	crygm2d12	-1.01	0.00E+00
ENSDARG00000030215	matn1	-1.03	7.50E-04
ENSDARG00000011640	syt5b	-1.03	1.10E-10
ENSDARG00000067639	prpf4	-1.04	4.67E-02
ENSDARG00000001760	tnxb	-1.04	2.09E-08
ENSDARG00000037921	gng13b	-1.04	0.00E+00
ENSDARG00000045808	rlbp1b	-1.06	2.41E-02
ENSDARG00000069988	ARID5A (2 of 2)	-1.07	3.41E-02
ENSDARG00000078440	CCDC88A	-1.08	1.70E-08
ENSDARG00000040321	rx2	-1.09	1.98E-03
ENSDARG00000092945	si:ch211-250g4.3	-1.11	0.00E+00
ENSDARG00000001976	si:ch211-13k12.1	-1.11	6.26E-03
ENSDARG00000037337	cnrip1b	-1.12	4.05E-02
ENSDARG00000044212	CR385063.1	-1.12	0.00E+00
ENSDARG00000023324	rab11bb	-1.13	8.54E-03
ENSDARG00000091148	zgc:162402	-1.13	7.16E-09
ENSDARG00000004358	gnb3a	-1.14	0.00E+00
ENSDARG00000041382	si:dkey-283b15.2	-1.15	4.35E-03
ENSDARG00000088330	si:ch211-5k11.2	-1.16	2.09E-06
ENSDARG00000055118	mylipb	-1.16	2.55E-02
ENSDARG00000068194	klf9	-1.16	1.05E-02
ENSDARG00000003991	fhl2b	-1.18	3.42E-02
ENSDARG00000069451	cx50.5	-1.20	1.98E-03
ENSDARG00000087345	CABZ01059415.2	-1.20	9.59E-06
ENSDARG00000051981	STX3 (2 of 2)	-1.20	8.23E-03
ENSDARG00000088636	wu:fa03e10	-1.21	0.00E+00
ENSDARG00000057629	slc30a8	-1.22	9.96E-07
ENSDARG00000093318	CRYGB	-1.24	8.68E-05
ENSDARG00000031952	mb	-1.25	0.00E+00
ENSDARG00000012504	rlbp1a	-1.26	8.73E-10
ENSDARG00000076572	crygm2d7	-1.27	1.07E-12
ENSDARG00000033382	grfin	-1.29	2.03E-02

Gene ID	Gene	Log2(fold_change)	q_value
ENSDARG00000007788	atp2b1b	-1.29	1.60E-02
ENSDARG00000062661	ABCA4 (1 of 2)	-1.29	2.84E-05
ENSDARG00000058556	CR854881.1	-1.31	2.68E-09
ENSDARG00000073874	crygm2d6	-1.32	0.00E+00
ENSDARG00000086912	zgc:86723	-1.33	0.00E+00
ENSDARG00000076055	RPGRIP1	-1.33	1.26E-02
ENSDARG00000086360	RP1 (2 of 2)	-1.33	1.94E-02
ENSDARG00000076192	ankrd1b	-1.40	0.00E+00
ENSDARG00000035544	agxt2l1	-1.40	3.88E-02
ENSDARG00000069817	crygm2d8	-1.42	0.00E+00
ENSDARG00000027495	elovl4b	-1.46	1.60E-11
ENSDARG00000028396	fkbp5	-1.50	0.00E+00
ENSDARG00000073750	crygm2d9	-1.50	9.85E-13
ENSDARG00000037656	C17H2orf71	-1.55	2.29E-02
ENSDARG00000007480	rpe65a	-1.58	1.36E-13
ENSDARG00000019902	rcv1	-1.58	0.00E+00
ENSDARG00000069826	crygm2d15	-1.62	0.00E+00
ENSDARG00000012126	zgc:109965	-1.62	9.69E-12
ENSDARG00000038634	CCK (1 of 2)	-1.68	1.58E-03
ENSDARG00000056511	arr3a	-1.71	7.92E-08
ENSDARG00000069615	CKMT2 (1 of 2)	-1.75	8.26E-05
ENSDARG00000075295	-	-1.76	7.06E-06
ENSDARG00000088589	ponzr3	-1.78	1.83E-06
ENSDARG00000094990	si:dkey-91f15.1	-1.87	2.33E-02
ENSDARG00000052223	rcvrna	-1.88	1.03E-07
ENSDARG00000038894	tmx3	-1.90	1.82E-07
ENSDARG00000087301	crygm2d14	-1.90	0.00E+00
ENSDARG00000076624	ptprb	-1.93	1.22E-11
ENSDARG00000076790	si:ch211-55g3.6	-2.07	0.00E+00
ENSDARG00000088687	zgc:165347	-2.11	0.00E+00
ENSDARG00000027236	rs1	-2.11	4.49E-06
ENSDARG00000057427	SV2B (3 of 3)	-2.21	7.83E-05
ENSDARG00000087440	ponzr4	-2.27	7.35E-10
ENSDARG00000045677	opn1sw1	-2.82	8.92E-03
ENSDARG00000094310	si:ch211-255g12.6	-2.86	0.00E+00
ENSDARG00000069827	crygm2d11	-3.05	5.59E-11
ENSDARG00000026855	cacna2d4a	-3.10	3.22E-03
ENSDARG00000044861	opn1lw2	-3.43	2.06E-04

Chapter 5 - Discussion

Individual PAHs interact with biological systems in numerous ways, resulting in complex responses in many organs and tissue types. To respond to exposures, organisms at all levels of biological complexity have the ability to detect, metabolize and excrete these multi-ringed structures that are ubiquitous in the environment. In vertebrates, the most well-known mediator of xenobiotic response is arguably the AHR, which can bind some PAH structures with high affinity. Metabolism and receptor affinity play large roles in the toxicity of AHR agonists. TCDD, one of the most toxic halogenated hydrocarbons, binds the AHR with high affinity but is not readily metabolized. Compounds naturally present in plants, such as indole 3-carbinol, are also AHR agonists but are more commonly thought of as beneficial components of the diet (Denison and Nagy 2003). Research on PAHs both in aquatic systems and mammals has highlighted a need to better understand both the AHR-dependent and -independent mechanisms by which PAH structures exert toxicological effects, and the concentrations at which these biological mechanisms become concerns for human and wildlife health.

Many studies have screened PAHs for their mutagenic activity, and PAHs are classified as carcinogenic or non-carcinogenic for human health risk assessment purposes. Because little is known about other toxicity mechanisms, it is not currently possible to classify PAHs as “inflammatory” or “ion channel disrupters”, which would be necessary for predicting risk of these effects from exposure to complex PAH mixtures. The involvement of metabolism and receptor binding in the toxicological mechanisms causes small difference in PAH structure to result in very different biological effects. The presence of a “bay” or “fjord” region in higher molecular weight PAHs affects DNA damage potential (Mattsson et al. 2009). A recent study demonstrated that this is also true for non-genotoxic effects of methylanthracenes; 1-methylanthracene (1-MeA), which contains a bay-like region, was compared with 2-methylanthracene (2-MeA) for inflammatory related effects (Osgood et al. 2013). In an alveolar cell line, 1-MeA induced inflammatory signaling associated with tumor promotion, including MAP Kinase signaling, p38 phosphorylation, and inhibited gap junctional intercellular communication, while 2-MeA did not (Osgood et al. 2013). Recognizing these differences is particularly important as we begin to assess the toxicity of

substituted PAHs. Associating molecular mechanisms with structural differences would greatly increase our predictive power for toxicological effects of this large family of compounds.

The objective of the research presented here was to create profiles of biological activities of diverse PAH structures during embryonic development. The zebrafish model can rapidly provide a rich *in vivo* dataset from which to tease apart different biological mechanisms. Morphology analysis can be used to assess toxicity potential with high sensitivity (Truong et al. 2011). Whole genome analysis of mRNA expression via microarrays and RNA-seq provides a snapshot of the transcriptional effects of exposure at a point in time. By comparing these snapshots between compounds, we identified common effects, biomarker genes, and proposed mechanisms for further investigation of PAH-mediated toxicity.

In chapter 2, we compared microarray mRNA profiles of three parent PAHs, dibenzothiophene (DBT), pyrene (PYR), and benz(a)anthracene (BAA). By analyzing early transcriptional changes at concentrations that eventually elicited biological effects, we identified genes that were differentially involved in toxicological effects of these PAHs. We also measured body burdens of PAHs at the exposure concentrations and time points employed in the microarray. This information was essential for discerning potential mechanism from body burden differences. PAHs are hydrophobic; they are readily absorbed by embryos but also adhere to plastic, complicating exposures. While the studies presented here were all conducted in glass vials, solubility likely played a substantial role in the biological effects observed for the parent PAHs. Precipitation of PAH occurs for both PYR and BAA at the 25 μ M concentration. PYR is slightly more soluble than BAA, and we expected some differences in body burden, but the extent to which this varied between compounds was surprising. The large difference in body burden between DBT and the 4-ring parent PAHs was important for interpreting the expression data. By comparing \log_2 FC values across all transcripts that were significantly induced by DBT or PYR, we found very similar patterns of expression. We found little evidence for distinct biological mechanisms between DBT and PYR, while BAA induced a very different profile of genes. BAA-induced genes were examined in further chapters. DBT and PYR, however, induced a large suite of inflammatory-related genes, which has been previously observed for PAHs in other model

systems. The exact mechanism of inflammation is not clear, and I observed no sign of a specific inflammatory site, using transgenic zebrafish with mpx-driven expression of GFP (neutrophils). I also observed a hyperactive phenotype elicited by PYR exposure. DBT also induced hyperactivity, but it decreased, while PYR-exposed embryos remained hyperactive for 5 hours (Appendix 2). Hyperactivity was observed at concentrations as low as 2.5 μ M; future studies will investigate the mechanism that results in this behavioral phenotype.

The role of the AHR in mediating PAH-induced developmental toxicity is not yet well-defined. In Chapter 3, we characterized an *ahr2* mutant zebrafish, which will be an important tool for defining the role of the AHR in both PAH-mediated toxicity as well as normal development. We determined that the TILLING-identified *ahr2* mutant was indeed a functional AHR2 knockout, and was completely resistant to TCDD-induced toxicity. We additionally investigated the effects of an alternative ligand, leflunomide, in the *ahr2*^{hu3335} line. Interestingly, we found that leflunomide induced liver-specific Cyp1a in the mutant line, and found that the AHR isoform AHR1A was responsible for mediating this induction. While this study showed that AHR1A is a functional receptor, future work is needed to characterize the functions of this receptor and potential roles in mediating toxicity.

Building off of a screen of substituted PAHs, we investigated the role of AHR2 in mediating the developmental toxicity of two similarly-structured OPAHs, BEZO and 7,12-B[a]AQ in Chapter 4. Intriguingly, we found that despite different CYP1A induction profiles, developmental effects of both BEZO and 7,12-B[a]AQ were mediated by AHR2. We conducted paired-end 50 bp RNA-seq to compare mRNA expression profiles of embryos exposed to the two compounds from 6-48 hpf. Using the Tuxedo suite of software, we identified novel transcripts that are promising targets for future investigation of AHR-dependent toxicological pathways. By comparing BEZO and 7,12-B[a]AQ transcriptional profiles, we found differences in groups of transcripts, such as eye-related genes, that suggest the AHR interacts with other transcription factors or coactivators to mediate the differential toxicological effects observed for these two compounds. Future studies using morpholino knockdown of other predicted interactors would be a promising way to determine their roles in the toxicity of BEZO and 7,12-B[a]AQ, as well as discover new AHR toxicity mechanisms.

We identified transcripts with common identifiers that could be compared across the microarray and RNA-seq platforms. By clustering transcripts by expression changes observed with all 5 PAHs, we identified genes that could be potential biomarkers of PAH-related toxicity. *Ctsl.1*, for example, was induced by BAA, BEZO, and 7,12-B[a]AQ. Cathepsin L1 is a protease that influences blood pressure, and a recent study identified a polymorphic locus in its promoter, which was associated with high blood pressure in a human population (Mbewe-Campbell et al. 2012). By examining the locus, the authors found it was located in an XRE, and determined that CTSL1 is AHR-responsive. To our knowledge, the effects of xenobiotic exposure on CTSL1 and blood pressure regulation have not yet been investigated. Chemokine receptor 4a (*cxc4a*) was induced mildly, but consistently, by all PAHs in these studies and would also be an interesting target for future investigation.

In the work presented here, we investigated global transcriptional responses to diverse PAH structures and began to identify expression patterns associated with PAH exposure. Investigating PAH toxicity in AHR2 deficient zebrafish added additional insight into potential toxicity mechanisms. This work, along with other recent studies of both the AHR and PAHs, demonstrates that the AHR has functions well beyond xenobiotic-activated binding to the canonical AHR-responsive genes. Unraveling the pathways by which PAHs differentially interact with the receptor will be an engaging direction for future research.

References

- Denison, M. S. and S. R. Nagy (2003). "Activation of the aryl hydrocarbon receptor by structurally diverse exogenous and endogenous chemicals." Annu Rev Pharmacol Toxicol **43**: 309-334.
- Jonsson, M. E., D. G. Franks, et al. (2009). "The tryptophan photoproduct 6-formylindolo[3,2-b]carbazole (FICZ) binds multiple AHRs and induces multiple CYP1 genes via AHR2 in zebrafish." Chem Biol Interact.
- Mattsson, A., B. Jernstrom, et al. (2009). "H2AX phosphorylation in A549 cells induced by the bulky and stable DNA adducts of benzo[a]pyrene and dibenzo[a,l]pyrene diol epoxides." Chem Biol Interact **177**(1): 40-47.
- Mbewe-Campbell, N., Z. Wei, et al. (2012). "Genes and environment: novel, functional polymorphism in the human cathepsin L (CTSL1) promoter disrupts a xenobiotic response element (XRE) to alter transcription and blood pressure." J Hypertens.
- Osgood, R. S., B. L. Upham, et al. (2013). "Polycyclic aromatic hydrocarbon-induced signaling events relevant to inflammation and tumorigenesis in lung cells are dependent on molecular structure." PLoS One **8**(6): e65150.
- Truong, L., S. L. Harper, et al. (2011). "Evaluation of embryotoxicity using the zebrafish model." Methods Mol Biol **691**: 271-279.

Chapter 6 - Future Directions

In the studies present in this dissertation, we employed a comparative transcriptomics approach to identify global changes in mRNA expression that lead to developmental effects of PAH exposure in developing embryos. We identified clusters of genes and associated biological processes that are misexpressed in response to different PAH exposures, and further investigated the role of AHR2 in mediating responses. The rich datasets presented in this dissertation could lead to many future research directions. The ion channel disruption/inflammatory/NfKB-related processes disrupted by DBT and PYR exposure are complex, and attempted to characterize endpoints more specifically related to these processes in Appendix 2. Further studies of the PYR behavioral response, in comparison with other PAHs and in combination with potential antagonists are in progress in the laboratory.

Involvement of the AHR in toxicity pathways and normal development remains an exciting and complex area for research. With three AHR isoforms, zebrafish provide an opportunity to unravel differential functions that may be partitioned between the isoforms. We showed the AHR1A is a functional receptor, and can mediate CYP1A expression. Beyond ability to induce that downstream target, little is known about function of AHR1A or AHR1B. Characterization of where they are expressed over the course of development, and their interactions with a variety of ligands could provide valuable information about different functions of the AHR. These studies will be easier to carry out in the *ahr2*^{hu3335} line.

The need to outcross the *ahr2*^{hu3335} line has put many exciting studies of endogenous AHR2 functions on hold, but there is promise to further investigate how loss of AHR2 affects developmental processes with them in the future. Beyond this, determining global transcriptional responses to PAH exposure in the AHR2 mutant line would be an exciting direction for research. In Chapter 4, we investigated the dependence of select transcriptional changes on AHR2. This could be continued with additional genes, but provides only a piece-wise picture, and we have continually found the AHR to be involved in mechanisms in ways we have not predicted. Analysis across the genome would provide information about the entirety of processes the AHR is affecting.

From the RNA-seq analysis, we were able to identify misexpressed transcripts, and compare across PAHs. This dataset however, could be analyzed in many more interesting ways. As annotation of the zebrafish genome improves, promoter analysis and/or prediction of non-coding RNA targeting may be able to better predict expression regulation than our current analysis based on known interactions in mammals. Some novel transcripts were identified and discussed in this dissertation; many are present within the dataset that would be interesting to pursue for interaction with the AHR and involvement in zebrafish development processes. Annotation of the zebrafish genome has improved much over the past 5 years, but there are many transcripts that remain un-annotated and could be important mediators of toxicity.

Comparison of all 5 PAH structures in these studies shed light on interesting patterns in expression. Better statistical comparisons across multiple treatment groups may help to identify promising transcriptional differences between BEZO and 7,12-B[a]AQ for further analysis. Comparing additional PAH structures, will of course add power to identify which structural differences may be responsible for mediating groups of transcripts involved in different biological processes. Not discussed here are other samples collected in parallel with our BEZO and 7,12-B[a]AQ samples, which included phenanthrene-quinone and environmental mixture exposed samples. Adding these to the analysis, and comparing patterns across the larger dataset will be an interesting future direction.

Finally, comparing the genes and responses identified here across model systems will be a valuable direction for future studies. Homologues of many genes identified here have similar functions in other species, and eventually could be developed into biomarkers of PAH effects relevant to human or wildlife populations. Determining first whether PAH exposure affects their expression in rodents or human cell lines remains to be determined, and an interesting area of future work.

Bibliography

- (2010). R: A language and environment for statistical computing. R. D. C. Team. Vienna, Austria.
- Abbott, B. D., J. E. Schmid, et al. (1999). "Adverse reproductive outcomes in the transgenic Ah receptor-deficient mouse." Toxicol Appl Pharmacol **155**(1): 62-70.
- Alexeyenko, A., D. M. Wassenberg, et al. (2010). "Dynamic zebrafish interactome reveals transcriptional mechanisms of dioxin toxicity." PLoS One **5**(5): e10465.
- Andreasen, E. A., M. E. Hahn, et al. (2002). "The zebrafish (*Danio rerio*) aryl hydrocarbon receptor type 1 is a novel vertebrate receptor." Mol Pharmacol **62**(2): 234-249.
- Andreasen, E. A., L. K. Mathew, et al. (2006). "Regenerative growth is impacted by TCDD: gene expression analysis reveals extracellular matrix modulation." Toxicol Sci **92**(1): 254-269.
- Andreasen, E. A., J. M. Spitsbergen, et al. (2002). "Tissue-specific expression of AHR2, ARNT2, and CYP1A in zebrafish embryos and larvae: effects of developmental stage and 2,3,7,8-tetrachlorodibenzo-p-dioxin exposure." Toxicol Sci **68**(2): 403-419.
- Antkiewicz, D. S., R. E. Peterson, et al. (2006). "Blocking expression of AHR2 and ARNT1 in zebrafish larvae protects against cardiac toxicity of 2,3,7,8-tetrachlorodibenzo-p-dioxin." Toxicol Sci **94**(1): 175-182.
- Archuleta, M. M., G. L. Schieven, et al. (1993). "7,12-Dimethylbenz[a]anthracene activates protein-tyrosine kinases Fyn and Lck in the HPB-ALL human T-cell line and increases tyrosine phosphorylation of phospholipase C-gamma 1, formation of inositol 1,4,5-trisphosphate, and mobilization of intracellular calcium." Proc Natl Acad Sci U S A **90**(13): 6105-6109.
- Baba, T., J. Mimura, et al. (2001). "Structure and expression of the Ah receptor repressor gene." J Biol Chem **276**(35): 33101-33110.
- Baird, W. M., L. A. Hooven, et al. (2005). "Carcinogenic polycyclic aromatic hydrocarbon-DNA adducts and mechanism of action." Environ Mol Mutagen **45**(2-3): 106-114.
- Barker, C. W., J. B. Fagan, et al. (1994). "Down-regulation of P4501A1 and P4501A2 mRNA expression in isolated hepatocytes by oxidative stress." J Biol Chem **269**(6): 3985-3990.
- Barron, M. G., M. G. Carls, et al. (2004). "Evaluation of fish early life-stage toxicity models of chronic embryonic exposures to complex polycyclic aromatic hydrocarbon mixtures." Toxicol Sci **78**(1): 60-67.
- Barron, M. G., R. Heintz, et al. (2004). "Relative potency of PAHs and heterocycles as aryl hydrocarbon receptor agonists in fish." Mar Environ Res **58**(2-5): 95-100.
- Beischlag, T. V., J. Luis Morales, et al. (2008). "The aryl hydrocarbon receptor complex and the control of gene expression." Crit Rev Eukaryot Gene Expr **18**(3): 207-250.
- Benjamini, Y. and Y. Hochberg (1995). "Controlling the False Discovery Rate - a Practical and Powerful Approach to Multiple Testing." Journal of the Royal Statistical Society Series B-Methodological **57**(1): 289-300.
- Billiard, S. M., M. E. Hahn, et al. (2002). "Binding of polycyclic aromatic hydrocarbons (PAHs) to teleost aryl hydrocarbon receptors (AHRs)." Comp Biochem Physiol B Biochem Mol Biol **133**(1): 55-68.

- Billiard, S. M., A. R. Timme-Laragy, et al. (2006). "The role of the aryl hydrocarbon receptor pathway in mediating synergistic developmental toxicity of polycyclic aromatic hydrocarbons to zebrafish." *Toxicol Sci* **92**(2): 526-536.
- Binder, R. L. and J. J. Stegeman (1984). "Microsomal electron transport and xenobiotic monooxygenase activities during the embryonic period of development in the killifish, *Fundulus heteroclitus*." *Toxicol Appl Pharmacol* **73**(3): 432-443.
- Bisson, W. H., D. C. Koch, et al. (2009). "Modeling of the aryl hydrocarbon receptor (AhR) ligand binding domain and its utility in virtual ligand screening to predict new AhR ligands." *J Med Chem* **52**(18): 5635-5641.
- Bock, K. W. (2012). "Ah receptor- and Nrf2-gene battery members: Modulators of quinone-mediated oxidative and endoplasmic reticulum stress." *Biochem Pharmacol* **83**(7): 833-838.
- Bostrom, C. E., P. Gerde, et al. (2002). "Cancer risk assessment, indicators, and guidelines for polycyclic aromatic hydrocarbons in the ambient air." *Environ Health Perspect* **110 Suppl 3**: 451-488.
- Brasier, A. R., M. Jamaluddin, et al. (2000). "Angiotensin II induces gene transcription through cell-type-dependent effects on the nuclear factor-kappaB (NF-kappaB) transcription factor." *Mol Cell Biochem* **212**(1-2): 155-169.
- Brasier, A. R. and J. Li (1996). "Mechanisms for inducible control of angiotensinogen gene transcription." *Hypertension* **27**(3 Pt 2): 465-475.
- Bugel, S. M., L. A. White, et al. (2010). "Impaired reproductive health of killifish (*Fundulus heteroclitus*) inhabiting Newark Bay, NJ, a chronically contaminated estuary." *Aquat Toxicol* **96**(3): 182-193.
- Burstyn, I., H. Kromhout, et al. (2005). "Polycyclic aromatic hydrocarbons and fatal ischemic heart disease." *Epidemiology* **16**(6): 744-750.
- Bussmann, J., S. A. Wolfe, et al. (2011). "Arterial-venous network formation during brain vascularization involves hemodynamic regulation of chemokine signaling." *Development* **138**(9): 1717-1726.
- Carney, S. A., J. Chen, et al. (2006). "Aryl hydrocarbon receptor activation produces heart-specific transcriptional and toxic responses in developing zebrafish." *Mol Pharmacol* **70**(2): 549-561.
- Carney, S. A., R. E. Peterson, et al. (2004). "2,3,7,8-Tetrachlorodibenzo-p-dioxin activation of the aryl hydrocarbon receptor/aryl hydrocarbon receptor nuclear translocator pathway causes developmental toxicity through a CYP1A-independent mechanism in zebrafish." *Mol Pharmacol* **66**(3): 512-521.
- Carney, S. A., A. L. Prash, et al. (2006). "Understanding dioxin developmental toxicity using the zebrafish model." *Birth Defects Res A Clin Mol Teratol* **76**(1): 7-18.
- Cavalieri, E. L. and E. G. Rogan (1995). "Central role of radical cations in metabolic activation of polycyclic aromatic hydrocarbons." *Xenobiotica* **25**(7): 677-688.
- Chew, G. L., A. Pauli, et al. (2013). "Ribosome profiling reveals resemblance between long non-coding RNAs and 5' leaders of coding RNAs." *Development* **140**(13): 2828-2834.
- Choi, H., W. Jedrychowski, et al. (2006). "International studies of prenatal exposure to polycyclic aromatic hydrocarbons and fetal growth." *Environ Health Perspect* **114**(11): 1744-1750.
- Ciganek, M., J. Neca, et al. (2004). "A combined chemical and bioassay analysis of traffic-emitted polycyclic aromatic hydrocarbons." *Sci Total Environ* **334-335**: 141-148.

- Collins, J. F., J. P. Brown, et al. (1998). "Potency equivalency factors for some polycyclic aromatic hydrocarbons and polycyclic aromatic hydrocarbon derivatives." Regul Toxicol Pharmacol **28**(1): 45-54.
- Couroucli, X. I., S. E. Welty, et al. (2002). "Regulation of pulmonary and hepatic cytochrome P4501A expression in the rat by hyperoxia: implications for hyperoxic lung injury." Mol Pharmacol **61**(3): 507-515.
- Cubbage, C. C. and P. M. Mabee (1996). "Development of the cranium and paired fins in the zebrafish *Danio rerio* (Ostariophysi, cyprinidae)." Journal of Morphology **229**(2): 121-160.
- Das, M., K. Garg, et al. (1994). "Attenuation of benzanthrone toxicity by ascorbic acid in guinea pigs." Fundam Appl Toxicol **22**(3): 447-456.
- Denison, M. S. and S. R. Nagy (2003). "Activation of the aryl hydrocarbon receptor by structurally diverse exogenous and endogenous chemicals." Annu Rev Pharmacol Toxicol **43**: 309-334.
- Detmar, J., M. Y. Rennie, et al. (2008). "Fetal growth restriction triggered by polycyclic aromatic hydrocarbons is associated with altered placental vasculature and AhR-dependent changes in cell death." Am J Physiol Endocrinol Metab **295**(2): E519-530.
- Dong, P. D., C. A. Munson, et al. (2007). "Fgf10 regulates hepatopancreatic ductal system patterning and differentiation." Nat Genet **39**(3): 397-402.
- Duarte-Salles, T., M. A. Mendez, et al. (2012). "Dietary benzo(a)pyrene and fetal growth: effect modification by vitamin C intake and glutathione S-transferase P1 polymorphism." Environ Int **45**: 1-8.
- Durant, J. L., W. F. Busby, Jr., et al. (1996). "Human cell mutagenicity of oxygenated, nitrated and unsubstituted polycyclic aromatic hydrocarbons associated with urban aerosols." Mutat Res **371**(3-4): 123-157.
- Durante, W. (2013). "Role of arginase in vessel wall remodeling." Front Immunol **4**: 111.
- Dwivedi, N., M. Das, et al. (2001). "Role of biological antioxidants in benzanthrone toxicity." Archives of Toxicology **75**(4): 221-226.
- Ebert, A. M., G. L. Hume, et al. (2005). "Calcium extrusion is critical for cardiac morphogenesis and rhythm in embryonic zebrafish hearts." Proc Natl Acad Sci U S A **102**(49): 17705-17710.
- Eden, E., R. Navon, et al. (2009). "GORilla: a tool for discovery and visualization of enriched GO terms in ranked gene lists." BMC Bioinformatics **10**: 48.
- Ema, M., N. Ohe, et al. (1994). "Dioxin binding activities of polymorphic forms of mouse and human arylhydrocarbon receptors." J Biol Chem **269**(44): 27337-27343.
- EPA, U. (2010). Development of a relative potency factor (RPF) approach for polycyclic aromatic hydrocarbon (PAH) mixtures (External review draft). U. S. E. P. Agency. Washington, DC.
- EPA, U. (2012). "Integrated Risk Information System." from <http://www.epa.gov/iris/>.
- Evans, B. R., S. I. Karchner, et al. (2008). "Repression of aryl hydrocarbon receptor (AHR) signaling by AHR repressor: role of DNA binding and competition for AHR nuclear translocator." Mol Pharmacol **73**(2): 387-398.
- Fan, R., D. Wang, et al. (2012). "Preliminary study of children's exposure to PAHs and its association with 8-hydroxy-2'-deoxyguanosine in Guangzhou, China." Environ Int **42**: 53-58.

- Fernandez-Salguero, P., T. Pineau, et al. (1995). "Immune system impairment and hepatic fibrosis in mice lacking the dioxin-binding Ah receptor." *Science* **268**(5211): 722-726.
- Fleming, C. R. and R. T. Di Giulio (2011). "The role of CYP1A inhibition in the embryotoxic interactions between hypoxia and polycyclic aromatic hydrocarbons (PAHs) and PAH mixtures in zebrafish (*Danio rerio*)." *Ecotoxicology* **20**(6): 1300-1314.
- Fukunaga, B. N. and O. Hankinson (1996). "Identification of a novel domain in the aryl hydrocarbon receptor required for DNA binding." *J Biol Chem* **271**(7): 3743-3749.
- Fukunaga, B. N., M. R. Probst, et al. (1995). "Identification of functional domains of the aryl hydrocarbon receptor." *J Biol Chem* **270**(49): 29270-29278.
- Gao, J., A. A. Voss, et al. (2005). "Ryanodine receptor-mediated rapid increase in intracellular calcium induced by 7,8-benzo(a)pyrene quinone in human and murine leukocytes." *Toxicol Sci* **87**(2): 419-426.
- Garner, L. V. and R. T. Di Giulio (2012). "Glutathione transferase pi class 2 (GSTp2) protects against the cardiac deformities caused by exposure to PAHs but not PCB-126 in zebrafish embryos." *Comp Biochem Physiol C Toxicol Pharmacol* **155**(4): 573-579.
- Gonzalez, F. J. and P. Fernandez-Salguero (1998). "The aryl hydrocarbon receptor: studies using the AHR-null mice." *Drug Metab Dispos* **26**(12): 1194-1198.
- Goodale, B. C., S. C. Tilton, et al. (2013). "Structurally distinct polycyclic aromatic hydrocarbons induce differential transcriptional responses in developing zebrafish." *Toxicol Appl Pharmacol*.
- Gu, Y. Z., J. B. Hogenesch, et al. (2000). "The PAS superfamily: sensors of environmental and developmental signals." *Annu Rev Pharmacol Toxicol* **40**: 519-561.
- Guengerich, F. P. (2000). "Metabolism of chemical carcinogens." *Carcinogenesis* **21**(3): 345-351.
- Gurbani, D., S. K. Bharti, et al. (2013). "Polycyclic aromatic hydrocarbons and their quinones modulate the metabolic profile and induce DNA damage in human alveolar and bronchiolar cells." *Int J Hyg Environ Health*.
- Hahn, M. E. (1998). "The aryl hydrocarbon receptor: a comparative perspective." *Comp Biochem Physiol C Pharmacol Toxicol Endocrinol* **121**(1-3): 23-53.
- Hahn, M. E. (2002). "Aryl hydrocarbon receptors: diversity and evolution." *Chem Biol Interact* **141**(1-2): 131-160.
- Hahn, M. E. (2002). "Biomarkers and bioassays for detecting dioxin-like compounds in the marine environment." *Sci Total Environ* **289**(1-3): 49-69.
- Hahn, M. E., S. I. Karchner, et al. (2006). "Unexpected diversity of aryl hydrocarbon receptors in non-mammalian vertebrates: insights from comparative genomics." *J Exp Zool A Comp Exp Biol* **305**(9): 693-706.
- Hansch, C., Albert, L., Hoekman, D. (1995). *Exploring QSAR: Volume 2: Hydrophobic, Electronic, and Steric Constants*, American Chemical Society.
- Hansen, A. M., L. Mathiesen, et al. (2008). "Urinary 1-hydroxypyrene (1-HP) in environmental and occupational studies--a review." *Int J Hyg Environ Health* **211**(5-6): 471-503.
- Hecht, S. S., S. G. Carmella, et al. (2010). "Analysis of phenanthrene and benzo[a]pyrene tetraol enantiomers in human urine: relevance to the bay region diol epoxide hypothesis of benzo[a]pyrene carcinogenesis and to biomarker studies." *Chem Res Toxicol* **23**(5): 900-908.

- Hermann, A., R. Donato, et al. (2012). "S100 calcium binding proteins and ion channels." Front Pharmacol **3**: 67.
- Hernandez-Ochoa, I., B. N. Karman, et al. (2009). "The role of the aryl hydrocarbon receptor in the female reproductive system." Biochem Pharmacol **77**(4): 547-559.
- Hertz-Picciotto, I., H. Y. Park, et al. (2008). "Prenatal exposures to persistent and non-persistent organic compounds and effects on immune system development." Basic Clin Pharmacol Toxicol **102**(2): 146-154.
- Hofsteen, P., J. Plavicki, et al. (2013). "Sox9b is Required for Epicardium Formation and Plays a Role in TCDD-induced Heart Malformation in Zebrafish." Mol Pharmacol.
- Hu, S. W., Y. J. Chan, et al. (2011). "Urinary levels of 1-hydroxypyrene in children residing near a coal-fired power plant." Environ Res **111**(8): 1185-1191.
- Huang da, W., B. T. Sherman, et al. (2009). "Systematic and integrative analysis of large gene lists using DAVID bioinformatics resources." Nat Protoc **4**(1): 44-57.
- Huang, L., C. Wang, et al. (2012). "Benzo[a]pyrene exposure influences the cardiac development and the expression of cardiovascular relative genes in zebrafish (Daniorerio) embryos." Chemosphere **87**(4): 369-375.
- Hylland, K. (2006). "Polycyclic aromatic hydrocarbon (PAH) ecotoxicology in marine ecosystems." J Toxicol Environ Health A **69**(1-2): 109-123.
- Incardona, J. P., M. G. Carls, et al. (2009). "Cardiac arrhythmia is the primary response of embryonic Pacific herring (*Clupea pallasii*) exposed to crude oil during weathering." Environ Sci Technol **43**(1): 201-207.
- Incardona, J. P., M. G. Carls, et al. (2005). "Aryl hydrocarbon receptor-independent toxicity of weathered crude oil during fish development." Environ Health Perspect **113**(12): 1755-1762.
- Incardona, J. P., T. K. Collier, et al. (2004). "Defects in cardiac function precede morphological abnormalities in fish embryos exposed to polycyclic aromatic hydrocarbons." Toxicol Appl Pharmacol **196**(2): 191-205.
- Incardona, J. P., H. L. Day, et al. (2006). "Developmental toxicity of 4-ring polycyclic aromatic hydrocarbons in zebrafish is differentially dependent on AH receptor isoforms and hepatic cytochrome P4501A metabolism." Toxicol Appl Pharmacol **217**(3): 308-321.
- Incardona, J. P., T. L. Linbo, et al. (2011). "Cardiac toxicity of 5-ring polycyclic aromatic hydrocarbons is differentially dependent on the aryl hydrocarbon receptor 2 isoform during zebrafish development." Toxicol Appl Pharmacol **257**(2): 242-249.
- Isidoro Tavares, N., P. Philip-Couderc, et al. (2009). "Angiotensin II and tumour necrosis factor alpha as mediators of ATP-dependent potassium channel remodelling in post-infarction heart failure." Cardiovasc Res **83**(4): 726-736.
- Jeng, H. A., C. H. Pan, et al. (2011). "Polycyclic aromatic hydrocarbon-induced oxidative stress and lipid peroxidation in relation to immunological alteration." Occup Environ Med **68**(9): 653-658.
- Jennings, A. A. (2012). "Worldwide regulatory guidance values for surface soil exposure to carcinogenic or mutagenic polycyclic aromatic hydrocarbons." J Environ Manage **110**: 82-102.
- Jennings, A. A. (2012). "Worldwide regulatory guidance values for surface soil exposure to noncarcinogenic polycyclic aromatic hydrocarbons." J Environ Manage **101**: 173-190.
- Jensen, B. A., C. M. Reddy, et al. (2010). "Developing tools for risk assessment in protected species: Relative potencies inferred from competitive binding of halogenated

- aromatic hydrocarbons to aryl hydrocarbon receptors from beluga (*Delphinapterus leucas*) and mouse." *Aquat Toxicol* **100**(3): 238-245.
- Jia, Y., D. Stone, et al. (2011). "Estimated reduction in cancer risk due to PAH exposures if source control measures during the 2008 Beijing Olympics were sustained." *Environ Health Perspect* **119**(6): 815-820.
- Jonsson, M. E., D. G. Franks, et al. (2009). "The tryptophan photoproduct 6-formylindolo[3,2-b]carbazole (FICZ) binds multiple AHRs and induces multiple CYP1 genes via AHR2 in zebrafish." *Chem Biol Interact*.
- Jonsson, M. E., M. J. Jenny, et al. (2007). "Role of AHR2 in the expression of novel cytochrome P450 1 family genes, cell cycle genes, and morphological defects in developing zebra fish exposed to 3,3',4,4',5-pentachlorobiphenyl or 2,3,7,8-tetrachlorodibenzo-p-dioxin." *Toxicol Sci* **100**(1): 180-193.
- Jules, G. E., S. Pratap, et al. (2012). "In utero exposure to benzo(a)pyrene predisposes offspring to cardiovascular dysfunction in later-life." *Toxicology*.
- Jung, D., C. W. Matson, et al. (2011). "Genotoxicity in Atlantic killifish (*Fundulus heteroclitus*) from a PAH-contaminated Superfund site on the Elizabeth River, Virginia." *Ecotoxicology* **20**(8): 1890-1899.
- Jung, K. H., J. H. Noh, et al. (2011). "Molecular signature for early detection and prediction of polycyclic aromatic hydrocarbons in peripheral blood." *Environ Sci Technol* **45**(1): 300-306.
- Jyethi, D. S., P. S. Khillare, et al. (2013). "Risk assessment of inhalation exposure to polycyclic aromatic hydrocarbons in school children." *Environ Sci Pollut Res Int*.
- Karchner, S. I., D. G. Franks, et al. (2005). "AHR1B, a new functional aryl hydrocarbon receptor in zebrafish: tandem arrangement of *ahr1b* and *ahr2* genes." *Biochem J* **392**(Pt 1): 153-161.
- Kerkvliet, N. I. (2009). "AHR-mediated immunomodulation: the role of altered gene transcription." *Biochem Pharmacol* **77**(4): 746-760.
- Kerley-Hamilton, J. S., H. W. Trask, et al. (2012). "Inherent and Benzo[a]pyrene-Induced Differential Aryl Hydrocarbon Receptor Signaling Greatly Affects Life Span, Atherosclerosis, Cardiac Gene Expression, and Body and Heart Growth in Mice." *Toxicol Sci* **126**(2): 391-404.
- Kim, K. T., T. Zaikova, et al. (2013). "Gold nanoparticles disrupt zebrafish eye development and pigmentation." *Toxicol Sci* **133**(2): 275-288.
- Kimmel, C. B., W. W. Ballard, et al. (1995). "Stages of embryonic development of the zebrafish." *Dev Dyn* **203**(3): 253-310.
- Kluver, N., L. Yang, et al. (2011). "Transcriptional response of zebrafish embryos exposed to neurotoxic compounds reveals a muscle activity dependent *hsb11* expression." *PLoS One* **6**(12): e29063.
- Knecht, A. L., B. C. Goodale, et al. (2013). "Comparative developmental toxicity of environmentally relevant oxygenated PAHs." *Toxicol Appl Pharmacol*.
- Kojic, S., D. Radojkovic, et al. (2011). "Muscle ankyrin repeat proteins: their role in striated muscle function in health and disease." *Crit Rev Clin Lab Sci* **48**(5-6): 269-294.
- Kraus, U., S. Breitner, et al. (2011). "Particle-associated organic compounds and symptoms in myocardial infarction survivors." *Inhalation Toxicology* **23**(7): 431-447.
- Krieger, J. A., J. L. Born, et al. (1994). "Persistence of calcium elevation in the HPB-ALL human T cell line correlates with immunosuppressive properties of polycyclic aromatic hydrocarbons." *Toxicol Appl Pharmacol* **127**(2): 268-274.

- Krieger, J. A., D. R. Davila, et al. (1995). "Inhibition of sarcoplasmic/endoplasmic reticulum calcium ATPases (SERCA) by polycyclic aromatic hydrocarbons in HPB-ALL human T cells and other tissues." Toxicol Appl Pharmacol **133**(1): 102-108.
- Kriek, E., M. Rojas, et al. (1998). "Polycyclic aromatic hydrocarbon-DNA adducts in humans: relevance as biomarkers for exposure and cancer risk." Mutat Res **400**(1-2): 215-231.
- Lahvis, G. P., R. W. Pyzalski, et al. (2005). "The aryl hydrocarbon receptor is required for developmental closure of the ductus venosus in the neonatal mouse." Mol Pharmacol **67**(3): 714-720.
- Langrish, J. P., X. Li, et al. (2011). "Reducing personal exposure to particulate air pollution improves cardiovascular health in patients with coronary heart disease." Environ Health Perspect **120**(3): 367-372.
- Layshock, J. A., G. Wilson, et al. (2010). "Ketone and Quinone-Substituted Polycyclic Aromatic Hydrocarbons in Mussel Tissue, Sediment, Urban Dust, and Diesel Particulate Matrices." Environmental Toxicology and Chemistry **29**(11): 2450-2460.
- Le Mevel, J. C., F. Lancien, et al. (2008). "Central cardiovascular actions of angiotensin II in trout." Gen Comp Endocrinol **157**(1): 27-34.
- Lee, M. S., S. Magari, et al. (2011). "Cardiac autonomic dysfunction from occupational exposure to polycyclic aromatic hydrocarbons." Occup Environ Med **68**(7): 474-478.
- Li, X., Y. Feng, et al. (2012). "The dose-response decrease in heart rate variability: any association with the metabolites of polycyclic aromatic hydrocarbons in coke oven workers?" PLoS One **7**(9): e44562.
- Livak, K. J. and T. D. Schmittgen (2001). "Analysis of relative gene expression data using real-time quantitative PCR and the 2(-Delta Delta C(T)) Method." Methods **25**(4): 402-408.
- Lundstedt, S., Y. Persson, et al. (2006). Transformation of PAHs during ethanol-Fenton treatment of an aged gasworks' soil. Chemosphere. England. **65**: 1288-1294.
- Lundstedt, S., P. A. White, et al. (2007). "Sources, fate, and toxic hazards of oxygenated polycyclic aromatic hydrocarbons (PAHs) at PAH-contaminated sites." Ambio **36**(6): 475-485.
- Mahler, B. J., P. C. Van Metre, et al. (2005). "Parking lot sealcoat: an unrecognized source of urban polycyclic aromatic hydrocarbons." Environ Sci Technol **39**(15): 5560-5566.
- Mandrell, D., L. Truong, et al. (2012). "Automated zebrafish chorion removal and single embryo placement: optimizing throughput of zebrafish developmental toxicity screens." J Lab Autom **17**(1): 66-74.
- Mao, C., L. Shi, et al. (2009). "Development of fetal brain renin-angiotensin system and hypertension programmed in fetal origins." Prog Neurobiol **87**(4): 252-263.
- Mathew, L. K., E. A. Andreasen, et al. (2006). "Aryl hydrocarbon receptor activation inhibits regenerative growth." Mol Pharmacol **69**(1): 257-265.
- Mathew, R., J. A. McGrath, et al. (2008). "Modeling polycyclic aromatic hydrocarbon bioaccumulation and metabolism in time-variable early life-stage exposures." Environ Toxicol Chem **27**(7): 1515-1525.
- Matsumura, F., A. Puga, et al. (2009). "Biological functions of the arylhydrocarbon receptor: beyond induction of cytochrome P450s. Introduction to this special issue." Biochem Pharmacol **77**(4): 473.

- Mattsson, A., B. Jernstrom, et al. (2009). "H2AX phosphorylation in A549 cells induced by the bulky and stable DNA adducts of benzo[a]pyrene and dibenzo[a,l]pyrene diol epoxides." Chem Biol Interact **177**(1): 40-47.
- Mbewe-Campbell, N., Z. Wei, et al. (2012). "Genes and environment: novel, functional polymorphism in the human cathepsin L (CTSL1) promoter disrupts a xenobiotic response element (XRE) to alter transcription and blood pressure." J Hypertens.
- McIntosh, B. E., J. B. Hogenesch, et al. (2010). "Mammalian Per-Arnt-Sim proteins in environmental adaptation." Annu Rev Physiol **72**: 625-645.
- Meeker, N. D. and N. S. Trede (2008). "Immunology and zebrafish: spawning new models of human disease." Dev Comp Immunol **32**(7): 745-757.
- Menzie, C. A., B. B. Potocki, et al. (1992). "Exposure to Carcinogenic Pahs in the Environment." Environmental Science & Technology **26**(7): 1278-1284.
- Meylan, W. M. and P. H. Howard (1995). "Atom Fragment Contribution Method for Estimating Octanol-Water Partition-Coefficients." Journal of Pharmaceutical Sciences **84**(1): 83-92.
- Moens, C. B., T. M. Donn, et al. (2008). "Reverse genetics in zebrafish by TILLING." Brief Funct Genomic Proteomic **7**(6): 454-459.
- Morey, J. S., J. C. Ryan, et al. (2006). "Microarray validation: factors influencing correlation between oligonucleotide microarrays and real-time PCR." Biol Proced Online **8**: 175-193.
- Mumtaz, M. and J. George (1995). Toxicological profile for polycyclic aromatic hydrocarbons (PAHs). Atlanta, GA, Agency for Toxic Substances and Disease Registry, U.S. Department of Health and Human Services.
- Murk, A. J., J. Legler, et al. (1996). "Chemical-activated luciferase gene expression (CALUX): a novel in vitro bioassay for Ah receptor active compounds in sediments and pore water." Fundam Appl Toxicol **33**(1): 149-160.
- Murray, I. A., C. A. Flaveny, et al. (2011). "Suppression of cytokine-mediated complement factor gene expression through selective activation of the Ah receptor with 3',4'-dimethoxy- α -naphthoflavone." Mol Pharmacol **79**(3): 508-519.
- Nacci, D., M. Huber, et al. (2009). "Evolution of tolerance to PCBs and susceptibility to a bacterial pathogen (*Vibrio harveyi*) in Atlantic killifish (*Fundulus heteroclitus*) from New Bedford (MA, USA) harbor." Environ Pollut **157**(3): 857-864.
- Narayanan, G. A., I. A. Murray, et al. (2012). "Selective aryl hydrocarbon receptor modulator-mediated repression of CD55 expression induced by cytokine exposure." J Pharmacol Exp Ther **342**(2): 345-355.
- Narayanan, S. P., J. Suwanpradid, et al. (2011). "Arginase 2 deletion reduces neuro-glial injury and improves retinal function in a model of retinopathy of prematurity." PLoS One **6**(7): e22460.
- Naumova, Y. Y., S. J. Eisenreich, et al. (2002). "Polycyclic aromatic hydrocarbons in the indoor and outdoor air of three cities in the U.S." Environ Sci Technol **36**(12): 2552-2559.
- Nebert, D. W., T. P. Dalton, et al. (2004). "Role of aryl hydrocarbon receptor-mediated induction of the CYP1 enzymes in environmental toxicity and cancer." J Biol Chem **279**(23): 23847-23850.
- Nebert, D. W., J. R. Robinson, et al. (1975). "Genetic expression of aryl hydrocarbon hydroxylase activity in the mouse." J Cell Physiol **85**(2 Pt 2 Suppl 1): 393-414.

- Nebert, D. W., A. L. Roe, et al. (2000). "Role of the aromatic hydrocarbon receptor and [Ah] gene battery in the oxidative stress response, cell cycle control, and apoptosis." Biochem Pharmacol **59**(1): 65-85.
- Nielsen, T., A. Feilberg, et al. (1999). "The variation of street air levels of PAH and other mutagenic PAC in relation to regulations of traffic emissions and the impact of atmospheric processes." Environmental Science and Pollution Research **6**(3): 133-137.
- Nikolsky, Y., E. Kirillov, et al. (2009). "Functional analysis of OMICs data and small molecule compounds in an integrated "knowledge-based" platform." Methods Mol Biol **563**: 177-196.
- O'Donnell, E. F., K. S. Saili, et al. (2010). "The anti-inflammatory drug leflunomide is an agonist of the aryl hydrocarbon receptor." PLoS One **5**(10).
- Osgood, R. S., B. L. Upham, et al. (2013). "Polycyclic aromatic hydrocarbon-induced signaling events relevant to inflammation and tumorigenesis in lung cells are dependent on molecular structure." PLoS One **8**(6): e65150.
- Ovrevik, J., V. M. Arlt, et al. (2010). "Differential effects of nitro-PAHs and amino-PAHs on cytokine and chemokine responses in human bronchial epithelial BEAS-2B cells." Toxicol Appl Pharmacol **242**(3): 270-280.
- Pandini, A., M. S. Denison, et al. (2007). "Structural and functional characterization of the aryl hydrocarbon receptor ligand binding domain by homology modeling and mutational analysis." Biochemistry **46**(3): 696-708.
- Pandini, A., A. A. Soshilov, et al. (2009). "Detection of the TCDD binding-fingerprint within the Ah receptor ligand binding domain by structurally driven mutagenesis and functional analysis." Biochemistry **48**(25): 5972-5983.
- Park, K. and A. L. Scott (2010). "Cholesterol 25-hydroxylase production by dendritic cells and macrophages is regulated by type I interferons." J Leukoc Biol **88**(6): 1081-1087.
- Patel, R. D., I. A. Murray, et al. (2009). "Ah receptor represses acute-phase response gene expression without binding to its cognate response element." Lab Invest **89**(6): 695-707.
- Perera, F., W. Y. Tang, et al. (2009). "Relation of DNA methylation of 5'-CpG island of ACSL3 to transplacental exposure to airborne polycyclic aromatic hydrocarbons and childhood asthma." PLoS One **4**(2): e4488.
- Perera, F. P., Z. Li, et al. (2009). "Prenatal Airborne Polycyclic Aromatic Hydrocarbon Exposure and Child IQ at Age 5 Years." Pediatrics.
- Petersen, G. I. and P. Kristensen (1998). "Bioaccumulation of lipophilic substances in fish early life stages." Environmental Toxicology and Chemistry **17**(7): 1385-1395.
- Peterson, R. E., H. M. Theobald, et al. (1993). "Developmental and reproductive toxicity of dioxins and related compounds: cross-species comparisons." Crit Rev Toxicol **23**(3): 283-335.
- Pfaffl, M. W. (2001). "A new mathematical model for relative quantification in real-time RT-PCR." Nucleic Acids Res **29**(9): e45.
- Planchart, A. and C. J. Mattingly (2010). "2,3,7,8-Tetrachlorodibenzo-p-dioxin upregulates FoxQ1b in zebrafish jaw primordium." Chem Res Toxicol **23**(3): 480-487.
- Polidori, A., J. Kwon, et al. (2010). "Source proximity and residential outdoor concentrations of PM(2.5), OC, EC, and PAHs." J Expo Sci Environ Epidemiol **20**(5): 457-468.

- Postlethwait, J., A. Amores, et al. (2004). "Subfunction partitioning, the teleost radiation and the annotation of the human genome." Trends Genet **20**(10): 481-490.
- Prasch, A. L., H. Teraoka, et al. (2003). "Aryl hydrocarbon receptor 2 mediates 2,3,7,8-tetrachlorodibenzo-p-dioxin developmental toxicity in zebrafish." Toxicol Sci **76**(1): 138-150.
- Price, R. L., W. Carver, et al. (1997). "The effects of angiotensin II and specific angiotensin receptor blockers on embryonic cardiac development and looping patterns." Dev Biol **192**(2): 572-584.
- Puga, A., C. Ma, et al. (2009). "The aryl hydrocarbon receptor cross-talks with multiple signal transduction pathways." Biochem Pharmacol **77**(4): 713-722.
- Ramesh, A., S. A. Walker, et al. (2004). "Bioavailability and risk assessment of orally ingested polycyclic aromatic hydrocarbons." Int J Toxicol **23**(5): 301-333.
- Ramirez, N., A. Cuadras, et al. (2011). "Risk assessment related to atmospheric polycyclic aromatic hydrocarbons in gas and particle phases near industrial sites." Environ Health Perspect **119**(8): 1110-1116.
- Reimers, M. J., J. K. La Du, et al. (2006). "Ethanol-dependent toxicity in zebrafish is partially attenuated by antioxidants." Neurotoxicol Teratol **28**(4): 497-508.
- Ren, A., X. Qiu, et al. (2011). "Association of selected persistent organic pollutants in the placenta with the risk of neural tube defects." Proc Natl Acad Sci U S A **108**(31): 12770-12775.
- Rennie, M. Y., J. Detmar, et al. (2011). "Vessel tortuosity and reduced vascularization in the fetoplacental arterial tree after maternal exposure to polycyclic aromatic hydrocarbons." Am J Physiol Heart Circ Physiol **300**(2): H675-684.
- Reynaud, S. and P. Deschaux (2006). "The effects of polycyclic aromatic hydrocarbons on the immune system of fish: a review." Aquat Toxicol **77**(2): 229-238.
- Saeed, A. I., V. Sharov, et al. (2003). "TM4: a free, open-source system for microarray data management and analysis." Biotechniques **34**(2): 374-378.
- Safe, S. H. (1998). "Development validation and problems with the toxic equivalency factor approach for risk assessment of dioxins and related compounds." J Anim Sci **76**(1): 134-141.
- Saili, K. S. (2012). Developmental neurobehavioral toxicity of bisphenol A in zebrafish (Danio rerio) [electronic resource] / by Katherine Schletz Saili. Corvallis, Or. :, Oregon State University.
- Sarkar, A., D. Ray, et al. (2006). "Molecular Biomarkers: their significance and application in marine pollution monitoring." Ecotoxicology **15**(4): 333-340.
- Sartor, M. A., M. Schnekenburger, et al. (2009). "Genomewide analysis of aryl hydrocarbon receptor binding targets reveals an extensive array of gene clusters that control morphogenetic and developmental programs." Environ Health Perspect **117**(7): 1139-1146.
- Schmidt, J. V. and C. A. Bradfield (1996). "Ah receptor signaling pathways." Annu Rev Cell Dev Biol **12**: 55-89.
- Schmidt, J. V., G. H. Su, et al. (1996). "Characterization of a murine Ahr null allele: involvement of the Ah receptor in hepatic growth and development." Proc Natl Acad Sci U S A **93**(13): 6731-6736.
- Schoeny, R. a. K. P. (1993). Provisional guidance for quantitative risk assessment of polycyclic aromatic hydrocarbons. U. S. E. P. Agency. Washington, DC.

- Scott, J. A., J. P. Incardona, et al. (2011). "AhR2-mediated, CYP1A-independent cardiovascular toxicity in zebrafish (*Danio rerio*) embryos exposed to retene." Aquat Toxicol **101**(1): 165-174.
- Shannon, P., A. Markiel, et al. (2003). "Cytoscape: a software environment for integrated models of biomolecular interaction networks." Genome Res **13**(11): 2498-2504.
- Shi, Z., N. Dragin, et al. (2010). "Organ-specific roles of CYP1A1 during detoxication of dietary benzo[a]pyrene." Mol Pharmacol **78**(1): 46-57.
- Shimizu, Y., Y. Nakatsuru, et al. (2000). "Benzo[a]pyrene carcinogenicity is lost in mice lacking the aryl hydrocarbon receptor." Proc Natl Acad Sci U S A **97**(2): 779-782.
- Singh, K. P., F. L. Casado, et al. (2009). "The aryl hydrocarbon receptor has a normal function in the regulation of hematopoietic and other stem/progenitor cell populations." Biochem Pharmacol **77**(4): 577-587.
- Singh, R. P., R. Khanna, et al. (2003). "Comparative effect of benzanthrone and 3-bromobenzanthrone on hepatic xenobiotic metabolism and anti-oxidative defense system in guinea pigs." Archives of Toxicology **77**(2): 94-99.
- Smith, B. W., S. S. Rozelle, et al. (2013). "The aryl hydrocarbon receptor directs hematopoietic progenitor cell expansion and differentiation." Blood.
- Song, M. K., M. Song, et al. (2012). "Identification of molecular signatures predicting the carcinogenicity of polycyclic aromatic hydrocarbons (PAHs)." Toxicol Lett **212**(1): 18-28.
- Suresh, R., A. Shally, et al. (2009). "Assessment of association of exposure to polycyclic aromatic hydrocarbons with bronchial asthma and oxidative stress in children: A case control study." Indian J Occup Environ Med **13**(1): 33-37.
- Svoboda, K. R., A. E. Linares, et al. (2001). "Activity regulates programmed cell death of zebrafish Rohon-Beard neurons." Development **128**(18): 3511-3520.
- Tang, D., T. Y. Li, et al. (2006). "PAH-DNA adducts in cord blood and fetal and child development in a Chinese cohort." Environ Health Perspect **114**(8): 1297-1300.
- Tanguay, R. L., C. C. Abnet, et al. (1999). "Cloning and characterization of the zebrafish (*Danio rerio*) aryl hydrocarbon receptor." Biochim Biophys Acta **1444**(1): 35-48.
- Teraoka, H., W. Dong, et al. (2003). "Induction of cytochrome P450 1A is required for circulation failure and edema by 2,3,7,8-tetrachlorodibenzo-p-dioxin in zebrafish." Biochem Biophys Res Commun **304**(2): 223-228.
- Tian, B., D. E. Nowak, et al. (2005). "A TNF-induced gene expression program under oscillatory NF-kappaB control." BMC Genomics **6**: 137.
- Tian, Y., S. Ke, et al. (1999). "Ah receptor and NF-kappaB interactions, a potential mechanism for dioxin toxicity." J Biol Chem **274**(1): 510-515.
- Tilton, S. C., T. L. Tal, et al. (2012). "Bioinformatics resource manager v2.3: an integrated software environment for systems biology with microRNA and cross-species analysis tools." BMC Bioinformatics **13**(1): 311.
- Timme-Laragy, A. R., C. J. Cockman, et al. (2007). "Synergistic induction of AHR regulated genes in developmental toxicity from co-exposure to two model PAHs in zebrafish." Aquat Toxicol **85**(4): 241-250.
- Timme-Laragy, A. R., S. I. Karchner, et al. (2012). "Nrf2b, novel zebrafish paralog of oxidant-responsive transcription factor NF-E2-related factor 2 (NRF2)." J Biol Chem **287**(7): 4609-4627.
- Timme-Laragy, A. R., L. A. Van Tiem, et al. (2009). "Antioxidant responses and NRF2 in synergistic developmental toxicity of PAHs in zebrafish." Toxicol Sci.

- Trapnell, C., L. Pachter, et al. (2009). "TopHat: discovering splice junctions with RNA-Seq." *Bioinformatics* **25**(9): 1105-1111.
- Trapnell, C., A. Roberts, et al. (2012). "Differential gene and transcript expression analysis of RNA-seq experiments with TopHat and Cufflinks." *Nat Protoc* **7**(3): 562-578.
- Truong, L., S. L. Harper, et al. (2011). "Evaluation of embryotoxicity using the zebrafish model." *Methods Mol Biol* **691**: 271-279.
- van Delft, J., S. Gaj, et al. (2012). "RNA-Seq provides new insights in the transcriptome responses induced by the carcinogen benzo[a]pyrene." *Toxicol Sci* **130**(2): 427-439.
- Van den Berg, M., L. S. Birnbaum, et al. (2006). "The 2005 World Health Organization reevaluation of human and Mammalian toxic equivalency factors for dioxins and dioxin-like compounds." *Toxicol Sci* **93**(2): 223-241.
- Van Metre, P. C. and B. J. Mahler (2005). "Trends in hydrophobic organic contaminants in urban and reference lake sediments across the United States, 1970-2001." *Environ Sci Technol* **39**(15): 5567-5574.
- Van Metre, P. C. and B. J. Mahler (2010). "Contribution of PAHs from coal-tar pavement sealcoat and other sources to 40 U.S. lakes." *Sci Total Environ* **409**(2): 334-344.
- Van Tiem, L. A. and R. T. Di Giulio (2011). "AHR2 knockdown prevents PAH-mediated cardiac toxicity and XRE- and ARE-associated gene induction in zebrafish (*Danio rerio*)." *Toxicol Appl Pharmacol* **254**(3): 280-287.
- Vanwezel, A. P. and A. Opperhuizen (1995). "Narcosis Due to Environmental-Pollutants in Aquatic Organisms - Residue-Based Toxicity, Mechanisms, and Membrane Burdens." *Critical Reviews in Toxicology* **25**(3): 255-279.
- Vlecken, D. H., J. Testerink, et al. (2009). "A critical role for myoglobin in zebrafish development." *Int J Dev Biol* **53**(4): 517-524.
- Vogel, C. F., E. Sciallo, et al. (2004). "Dioxin increases C/EBPbeta transcription by activating cAMP/protein kinase A." *J Biol Chem* **279**(10): 8886-8894.
- Walgraeve, C., K. Demeestere, et al. (2010). "Oxygenated polycyclic aromatic hydrocarbons in atmospheric particulate matter: Molecular characterization and occurrence." *Atmospheric Environment* **44**(15): 1831-1846.
- Wan, B., J. W. Yarbrough, et al. (2008). "Structure-related clustering of gene expression fingerprints of thp-1 cells exposed to smaller polycyclic aromatic hydrocarbons." *SAR QSAR Environ Res* **19**(3-4): 351-373.
- Wang, W., N. Jariyasopit, et al. (2011). "Concentration and photochemistry of PAHs, NPAHs, and OPAHs and toxicity of PM2.5 during the Beijing Olympic Games." *Environ Sci Technol* **45**(16): 6887-6895.
- Wassenberg, D. M., A. L. Nerlinger, et al. (2005). "Effects of the polycyclic aromatic hydrocarbon heterocycles, carbazole and dibenzothiophene, on in vivo and in vitro CYP1A activity and polycyclic aromatic hydrocarbon-derived embryonic deformities." *Environ Toxicol Chem* **24**(10): 2526-2532.
- Wei, S. L., B. Huang, et al. (2012). "Characterization of PM2.5-bound nitrated and oxygenated PAHs in two industrial sites of South China." *Atmospheric Research* **109**: 76-83.
- White, S. S. and L. S. Birnbaum (2009). "An overview of the effects of dioxins and dioxin-like compounds on vertebrates, as documented in human and ecological epidemiology." *J Environ Sci Health C Environ Carcinog Ecotoxicol Rev* **27**(4): 197-211.
- Wienholds, E., F. van Eeden, et al. (2003). "Efficient target-selected mutagenesis in zebrafish." *Genome Res* **13**(12): 2700-2707.

- Wiens, G. D. and G. W. Glenney (2011). "Origin and evolution of TNF and TNF receptor superfamilies." Dev Comp Immunol **35**(12): 1324-1335.
- Wilhelm, M., J. K. Ghosh, et al. (2012). "Traffic-related air toxics and term low birth weight in Los Angeles County, California." Environ Health Perspect **120**(1): 132-138.
- Willett, K. L., D. Wassenberg, et al. (2001). "In vivo and in vitro inhibition of CYP1A-dependent activity in *Fundulus heteroclitus* by the polynuclear aromatic hydrocarbon fluoranthene." Toxicol Appl Pharmacol **177**(3): 264-271.
- Wills, L. P., C. W. Matson, et al. (2010). "Characterization of the recalcitrant CYP1 phenotype found in Atlantic killifish (*Fundulus heteroclitus*) inhabiting a Superfund site on the Elizabeth River, VA." Aquat Toxicol **99**(1): 33-41.
- Wilson, S. R., A. D. Joshi, et al. (2013). "The tumor suppressor Kruppel-like factor 6 is a novel aryl hydrocarbon receptor DNA binding partner." J Pharmacol Exp Ther **345**(3): 419-429.
- Wirgin, I., N. K. Roy, et al. (2011). "Mechanistic basis of resistance to PCBs in Atlantic tomcod from the Hudson River." Science **331**(6022): 1322-1325.
- Wittkopp, N., E. Huntzinger, et al. (2009). "Nonsense-mediated mRNA decay effectors are essential for zebrafish embryonic development and survival." Mol Cell Biol **29**(13): 3517-3528.
- Wu, C., H. Lu, et al. (2011). "Molecular and Pathophysiological Features of Angiotensinogen: A Mini Review." N Am J Med Sci (Boston) **4**(4): 183-190.
- Wu, M. T., T. C. Lee, et al. (2011). "Whole genome expression in peripheral-blood samples of workers professionally exposed to polycyclic aromatic hydrocarbons." Chem Res Toxicol **24**(10): 1636-1643.
- Xiong, K. M., R. E. Peterson, et al. (2008). "Aryl hydrocarbon receptor-mediated down-regulation of *sox9b* causes jaw malformation in zebrafish embryos." Mol Pharmacol **74**(6): 1544-1553.
- Xu, X., H. Hu, et al. (2013). "Studying the effects of polycyclic aromatic hydrocarbons on peripheral arterial disease in the United States." Sci Total Environ **461-462C**: 341-347.
- Yu, H. (2002). "Environmental carcinogenic polycyclic aromatic hydrocarbons: photochemistry and phototoxicity." J Environ Sci Health C Environ Carcinog Ecotoxicol Rev **20**(2): 149-183.

Appendices

Appendix 1 - Developmental toxicity of DBT, BAA and PYR in *ahr2^{hu3335}* zebrafish

Objective

The developmental toxicity of BAA, DBT and PYR was compared between wild-type 5D embryos (*ahr2*⁺) and embryos with non-functional AHR2 (*ahr2^{hu3335}*) in order to determine whether developmental toxicity of these three PAHs was mediated by *ahr2*.

Methods

Embryos were exposed to 25 uM benz(a)anthracene (BAA), dibenzothiophene (DBT), pyrene (PYR) or 1% DMSO vehicle control dissolved in embryo media from 6-48 hpf in glass vials. Exposures were conducted at 28C on a rocker, protected from light. At 48 hpf, exposure solutions were removed, embryos were rinsed 4 times and solution was replaced with 2 ml fresh embryo media. Embryos were incubated in the dark until 120 hpf, when they were evaluated for developmental malformations.

Results

As observed previously (Chapter 2), we observed significant malformation incidence in *ahr2*⁺embryos exposed to 25µM BAA, DBT and PYR (Figure 1A). In *ahr2^{hu3335}* embryos, 25 uM BAA did not cause a significant increase in any malformations. DBT and PYR, however, did cause increases in malformations, suggesting that they cause toxicity through *ahr2*-independent mechanisms.

Conclusions

With these studies, we confirmed the dependence of BAA-induced developmental toxicity on AHR2. We also demonstrate that absence of AHR2 does not protect from DBT and PYR-induced toxicity. This has been previously observed in AHR2-deficient (AHR2 morpholino injected) embryos exposed to these compounds (Incardona, Day et al. 2006). Background malformations and low quantity of embryos precluded the use of the *ahr2^{hu3335}* line for the remaining studies in this dissertation. It is generally accepted that 5 outcrosses are required to sufficiently dilute background mutations in zebrafish lines generated by TILLING. At the writing of this thesis, the fourth outcrossed generation is spawning more reliably and better

quality eggs. The *ahr2*^{hu3335} shows promise for future work investigating AHR related questions in zebrafish.

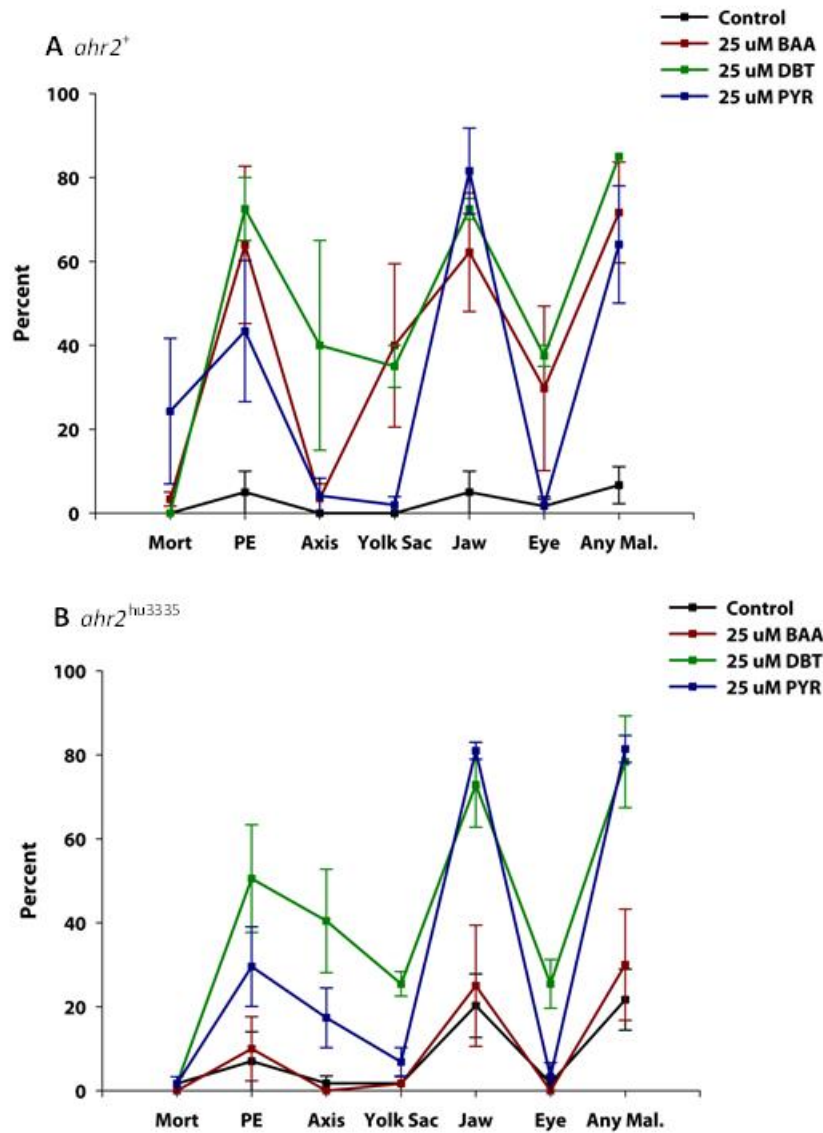


Figure A1-1

Profile plots of malformations observed at 5 dpf in PAH-treated wild-type and *ahr2*-null embryos indicate subtle differential responses between PAHs. PAH exposures did not induce significant mortality (Mort) in either fish line, but pericardial edema (PE), axis, yolk sac, jaw, and eye malformations were observed. All three PAH treatments caused a significant increase in the percent of wild-type embryos with at least one malformation (Any Mal.). BAA did not cause a significant increase in malformations in *ahr2*^{hu3335} embryos compared to control. Data represent 3 independent replicates analyzed by One-way Analysis of Variance with Tukey's post-test for pairwise comparisons.

Appendix 2 - Characterization of behavioral and neutrophil responses to PAH exposure

Objective

During developmental toxicity studies, we observed hyperactivity at 3 and 4 days post fertilization in embryos exposed to pyrene (PYR). By 120 hpf, when toxicity evaluations are conducted, behavior was no longer noticeable. We hypothesized that embryos were sensing and responding to PYR in a more immediate manner, and not because of effects on development. In this preliminary study we investigated whether zebrafish respond to acute PAH exposure at 120 hpf, when organ systems are fully developed.

In our microarray study (Chapter 2) we observed a large number of inflammatory-related transcripts misexpressed in response to PAH exposure. PAHs are also known skin irritants. We investigated whether localized inflammatory activity could be observed following PAH exposure using a transgenic zebrafish line (mpx:gfp) that expresses green fluorescent protein in neutrophils (Elks, Loynes et al. 2011).

Methods

Behavioral challenge assay

Zebrafish were dechorionated and placed individually into wells of a 96-well plate at 6 hpf in 100 μ l embryo media. They were incubated with normal lighting conditions until 120 dpf. 100 μ l of exposure solution (DBT, PYR or BAA) was then added to each well, to a final concentration of 1% DMSO. Embryos were exposed to 0, 1, 2.5, 5, 10 or 25 μ M final concentrations of PAH. Behavior was recorded under lit conditions using Viewpoint Zebraboxes, starting 10 min following exposure for 5 hours. Distance traveled was calculated per minute for each fish. Data represent the mean of 32 fish per exposure group.

Imaging neutrophil response

GFP:mpo zebrafish were exposed to 25 μ M PYR or 1% DMSO control in a 96-well plate at 72 hpf. 8 embryos from each group were anesthetized and imaged on a zeiss axiovert microscope using a 5X objective at 2, 4, 8 and 24 hours post exposure. Images were created from z-stack of 5 slices.

Results

Behavioral challenge assay

In this preliminary dataset, we observed distinct differences in behavioral patterns of fish exposed to DBT, PYR and BAA. Movement was heightened by exposure to all PAHs for the first hour of the study. Zebrafish exposed to DBT and BAA returned to activity levels comparable to controls after ~ 1.5 hr (Figure 1A, 1B). The 25uM DBT group remained more active, at 80 millimeters per minute, for almost 3 hours. In contrast, PYR-exposed zebrafish were less active immediately following exposure, but activity increased to ~120 millimeters per minute 1 hr after exposure in the 10 and 25 uM exposure groups (Figure 1C). Activity remained elevated for the duration of the study. We observed a concentration-response in hyperactivity, where zebrafish exposed to 2.5 uM PYR also had activity elevated above controls for the 5 hr exposure. This preliminary data demonstrates that zebrafish can immediately sense PAHs, and respond uniquely to PYR. The sensory mechanism and cause of activity remains unknown.

Imaging neutrophil response

From the whole-embryo images collected, we were not able to discern any specific areas of neutrophil activity in the PYR-exposed embryos. We found that neutrophil number and location was variable between fish. While a quantitative method may be able to detect small changes that are not readily observable, we were not able to identify a specific area in the fish that exhibited increased localization of these cells involved in the inflammatory response (Figure 2A). We note that we were only visualizing neutrophils; macrophages are also active at these developmental time points and could be more involved in response to PAH exposure. The waterborne exposure also would not necessarily be expected to result in a localized response.

Conclusions

In this preliminary data, we found that zebrafish can sense and immediately respond to PAH exposure with increased swimming behavior at 5 dpf. This was also observed anecdotally at 3 and 4 dpf. PYR induced a unique response, wherein zebrafish exhibited increased swimming activity for the duration of the study (5 hours). We test lower concentrations, and found increased activity at 2.5 uM, which is 10 fold lower than the concentration that

induced developmental malformations (in glass vial exposures). Fish have been shown to exhibit increased activity in response to water contaminants (Hellou 2011). The sensory mechanism, however, is not known. Given their structural similarity, the difference in response to PYR and BAA is particularly intriguing and under further investigation.

PAHs can cause skin irritation, and induce inflammatory activity in a number of model systems. We hypothesized that an inflammatory response to PYR might result in differential neutrophil localization. We did not observe any notable difference, however, in transgenic mpx:gfz zebrafish at 2, 4, 8 or 28 hours post exposure. Other cell types may be more involved in inflammatory response to PAHs, or this method may not be sufficient to discern differences.

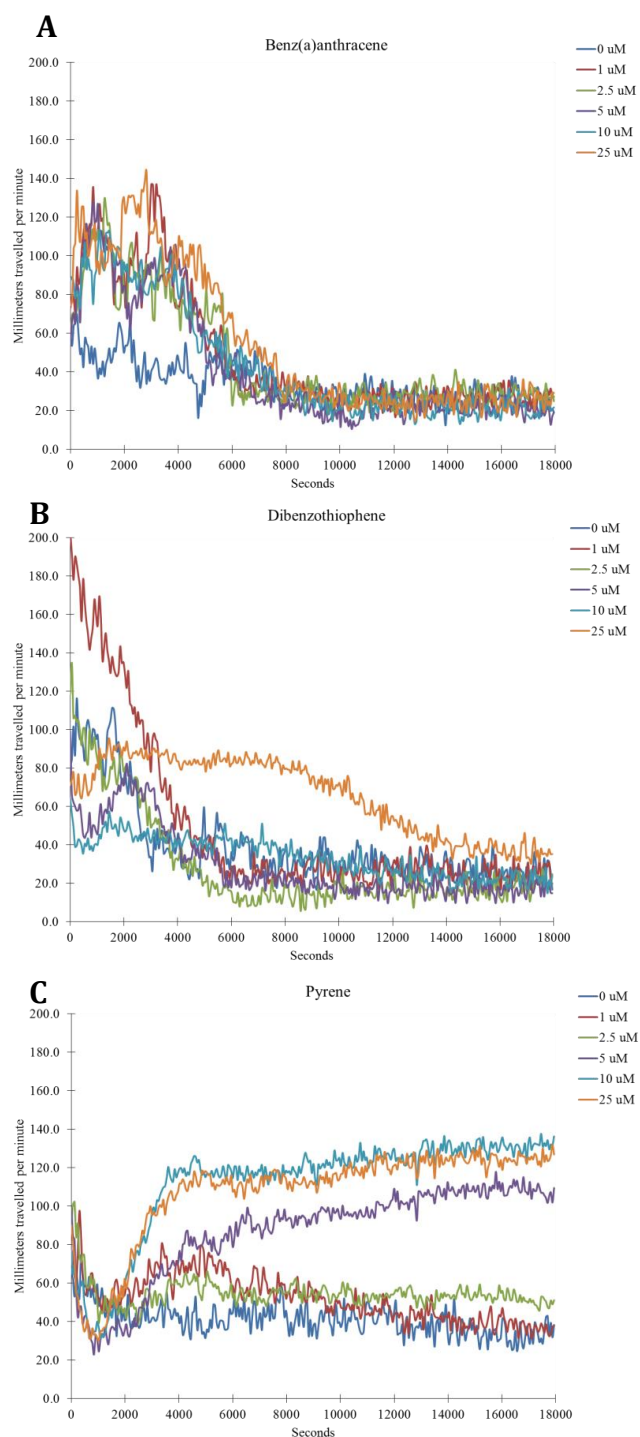


Figure A2-1

Activity of zebrafish (120 hpf) exposed to BAA (**A**), DBT (**B**), or PYR (**C**) was recorded for 5 hours following exposure.

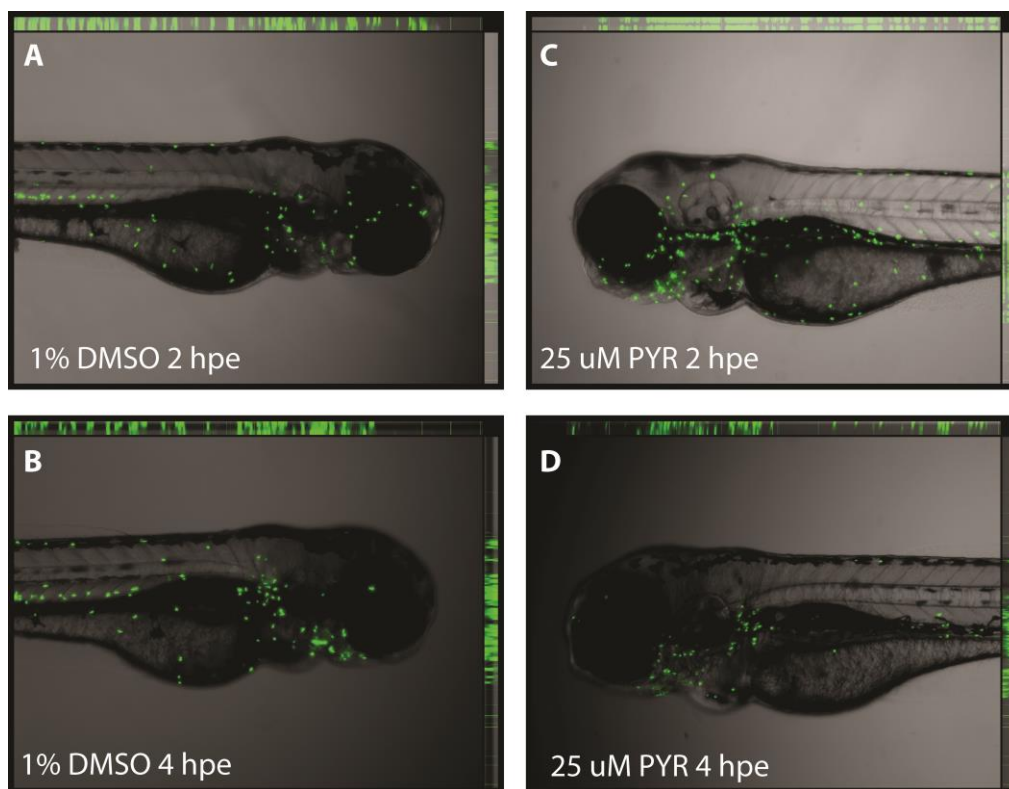


Figure A2-2 No treatment-related differences in neutrophil localization following PYR exposure

Representative images of 3 dpf zebrafish exposed to 1% DMSO at 2 and 4 hours post exposure (**A, B**). Treatment effects were not observed in embryos exposed to 25 μ M PYR at 2 and 4 hpe (**C,D**).

References

- Elks, P. M., C. A. Loynes, et al. (2011). "Measuring inflammatory cell migration in the zebrafish." *Methods Mol Biol* **769**: 261-275.
- Hellou, J. (2011). "Behavioural ecotoxicology, an "early warning" signal to assess environmental quality." *Environ Sci Pollut Res Int* **18**(1): 1-11.
- Incardona, J. P., H. L. Day, et al. (2006). "Developmental toxicity of 4-ring polycyclic aromatic hydrocarbons in zebrafish is differentially dependent on AH receptor isoforms and hepatic cytochrome P4501A metabolism." *Toxicol Appl Pharmacol* **217**(3): 308-321.